

GLUCOSE AND HUMAN VASCULAR ENDOTHELIAL CELL AGEING

Thesis submitted for the degree of Doctor of Philosophy
(as part of the MB PhD ChB programme)

1.1 DIABETES at the University of Leicester

1.2 ENDOTHELIAL CELL PHYSIOLOGY

1.3 Atherosclerosis

1.3.1 THE NATURE OF ATHEROSCLEROSIS

1.3.2 ATHEROSCLEROSIS

1.4 ENDOTHELIAL CELL PHYSIOLOGY

1.4.1 ENDOTHELIAL DYSFUNCTION AND AILING

1.4.2 ENDOTHELIAL DYSFUNCTION AND AILING

1.4.3 ENDOTHELIAL DYSFUNCTION AND AILING

1.5 CELLULAR SENESCENCE

1.5.1 CELLULAR SENESCENCE

1.5.2 THE MITOCHONDRIUM AND CELLULAR SENESCENCE

1.5.3 CELLULAR SENESCENCE

1.6 TELOMERE PHYSIOLOGY

1.6.1 THE STRUC

1.6.2 TELOMERE

1.6.3 DNA DAMAGE

1.6.4 TELOMERE

1.7 CELLULAR SENESCENCE

1.7.1 SENESCENCE AND CELLULAR SENESCENCE

1.7.2 SENESCENCE AND CELLULAR SENESCENCE

1.7.3 SENESCENCE AND CELLULAR SENESCENCE

By

Raman Verma

Department of Cardiovascular Sciences

University of Leicester



September 2004

UMI Number: U196318

All rights reserved

INFORMATION TO ALL USERS

The quality of this reproduction is dependent upon the quality of the copy submitted.

In the unlikely event that the author did not send a complete manuscript and there are missing pages, these will be noted. Also, if material had to be removed, a note will indicate the deletion.



UMI U196318

Published by ProQuest LLC 2013. Copyright in the Dissertation held by the Author.
Microform Edition © ProQuest LLC.

All rights reserved. This work is protected against
unauthorized copying under Title 17, United States Code.



ProQuest LLC
789 East Eisenhower Parkway
P.O. Box 1346
Ann Arbor, MI 48106-1346

CONTENTS

Title Page	
Contents	(i)
Abstract	(vi)
Acknowledgements	(vii)
Abbreviations	(viii)
<u>Chapter 1 : INTRODUCTION</u>	1
1.1 DIABETES	2
1.2 ENDOTHELIAL CELL PHYSIOLOGY	3
1.3 ATHEROSCLEROSIS	4
1.3.1 THE NATURE OF ATHEROSCLEROSIS	4
1.3.2 ATHEROSCLEROSIS INITIATION	4
1.4 ENDOTHELIAL DYSFUNCTION	5
1.4.1 ENDOTHELIAL DYSFUNCTION AND AGEING	5
1.4.2 ENDOTHELIAL DYSFUNCTION AND DIABETES	6
1.4.3 ENDOTHELIAL DYSFUNCTION AND OXIDATIVE STRESS	7
1.5 OXIDATIVE STRESS AND AGEING	8
1.5.1 THE FREE RADICAL THEORY OF AGEING	8
1.5.2 THE MITOCHONDRIAL THEORY OF AGEING	10
1.5.3 DIABETES AND AGEING	11
1.6 TELOMERE BIOLOGY	12
1.6.1 THE STRUCTURE OF HUMAN TELOMERES	13
1.6.2 TELOMERE SHORTENING	15
1.6.3 DNA DAMAGE AND TELOMERE ATTRITION	18
1.6.4 TELOMERE ATTRITION AND SENESENCE	19
1.7 CELLULAR SENESENCE	21
1.7.1 SENESENCE AND CELL CYLCE ARREST	23
1.7.2 SENESENCE AND OXIDATIVE STRESS	25
1.7.3 SENESENCE AND THE VESSEL WALL	26

1.8	MITOCHONDRIAL PHYSIOLOGY	27
1.8.1	MITOCHONDRIAL DNA DAMAGE	30
1.8.2	MITOCHONDRIA AND AGEING	32
1.8.3	MITOCHONDRIA AND DIABETES	33
1.9	BIOLOGY OF OXIDATIVE STRESS	34
1.9.1	FREE RADICALS	34
1.9.2	REACTIVE SPECIES	34
1.9.2.1	SUPEROXIDE RADICAL ($O_2^{\bullet-}$)	34
1.9.2.2	HYDROGEN PEROXIDE (H_2O_2)	35
1.9.2.3	HYDROXYL RADICAL (OH^{\bullet})	35
1.9.2.4	NITRIC OXIDE (NO)	36
1.9.3	ANTIOXIDANTS	37
1.9.4	ENZYMATIC DEFENCES	37
1.9.4.1	SUPEROXIDE DISMUTASE (SOD)	37
1.9.4.2	CATALASES	38
1.9.4.3	GLUTATHIONE PEROXIDASE (Gpx)	38
1.9.5	NON-ENZYMATIC DEFENCES	39
1.9.6	CHEMICAL REACTIONS OF ROS	39
1.9.7	DNA DAMAGE	40
1.9.7.1	BASE MODIFICATIONS	40
1.9.7.2	SUGAR DAMAGE	42
1.10	MECHANISMS OF GLUCOSE DAMAGE	42
1.10.1	GLUCOSE TRANSPORT	42
1.10.2	MECHANISMS OF GLUCOSE TOXICITY	44
1.10.2.1	INCREASED GLUCOSE METABOLISM	44
1.10.2.2	POLYOL PATHWAY	46
1.10.2.3	PROSTANOID SYNTHESIS	47
1.10.2.4	NON-ENZYMATIC GLYCATION	48
1.11	DIABETES AND OXIDATIVE STRESS	49
1.12	DNA REPAIR	52
1.12.1	EXCISION REPAIR	53
1.12.2	DOUBLE-STRAND BREAK REPAIR	56
1.12.3	MITOCHONDRIAL DNA REPAIR	56
	HYPOTHESIS	57
	AIMS AND OBJECTIVES	57

<u>Chapter 2 : MATERIALS AND METHODS</u>	58
2.1 MATERIALS	58
2.2 METHODS	58
2.2.1 COMET ASSAY TECHNIQUE	58
2.2.2 HUMAN UMBILICAL VEIN CELL CULTURE	62
2.2.3 β -GALACTOSIDASE STAINING	63
2.2.4 SOUTHERN ANALYSIS PROCEDURE	63
2.2.5 DNA REPAIR NUCLEOTIDE INCISION ASSAY	65
2.2.6 WESTERN BLOT ANALYSIS	69
2.2.7 MITOCHONDRIAL STUDIES	70
2.2.7.1 CELL CULTURE	70
2.2.7.2 COMET ASSAY	71
2.2.7.3 DNA STUDIES	72
2.2.7.4 PROTEIN STUDIES	75
2.2.8 STATISTICS	78
<u>CHAPTER 3 : GLUCOSE-INDUCED HUVEC DNA DAMAGE</u>	79
3.1 INTRODUCTION	79
3.2 AIM	80
3.3 METHODS	80
3.4 RESULTS	82
3.4.1 SHORT-TERM TIME COURSE OF GLUCOSE-INDUCED HUVEC DNA DAMAGE	82
3.4.2 LONGER-TERM GLUCOSE-MEDIATED HUVEC DNA DAMAGE TIME COURSE	84
3.4.3 EFFECT OF GLUCOSE CONCENTRATION ON HUVEC DNA DAMAGE	87
3.4.4 POSSIBLE MECHANISM FOR HIGH GLUCOSE-INFLICTED HUVEC DNA DAMAGE: OSMOSIS	90
3.4.5 EFFECT OF <i>N</i> -ACETYLCYSTEINE INCUBATION ON GLUCOSE-INDUCED HUVEC DNA INJURY	93
3.4.6 FPG COMET ANALYSIS OF HIGH GLUCOSE ASSOCIATED HUVEC DNA INJURY	96
3.5 DISCUSSION	98

3.6	CONCLUSIONS	101
3.7	FUTURE WORK	102
<u>CHAPTER 4 : GLUCOSE-INDUCED HUVEC SENESENCE</u>		103
4.1	INTRODUCTION	103
4.2	AIM	104
4.3	METHODS	104
4.4	RESULTS	105
4.4.1	HUVEC PROLIFERATION	105
4.4.2	HUVEC DNA DAMAGE DURING PROLONGED HIGH GLUCOSE EXPOSURE	109
4.4.3	β -GALACTOSIDASE ACTIVITY	114
4.5	DISCUSSION	117
4.6	CONCLUSIONS	120
4.7	FUTURE WORK	120
<u>CHAPTER 5 : HUVEC TELOMERE ATTRITION</u>		122
5.1	INTRODUCTION	122
5.2	AIM	123
5.3	METHODS	123
5.4	RESULTS	124
5.4.1	GLUCOSE-INDUCED TELOMERE ATTRITION	124
5.4.2	TELOMERE REDUCTION WITH N-ACETYLCYSTEINE	130
5.5	DISCUSSION	132
5.6	CONCLUSIONS	136
5.7	FUTURE WORK	136
<u>Chapter 6 : HUVEC DNA REPAIR</u>		137
6.1	INTRODUCTION	137
6.2	AIM	138
6.3	METHODS	139
6.4	RESULTS	140
6.4.1	COMPARISON OF 8-oxo-dG INCISION IN HeLa, HUVECs AND HUASMCs	140

6.4.2	EFFECT OF HIGH GLUCOSE ON 8-oxo-dG EXCISION IN HUVECs	144
6.4.3	Ref-1 EXPRESSION IN HeLa, HUVECs AND HUASMCs	147
6.4.4	Ref-1 EXPRESSION IN HIGH GLUCOSE-TREATED HUVECs	150
6.5	DISCUSSION	153
6.6	CONCLUSIONS	155
6.7	FUTURE WORK	155
<u>Chapter 7 : HUVEC MITOCHONDRIAL DNA CONTENT</u>		156
7.1	INTRODUCTION	156
7.2	AIM	157
7.3	METHODS	157
7.4	RESULTS	158
7.5	DISCUSSION	161
7.6	CONCLUSIONS	162
7.7	FUTURE WORK	162
<u>Chapter 8 : HUVEC MITOCHONDRIAL COMPLEX IV EXPRESSION</u>		164
8.1	INTRODUCTION	164
8.2	AIM	165
8.3	METHODS	165
8.4	RESULTS	166
8.5	DISCUSSION	170
8.6	CONCLUSIONS	171
8.7	FUTURE WORK	171
<u>Chapter 9 : SUMMARY AND FINAL CONCLUSIONS</u>		172
9.1	LIMITATIONS OF THE STUDY AND FUTURE DIRECTIONS	176
REFERENCES		178

GLUCOSE AND HUMAN VASCULAR ENDOTHELIAL CELL AGEING

Raman Verma

Diabetes mellitus is associated with premature atherosclerosis and accelerated endothelial cell ageing. Elevated glucose concentrations, through oxidative stress, have been implicated in endothelial dysfunction and ageing but the mechanisms have remained undefined. Additionally, there is evidence that telomeric DNA, an index of cell age, is especially susceptible to oxidation. Thus, this study examined whether raised extracellular glucose concentrations (through increased oxidative stress) could induce DNA damage and hasten human vascular endothelial cell (HUVEC) senescence.

HUVEC DNA damage was measured using the comet assay. Senescence was detected by β -Galactosidase staining at pH 6. Telomere lengths and mitochondrial genome copy numbers were obtained through Southern analysis. 8-oxoguanine excision was assessed by a nucleotide incision assay. Western blotting demonstrated Ref-1 and electron transport chain complex IV (subunit I) expression.

DNA damage peaked after four hours of high glucose (HG; 22mM) exposure. This was D-glucose specific and concentration dependent. DNA damage was attenuated by *N*-acetylcysteine ($p < 0.01$) and augmented by formamidopyrimidine DNA glycosylase ($p < 0.05$), indicating that HG induced oxidative lesions. DNA damage was associated with premature HUVEC senescence ($p = 0.011$) and accelerated telomere shortening ($p = 0.03$). *N*-acetylcysteine did not prevent telomere attrition. 8-oxoguanine incision and Ref-1 expression decreased during 24-hour HG treatment, suggesting that HG could disrupt the efficiency of oxidative DNA lesion repair. No difference in mitochondrial DNA content in HG exposed HUVECs was found. However, complex IV (subunit I) expression fell in HG conditioned HUVECs ($p = 0.006$), implying that HG could affect mitochondrial activity.

This study demonstrates for the first time that elevated glucose concentrations promote oxidative DNA damage in human vascular cells. This leads to accelerated telomere attrition, prompts premature human endothelial cell senescence and may profoundly disturb mitochondrial function. These observations provide a novel mechanism to implicate glucose in accelerated vascular ageing in diabetes.

ACKNOWLEDGEMENTS

I would like to take this opportunity to thank a number of people. Firstly, I would like to express my gratitude to Professor Bryan Williams, Dr Richard Hastings, Carol Orme and Dr Karl Herbert who were all instrumental in the development of the work in my thesis. Additionally, I am grateful to the whole Cardiovascular Sciences Department (including Dr Harprit Singh, Hash Patel, Janet Harris, Anne Taylor, Professor Herbert Thurston, Dr Adrian Stanley, Dr Philip Swales, Dr David Lodwick, Dr Robert Norman and Mairead Dewar) for making me feel welcome and part of the group. I truly could not have wished to join a better team. Further, I would like to thank the Leicester and Warwick Medical School for allowing me to take two years away from my medical studies and for arranging my seamless return.

I am indebted to my parents. They have been with me at every step of the way and are the wind beneath my wings. Also, a special thanks to my friends for all their encouragement, wise words and love.

The two-year period leading to the completion of the PhD phase of the MB PhD ChB programme has indeed been very challenging. But, it has been a fun packed adventure, full of thrills and spills. Overall, it has been a blast!!

ABBREVIATIONS

(h)OGG	(human) 8-oxoG-DNA glycosylase
8-oxo-dG	8-hydroxy-2-deoxyguanosine
A	adenine
ADP	adenosine diphosphate
AGE	advanced glycated end-product
AP site	apurinic or apyrimidinic site
APE	AP endonuclease
ATP	adenosine triphosphate
BAEC(s)	bovine aortic endothelial cell(s)
BER	base excision repair
bp	base pairs
bp/PD	base pairs per population doubling
C	cytosine
DNA	deoxyribonucleic acid
DSB(s)	double-strand break(s)
dsDNA	double-stranded DNA
EDCF	endothelium-derived constricting factor
EDHF	endothelium-derived hyperpolarizing factor
EDRF	endothelium-derived relaxing factor
ETC	electron transport chain
FPG	formamidopyrimidine DNA glycosylase
G	guanine
Gpx	glutathione peroxidase
GSH	reduced glutathione
GSSG	oxidised glutathione
H₂O₂	hydrogen peroxide
HG	high glucose (22mM)
HOCl	hypochlorous acid
HUASMC(s)	human umbilical aortic smooth muscle cell(s)
HUVEC(s)	human umbilical vein endothelial cell(s)
i.e.	id est
IDDM	insulin-dependent diabetes mellitus
Ig	immunoglobulin
LDL	low-density lipoprotein
mRNA	messenger RNA
mt-DNA	mitochondrial DNA
NAC	<i>N</i> -acetylcysteine
NER	nucleotide excision repair
NF-κB	nuclear factor kappa B
NG	normal glucose (5.5mM)
NIDDM	non-insulin-dependent diabetes mellitus
NO	nitric oxide
NOS	nitric oxide synthase
O₂^{•-}	superoxide radical
OH[•]	hydroxyl radical
ONOO⁻	peroxynitrite

P	passage number
PAI-1	plasminogen activator inhibitor-1
PARP	poly(ADP-ribose)polymerase
PCNA	proliferating cell nuclear antigen
PD	population doubling
PKC	protein kinase C
RAGE	receptor for AGE
Ref-1	repair endonuclease fraction-1
RNA	ribonucleic acid
ROS	reactive oxygen species
RPA	replication protein A
SAMP	accelerated senescence-prone, short-lived
SAMR	accelerated senescence-resistant, long-lived
SA-β-Gal	senescence associated- β -galactosidase
SCGE	single cell gel electrophoresis
SMC(s)	smooth muscle cell(s)
SOD	superoxide dismutase
T	thymine
TGF-β	transforming growth factor- β
TRF	telomere repeat-binding factor
UV	ultraviolet
v/v	volume by volume
VSMC(s)	vascular smooth muscle cells(s)
w/v	weight by volume

Chapter 1 : INTRODUCTION

The central theme of this thesis is that various cardiovascular risk factors act through a final common pathway which involves the induction of intracellular oxidative stress and subsequently, DNA oxidation. One such factor, diabetes mellitus, has long been associated with premature cardiovascular disease.¹ Additionally, research has demonstrated that functionally, the diabetic vasculature behaves as though it were older than the patient's chronological age.² This suggested a process of accelerated "vascular ageing" and numerous influences have been implicated in this phenomenon. Of special interest, are those focusing on the disturbed diabetic metabolic milieu caused by the elevated extracellular glucose concentration. Furthermore, there was evidence that telomeric DNA, an index of cell age, was especially susceptible to oxidation.³ Moreover, it was well accepted that telomeres shortened with replication and that this process could be hastened by oxidative stress.³ This quickened rate of telomere attrition could then, in turn, lead to premature cell senescence and thus, ageing.

This thesis examined for the first time, the impact of elevated glucose levels upon the molecular ageing, DNA homeostasis and mitochondrial function of endothelial cells. This thesis begins with an insight into diabetes, endothelial physiology and atherosclerosis. Detailed discussions of telomeres, cell senescence, ageing and their interrelationships then follow. In addition, there are summaries on free radical biology, mitochondrial activity, DNA damage and its repair. Finally, the experimental methods are described and the results presented before the conclusions are drawn and the future considered.

1.1 DIABETES

Diabetes mellitus is a major worldwide disorder that is defined by elevated blood glucose (hyperglycaemia) concentrations.⁴⁻⁸ It is a chronic disease caused by the impaired production of, or tissue response to, insulin.¹ Epidemiological studies have suggested that its prevalence will rise from 6% to over 10% in the next decade, with 220 million diabetic patients world-wide in the year 2010 and 300 million in 2025.⁸⁻¹¹ The major contributor to this increase will be type 2 diabetes (non-insulin-dependent diabetes mellitus; NIDDM) which is characterised by insulin resistance and/or abnormal insulin secretion, either of which may predominate.¹⁰⁻¹⁴ In type I (juvenile onset; insulin-dependent), insulin secretion is absent or impaired due primarily to autoimmune-mediated destruction of pancreatic β -cell islets.^{1, 10, 11, 14}

The complications of diabetes include systemic vascular disease (accelerated atherosclerosis), microvascular eye disease causing bleeding and retinal degeneration (diabetic retinopathy), cataracts, kidney damage leading to renal failure and damage to the peripheral nerves (peripheral neuropathy).^{12, 15} The retina, kidney, blood vessels and nerves are all freely permeable to glucose and hence, suffer the most.^{4, 15} Adults with diabetes have an annual mortality rate of 5.4% (twice the level of age-matched adults without diabetes) and their life expectancy is decreased, on average, by 5-10 years.¹⁶ Further, diabetes is one of the main risk factors for coronary heart disease and the relative danger of heart attack is approximately three times higher in diabetics.¹⁷⁻¹⁹ Cardiovascular disease accounts for 75% of all deaths in patients with type 2 diabetes and in a recent study, fatal cardiovascular events were 70 times more common than deaths due to microvascular complications.^{16, 18, 20-22}

1.2 ENDOTHELIAL CELL PHYSIOLOGY

The endothelium is a large, highly specialised, versatile, multifactorial and metabolically active organ.¹⁹ In man, it consists of about $1-6 \times 10^{13}$ cells with a total surface area of 100m^2 and weighs approximately 1kg.^{1, 23-25} It is composed of a confluent monolayer of thin, flattened, polygonal or elongated cells that line the entire luminal surface of the heart and blood vessels.^{2, 26-28} A typical endothelial cell is 25-50 μm long, 10-15 μm wide and contains the organelles common to all eukaryotic cells, in addition to a unique set of intracellular storage vesicles, the Weibel-Palade bodies.^{29, 30} These enclose a variety of proteins, like the von Willebrand factor and P-selectin.¹

Endothelial cells play an indispensable role in all aspects of cardiovascular physiology and homeostasis.^{1, 27, 28, 31, 32} For example, they act as a permeability barrier between flowing blood and the vascular wall. Secondly, they regulate vasomotor tone, which in turn, determines the blood flow and pressure. In addition, they regulate vascular smooth muscle cell (VSMC) growth, modulate immunosuppression and have pro- and anti-thrombotic activities. Furthermore, endothelial cells must integrate contrasting extracellular signals and cellular responses in different regions of the vascular tree.

It has been increasingly advocated that endothelial cells are heterogenous and that their function and phenotype are specialised to match their particular location.^{19, 23} Normally, the endothelium behaves in an inhibitory mode – preventing VSMC contraction and growth, platelet aggregation, thrombosis and white cell adhesion.^{1, 33} In order to control the vascular tone, the endothelium produces and releases a number of vasoactive substances, including:

- endothelium-derived relaxing factors (EDRFs) → nitric oxide (NO), prostacyclin and endothelium-derived hyperpolarizing factor (EDHF), and

- endothelium-derived constricting factors (EDCFs) → cyclooxygenase-derived factors (thromboxane A₂ and prostaglandin H₂), endothelin, reactive oxygen species (ROS) and angiotensin II.^{1, 24, 26, 31, 33-35}

1.3 ATHEROSCLEROSIS

1.3.1 THE NATURE OF ATHEROSCLEROSIS

Cardiovascular disease is the chief cause of death in the United States and Europe.^{1, 7, 12} Most heart attacks and strokes are secondary to the condition of atherosclerosis, an arterial disease characterised by the development of a thickening in the inner layer of the vessel wall.^{36, 37} It is a multi-factorial process that is probably initiated in childhood but only becomes clinically apparent in later life.^{1, 38}

1.3.2 ATHEROSCLEROSIS INITIATION

The origin of atherosclerosis is still uncertain, however, a popular current theory is that it begins with damage to the vascular endothelium (“response to injury hypothesis”).^{37, 39-41} The damaging events could include mechanical damage, viral infection, exposure to blood-borne toxins and elevated levels of normal metabolites, such as glucose or homocysteine (amino acid).^{28, 36, 42, 43} The endothelial injury is then followed by the attachment of monocytes, which in turn, enter the vessel wall and develop into macrophages.¹ These cells, together with smooth muscle cells (SMCs) are believed to be involved in the overall atherosclerotic process, possibly mediated via an oxidative pathway.^{38,}

44-50

1.4 ENDOTHELIAL DYSFUNCTION

Most arterial diseases, including atherosclerosis, are typified by a deterioration of the endothelium-derived vasodilator functions.^{2, 31, 35, 51, 52} This endothelial “dysfunction” could be attributed to decreased vasodilator secretion; increased vasoconstrictor production, sensitivity, or inactivation; vasodilator resistance; or impaired vasodilator diffusion to the underlying VSMCs.^{2, 19, 31, 33, 53}

It is evident that endothelial malfunction also contributes to the maintenance and progression of ageing and diabetes.^{31, 33, 54} However, there is little, if any, clear proof that altered endothelial function is a primary factor in their pathogenesis.⁵⁵

1.4.1 ENDOTHELIAL DYSFUNCTION AND AGEING

Declining vascular compliance has been proven to develop with age and is probably related to reductions in elastin, collagen degeneration and increased arterial wall thickness.^{1, 19, 49, 54} Studies have also suggested that advancing age is associated with progressive endothelial dysfunction, which in turn, may partially explain the increased cardiovascular risk in the elderly.^{1, 19, 33, 52} For example, endothelin-1-induced endothelium-dependent release of NO and EDHF is absent in old rats; thus, leaving the potent vasoconstrictor unchecked.^{26, 31} Similarly, in otherwise healthy individuals, age was linked to impaired endothelium-dependent vasodilatation to acetylcholine in the forearm circulation and in epicardial coronary arteries.^{1, 33} Additionally, it is thought that the superoxide radical ($O_2^{\bullet-}$) steady state concentration in older vasculature may shorten the half-life of released NO and therefore, promote endothelial malfunction.^{26, 31, 37, 54} Furthermore, such radicals are known to be involved in EDRF breakdown.^{31, 54} Hence, at present, the mechanisms of age-related endothelial dysfunction and the extent to which they contribute to ageing are unclear.

1.4.2 ENDOTHELIAL DYSFUNCTION AND DIABETES

In diabetes, the endothelium produces high levels of vasoconstrictors and pro-coagulants but fewer vasodilators.^{2, 26, 27, 51, 53, 56} Thus, the diabetic vasculature displays a phenotype similar to that noted in the aged endothelium. Additionally, *in vitro*, endothelial cells exposed to high glucose increase their synthesis of extracellular matrix components (like collagen and fibronectin) and show decreased proliferation, migration and fibrinolytic potential as well as increased apoptosis.^{17, 27, 31, 53, 57, 58}

The mechanisms underlying this endothelial dysfunction are unclear.^{58, 59} However, the high glucose concentrations that constantly bathe the endothelium of diabetic patients have the capacity to disturb endothelial function profoundly.^{19, 26, 29, 56} For example, recent studies have shown that a number of free radical scavengers reverse the declining endothelium-dependent relaxations caused by elevated glucose.^{26, 31, 53} The various hyperglycaemic-related hypotheses include; increased polyol pathway flux, activation of protein kinase C (PKC), advanced glycated end-product (AGE) accumulation and heightened oxidative stress.^{2, 22, 26, 27, 31, 34, 59-62} There are several areas of overlap between these principal mediators of glucose-induced endothelial damage.^{53, 63} Therefore, it is predicted that they may interact through a final common pathway involving the induction of oxidative stress.

1.4.3 ENDOTHELIAL DYSFUNCTION AND OXIDATIVE STRESS

Oxidative damage may be important in the early stages of atherosclerosis, through endothelial injury or dysfunction.^{2, 25, 26, 29, 47, 64-72} The balance between oxidant generation and the effectiveness and spatial availability of antioxidants determines the net oxidative status of the vessel wall. The relative contributions of each cell type have yet to be defined, however, endothelial cells are very sensitive to oxidative stress and are both critical targets and sources of ROS.^{25, 31, 73-80} For example, they possess NADH/NADPH oxidase, the mitochondrial respiratory chain, xanthine oxidoreductase and purine nucleotide phosphorylase.^{58, 72, 79, 81-84} Microsomal enzymes, such as lipoxygenases and cyclooxygenases, generate peroxides and oxygen radicals that may also be involved in the initial promotion of oxidative damage within endothelial cells.^{33, 53, 84} The glutathione redox cycle is the major route for hydrogen peroxide (H₂O₂) scavenging in endothelial cells hence, it is likely to underlie the fate of these cells.^{12, 21, 26, 76, 77} Additionally, endothelial cells have the capacity to form transforming growth factor-β (TGF-β) which can cause the reduction of glutathione levels and increased H₂O₂ release in these cells.^{27, 85}

In diabetic animals, endothelial cells are described to undergo morphological and functional alterations, and intercellular junction weakening.⁸⁶ *In vitro*, high ambient glucose has been demonstrated to affect endothelial and other vascular cells at the cellular level through oxidative stress.^{21, 65, 66, 68, 69, 75, 81, 87-89} For example, Ho *et al.* (2000) discovered that high glucose treatment of Human Umbilical Vein Endothelial Cells (HUVECs) increased 2', 7'-dichlorofluorescein diacetate fluorescence (indicator of intracellular oxidant production) in a time- and dose-dependent manner, while ascorbic acid (antioxidant) completely suppressed this rise in fluorescence.^{67, 86, 90} Meanwhile, Graier *et al.* (1996) showed that high glucose could stimulate superoxide (O₂^{•-}) generation and enhance cell-mediated low-density lipoprotein (LDL) peroxidation in endothelial cells.^{56, 72}

1.5 OXIDATIVE STRESS AND AGEING

Numerous influences have been implicated in the process of accelerated ageing. Of special interest, in this thesis, are those focusing on the disturbed diabetic metabolic environment caused by the elevated extracellular glucose concentration. Excessive glucose is known to cause the enhancement of oxidative stress levels and data has emerged that the latter may play an important role in the aetiology of diabetic complications. In addition, there is evidence that telomeric DNA (capping chromosomal ends), acts as an index of cell age and is especially susceptible to oxidation. Moreover, it is well accepted that these regions shorten with replication and that the process could be hastened by increased oxidative stress. This quickened rate of telomere attrition could then, in turn, lead to early endothelial cell senescence and thus, ageing to result ultimately in premature cardiovascular disease.

1.5.1 THE FREE RADICAL THEORY OF AGEING

Studies into oxidative damage have paved the way to a popular current theory regarding the mechanism of ageing: “the free radical theory of ageing”. It holds that natural ageing results from random deleterious tissue damage caused by free radicals produced during normal aerobic metabolism.¹² This proposition was based on experimental observations in which radiation exposure to laboratory animals appeared to age the animals very rapidly and cause an increase in free radical levels.⁹¹ Furthermore, it was recently found that free radical inhibitors prolonged the lifespan of the nematode *Caenorhabditis elegans*, and the fruit fly *Drosophila melanogaster*, while the selective knockout of ROS signalling pathways protracted the lives of mice.^{12, 38, 92-103} Additionally, an increasing number of age-related and degenerative diseases have been found to have an aetiological component associated with ROS generation.^{49, 98, 100, 101, 104-107}

Oxygen free radicals are thought to be ubiquitous and *in vitro* studies have demonstrated that about 2-4% of the oxygen consumed is converted into $O_2^{\bullet-}$.^{91, 92, 108-110} It has also been calculated that a typical human cell metabolises approximately 10^{12} oxygen molecules daily, and therefore, generates about 3×10^9 H_2O_2 molecules per hour.^{12, 111} The targets of such radicals are proteins, lipids and DNA with the resultant oxidative damage to the latter producing large numbers of poorly characterised DNA adducts, abasic sites, and single- and double-stranded breaks.^{112, 113} Such DNA breakages are particularly important within the telomere because their structures are thought to be the preferential targets for the free radicals. Research has demonstrated that the G-triplet sequence in the telomere ($5' \text{TTAGGG} 3'$) is especially sensitive to oxidative insult.^{3, 114-116} Further, deficiencies in the telomeric repair of oxidatively generated single-strand breaks have been described.^{3, 117, 118}

Within each cell, the mitochondria use approximately 90% of the cell's oxygen, making them the greatest free radical source. Hence, the mitochondria become the targets of their own ROS yields and consequently, their levels of steady-state oxidative damage are relatively higher when compared to other organelles. In fact, research has demonstrated that the injury to mitochondrial DNA is particularly striking. For instance, the levels of mitochondrial 8-hydroxy-2-deoxyguanosine (8-oxo-dG; indicator of oxidative DNA damage) are noted to be higher and to persist for longer than those found in nuclear DNA even though there are DNA-protective mechanisms in both these organelles.¹¹⁹⁻¹²¹

1.5.2 THE MITOCHONDRIAL THEORY OF AGEING

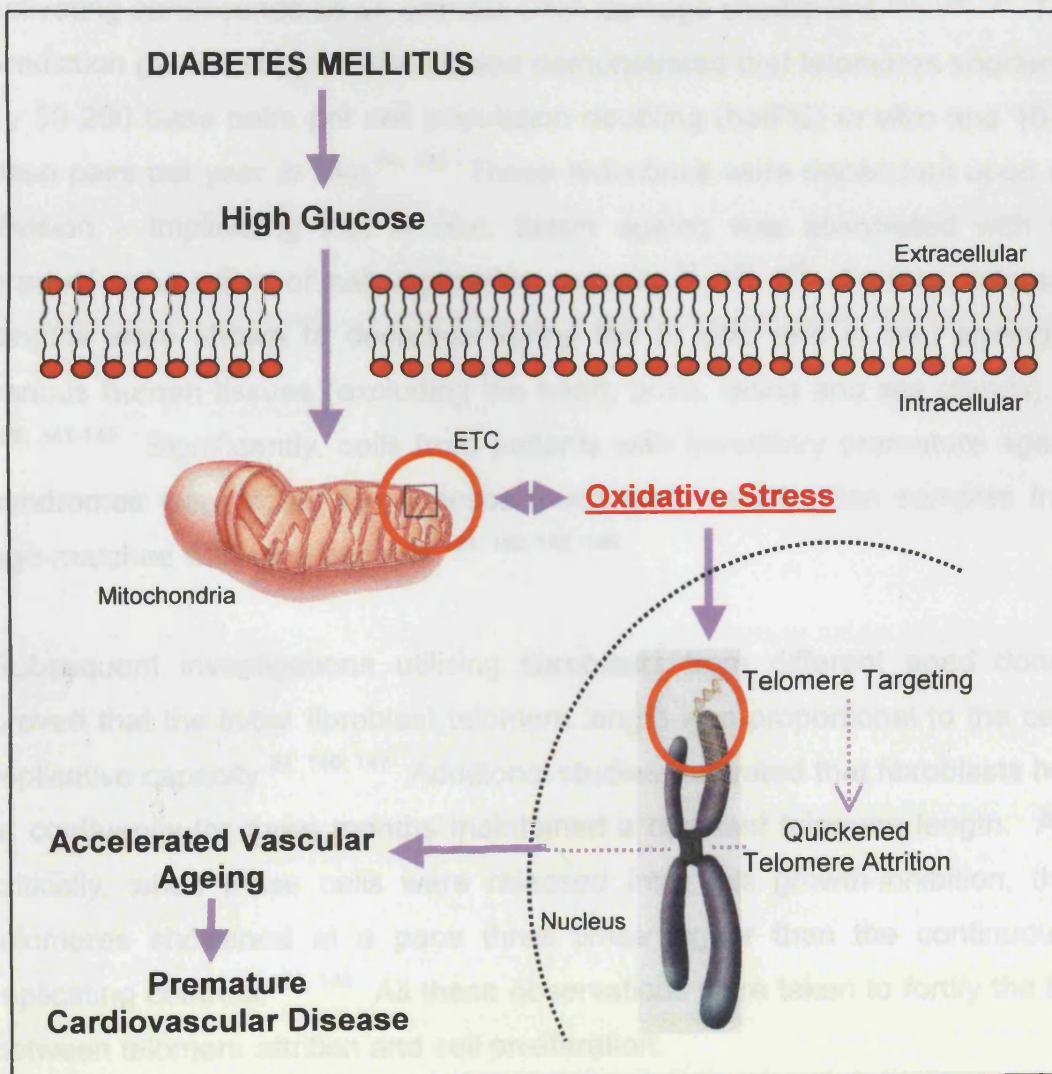
As mitochondria produce the most cellular energy and consume the majority of intracellular oxygen, the free radical theory of ageing is now often synonymously thought of with the “rate of living” hypothesis.^{77, 95, 98, 122, 123} This speculates that higher organismal metabolic rates result in greater ROS production, and therefore, shorter lifespans.^{77, 95, 98, 102} This proposal has been strengthened by the observation that caloric restriction, a regimen known to increase animal mean lifespan, maintains mitochondrial function and lowers oxidant production. For example, the mitochondrial rate of ROS formation from calorically limited mice was significantly reduced when compared to their *ad libitum*-fed counterparts.^{95, 105, 124, 125} Additionally, their age-associated accumulations of oxidatively damaged proteins, lipids and DNA were all attenuated.^{95, 105, 124, 125} Similarly, the lifespan of the housefly is lengthened by more than twofold by the removal of their wings.⁹⁸ Furthermore, their oxidant generation rates and subsequent levels of oxidatively modified products were all diminished.⁹⁸

Mitochondrial decay is now considered to be an important factor in ageing caused, in part, by ROS released from the “electron transport chain”.^{94, 96, 124, 126} Mitochondria are the targets of their own deleterious oxidant yields and consequently, their steady-state oxidative damage is relatively higher when compared to other organelles.^{100, 125, 127-129} Further, the percentage of oxygen converted into $O_2^{\bullet-}$ increases with age.^{130, 131} This, in turn, leads to a spiralling cycle of elevated injury to the mitochondrial, cytosolic and nuclear compartments, which would then adversely affect cell function and ultimately result in a loss of ATP-generating capacity. This could become especially important in times of great energy demand (DNA repair, for instance) as vital ATP-dependent reactions would be compromised.¹³²

1.5.3 DIABETES AND AGEING

All in all, we have considered diabetes to be a state of accelerated vascular ageing. Therefore, this thesis examines whether this ageing is due to glucose-driven oxidative damage to telomeric and mitochondrial DNA, culminating in premature endothelial cell senescence (figure 1-1).

Figure 1-1: The potential mechanism for accelerated vascular ageing in diabetes mellitus. ETC, electron transport chain of mitochondria.



1.6 TELOMERE BIOLOGY

“Replicative senescence” describes the mortality of human somatic cells, that is, the exhaustion of their division potential after a number of population doublings.^{133, 134} The number of divisions that normal cells complete before they senesce depends on the species, age and genetic background of the donor, as well as the particular cell type.^{133, 135} The discovery that the ends of chromosomes (telomeres) shorten with each cell division in human somatic cells, but not in immortal tumour cells, led to the suggestion that telomeres might act as “mitotic clocks”, counting the number of cell divisions and activating senescence as an ultimate DNA damage checkpoint.^{133, 136, 137} This prediction gained support when it was demonstrated that telomeres shortened by 30-200 base pairs per cell population doubling (bp/PD) *in vitro* and 10-50 base pairs per year *in vivo*.^{94, 138} These reductions were dependent upon cell division – implicating that *in vivo*, tissue ageing was associated with the gradual exhaustion of cell replicative capacity.^{12, 139, 140} Further, telomere lengths were shown to decrease during the *in vitro* and *in vivo* ageing of various human tissues (excluding the heart, brain, retina and sex glands).^{133-138, 141-145} Significantly, cells from patients with hereditary premature ageing syndromes were noted to senesce much more rapidly than samples from age-matched wild-type controls.^{121, 140, 145, 146}

Subsequent investigations utilising fibroblasts from different aged donors proved that the initial fibroblast telomere length was proportional to the cell’s replicative capacity.^{94, 140, 147} Additional studies illustrated that fibroblasts held at confluency for three months maintained a constant telomere length. And critically, when these cells were released from this growth-inhibition, their telomeres shortened at a pace three times higher than the continuously replicating controls.^{140, 148} All these observations were taken to fortify the link between telomere attrition and cell proliferation.

Importantly, research into the ectopic expression of telomerase (the enzyme which lengthens telomeres in some cells) lead to telomere elongation followed

by the immortalisation of some human cells.^{121, 140, 149} Moreover, the specific and successful inhibition of telomerase in tumour cells resulted in telomere shortening and growth arrest with the occurrence of a senescent phenotype.^{121, 150}

1.6.1 THE STRUCTURE OF HUMAN TELOMERES

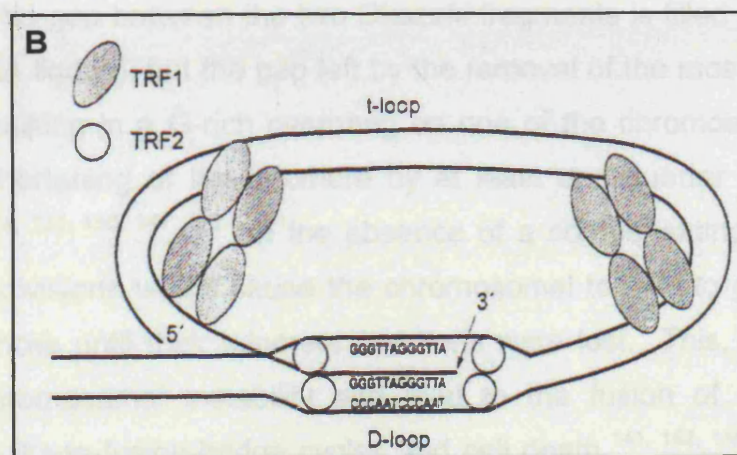
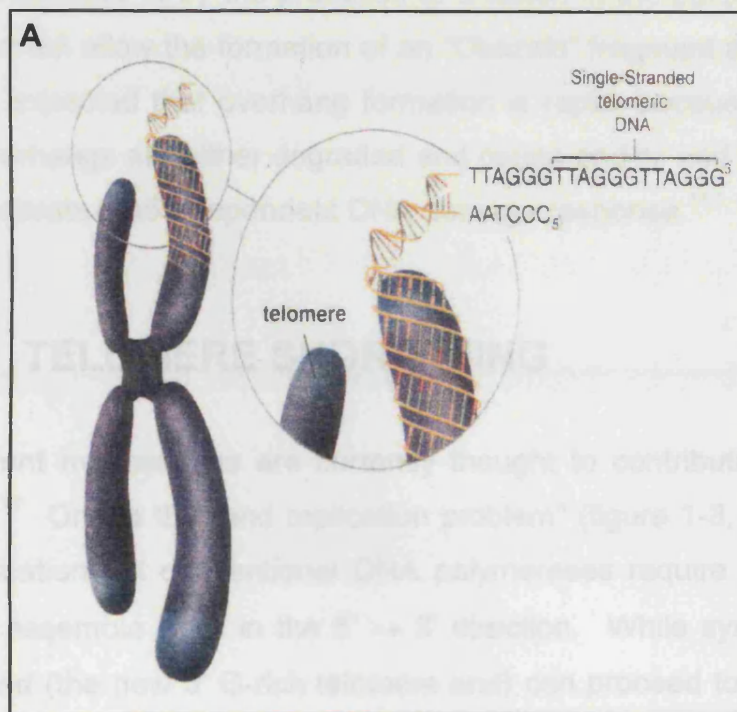
Human telomeres do not contain protein-encoding genes instead, they consist of $5'$ TTAGGG $3'$ repeats whose functions, though not fully understood, involve the stabilisation of chromosomal ends, the protection of genes in the sub-telomeric regions, the attachment of chromosomes to the nuclear matrix and chromosomal separation during mitosis.^{134, 135, 149, 151-156}

Telomere lengths are highly heterogeneous, even within a cell.^{133, 134} Generally, the longest telomeres are found in the germ-line (between 15-20 kilobases in length), whereas in senescent fibroblast cultures, telomere length was 5-6 kilobases.^{141, 149} They consist of a single-stranded overhang of approximately 100-280 nucleotides at the $3'$ -end (the G-rich strand), closely spaced nucleosomes and a number of telomere-specific proteins (figure 1-2, page 14).^{135, 140, 151, 157-160} The best characterised of these are the human telomeric repeat-binding factors (TRF) 1 and 2.^{137, 161-163} TRF 1 has been shown to bind to duplex TTAGGG and negatively regulate telomerase activity, while TRF 2 appears to maintain the $3'$ -overhang and influence the conformation of the G-rich strand.¹⁶¹⁻¹⁶⁷

Classically, telomeres had been regarded as linear structures.¹¹⁷ However, it was recently shown by electron microscopy, that telomeres formed "lasso-like" loops when combined with TRF 2 (figure 1-2 (B), page 14).^{162, 163, 168, 169} The single-stranded $5'$ TTAGGG $3'$ overhangs were revealed to fold back and invade the upstream telomeric DNA duplex to form a "Displacement loop" ("D"-loop) with the complementary $3'$ AATCCC $5'$ sequences.^{117, 153, 162} The overhang also encroached upon a partial unwinding at the base of the telomeric double-stranded DNA forming a "telomere loop" ("t"-loop).^{153, 163, 168} It appears that

these t-loops exist at the ends of most, if not all, human telomeres as they probably act to protect single-stranded chromosomal ends.^{153, 162, 164} Their sizes are highly variable, but tend to increase with telomere length.^{163, 169}

Figure 1-2: A) Chromosome with telomeric DNA cap. B) Formation of telomere loops. The single-stranded 3'-overhang at the very ends of telomeres invades upstream double-stranded telomeric sequences and hybridises to complementary sequences, thereby forming a displacement loop (D-loop). TRF 2 is thought to stabilise this structure. Telomeric DNA loops out and might be stabilised by TRF 1 proteins. TRF, telomeric repeat-binding factor; t-loop, telomere loop. (Adapted from reference 153)



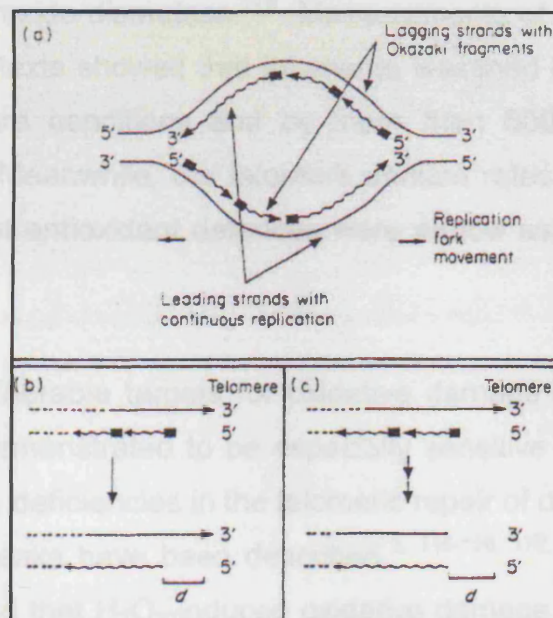
T-loops must be very dynamic structures as they have to be opened during DNA replication for the passage of the DNA polymerase machinery.^{162, 163} *In vitro*, TRF 2 is sufficient to catalyse the formation of t-loops, indicating that it could both partially unwind a region of duplex DNA (D-loop formation) and promote the overhang invasion.^{162, 168, 170} Additionally, TRF 1 may be involved in aiding the telomere coiling.^{162, 163, 165} During or after the completion of telomere DNA replication, new overhangs have to be generated before the t-loops can be reformed.^{117, 162} This could happen either by the elongation of the G-rich strand by telomerase, limited degradation of the C-rich strand by a specific exonuclease or by the presence of a lesion in the parental overhang (which would not allow the formation of an “Okazaki” fragment at this site).^{135, 158, 165} It is expected that overhang formation is rapid, because free single-stranded overhangs are either degraded and cause end-to-end chromosomal fusions or activate a p53-dependent DNA damage response.^{117, 163}

1.6.2 TELOMERE SHORTENING

Three different mechanisms are currently thought to contribute to telomere shortening.¹¹⁷ One is the “end replication problem” (figure 1-3, page 16). In normal replication, all conventional DNA polymerases require a primer and template to assemble DNA in the 5' → 3' direction. While synthesis of the leading strand (the new 3' G-rich telomere end) can proceed to the very end of the template, production of the lagging strand occurs via a multitude of Okazaki fragments primed by short RNAs (about 8-12 nucleotides long).^{135, 153, 171, 172} The gap between the two Okazaki fragments is filled in and ligated later (by DNA ligase), but the gap left by the removal of the most distal primer remains, resulting in a G-rich overhang on one of the chromosome ends as well as a shortening of the telomere by at least one quarter of the primer length.^{117, 118, 135, 136, 141, 172} In the absence of a compensating mechanism, successive divisions would cause the chromosomal termini to gradually lose their sequences until their telomere functions were lost. This, in turn, could result in chromosomal instability and lead to the fusion of non-telomeric regions, breakage-fusion-bridge cycles and cell death.^{141, 152, 158} Historically,

the end replication problem was regarded as the exclusive cause of telomere shortening.^{117, 173} However, in reality, the end replication problem, whilst important, would be inadequate to explain the observed telomere shortening rates in human cells. In fact, it could only account for the loss of less than 10 bp/PD.^{94, 118, 141, 152, 159, 169}

Figure 1-3: The end replication problem. (a) Schematic of the DNA replication fork at an origin of replication. The RNA primer (filled block) and newly replicated DNA (wavy lines) are shown. (b) and (c) Schematic of possible events on the lagging strand at either telomere. (b) After the removal of the RNA primer that initiates the terminal Okazaki fragment, a single strand deletion "d" remains at the 5' end of the newly replicated strand. (c) Degradation of the overhang generated by incomplete replication results in a double-stranded deletion. (Adapted from reference 173)



When it was found that most telomeres contained G-rich overhangs, the action of a C-strand specific exonuclease was suggested.^{139, 153, 158, 157} The action of this exonuclease could shorten each telomere by half the overhang length per round of replication.^{135, 158} It is currently not yet clear if overhangs of that size exist on one or both chromosomal ends as there are experimental arguments for both observations.^{117, 135, 157} Therefore, it is not clear if t-loops are the only chromosome end structures. However, it is hard to imagine that principally different structural and functional rules are valid on the two chromosomal extremities.

Neither of the previous models takes into account the possibility that telomere shortening also depends on external influences, especially oxidative DNA damage. A number of oxidative stress conditions, including treatment with H₂O₂, can induce a senescence-like cell arrest prematurely.^{114, 118, 136, 174, 175} In fact, oxidative stress can vary the telomere shortening rate in cultured human fibroblasts by more than one order of magnitude.^{3, 49, 118, 114, 174} For example, fibroblast telomeres are diminished five times faster if they are subjected to chronic hyperoxia or subtoxic concentrations of either H₂O₂ or *tert*-butyl-hydroperoxide.^{176, 177} A similar acceleration of telomere loss was also seen in fibroblasts from patients with Fanconi anaemia, a condition that results in increased oxidative stress.¹⁷⁸ Conversely, the rate of telomere loss was decreased if fibroblasts were treated with various antioxidants, like extracellular superoxide dismutase.¹⁷⁹ Measurements of telomere shortening rates in these contexts showed that telomeres lessened by about 100 bp/PD under basal culture conditions and by more than 600 bp/PD under mild hyperoxia.^{180, 181} Meanwhile, the telomere attrition rates in fibroblast strains with highly efficient antioxidant defences were as low as 15-20 bp/PD under both conditions.⁹⁴

Telomeres are vulnerable targets for oxidative damage as the telomeric G-triplet has been demonstrated to be especially sensitive to oxidative injury.^{3, 114-116} Additionally, deficiencies in the telomeric repair of oxidatively generated single-stranded breaks have been described.^{3, 115-118, 172, 182} Furthermore, it has been illustrated that H₂O₂-induced oxidative damage to DNA is sufficient to promote the instability of repetitive sequences.^{114, 115, 149, 183} Together, this data strongly indicates that telomere damage is a major mechanism in triggering replicative senescence.^{116, 118, 144} However, how this trigger functions is as yet, unknown.

The t-loop structure suggests a possible explanation for the telomere repair deficiency: the D-loops may block the access of repair complexes to the entire DNA within the t-loop.^{117, 139, 162, 163, 184} Thus, only repair coupled to replication could be functional within the t-loop. The repair efficiency of ultraviolet (UV)-induced pyrimidine dimers in telomeres has been shown to be intermediate

between that in an active and inactive gene.^{3, 182} However, Kruk *et al.* (1995) found efficient repair of such damage.^{148, 185} It is possible that the situation may be different for the repair of other types of DNA damage. For example, in an experiment which used H₂O₂ treatment to induce single-stranded breaks all over the genome, proficient repair diminished the frequency of the single-stranded breaks down to the background frequency (one per 10⁶ base pairs) within less than 24 hours in the bulk of the genome.^{3, 115, 116, 168, 186} But, a significant fraction of the telomeric single-stranded sites remained unrepaired, even after 20 days.^{117, 116, 186}

1.6.3 DNA DAMAGE AND TELOMERE ATTRITION

In mammals, studies on replication bypassing a thymidine dimer (UV lesion) showed that it was transiently stalled and that the position of the lesion determined the effect on replication.¹⁴⁴ For example, if the lesion was on the lagging strand template, both leading and lagging strand synthesis could proceed with only a temporary interruption to the lagging strand production by one Okazaki fragment (about 100-200 nucleotides).^{116, 139} If, on the other hand, the lesion was on the leading strand template, lagging strand synthesis could proceed for more than 1000 nucleotides before translesional synthesis of the leading strand would occur.¹⁶⁸ Meanwhile, the replication fork would continue and consequently, leave the leading strand template as a single-stranded, unreplicated stretch.

With respect to telomeres, single-stranded breaks could translate into accelerated telomere shortening as soon as the cells replicate their DNA. For instance, a lesion in the G-rich strand (the template for the lagging strand) should not affect telomere length in the daughter strand, except when it is within the most distal 150 nucleotides. Such a lesion, in the G-rich overhang, would prohibit the formation of the most outlying Okazaki fragment – giving one possible way to reproduce the G-rich overhang.¹³⁵ Interestingly, a telomeric lesion in the C-rich strand (the template to the leading strand) would have a much stronger effect.¹¹⁷ If leading strand synthesis could be stalled

until the replication fork reached the distal end of the telomere, the polymerase complex could fall off and translesional synthesis would not occur, thus leaving the newly synthesized 3'-end greatly recessed.¹¹⁷ Nonetheless, single-stranded C-rich telomeric DNA has never been found, hence, the resulting 5'-end protrusion must be degraded by an exonuclease which would lead to overall telomere shortening.^{135, 157}

These predictions should be true for lesions capable of transiently blocking DNA replication, such as bulky lesions and abasic sites. But, it is not yet clear whether the same applies to telomeric single-stranded breaks.

1.6.4 TELOMERE ATTRITION AND SENESENCE

Currently there is only speculation in mammalian cells, however, experiments in lower eukaryotes have proposed several theories connecting telomere attrition to senescence. One proposal is that critically short telomeres could signal a p53-dependent DNA damage checkpoint response from which cells cannot recover.^{135, 142, 187, 188} p53 has additionally been shown to be associated with the replication and repair protein "RPA" (replication protein A).^{144, 162, 168} Thus, when DNA damage occurs, RPA could bind to single-stranded DNA and release p53, which would in turn, block cell division. The p53 protein level, which should be increased in the damage response has, however, also been reported to be unchanged in some studies.^{119, 187, 189-195} Alternatively, the telomere shortening could lead to the destabilisation of telomeres from the nuclear envelope or matrix, leading to a signal for checkpoint arrest.

Another hypothesis is that telomeres could bind or sequester transcription factors or other proteins involved in the activation or repression of genes.¹⁶⁶ Thus, as the telomere length declines, these factors would become available to non-telomeric sites, where they could act to repress or activate genes that interfere with cellular function. However, currently, there is no molecular data to support this in mammalian cells. Finally, there is the telomere position

effect (TPE) supposition.^{94, 196} This postulates that the heterochromatin structure of DNA near the telomere may repress regulatory genes that could act to arrest cell growth and alter cell differentiation. As the telomere shortens, the field of heterochromatin would diminish and free these putative regulators. Alternatively, telomere shortening could alter gene expression by repositioning specific chromosomal arms within the nucleus.^{94, 166} Again, although observed in yeast, there is little data to suggest the existence of TPE in human cells.¹²¹ Moreover, as yet, no connection between TPE and senescence has been established.

The p53-dependent pathway is favoured because it is the simplest model – it does not require new routes for signalling cell cycle exit, it only necessitates that a sufficient amount of DNA is lost from a chromosome end to render the telomere functionally inactive.^{153, 197} Data has shown that telomere shortening triggers a p53-dependent DNA damage response not only in human cells, but also in mouse cells and tissues.^{116, 144, 163, 198} Additionally, late generation telomerase-knockout tissues and fibroblasts display shorter telomeres and apoptosis or cell cycle arrest, respectively.^{143, 149, 191} Both these phenotypes were rescued by p53 knockout, thus, research now points to senescence being an irreversible cell cycle block (G0/G1-phase) triggered by the activation of the p53 pathway.^{116, 153} However, it is not completely clear how DNA damage triggers p53 activation.¹⁹⁹

The correlation between telomere loss and senescent cell cycle arrest is, however, more complicated; given that different fibroblast strains senesce at varied average telomere lengths and very short telomeres are prevented from signalling cell cycle arrest or apoptosis by the addition of telomerase. Evidence has suggested that it is no longer the smallest telomere(s) on any chromosome within a cell that triggers the arrest because very short telomeres are now found on single chromosomes (especially on human chromosome 17) for many population doublings before senescence.²⁰⁰ Instead, new data has highlighted the importance of the higher order telomeric structure. It is proposed that a minimal telomere length is required for t-loop

formation and that failure to produce it could lead to senescence.^{153, 162} The ability to form this loop could be impaired by either telomere trimming below a threshold limit or by the accumulation of telomeric damage, which would interfere with the loop's torsional stability.^{181, 200} Furthermore, von Zglinicki *et al.* (2000) found that free single-stranded G-rich telomeric DNA could signal p53-dependent arrest.^{94, 188} Accordingly, any treatment that could lead to the unscheduled release of the terminal G-rich single-stranded overhang would also activate the DNA damage checkpoint machinery, and therefore, induce senescence.^{94, 181, 200}

1.7 CELLULAR SENESCENCE

Most mammalian cells will senesce, including endothelial and smooth muscle cells.^{201, 202} Nevertheless, there are a few exceptions:^{190, 197, 203}

- germ-line cells – somatic cells acquire a finite replicative lifespan during embryonic development. Very little is known about when, where or how this occurs;
- some stem cells – this has not yet been fully investigated; and
- many malignant tumours.

Accompanying the inability to respond to stimulation by physiological mitogens, senescent cells demonstrate a decrease in cell cycle regulated enzymatic activity, protein synthesis and degradative efficiency.^{197, 204} Moreover, nuclear and chromosomal aberrations occur at a higher frequency.²⁰⁴ Furthermore, some cells acquire resistance to the induction of apoptosis.^{121, 205-208} Compared to their young counterparts, senescent cells are larger (they have more cytoplasm), grow to a lower saturation density and have shorter telomeres.^{94, 139, 155, 189, 204} The senescence response can also induce changes to differentiated cellular functions (i.e. a “phenotypic shift”). For example, senescent fibroblasts can adopt a matrix-degrading phenotype while senescent adrenal cortical epithelial cells secrete an altered profile of steroid hormones.^{169, 206, 208} Importantly, the over expressed secreted

molecules can act to disrupt both the local environment and distant tissues.²⁰⁹ In contrast to the growth inhibition, very little is known about the mechanisms accountable for the operative changes that follow senescence. However, growth arrest and functional transformations are tightly linked, and together define the senescent phenotype.^{169, 206, 208}

The number of divisions that normal cells complete before they senesce, depends on the cell type, species, age and genetic background of the donor.¹⁹³ There are at least six lines of evidence that support the association between replicative senescence *in vitro* and ageing *in vivo*:

1. *In vitro* replicative potential has been inversely related to the tissue donor age.^{107, 136, 142, 210-212} This was observed in fibroblasts; smooth muscle, lens epithelial, adrenocortical, human pancreatic β - and endothelial cells; epidermal keratinocytes and T-lymphocytes.^{143, 153, 183, 193, 207, 211} In fact, the growth potential of primary fibroblast cultures was found to decline at a rate of 0.2 population doublings (PDs) per year of donor age.^{121, 142}
2. Cells from subjects with inherited premature ageing syndromes, such as Hutchinson-Gilford, have a reduced lifespan.^{121, 212} While other genetic syndromes, such as Werner's, Down's and Dyskeratosis congenita, are associated with accelerated telomere loss.^{107, 121, 213} Generally, the reasons for death in these individuals are premature cancer and cardiovascular disease, which are also the common causes of mortality in normal elderly individuals.^{121, 191}
3. In general, cells from long-lived species replicate more than those from short-lived species.^{121, 214} For example, the average life expectancy for humans and rodents is 70 and 3 years respectively.¹⁴⁰ Subsequently, human embryo fibroblasts proliferate for 50-55 PDs, whereas rodent fibroblasts replicate for a maximum of 30 PDs.¹²¹

4. Senescent cells appear *in vivo*, as judged by enzymatic markers characterised *in vitro*.^{207, 215, 216} The senescence biomarker, senescence associated- β -galactosidase (SA- β -Gal), has been identified in aged cells from both *in vitro* and *in vivo* conditions and was originally discovered in the skin biopsy samples from elderly individuals.^{121, 212, 215, 216}
5. A number of genes change their expression during cell senescence to mimic the pattern of ageing *in vivo*.^{121, 190, 217} A good example of this is collagenase-1-gene, which is often over expressed in senescent cells and the tissues of elderly individuals.^{140, 193, 218}
6. As one of the likely components of tumour suppression, cellular senescence is necessary (but not sufficient) for an extended lifespan.^{136, 153, 210, 218}

The longevity of a cell and organism as a whole, nonetheless, depends on multiple factors because the processes underlying ageing and senescence are not identical.^{189, 197, 219} Additionally, there is much data that implicates environmental factors in many age-related diseases, such as atherosclerosis.¹

1.7.1 SENESCENCE AND CELL CYCLE ARREST

Senescence is neither due to a DNA synthesis machinery deficiency nor a generalised collapse in growth factor signal transduction.^{194, 217} Rather, it is caused by the selective repression of a few growth-regulating genes, the expression of which is crucial for G1 progression and thus, DNA synthesis.^{4, 189, 191, 195, 220} As senescence approaches, the cell cycle transit time increases (due to a prolonged G1-phase). Moreover, at senescence, the cells typically arrested with a G1-phase DNA content.^{116, 136, 193, 194, 198} This irreversible cell cycle arrest is the hallmark of senescence. Subsequently, it was suggested that G1 cell cycle checkpoints could be the critical senescent controls. Indeed, studies into these checkpoints revealed that senescent cells contained an activated p53 transcription factor, elevated levels of p21 and

p16, and could not hyper-phosphorylate the retinoblastoma tumour suppressor protein (pRb).^{119, 136, 140, 189-193, 197, 217, 221-223}

The replicative loss in senescence has been studied most extensively in human fibroblasts. From these investigations, it became clear that the key growth regulators are the *c-fos*, helix-loop-helix and early growth response-1 genes, and components of the E2F transcription factor (E2F-1 and E2F-5).^{48, 190, 204, 212, 217} In addition, pRb remained in its growth suppressive (under-phosphorylated) form.^{189, 197, 224} Furthermore, senescent fibroblasts over expressed two negative growth regulators: p21 and p16.^{189, 190, 194} These inhibit cyclin-dependent protein kinases (CdKs), which along with their activating regulatory subunits (cyclins), phosphorylate Rb and allow G1- to S-phase progression.^{116, 217} p21 is an inhibitor of CdK generation, proliferating cell nuclear antigen (PCNA)-mediated DNA replication and of E2F.^{195, 197, 225} Meanwhile, p16 forms a complex with cyclin D and negatively regulates cyclin D-dependent kinases.^{193, 197} Hence, the high levels of p21 and p16 seem responsible for the accumulation of inactive CdK complexes, the lack of E2F activity and the under-phosphorylation of pRb in senescent cells.^{121, 191, 194, 205, 207, 220, 226}

The signals leading to p53, p21 and p16 activation need elucidation. It is known that p21 and p16 are heightened during the induction of premature senescence by both H₂O₂ and hyperactive Ras (linked to free radical generation).^{217, 227, 228} Additionally, p53 elevation or activation of its DNA binding activity can cause an increase in the transcription of the p21 gene.^{189, 197, 198, 226} In fact, the p21 gene contains p53 cis-elements in its promoter region.^{4, 117} However, the p21 gene can also augment its transcription in response to DNA damaging agents without p53.^{119, 194} p21 may also play a role in the functional alterations that occur in senescent cells, although how it does so is not yet understood.²⁰⁶

1.7.2 SENESENCE AND OXIDATIVE STRESS

Many studies indicate that ROS are important drivers for the development of the senescent phenotype.^{98, 100, 112, 229} For example, fibroblasts grown in low oxygen tension exhibit a prolonged lifespan, whereas, cells cultured in higher oxygen concentrations have a lowered lifespan and an accelerated rate of telomere shortening per population doubling.^{95, 96} Similarly, fibroblasts treated with H₂O₂ and hyperactive Ras activate a rapid, senescence-like growth arrest. Moreover, the latter was reversed by either ambient oxygen reduction or antioxidant supplementation.^{146, 228} Importantly, the senescent fibroblasts produced larger amounts of ROS themselves such that a three-fold increase in H₂O₂ was noted, along with an elevation in catalase (antioxidant) mRNA and activity.²³⁰ Indeed, DNA oxidation measurements indicated that senescent cells suffered greater oxidative DNA damage than young cells – they contained 30% more 8-oxo-dG (an indicator of oxidative DNA damage) and four times as many free 8-oxo-Gua bases.^{94, 121} Furthermore, the addition of α -phenyl-*t*-butyl-nitron (antioxidant) prolonged their lifespan in a dose-dependent fashion.⁹⁴

Additionally, the elevated oxidative stress observed in the SAMP (accelerated senescence-prone, short-lived) mice strains explained their accelerated senescence process, shorter lifespan, earlier onset and more rapid progression of age-associated pathological phenotypes when compared to the SAMR (accelerated senescence-resistant, long-lived) strains.²³¹ In addition, cultures of isolated fibroblast-like cells from these SAMP strains demonstrated the association between senescence acceleration and a hyper-oxidative status.²³² Altogether, these results raise the possibility that moderate, sustained increases in ROS production could act as activation triggers for the senescence programme.²²⁷

1.7.3 SENESCENCE AND THE VESSEL WALL

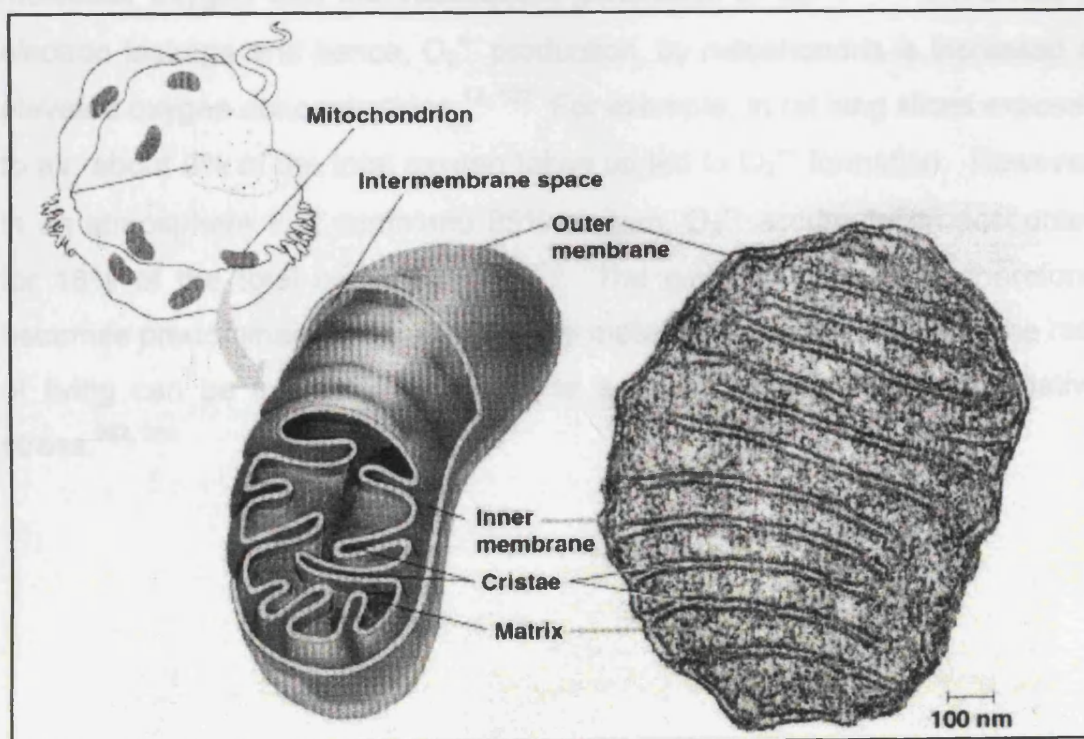
A variety of known senescence-specific changes have the potential to contribute to atherosclerosis.^{39, 201} The cells that make up the vascular wall include smooth muscle cells (in large vessels) or fibroblasts (in capillaries) and an overlying endothelium.¹ The response of an endothelial or smooth muscle cell to either an injurious or growth stimulus is probably a function of its age.^{18, 134, 218} For example, stimuli that would in a young endothelial cell induce a proliferative response, might, in an old vessel, lead to death and endothelial denudation.^{70, 209} Similarly, in an aged artery, proliferating cells could rapidly senesce and lead to a friable intima.⁴⁸ Ross *et al.* (1976) and others suggested that cells derived from regions of atherosclerotic plaques undergo more cellular divisions than cells from non-plaque areas, rendering them older and nearer to their maximum replicative capacity.^{121, 223} Indeed, it was shown that telomere length was inversely correlated with atherosclerotic grade.¹⁹⁶ Additionally, strong SA- β -Gal staining has been observed in coronary artery atherosclerotic lesions.⁴¹

In vitro, senescent HUVECs, show increased urokinase-type plasminogen activator and plasminogen activator inhibitor-1 (PAI-1) by more than 50-fold relative to their controls.²¹⁸ Both these molecules play a central role in the regulation of haemostasis and the altered PAI-1 regulation has been strongly implicated in the pathogenesis of age-related cardiovascular disease.^{193, 218, 233} Normally, the PAI-1 activity would be downregulated by factors produced by the neighbouring SMCs or fibroblasts.¹ Other changes that are potentially relevant to atherosclerosis include the reduced angiotensin-converting enzyme activity of senescent bovine endothelial cells, the elevated production of elastase by senescent SMCs and of thrombospondin by senescent fibroblasts, which may all contribute to vascular degeneration.^{39, 193, 218}

1.8 MITOCHONDRIAL PHYSIOLOGY

There are several thousand mitochondria present in an average somatic cell, each containing multiple copies (2-10) of the mammalian mitochondrial DNA (mt-DNA).²³⁴⁻²³⁹ Mt-DNA is a closed circular double-stranded molecule of about 16 kilobases and is located in the area defined by the inner mitochondrial membrane (figure 1-4).^{234, 240-244} Interestingly, mt-DNA has a genetic code that differs from the nuclear genome. It is characterised by a compact structure with very few intergenic spacing sequences, no introns and overlapping genes.^{241, 245} The only non-coding region is the “D-loop”, which is proposed to play a role in regulating mt-DNA replication and transcription.^{128, 245, 246} Mt-DNA encodes 37 genes – 24 encode the mt-DNA translational machinery (22 transfer and two ribosomal RNAs), while the remaining thirteen genes encode for some of the electron transport chain subunits.^{12, 68, 234, 247} It is this chain that enables oxidative phosphorylation and thus, cellular ATP generation.

Figure 1-4: Diagram of a mitochondrion. (Adapted from reference 248)



Approximately 85-90% of oxygen taken up by the cell is utilized by the mitochondria to manufacture most of the ATP needed.¹² The essence of metabolic energy production involves the oxidation of food materials, that is, they lose electrons, which are accepted by electron carriers, such as NAD⁺ and flavins (FMN, FAD).^{249, 250} The resulting reduced NADH and flavins (FMNH₂, FADH₂) are then re-oxidised by oxygen in mitochondria, forming ATP.^{251, 252} The oxidation is catalysed in a stepwise manner by a chain of five enzyme complexes, so that the energy is released gradually (figure 1-5, page 29).^{12, 253}

Mitochondrial O₂^{•-} production occurs primarily at two discrete points in the electron transport chain, namely at complex I (NADH dehydrogenase) and at complex III (ubiquinone-cytochrome c reductase).^{49, 125, 247, 256-260} Under normal metabolic conditions, complex III is the main site for ROS production.⁹⁵ With respect to human ageing, the Achilles' heel of this system lies in the formation of the free radical semiquinone anion species (•Q⁻) that occurs as an intermediate in the regeneration of coenzyme Q (figure 1-6, page 30). Once formed, •Q⁻ can readily and non-enzymatically transfer electrons to molecular oxygen with the subsequent generation of O₂^{•-}.^{95, 261} The rate of electron leakage and hence, O₂^{•-} production, by mitochondria is increased at elevated oxygen concentrations.^{12, 102} For example, in rat lung slices exposed to air, about 9% of the total oxygen taken up led to O₂^{•-} formation. However, in an atmosphere that contained 85% oxygen, O₂^{•-} accumulation accounted for 18% of the total oxygen uptake.¹² The generation of ROS, therefore, becomes predominantly a function of the metabolic rate and, as such, the rate of living can be indirectly translated to a corresponding scale of oxidative stress.^{262, 263}

Figure 1-5: A schematic representation of the mitochondrial oxidative phosphorylation system. Protons (H⁺) are pumped from the matrix to the IMS (intermembranous space) through complex I, III, IV. They flow back into the matrix through complex V with concomitant production of ATP. Complex I is responsible for the dehydrogenation of NADH and the transportation of electrons to coenzyme Q. This electron transport is coupled to the translocation of protons across the mitochondrial inner membrane and creates a proton gradient that is the proton-motive force for the production of ATP by F₁-F₀ ATP synthetase. Complex II (succinate: ubiquinone oxidoreductase) catalyses the oxidation of succinate to fumarate during which, electrons are transported from FADH₂ to the ubiquinone pool. Complex III catalyses the electron transfer from ubiquinol to cytochrome c with the coupled translocation of protons across the mitochondrial inner membrane. Complex IV (cytochrome c oxidase) couples the transfer of electrons from reduced cytochrome c to oxygen leading to a translocation of protons across the mitochondrial inner membrane. The resulting electrochemical gradient is used to drive the synthesis of ATP. Complex V (F₁-F₀ ATP synthetase) catalyses the synthesis of ATP from ADP and P_i (inorganic phosphate) using the energy of the proton motive force across the inner mitochondrial membrane. (Adapted from references 254 and 255)

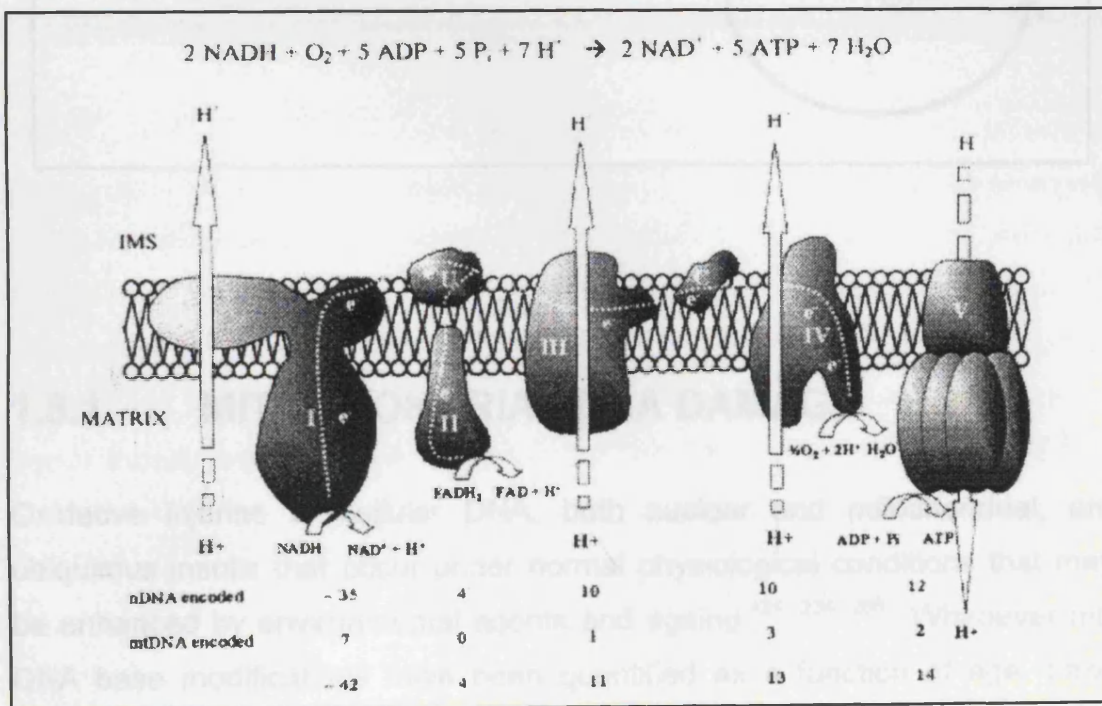
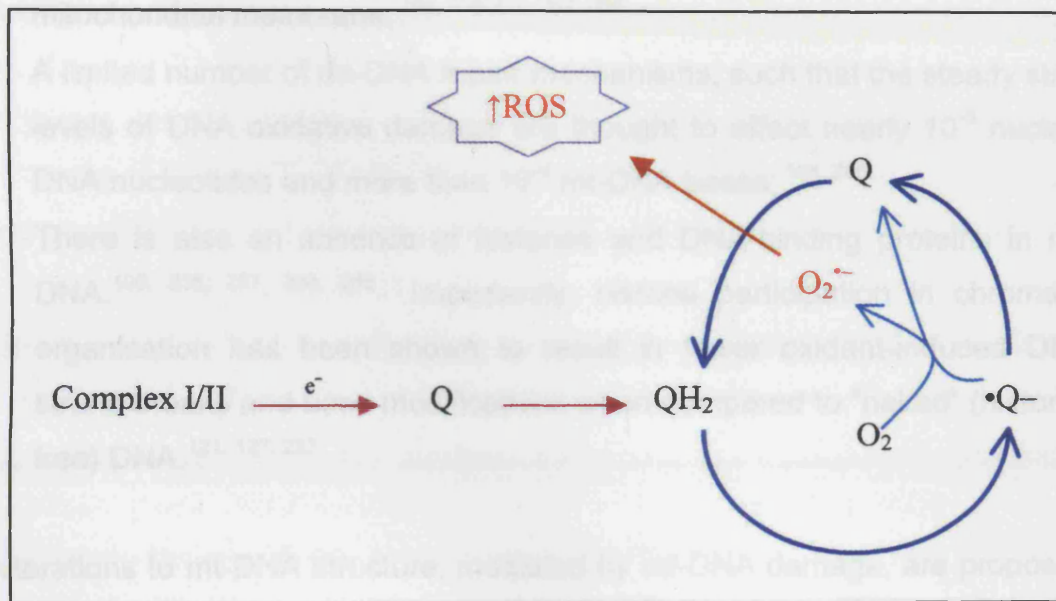


Figure 1-6: The Q cycle. Electrons from complex I or II are transferred to coenzyme Q (Q), also called ubiquinone. The resulting reduced form (QH₂) of coenzyme Q subsequently undergoes two sequential one-electron reductions (the Q cycle). The unstable intermediate in the Q cycle ($\cdot\text{Q}^-$) can lead to superoxide formation by transferring electrons directly to molecular oxygen. The generation of superoxide ($\text{O}_2^{\cdot-}$) is non-enzymatic and hence, the higher the rate of metabolism, the greater the production of reactive oxygen species (ROS). (Adapted from reference 95)



1.8.1 MITOCHONDRIAL DNA DAMAGE

Oxidative injuries to cellular DNA, both nuclear and mitochondrial, are ubiquitous insults that occur under normal physiological conditions that may be enhanced by environmental agents and ageing.^{121, 234, 256} Whenever mt-DNA base modifications have been quantified as a function of age, base alterations increased during ageing and mt-DNA adduct levels were higher than those in the nuclear DNA.¹²¹ Consequently, the mitochondrial genome is proposed to be more sensitive to oxidant damage than nuclear DNA.^{83, 264} Richter *et al.* (1988) reported that oxidative damage to mt-DNA was more

extensive than in nuclear DNA.^{121, 265, 266} Furthermore, Van Houten (1997) and others confirmed this observation and additionally noted that ROS-induced injury persisted for longer in mt-DNA.^{108, 121, 146} This heightened vulnerability of mt-DNA to oxidative damage is likely to be due to a number of factors, including:

- The mitochondrial genome's small size and high informational content;¹⁰⁰
- The close proximity of mt-DNA to the free radical generating inner mitochondrial membrane;^{100, 235-237, 267, 268}
- A limited number of mt-DNA repair mechanisms, such that the steady state levels of DNA oxidative damage are thought to affect nearly 10^{-5} nuclear DNA nucleotides and more than 10^{-4} mt-DNA bases;^{101, 266}
- There is also an absence of histones and DNA-binding proteins in mt-DNA.^{100, 235, 237, 238, 266} Importantly, histone participation in chromatin organisation has been shown to result in fewer oxidant-induced DNA strand breaks and base modifications when compared to "naked" (histone-free) DNA.^{121, 127, 237}

Alterations to mt-DNA structure, mediated by mt-DNA damage, are proposed to play a role in mt-DNA deletion generation.²⁶⁷ Age-correlations between mt-DNA oxidative adduct aggregation and deletions are consistent with this hypothesis.^{12, 121, 127, 234} For example, an age-associated exponential accumulation of 8-oxo-dG in mt-DNA from human diaphragmatic and cardiac tissues was shown to equate to the multiple mt-DNA deletions noted to occur within these tissues during ageing.^{12, 121} In addition to mt-DNA deletions, there is also evidence for an increase in the incidence of point mutations in mt-DNA with age.^{262, 267, 269, 270}

1.8.2 MITOCHONDRIA AND AGEING

Mitochondrial ROS production has been shown to be inversely correlated with mean lifespan.^{49, 271} Generally, long-lived animals tended to have lower mitochondrial free radical generation rates, and therefore, decreased mt-DNA oxidative damage.⁹² This led to the proposal that mt-DNA injury accumulation was a major determinant of the rate of ageing.¹⁰⁰ Further studies have shown that the rises in mt-DNA lesions correlate with muscle fibre ageing.²⁷² Additionally, higher steady-state levels of oxidative insults to nucleic acids were noted.^{237, 273} Subsequent studies reported that increased levels of oxidative stress, culminated in elevated 8-oxo-dG content in the mt-DNA of most aged tissues.^{49, 242, 274-276} In particular, ageing cardiac mitochondria appeared to have a heightened sensitivity to oxidative modification.^{49, 242, 274-276} Moreover, the production of ROS was greater in the cardiac mitochondria isolated from senescent mice when compared to younger mice.⁴⁹ Overall, the mitochondria gathered from senescent animals exhibited higher rates of ROS formation compared to the younger animals.^{49, 94, 127, 275, 277} In fact, base damage, point mutations and various mt-DNA deletions have all been reported to be amplified in senescent tissues.¹²¹

On the whole, ageing is thought to increase ROS mitochondrial production. Ageing defects in this organelle's electron transport chain are believed to be the probable sources for the raised oxidative injury.^{49, 127, 277} Investigations have highlighted decreases in the activity of complexes I, III and IV with advancing age but complex II appears unaltered.^{70, 127, 270, 277-279} Significantly, many of the subunits comprising complexes I, III and IV are partly encoded by mt-DNA while complex II is entirely encoded by nuclear DNA. Additionally, it is reported that complex II could be involved in the ROS elevation seen in people with diabetes – a role for it has been suggested in advanced glycation end-product (AGE) formation and sorbitol accumulation.^{256, 280}

1.8.3 MITOCHONDRIA AND DIABETES

Mitochondrial integrity and function are influenced by ageing and diabetes.^{234, 269} Studies have suggested that approximately 0.5-1.5% of all people with diabetes exhibit pathogenic mt-DNA mutations such as duplications, point mutations and large-scale deletions (especially the “common 4977 base pair deletion”).^{94, 127, 281} Mt-DNA mutations have been found in the region of the common deletion in skeletal muscle of older men and women with impaired glucose tolerance or diabetes mellitus and these have been speculated to be a consequence of ageing, possibly exacerbated by the oxidative damage, potentiated by hyperglycaemia.^{9, 282} Furthermore, high glucose concentrations are shown to contribute to common deletion accumulation, as well as to the development of other mutations in VSMCs *in vitro*.^{43, 282} Such glucose-related mt-DNA deletions have additionally been seen in HUVECs.²⁸² Diabetes may also be associated with quantitative changes in mt-DNA. For example, Antonetti *et al.* (1995) and others reported that mt-DNA copy number was approximately 50% lower in the skeletal muscles of people with both type 1 and 2 diabetes.^{121, 283-286} In addition, Lee *et al.* (1998) claimed that lymphocyte mt-DNA copy number decreased prior to the development of type 2 diabetes and suggested that the absolute decrease in the levels of mt-DNA might be a causal factor in the pathogenesis of diabetes.²⁸³⁻²⁸⁶

There is, as yet, no convincing evidence as to whether the reduction of mt-DNA copy number causes enough disturbances to glucose metabolism in peripheral tissues such as liver cells to directly contribute to the development of diabetes *per se*.^{127, 247, 281} Moreover, although the common deletion has been described to have an increased susceptibility to oxidative damage, the phenotypic consequences of this deletion are still undefined.²⁸²

1.9 BIOLOGY OF OXIDATIVE STRESS

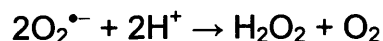
1.9.1 FREE RADICALS

Free radicals are species that are capable of independent existence and have one or more unpaired electrons.¹² Reactive oxygen species is a term used collectively to describe oxygen radicals (for instance, $O_2^{\bullet-}$ and OH^{\bullet}) and some non-radical derivatives of oxygen (for example, H_2O_2 , $HOCl$ and $ONOO^-$).¹² The half-lives and reactivity of the ROS vary greatly.²⁸⁷ OH^{\bullet} is both the most reactive and short-lived.²⁸⁷ Oxidative stress is stated to occur when ROS formation surpasses the neutralising capacity of the local antioxidant defence mechanisms.^{12, 42} This could be due to an excessive production of ROS, a depletion of antioxidants, or both.

1.9.2 REACTIVE SPECIES

1.9.2.1 SUPEROXIDE RADICAL ($O_2^{\bullet-}$)

In aqueous solutions, $O_2^{\bullet-}$ is extensively hydrated and poorly reactive, behaving as a weak oxidising agent.^{12, 33} It is most active in a hydrophobic environment and crosses biological membranes slowly unless there are anion channels (only in erythrocytes).²⁸⁷ $O_2^{\bullet-}$ undergoes the following dismutation reaction:²⁸⁸



Within the vessel wall, $O_2^{\bullet-}$ is produced from numerous sources such as the mitochondrial respiratory chain; small molecular cellular constituents like, flavins, thiols and catecholamines; the metabolism of arachidonic acid by cyclooxygenases, lipoxygenases and cytochrome P450 monooxygenases; xanthine oxidase and the NADH/NADPH oxidase.^{38, 49, 52, 92, 102, 146, 288}

1.9.2.2 HYDROGEN PEROXIDE (H₂O₂)

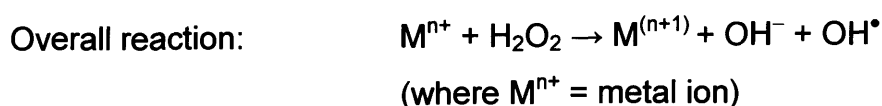
The addition of another electron to O₂^{•-} produces the peroxide ion (O₂²⁻) which, at physiological pH, immediately protonates to give H₂O₂.^{116, 204} H₂O₂ is quite stable, relatively long-lived and, under normal conditions, can be present in cells at a concentration of 10⁻⁸M.¹² In aqueous solutions, H₂O₂ is formed by the spontaneous or catalysed dismutation reaction of O₂^{•-} and by oxidase enzymes such as those involved in phagocytosis.^{287, 288} Unlike O₂^{•-}, H₂O₂ structurally resembles water and thus, readily diffuses across biological membranes and may additionally travel through water channels (aquaporins).¹² Hence, *in vivo*, H₂O₂ readily mixes with water and is very diffusible within and between cells.¹²

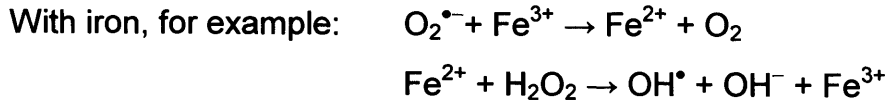
Generally, H₂O₂ is not very reactive. However, it can be reduced to yield OH[•] by transition metal ion catalysis.¹² OH[•] is believed to account for much of the damage sustained by DNA in H₂O₂-treated cells.^{92, 95, 146, 289}

1.9.2.3 HYDROXYL RADICAL (OH[•])

OH[•] is the most toxic ROS, interacting with nearly every molecule in its vicinity.^{12, 204} Its very short life span and intense reactivity implies that OH[•] acts at or close to its site of formation.^{12, 287} Additionally, OH[•] reactions with biomolecules produces extra radicals, which will cause further damage since they can diffuse away and attack other specific molecules.^{290, 291}

The toxicity of O₂^{•-} and H₂O₂ is often attributed to their transformation into OH[•].^{92, 292} The mechanism for this is based on transition metal ion chemistry involving iron or copper ions:





OH[•] generation occurs at specific locations – the sites at which iron or copper ions are bound to biomolecules, like DNA.^{146, 289} OH[•] scavengers find the ensuing damage very difficult to intercept because the places of OH[•] formation and reaction are very close. Therefore, the harm inflicted by ROS depends upon the availability and whereabouts of the metal ion catalysts. *In vivo*, antioxidant defences act to ensure that these ions are not freely available and are kept bound to their transport and storage proteins.¹²

1.9.2.4 NITRIC OXIDE (NO)

NO (a reactive nitrogen species) is synthesized from L-arginine by NO synthase, which is present in three separate isoforms produced by different genes.¹² NO is quite stable, freely diffusible and benign for a free radical, with a lifetime of several seconds.²⁹³ Under normal conditions, NO has many physiological functions as a neuronal messenger and modulator of SMC contraction.^{92, 293} However, NO can interact very rapidly with O₂^{•-} to generate ONOO⁻, the molecule that accounts for much of the NO toxicity.^{294, 295} In fact, the reactivity of ONOO⁻ is roughly the same as that of OH[•].^{12, 295} Its toxicity is derived from its ability to directly nitrate and hydroxylate the aromatic rings of amino acid residues, and to react with sugars, lipids, proteins and DNA.¹⁴⁶ Additionally, ONOO⁻ can affect cellular energy status by inactivating key mitochondrial enzymes and it may also trigger calcium release from the mitochondria.^{49, 295}

1.9.3 ANTIOXIDANTS

Antioxidants are substances that can delay or inhibit oxidative damage to a target molecule.¹² Human defences comprise agents that catalytically remove ROS like superoxide dismutases and catalases; proteins that minimise the availability of pro-oxidants such as iron and copper ions (examples include transferrin and caeruloplasmin); other proteins like heat shock proteins and low-molecular-mass agents that scavenge ROS (glutathione and α -tocopherol, for instance).^{12, 63, 146, 290, 291, 296, 297}

The evolution of numerous overlapping defences is indicative of the need to limit oxidative damage. *In vivo*, antioxidants exist in balance with ROS and there are no antioxidant reserves, probably due to the beneficial functions that can be performed by ROS such as phagocytosis.¹²

1.9.4 ENZYMATIC DEFENCES

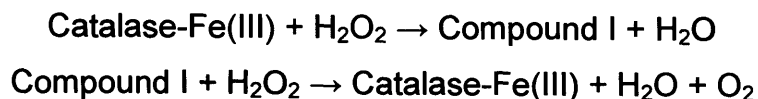
1.9.4.1 SUPEROXIDE DISMUTASE (SOD)

Superoxide dismutase resides in all aerobic organisms and accelerates the dismutation of $O_2^{\bullet-}$ to H_2O_2 .¹² Three different types of SOD have been identified in humans:^{102, 109, 129, 146, 290, 298, 299, 300, 301}

- SOD containing copper and zinc (CuZnSOD; SOD 1) – found in the cytosol and occasionally in lysosomes, the nucleus and the space between the inner and outer mitochondrial membranes;
- SOD incorporating manganese (MnSOD; SOD 2) – present in mitochondria; and
- Extracellular SOD (EC-SOD; SOD 3) – located between the endothelium and VSMC layer, it scavenges $O_2^{\bullet-}$ to prevent NO degradation.

1.9.4.2 CATALASES

Catalases exist in most aerobic cells and are responsible for the conversion of H_2O_2 into water and oxygen:^{12, 102, 109, 146, 298, 301, 302}

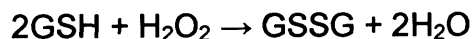


The exact structure of compound I is uncertain and NADPH is also needed for the continued functioning of catalase.¹² The above equations show that the complete removal of H_2O_2 requires the impact of two H_2O_2 molecules upon a single catalase active site. However, this will become less likely as the H_2O_2 concentration decreases.

Catalases are found in peroxisomes (which also contain many of the enzymes that generate H_2O_2) and at low levels in the cytosol and heart mitochondria.^{49, 102, 302} Fortunately, peroxisomal catalases can diffuse across membranes and help in the detoxification of H_2O_2 formed in other cellular components.^{49, 102}

1.9.4.3 GLUTATHIONE PEROXIDASE (Gpx)

This enzyme catalyses the removal of H_2O_2 and is present in the cytosol, mitochondria, endoplasmic reticulum and nuclei.^{12, 92, 290, 302} It converts reduced glutathione (GSH) into oxidised glutathione (GSSG) at the expense of H_2O_2 :^{243, 303}



The GSH is then regenerated by glutathione reductase – a NADPH-dependent enzyme.^{104, 106, 304} Normally, the electrons produced during pentose phosphate pathway aerobic metabolism allow the reduction of oxidised NADPH and the replenishment of GSH.^{146, 304} However, in hyperglycaemia, elevated free radical levels raise H_2O_2 concentrations and

therefore, incite increased GSH oxidation.⁴⁹ Additionally, NADPH depletion, caused by hyperglycaemic-induced polyol pathway activation and reduced pentose phosphate pathway NADPH production, impair GSH regeneration.^{12, 49}

1.9.5 NON-ENZYMATIC DEFENCES

The non-enzymatic antioxidants encompass: glutathione, ascorbic acid, α -tocopherol, β -carotene and uric acid.¹² These remove free radicals by reacting with them non-catalytically, thereby stopping chain reactions such as lipid peroxidation.

1.9.6 CHEMICAL REACTIONS OF ROS

Oxidative damage to DNA, proteins and lipids has been shown to accumulate with age.^{100, 121} The spectrum of DNA oxidative damage involves alterations to all four DNA bases and includes more than twenty different products. Among the base modifications studied as a function of age, oxidative injury to DNA is the most extensively documented, and probably the most abundant class of lesions continually introduced into the genome.

There are many well-documented correlations between oxidant levels, DNA repair and longevity. Firstly, there is a direct correlation between DNA repair and the lifespan of a species.^{49, 121, 140} Furthermore, an inverse association exists between endogenous oxidant levels and lifespan.^{49, 121, 140} Additionally, mitochondrial respiration rates correlate negatively with maximum species longevity; and finally, a direct relationship between antioxidant defence systems and lifespan has been noted.^{49, 66, 121, 140} Supplementary support comes from Orr and Sohal (1994), who showed a gene dosage-dependent extension of maximum lifespan in transgenic *Drosophila* containing additional germ line copies of catalase and SOD genes.^{98, 121}

Moreover, it is suggested that alterations to cellular DNA may contribute to atherosclerotic plaque formation.⁴⁶ Oxidative DNA damage has been observed to accumulate in such plaques of humans and animals, while antioxidants like probucol, butylated hydroxytoluene, vitamin E and β -carotene are reported to inhibit atherosclerotic development.³⁰⁵⁻³⁰⁷ The focus of this study was to examine the effects of ROS on DNA, consequently, the details of oxidative reactions with lipids and proteins are not discussed in detail here.

1.9.7 DNA DAMAGE

DNA injury is one of the most critical threats to cellular homeostasis and life because it can cause disruption to DNA transcription and replication.^{46, 92, 100, 308, 309} It has been estimated that around 2×10^4 DNA damaging events occur in every cell of the human body everyday and that a significant portion of this damage is caused by ROS.^{92, 310, 311} ROS lead to DNA damage either through direct chemical attack or by indirect mechanisms i.e., the activation of Ca^{2+} -dependent endonucleases due to raised free intracellular Ca^{2+} .^{291, 312, 313} Furthermore, free Ca^{2+} can fragment DNA and interfere with DNA replication and repair enzymes.^{291, 312-314}

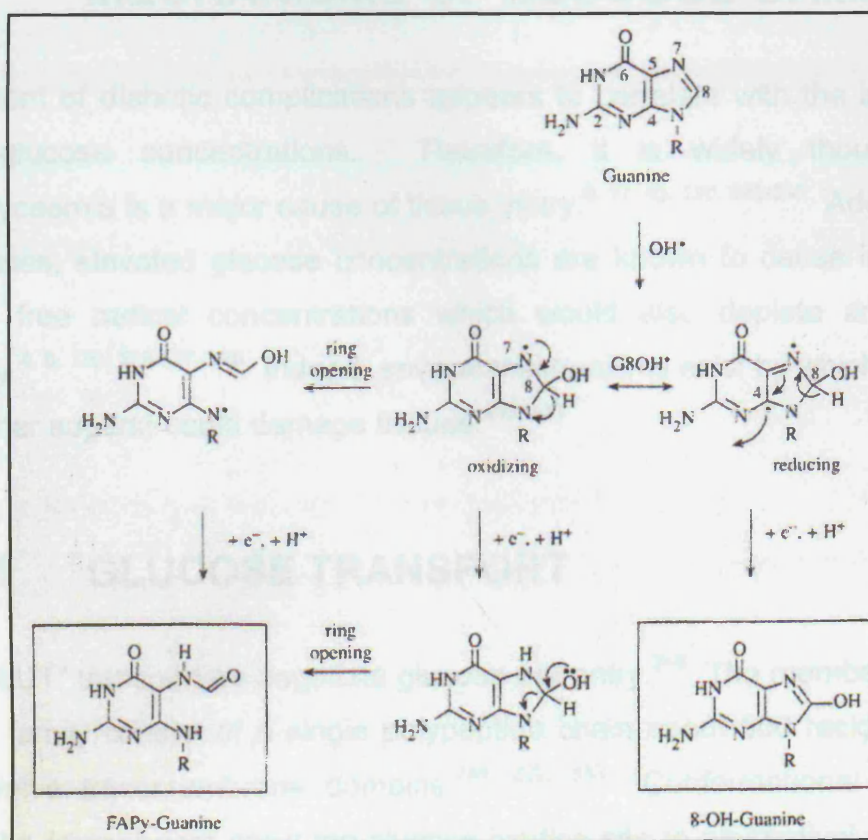
1.9.7.1 BASE MODIFICATIONS

DNA bases are chemically reactive, and therefore, susceptible to covalent modification. Purines are generally more reactive than pyrimidines.¹²¹ Base alterations include deaminations, oxidative adducts and ring openings, alkylation adducts, reactions with reducing sugars, bond formation with aldehydes and reactions with proteins or other macromolecules. At physiological levels, $\text{O}_2^{\bullet-}$ and H_2O_2 do not appear to react with DNA bases or sugars at significant rates.^{12, 113} By contrast, OH^\bullet and ONOO^- can generate a multitude of products, as they attack sugars, purines, pyrimidines and the phosphodiester DNA backbone causing single- and double-stranded breaks, DNA-DNA and DNA-protein crosslinks and base modifications.^{92, 290, 315-318}

For example, both OH^\bullet and ONOO^- can irreversibly react with the most readily oxidised base, guanine, at ring positions C-4, C-5 or C-8.^{291, 312, 318-320} The eighth position is the most readily oxidized (figure 1-7) and produces a radical that can be reduced to 8-hydroxy-7, 8-dihydroguanine, oxidised to 8-oxoguanine or undergo imidazole ring opening, to give 2, 6-diamino-4-hydroxyl-5-formamidopyrimidine (FAPyG).^{290, 321-323} The products resulting from C4 and C5- OH^\bullet are unknown. Similarly, OH^\bullet can add onto adenine at C4, C5 or C8.^{291, 321}

Pyrimidines are particularly susceptible to OH^\bullet assault.²⁹¹ A major reaction involves OH^\bullet attack on the C5-C6 double bond as the electrophilic OH^\bullet is attracted to the high electron density at C5.¹²

Figure 1-7: Guanine modification by hydroxyl radicals. (Adapted from reference 12)



1.9.7.2 SUGAR DAMAGE

OH[•] can cause sugar fragmentation, base loss (producing abasic sites) and strand breaks.^{113, 312} All positions in the sugar moiety are vulnerable and result in C-centred radicals due to hydrogen abstraction by OH[•].¹¹³ In the presence of oxygen, these rapidly convert into sugar peroxy radicals, which then undergo a series of undefined reactions.^{290, 312}

Radicals can also attack nuclear proteins.^{94, 204} The resulting protein-derived radicals can cross-link to base-derived radicals if the two meet in chromatin, giving DNA-protein cross-links (thymine to tyrosine, for instance) that could interfere with chromatin unfolding and DNA repair, replication and transcription.^{12, 113, 291, 324}

1.10 MECHANISMS OF GLUCOSE DAMAGE

The extent of diabetic complications appears to correlate with the increased blood glucose concentrations. Therefore, it is widely thought that hyperglycaemia is a major cause of tissue injury.^{6, 17, 45, 120, 325-330} Additionally, in diabetes, elevated glucose concentrations are known to cause increased plasma free radical concentrations which would also deplete antioxidant capacity.^{4, 5, 120, 325-327, 329} Indeed, several mechanisms exist by which glucose (and other sugars) could damage tissues.^{293, 331}

1.10.1 GLUCOSE TRANSPORT

The “GLUT” transporters negotiate glucose cell entry.²⁴⁸ The members of this protein family consist of a single polypeptide chain about 500 residues long with twelve transmembrane domains.^{248, 332, 333} Conformational changes within the transporters allow the glucose-binding site to alternatively face the cell's inside and outside when occupied by a sugar.^{248, 334} GLUT transporters

are widely distributed throughout mammalian cells (table 1-1) with GLUT 1, GLUT 3 and GLUT 4 having the highest affinities for glucose.³³⁵⁻³³⁷

Table 1-1: GLUT transporter details. The underlined isoforms are known to occur in the vasculature. (Adapted from references 21, 248, 332-334, 337-345)

TRANSPORTER	DETAILS
<u>GLUT 1</u>	Activated early in development and persists in virtually all adult tissues, albeit to varying degrees. Present in most cultured cell lines.
GLUT 2	Low affinity transporter identified in cells near the abluminal surface of liver cells, small intestine and kidney. May also facilitate glucose uptake or efflux from tissues depending on their nutritional status.
<u>GLUT 3</u>	Detected in human endothelium of intraplacental microvessels, where it was proposed to play a role with GLUT 1 in sustaining glucose supply to the developing foetus.
<u>GLUT 4</u>	Insulin-sensitive glucose transporter expressed mainly in adult skeletal muscle, cardiac muscle and adipose tissue with lower abundance in the vasculature.
GLUT 5	Constitutively expressed in the plasma membrane of muscle and adipocytes.
GLUT 6	Detected in brain, spleen, leukocytes and adipose tissue.
GLUT 8	Expressed in adipocytes.
GLUT 11	Only demonstrated in human heart and skeletal muscle

Little is known about glucose transporters and their regulation in the vascular system. Nonetheless there is no evidence that GLUT 2, 5, 6, 8 and 11 are expressed in the vasculature.³⁴³⁻³⁴⁵ SMCs have exhibited an adaptive response to changes in extracellular glucose by modifying their hexose-transport activity.^{338, 340, 343} However, endothelial cells lack this autoregulatory mechanism and therefore, appear to be “glucose-blind”.^{339, 340, 343} The transport of glucose into endothelial cells appears to be largely passive – being driven by the extracellular : intracellular glucose concentration gradient (B. Williams, personal communication). This glucose transport insensitivity during hyperglycaemia remains puzzling, but may explain why endothelial cells are more vulnerable to high glucose effects than SMCs.

1.10.2 MECHANISMS OF GLUCOSE TOXICITY

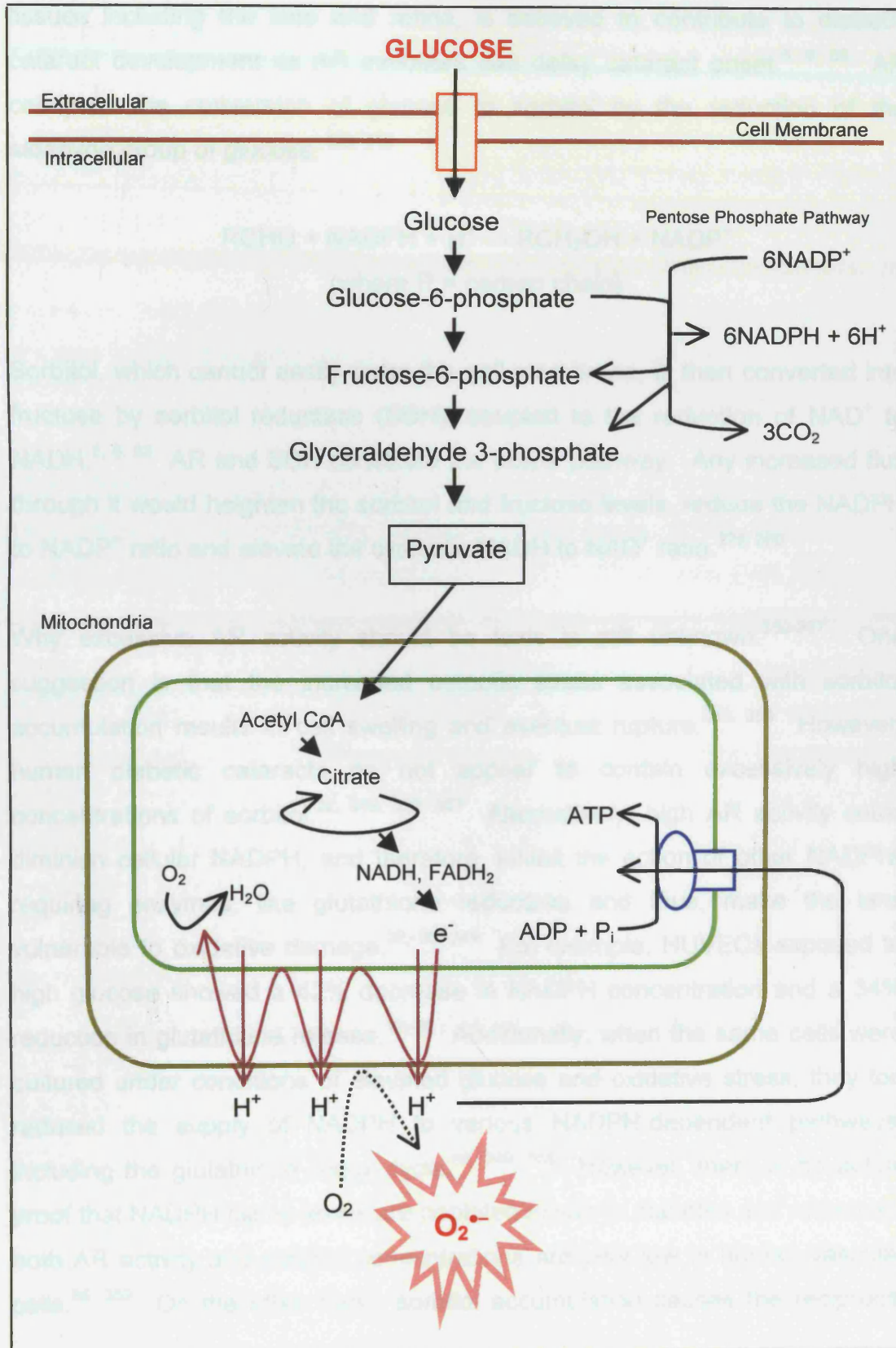
ROS generation may play an important role in the aetiology of diabetic complications.^{4-6, 325-327, 335, 346} This hypothesis is supported by evidence that biochemical pathways associated with hyperglycaemia (glycolysis, glucose autoxidation, polyol pathway, prostanoid synthesis and protein glycation) can all increase the production of free radicals.^{7, 19, 21, 26, 62, 65, 81, 85, 87, 259, 284, 347}

1.10.2.1 INCREASED GLUCOSE METABOLISM

During cellular respiration, cells use the potential energy stored in chemical bonds in food molecules to create ATP that, in turn, is needed to power the cell's many different metabolic reactions.²⁴⁸ Glucose is a major ATP source and once it has entered a cell, it is catabolised by glycolysis, the citric acid cycle and the mitochondrial electron transport system.²⁴⁸

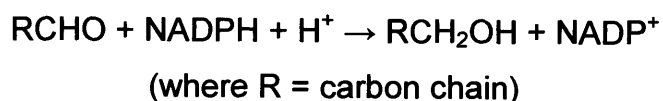
The mitochondrial electron transport system involves an energy transfer by electron translocation via a series of oxidation-reduction reactions in the mitochondrial inner membrane.³³³ Collectively, electrons are relocated to oxygen with some of the resultant chemical energy then used to manufacture ATP. However, this process is inefficient and a leakage of electrons is thought to allow $O_2^{\bullet-}$ production.³³³ Moreover, ROS generation is predicted to increase if the influx of electrons is higher than their expenditure.²⁴⁸ This typically occurs when the proton gradient is elevated (when too few protons are utilized to formulate ATP as a result of relatively high ATP and low ADP concentrations). Such a situation would also normally inhibit glycolysis and the entry of further energy substrates into the mitochondria.³⁴⁸ However, it has been proposed that high glucose may override this control mechanism (figure 1-8, page 45).^{38, 83} For example, in aortic endothelial cells, elevated glucose levels have been shown to cause a significant increase in mitochondrial electron transport chain ROS formation.³⁸

Figure 1-8: Effect of substrate availability on reactive oxygen species production. Raised extracellular glucose is thought to increase glycolysis, and therefore, elevate superoxide ($O_2^{\bullet-}$) production. e^- , electron; O_2 , oxygen. (Adapted from reference 38)



1.10.2.2 POLYOL PATHWAY

The enzyme aldose reductase (AR), which is found in many mammalian tissues including the lens and retina, is believed to contribute to diabetic cataract development as AR inhibitors can delay cataract onset.^{5, 6, 63} AR catalyses the conversion of glucose to sorbitol by the reduction of the aldehyde group of glucose:^{329, 349}



Sorbitol, which cannot easily cross the cell membrane, is then converted into fructose by sorbitol reductase (SDH), coupled to the reduction of NAD^+ to NADH .^{5, 6, 63} AR and SDH constitute the polyol pathway. Any increased flux through it would heighten the sorbitol and fructose levels, reduce the NADPH to NADP^+ ratio and elevate the cytosolic NADH to NAD^+ ratio.^{329, 350}

Why excessive AR activity should be toxic is still unknown.³⁵⁰⁻³⁵⁷ One suggestion is that the increased osmotic stress associated with sorbitol accumulation results in cell swelling and eventual rupture.^{353, 354} However, human diabetic cataracts do not appear to contain excessively high concentrations of sorbitol.^{22, 349, 352, 357} Alternatively, high AR activity could diminish cellular NADPH , and therefore, inhibit the action of other NADPH -requiring enzymes, like glutathione reductase and thus, make the lens vulnerable to oxidative damage.^{22, 88, 349} For example, HUVECs exposed to high glucose showed a 42% decrease in NADPH concentration and a 34% reduction in glutathione release.^{12, 85} Additionally, when the same cells were cultured under conditions of elevated glucose and oxidative stress, they too reduced the supply of NADPH to various NADPH -dependent pathways, including the glutathione redox cycle.^{88, 349, 358} However, there is no actual proof that NADPH tissue levels are depleted *in vivo* in diabetes and moreover, both AR activity and sorbitol concentrations are very low in human vascular cells.^{85, 359} On the other hand, sorbitol accumulation causes the reciprocal

depletion of taurine, an intracellular osmolyte and endogenous antioxidant, which would compromise antioxidant defences.³⁵⁸

1.10.2.3 PROSTANOID SYNTHESIS

The hyperglycaemic-induced increase in the NADH to NAD⁺ ratio is referred to as “hyperglycaemic pseudohypoxia” and is thought to play a role in diabetic complications.^{4, 5, 9, 328, 354} Both true hypoxia and pseudohypoxia can generate free radicals: the former through ischaemia/reperfusion injury and the latter via increased synthesis of prostaglandin H₂ from prostaglandin G₂ through the enzyme hydroperoxidase (which also uses NADH as a cofactor).^{4, 5, 9, 89, 274, 354, 360}

The altered redox state prompted by the increased NADH/NAD⁺ ratio may also influence the availability of tetrahydrobiopterin (BH₄), an essential cofactor for nitric oxide synthase (NOS).^{5, 328, 361, 362} During BH₄ depletion, NOS becomes “uncoupled”, resulting in increased O₂^{•-}, rather than NO production.^{75, 328, 361} In diabetic animal models, BH₄ supplementation has indeed been shown to improve faulty endothelium-dependent vasorelaxation.^{328, 329, 361} However, whether BH₄ enhances impaired NO activity *in vivo* in diabetic patients still remains to be established. Furthermore, the increased cytosolic NADH/NAD⁺ ratio encourages *de novo* synthesis of diacylglycerol (DAG) from glycolytic intermediates.^{12, 22, 360, 363, 364, 360} Such elevated DAG levels activate PKC, which in turn, is associated with endothelial dysfunction caused by heightened free radical formation.^{22, 328, 363, 365} A possible explanation for this ROS increase is the activation of TGF-β and thromboxane A₂ (TXA₂) by PKC.^{28, 81, 329, 365} TGF-β can activate monocytes that produce radicals through NADPH oxidases while TXA₂ is connected to ROS generation through increased cytochrome P450 activity.^{12, 366}

1.10.2.4 NON-ENZYMATIC GLYCATION

Glucose can also be toxic by virtue of its ability to behave chemically as an aldehyde.^{4, 12} Aldehydes are reactive substances that can bind to proteins, phospholipids and DNA.³⁶⁷ This modification by glucose is referred to as “non-enzymatic glycation”. It involves a series of complex steps, few of which are known with certainty because these molecules can undergo a variety of intramolecular rearrangements, producing intermediates that are also sensitive to oxidative modification.^{12, 367}

Glycation products can be oxidised to give AGEs, which are formed inside and outside cells as a function of glucose concentration.¹² Recent work has supported a central role for ROS in both AGE formation and in AGE-induced pathological gene expression alterations.^{5, 12, 121} AGE formation is irreversible, occurs over months to years and can cause tissue damage.^{6, 12, 367} For example, their accumulation in collagen decreases the elasticity of connective tissue, impairs blood vessel function and damages the kidney basement membranes.^{5, 6, 353, 368-370} Additionally, AGEs are thought to contribute to endothelial cell injury, while in diabetics, AGEs are present on circulating LDLs and in atherosclerotic lesions.^{353-357, 371-373}

Another method for AGE formation involves the initial oxidation of glucose (“autoxidation”) and then its reaction with proteins.³⁵⁷ This whole process is called “glycooxidation”. Monosaccharide oxidation is catalysed by traces of iron and copper ions to produce $O_2^{\bullet-}$, H_2O_2 , OH^{\bullet} and toxic carbonyls.^{12, 374} These all damage lipids, proteins and DNA in addition to accelerating AGE formation, which would in turn, supply more free radicals.³⁷⁵

AGEs had been thought to only form on long-lived extracellular macromolecules, as the rate of glucose-induced AGE formation was slow.^{357, 368, 373} However, recently, it was shown that AGEs formed on proteins *in vivo*.¹² After a week, AGE content increased 13.8-fold in endothelial cells cultured in high glucose.^{12, 140, 368, 376} This extremely rapid rate of AGE formation is believed to reflect the hyperglycaemic-mediated increases in

intracellular glycolytic intermediates; like fructose, glyceraldehyde-3-phosphate and glucose-6-phosphate, which are much more reactive than glucose.^{140, 376} Also, intracellularly, glucose and other sugars can form AGEs by their adduction to DNA in a reaction with the amino groups of bases. This can affect all aspects of DNA metabolism, causing increased mutation rates, ineffective repair and cross-linking of the DNA to local histone proteins.^{28, 246, 377}

Both glycated and AGE-modified proteins can lead to oxidative stress. They directly release $O_2^{\bullet-}$ or H_2O_2 and activate phagocytes.^{12, 14} Several cells, including monocytes, endothelial cells, SMCs and macrophages, recognise AGEs using a cell surface receptor, "RAGE".^{378, 379} RAGE enables monocyte migration and glycosylated cell recognition and engulfment by macrophages. On endothelial cells RAGE stimulation activates NF- κ B, up-regulates adhesion molecule production, increases vascular permeability, decreases glutathione levels and enhances vessel wall protein and lipoprotein deposition.^{12, 62, 146, 280, 380, 381} Moreover, its expression is enhanced in diabetic vasculopathy and in arteriosclerotic lesions.¹²¹ However, RAGE activity and function *in vivo* remains unclear and the pathological significance of AGE-induced oxidative stress in biological systems is still uncertain.

1.11 DIABETES AND OXIDATIVE STRESS

There appears to be higher levels of oxidative stress in diabetic patients.^{4, 120, 325} However, the significance of this in the underlying pathology is still uncertain. Moreover, it is impossible at this stage to define whether:

- hyperglycaemia impairs antioxidant defences;^{4, 329}
 - hyperglycaemia increases radical generation;^{329, 382}
 - subjects with impaired antioxidant defences are susceptible to diabetes;³⁸³
- or
- subjects with abnormally high radical generation rates are diabetes-prone.⁵⁵

There is a wealth of evidence that links hyperglycaemia to increased oxidative stress. For example, the increased production of malondialdehyde, a marker of lipid peroxidation and cellular OH[•] damage, has been found in erythrocyte membranes from people with diabetes.^{12, 384} Further, the erythrocyte GSH content is inversely related to glycaemic control.^{9, 12, 383}

Clinical studies by Halliwell and Nourooz-Zadeh (1997) demonstrated an approximate twofold increase in the plasma oxidative stress measures of 8-epi-prostaglandin F_{2α} (8-epi PGF_{2α}; a marker derived from free radical oxidation of phospholipids containing arachidonic acid) and ROOH (a reliable marker of hydroperoxides) in diabetic patients when compared to healthy subjects.^{12, 385-387} The relationship between hydroperoxides and the level of the antioxidant RRR-α-tocopherol (vitamin E) was also assessed.³⁰⁸ Subsequently, a three- to six-fold imbalance between increased levels of oxidative stress and the depletion of RRR-α-tocopherol was observed in the plasma of diabetic patients. In addition, Davi *et al.* (1999) reported that the increased urinary release of 8-epi-PGF_{2α} detected in type 1 and 2 diabetic patients could be normalised by the improvement of glycaemic control.^{12, 388}

Others have documented a relationship between the markers of lipid peroxidation, serum O₂^{•-} and glycaemic control in both type 1 and type 2 diabetes.^{4, 5, 63, 120, 325, 384, 389-392} Using 8-oxo-dG as an indicator of oxidative DNA damage, Dandona *et al.* (1996) showed that DNA damage in type 1 diabetes was four times higher than in non-diabetic controls.^{325, 326} In other investigations, type 1 and 2 diabetic patients showed greater oxidative DNA damage, with increased ROS generation.^{19, 121, 325, 327-329, 393} Importantly, these observations support previous findings linking hyperglycaemia with DNA glycosylation and decreased DNA repair.^{121, 284, 393-396}

Antioxidant enzymes levels have been shown to be increased or unaltered in the nonvascular beds of diabetic animals.^{5, 120, 325, 328, 329} However, in the vascular beds and cardiac tissues of diabetic animals, there was an increase in catalase, but not SOD or Gpx, which has been interpreted as proof that

diabetic blood vessels are chronically exposed to H_2O_2 .^{325-328, 346, 394} These discrepancies may have resulted from enzyme activity fluctuations and differences in the types of tissue under examination. Similarly, the finding that diabetic patients have lower enzymatic and non-enzymatic antioxidant defences remains controversial and has often been misinterpreted – it is likely that they represent chronic consumption, and therefore, the depletion of antioxidant defences is due to chronic oxidant stress.

Hyperglycaemia has been shown to increase LDL susceptibility to oxidation through glucose-mediated $O_2^{\bullet-}$ generation.^{12, 17, 28, 56, 64, 299, 397-399} The resultant fully oxidised LDLs appeared to be able to induce the transformation of macrophages and SMCs into foam cells, an effect also shared by glycosylated LDLs.^{6, 13, 17, 43, 396, 400} In fact, *in vitro* experiments demonstrated that the extent of LDL glycation varied with the duration of LDL incubation and glucose concentration.^{9, 377} Thus, hyperglycaemia was coupled to lipoprotein composition abnormalities and both, in turn, are atherogenic.

All in all, there are multiple sources of evidence that associate diabetes with increased ROS production and it is likely that the latter leads to the consumption of cellular antioxidant defences.

1.12 DNA REPAIR

All aerobic cells require repair enzymes to rectify damaged DNA. Such enzymes need to work accurately and efficiently as cells usually arrest their division until restoration is completed.^{113, 195, 226, 401, 402} Even though DNA polymerases show high fidelity due to their error correcting properties, mistakes are still made and so repair becomes essential.^{204, 248, 403}

DNA isolated from aerobic cells contain low levels of DNA base damage and this increases with age, suggesting that the repair enzymes do not remove all of the modified bases.²⁹⁰ Damage recognition could be the rate-limiting step during repair because over 10^9 mammalian base pairs have to be patrolled in order to locate the lesions.^{248, 267} Interestingly, the steady-state levels of base damage products have been observed to increase in many diseases associated with raised ROS production.^{12, 290, 311, 404}

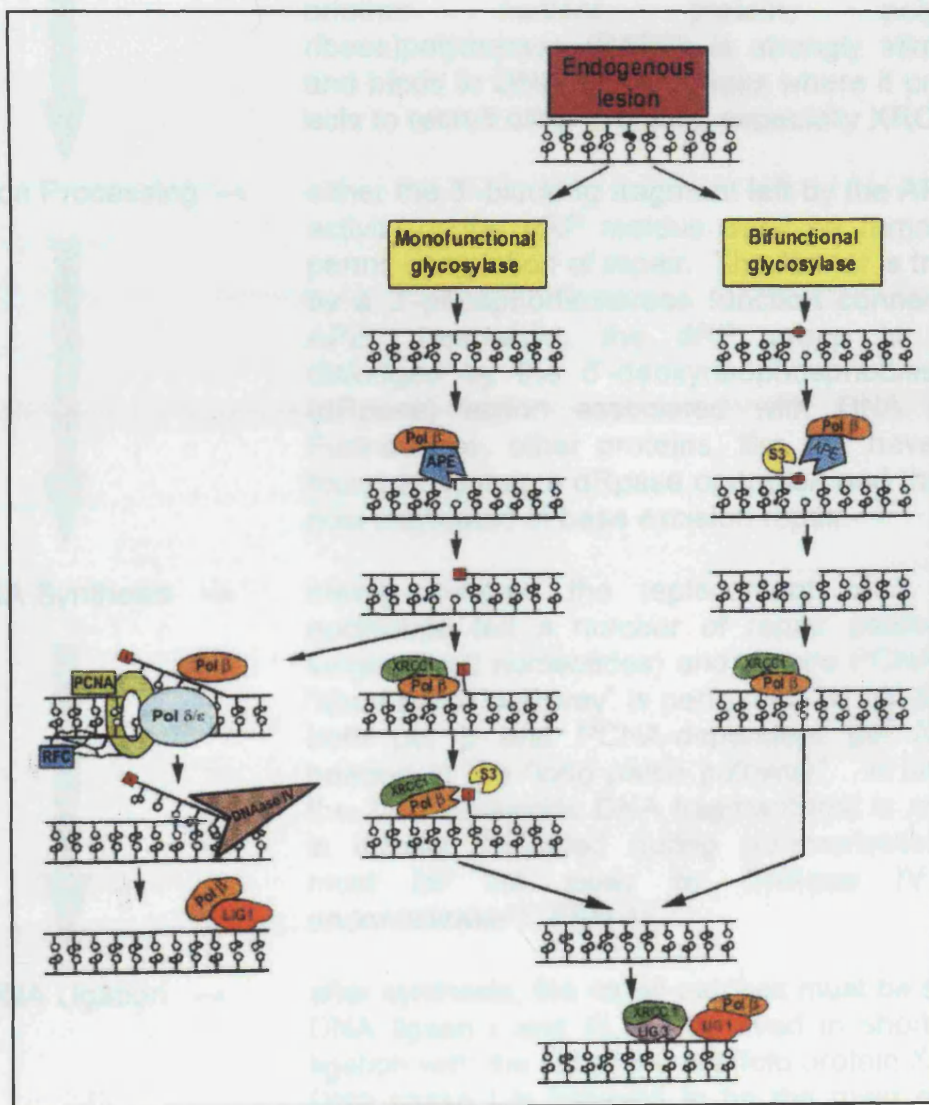
Due to the deleterious consequences of DNA damage for the cell, organism and species, cells possess sophisticated systems for rapidly repairing damaged DNA and preserving its information content. Such repair pathways include "Direct Reversal" (single enzymes catalyse the reversal and DNA ligase rejoins the single-strand breaks), "Mismatch Repair" (correction of mispaired bases, often due to an error in replication), "Recombinational Repair" (occurs when both DNA helix strands are damaged and there is no intact template for the DNA polymerase to copy) and "Excision Repair" (involved in much of the cellular DNA repair, especially to oxidative DNA damage).^{49, 121, 140, 405-410}

1.12.1 EXCISION REPAIR

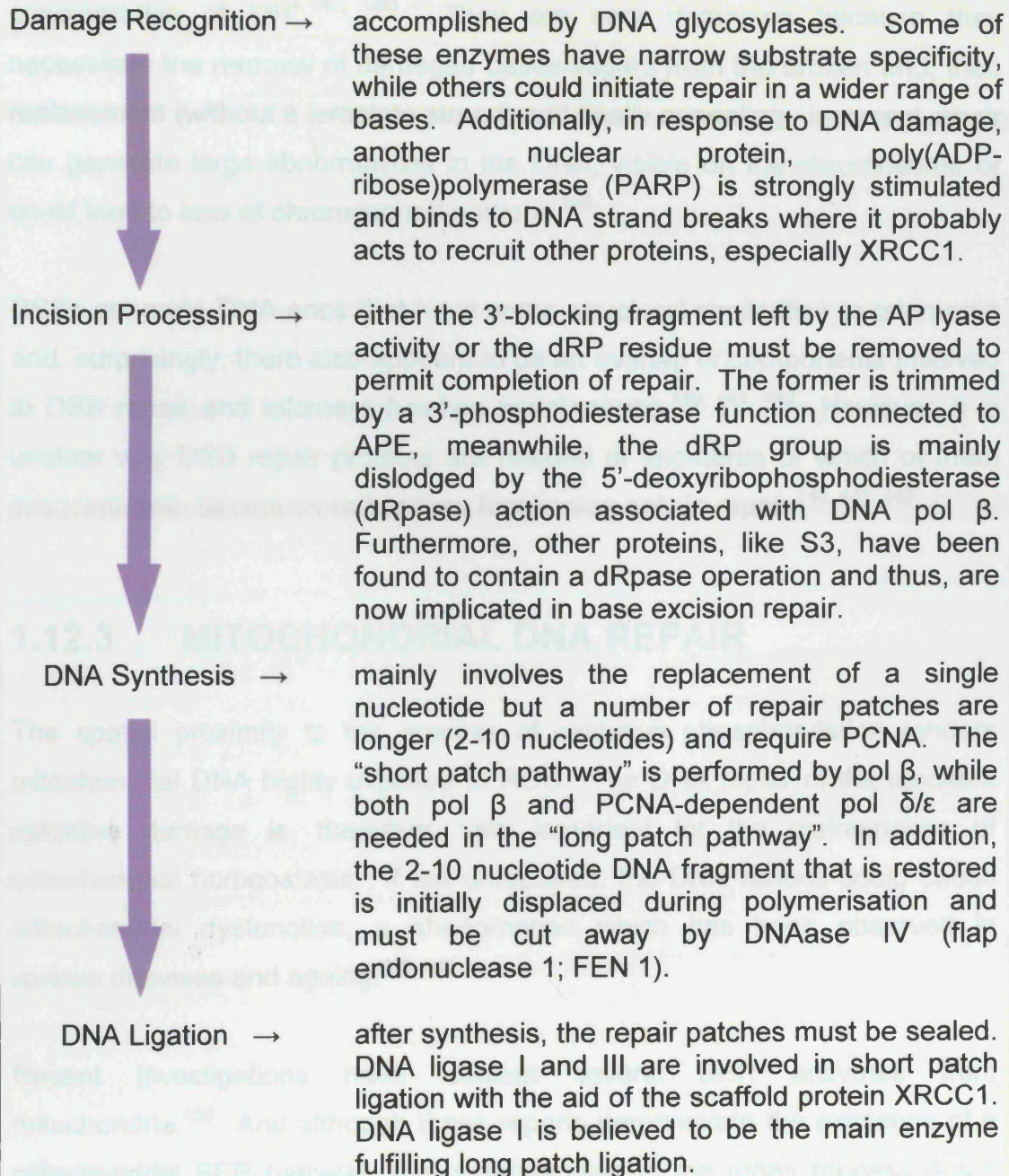
Essentially, mispaired, oxidised and deaminated bases are removed from DNA by the same types of mechanisms. In the first type, the damaged base is removed directly (“base excision repair”; BER).¹¹³ DNA glycosylase enzymes hydrolyse the bond linking the abnormal base to the sugar-phosphate backbone.¹¹³ Their action leaves behind an apurinic or apyrimidinic site (AP site). Such sites can also arise from spontaneous base loss in DNA.^{12, 182} These sites are mutagenic and hinder DNA transcription and replication. Enzymes (sometimes part of the glycosylase itself) recognise AP sites and nick the DNA on both sides of the missing base (an AP lyase cleaves the 3'-side and an AP endonuclease the 5'-side), so releasing an AP-deoxyribose. DNA polymerase then fills in the one-nucleotide gap with the correct base as dictated by the undamaged complementary strand. Finally, a ligase seals the DNA (figure 1-9, page 54 and box 1-1, page 55).²⁴⁸

In the second type, DNA is cut on both sides of the lesion by a multisubunit ATP-dependent exonuclease complex. A helicase then removes the damaged oligonucleotide leaving a gap of 27-29 nucleotides in eukaryotes. A DNA polymerase fills this gap (using information from the undamaged strand of DNA) and a ligase seals the DNA leading to the restoration of the original DNA sequence.^{113, 182} This process is called “nucleotide excision repair” (NER). It is the most general repair pathway in all organisms and is responsible for the renovation of a wide range of damage.^{12, 113, 182} It is particularly efficient in dealing with bulky lesions that distort the DNA double helix and may contribute to oxidative damage repair, although this remains unclear.^{46, 121, 310, 411}

Figure 1-9: Outline of the DNA base excision repair pathways in mammals. Glycosylases are classified as monofunctional or bifunctional according to whether they possess an AP lyase activity. Monofunctional glycosylases only remove the damaged base to leave an AP site, which is then incised at the 5'-terminus by an AP endonuclease (APE) leaving a 5'-terminal 2-deoxyribose-5-phosphate (dRP) and 3'-OH priming terminus. In case of bifunctional glycosylases, the AP site generated is cut further at the 3'-side via β -elimination to produce an obstructive 3'-end. XRCC1, X-ray cross-complementing 1; Pol $\beta/\delta/\epsilon$, DNA polymerase $\beta/\delta/\epsilon$; PCNA, proliferating cell nuclear antigen; RFC, replication factor C; LIG1, DNA ligase I; LIG3, DNA ligase III. (Adapted from reference 411)



Box 1-1: Breakdown of base excision repair. dRP, 5'-terminal 2-deoxyribose-5-phosphate; XRCC1, X-ray cross-complementing 1; APE, AP endonuclease; Pol $\beta/\delta/\epsilon$, DNA polymerase $\beta/\delta/\epsilon$; PCNA, proliferating cell nuclear antigen. (Adapted from references 49, 121, 140, 187, 191, 319, 324, 375, 412-438)



1.12.2 DOUBLE-STRAND BREAK REPAIR

Methods that cope with DNA double-strand breaks (DSBs) must exist because such breaks occur naturally during recombination.³⁷⁴ With regard to oxidative stress, DSBs probably result from multiple OH[•] attacks on a short DNA stretch with the number of breaks increasing in proportion to the concentration of OH[•].^{140, 290} They are very damaging because they necessitate the removal of damaged bases/sugars from the broken end, their replacement (without a template strand) and finally annealing. Incorrect repair can generate large abnormalities in the DNA, visible on the chromosome or could lead to loss of chromosomal portions.²⁴⁸

DSBs generate DNA ends that have some structural similarities to telomeres and, surprisingly, there also appears to be an overlap of components involved in DSB repair and telomere function maintenance.^{140, 441, 442} However, it is unclear why DSB repair proteins are needed at telomeres or which of them associate with telomeres rather than functioning only in repair.^{140, 441, 442}

1.12.3 MITOCHONDRIAL DNA REPAIR

The spatial proximity to the process of oxidative phosphorylation renders mitochondrial DNA highly exposed to ROS. The DNA repair of the resultant oxidative damage is, therefore, very important for the maintenance of mitochondrial homeostasis. If left unrepaired, the DNA lesions could cause mitochondrial dysfunction, a phenomenon which has been observed in various diseases and ageing.^{439, 440}

Recent investigations have isolated several BER enzymes from mitochondria.⁴³⁹ And although these reports demonstrate the existence of a mitochondrial BER pathway, the understanding of the repair process is still very limited.

HYPOTHESIS

I propose that diabetes is a state of accelerated human endothelial cell ageing. This ageing is due to glucose-driven oxidative damage to telomeric and mitochondrial DNA, culminating in premature endothelial cell senescence.

AIMS AND OBJECTIVES

The work contained in this thesis explores this hypothesis in cultured HUVECs with the following specific aims:

1. To define and characterise the effects of elevated extracellular glucose concentrations on HUVEC DNA damage.
2. To ascertain whether glucose-induced HUVEC DNA damage is mediated via glucose-driven oxidative stress.
3. To determine the effects of elevated extracellular glucose concentrations on the growth characteristics of HUVECs and the development of cell senescence.
4. To define the effects of elevated extracellular glucose concentrations on the rate of telomere attrition in HUVECs and whether any enhanced attrition is dependent on glucose-driven oxidative stress.
5. To examine the efficiency of DNA repair in HUVECs and the impact of elevated extracellular glucose concentrations on DNA repair.
6. To determine whether elevated extracellular glucose concentrations lead to an accelerated loss of mitochondrial DNA in HUVECs.
7. To determine the effects of elevated extracellular glucose concentrations on the expression of mitochondrial electron transport chain proteins in HUVECs.

Chapter 2 : MATERIALS AND METHODS

2.1 MATERIALS

The tissue culture reagents were purchased from Invitrogen (Paisley) and unless otherwise stated, all the other chemicals were purchased from either Sigma (Dorset) or Fisher (Leicestershire).

2.2 METHODS

2.2.1 COMET ASSAY TECHNIQUE

Primary endothelial cell cultures were established from human umbilical veins taken from umbilical cords at delivery. A colleague set up the initial cultures and froze the HUVECs for storage using standard techniques.^{443, 444, 445, 446}

These were rejuvenated, seeded, maintained on 1% (v/v) gelatin coated 25cm² flasks (Nunc Brand Products; Roskilde, Denmark) with 4ml HUVEC media and incubated at 37°C (5% (v/v) CO₂–95% (v/v) air atmosphere) until usage. Separate HUVEC lines were used for every experiment. The media contained Medium 199, 20% (v/v) foetal calf serum, penicillin (100iu/ml)-streptomycin (100µg/ml) mix, 0.5% (v/v) endothelial cell growth factor, heparin (10iu/ml; CP Pharmaceuticals; Wrexham), 200µM sodium pyruvate and 20mM N-[2-hydroxyethyl]piperazine-N'-[2-ethane-sulfonic acid] (HEPES).

To begin with, cleaned etched microscope slides (Merck; Dorset) were chilled on ice for 10 minutes before being dipped into 1% (w/v) normal melting point (NMP) agarose (Invitrogen). The slides were then dried at 50°C for 1-2 hours. During this period, the cells were prepared.

In dimmed light (to minimise UV-induced DNA damage), the cells were washed with 6ml warmed phosphate-buffered saline (PBS; Dulbecco's), aspirated and incubated with 1ml warmed 0.1% (w/v) trypsin-0.02% (w/v) diaminoethanetetra-acetic acid disodium salt (EDTA). After 3 minutes, 3ml

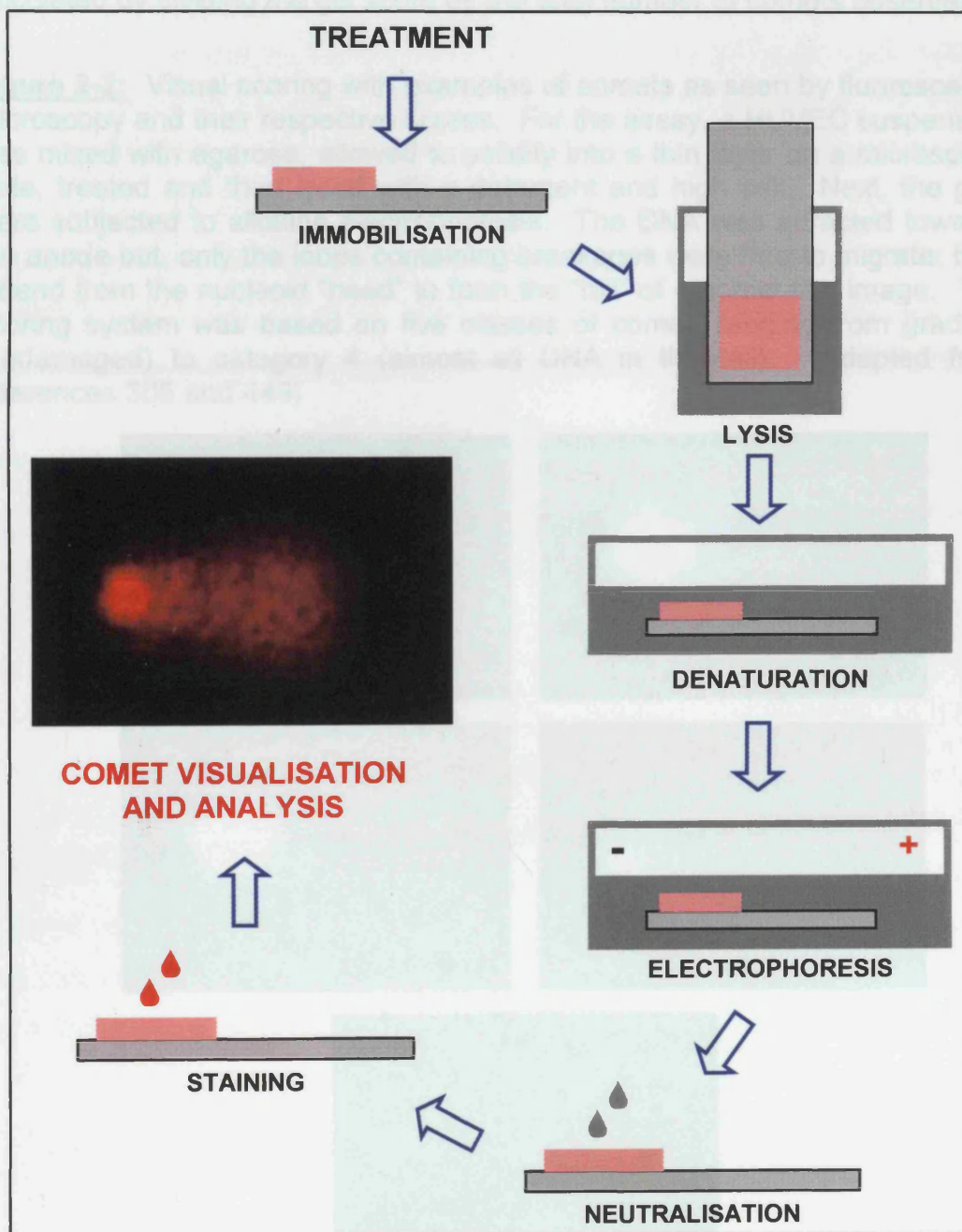
cold PBS was added and the solutions mixed. HUVECs were collected, centrifuged for 5 minutes at 172g and the supernatant discarded. The resultant pellet was re-suspended in 1ml PBS and counted in an Improved Neubauer haemocytometer. The appropriate cell number was then centrifuged for 3 minutes at 3300g. The supernatant was again discarded and the pellet warmed before being re-suspended in 0.6% (w/v) low melting point (LMP) agarose in PBS at 37°C. Approximately 2×10^4 HUVECs (in 50µl LMP agarose) were added onto each slide, overlaid with a cover slip and cooled for 10 minutes on ice. The cover slips (18x18mm) were then removed and the slides positioned into Wilson jars containing the treatment solutions. The treatment conditions varied from experiment to experiment and the details of each assay are described in the results section.

After their conditioning, the slides were immersed into cleaned Wilson jars containing 25ml ice-cold freshly prepared lysis solution (2.5M NaCl, 100mM EDTA, 10mM Tris, 1% (v/v) Triton X-100, pH 10) and left overnight at 4°C. The following day, the slides were washed in 1xTE buffer (10mM Tris-HCl, 1mM EDTA, pH 8) for 15 minutes before being covered with fresh electrophoresis buffer (0.3M NaOH, 1mM EDTA, pH ≥ 13) for 20 minutes in a horizontal electrophoresis unit on ice. Electrophoresis was then performed at 25V and 300mA for 20 minutes. Next, the slides were washed in neutralisation buffer (0.4M Tris, pH 7.5) for 15 minutes. Thereafter, the slides were fixed with ethanol for 5 minutes and allowed to dry for 1-2 hours at room temperature. Immediately prior to visualisation, under a green-blue florescent light (wavelength 485nm), each cell layer was re-hydrated with 60µl SYBR™ Green (1:10000 dilution; Molecular Probes; Eugene, USA) or 60µl ethidium bromide (10µg/ml), and overlaid with a cover slip (figure 2-1, page 60).

The comets were clearly distinguishable and assessed through a scoring system.^{447, 448} A KOMET computer (Kinetic Imaging; Liverpool) was also used for comet analysis and this allowed more detailed recordings of individual comet datum using a Nikon Super High Pressure Mercury Lamp microscope (Nikon Eclipse E400; Liverpool) and the KOMET 5 Single Cell Gel Electrophoresis Analysis (Kinetic Imaging) software linked to a Charge

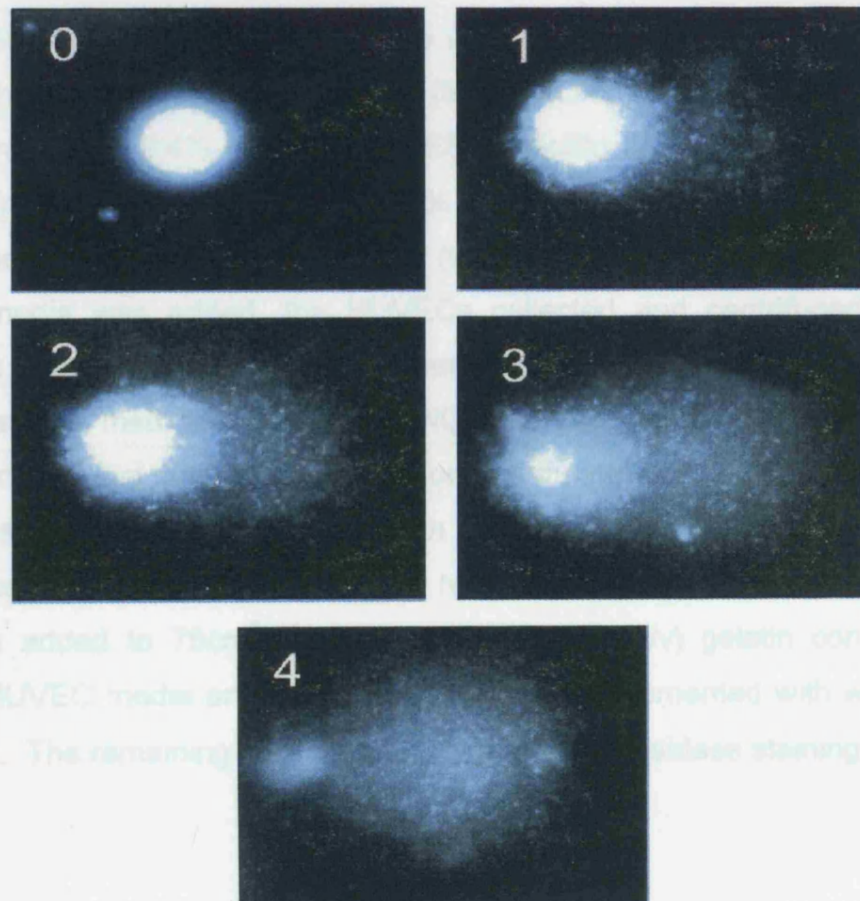
Coupled Device (CCD) camera. All the slides were scored in a blind fashion with at least 100-150 cells being viewed by randomly selecting multiple microscopic fields.

Figure 2-1: Diagrammatic representation of the comet assay technique. Experimentally, a treated HUVEC suspension was mixed with agarose, allowed to solidify into a thin layer (pink) on a microscope slide (light grey) and then lysed with a detergent and high salt. Next, the HUVEC DNA was denatured and the gels were subjected to alkaline electrophoresis. Thereafter, the slides were washed with neutralisation buffer and immediately prior to visualisation, the gel layer was re-hydrated with a staining solution.



The comets were judged either visually or by using densitometry linked to a computer-based image analysis programme. In both methods, completely obliterated comets and those at the gel edges were avoided because they tended to contain anomalously high damage levels. The scoring system was based on five recognisable classes of comet, ranging from grade 0 (undamaged, no discernible tail) to category 4 (almost all DNA in the tail, insignificant head), to distinguish between the different DNA injury levels (figure 2-2).³⁰⁵ Each comet was therefore given a value and every gel an overall score. This allowed the DNA damage per cell for each gel to be calculated by dividing the gel score by the total number of comets observed.

Figure 2-2: Visual scoring with examples of comets as seen by fluorescence microscopy and their respective scores. For the assay, a HUVEC suspension was mixed with agarose, allowed to solidify into a thin layer on a microscope slide, treated and then lysed with a detergent and high salt. Next, the gels were subjected to alkaline electrophoresis. The DNA was attracted towards the anode but, only the loops containing breakages were free to migrate: they extend from the nucleoid “head” to form the “tail” of a comet-like image. The scoring system was based on five classes of comet, ranging from grade 0 (undamaged) to category 4 (almost all DNA in the tail). (Adapted from references 305 and 449)



2.2.2 HUMAN UMBILICAL VEIN CELL CULTURE

Primary endothelial cell cultures were established from human umbilical veins taken from umbilical cords at delivery. A colleague set up the initial cultures and froze these cells for storage using standard techniques.^{443, 444, 445, 446} At the start of the experiment, the HUVECs were rejuvenated, seeded on 75cm² flasks coated with 1% (v/v) gelatin and maintained in HUVEC media. Separate HUVEC lines were used for every experiment. All the cultures were incubated in 12ml media at 37°C (5% (v/v) CO₂–95% (v/v) air atmosphere). When confluent, the HUVECs were passaged and 6x10⁵ cells were seeded per 75cm² flask. To study the effects of high glucose (HG), the growth media was supplemented with freshly prepared D-glucose to achieve a final concentration of 22mM. Exposure to HG began at passage three. The control glucose concentration (normal glucose; NG) was 5.5mM. Media was changed every two days to keep the glucose concentrations relatively constant.

When sub-culturing, all the flasks were aspirated, washed twice with 15ml warmed 1x Modified Essential Media (MEM) (Life Technologies, Paisley) supplemented with 2.4% (v/v) 1M HEPES, penicillin (200iu/ml)-streptomycin (200µg/ml) mix, 2.5µg/ml fungizone, 0.2% (v/v) 1M NaOH and incubated with 3ml warmed 0.1% (w/v) trypsin-0.02% (w/v) EDTA. After 2 minutes, 6ml warmed media was added, the HUVECs collected and centrifuged for 5 minutes at 172g. The resultant pellets were aspirated and then re-suspended in 3ml warmed medium. Next, the NG and HG cells were pooled into separate centrifugal tubes and stored on ice during counting. Cells were counted using 0.2% (w/v) Trypan blue in PBS, gently agitated for 2 minutes and counted in an Improved Neubauer haemocytometer. Next, 6x10⁵ cells were then added to 75cm² flasks coated with 1% (v/v) gelatin containing warmed HUVEC media and the HG flasks were supplemented with warmed D-glucose. The remaining cells were used for β-Galactosidase staining and in

the making of genomic DNA plugs for telomere analysis (sections 2.2.3 and 2.2.4, respectively).

2.2.3 β -GALACTOSIDASE STAINING

Cells were seeded on 25cm² flasks coated with 1% (v/v) gelatin containing 4ml HUVEC media and stained 48 hours later. HUVECs were washed twice in 6ml warmed PBS and fixed for 3¼ minutes at room temperature with 4ml 1% (v/v) formalin in PBS. After two further washes in 6ml warmed PBS, cultures were incubated for 24 hours at 37°C in 2.5ml warmed senescence-associated β -Galactosidase (SA- β -Gal; pH 6.0) staining solution containing 1mg/ml 5-bromo-4-chloro-3-indolyl- β -D-galactopyranoside (X-Gal), 5mM potassium ferricyanide, 5mM potassium ferrocyanide, 150mM NaCl, 2mM MgCl₂, and 40mM NaH₂PO₄ (pH 6.0).

β -Galactosidase staining was microscopically (Nikon Diaphot-TMD; New York, USA) revealed by the presence of a blue, insoluble precipitate within the cell. The percentage of SA- β -Gal-positive cells was determined by counting at least 700 cells in each sample under bright field illumination. To ensure a representative count, each 25cm² flask was divided into quarters and at least 175 cells were counted in each quarter.

2.2.4 SOUTHERN ANALYSIS PROCEDURE

Cells were centrifuged for 3 minutes at 1700g with the supernatant being discarded. They were then washed once in 1ml cold PBS, centrifuged and aspirated. The resultant pellet was re-suspended in Buffer L (0.1M EDTA, 10mM Tris, 20mM NaCl, pH 7.5) at a concentration of 1x10⁴ cells/ μ l. Next, the cells were briefly warmed at 42°C before an equal volume of 1.2% (w/v) LMP agarose (FMC Bioproducts; Maine, USA) in Buffer L was added. The solutions were mixed to form a homogenous suspension and before the HUVECs settled, they were drawn into cleaned rubber tubing and placed on ice for 10 minutes. Thereafter, the plugs were removed from their tubing,

immersed in their digestion buffer (5 volumes of Buffer L containing 1% (v/v) sarkosyl and 1mg/ml proteinase K) and incubated at 50°C. Two days later, the plugs were washed for 30 minutes each in 50 volumes of TE (10mM Tris-HCl, 1mM EDTA, pH 7.5), TE (10 volumes) with 1mM phenyl-methylsulphonyl-fluoride (PMSF) followed by two further washes in TE (50 volumes). Finally, the plug was stored in 4ml 0.5M EDTA at 4°C until restriction enzyme digestion. For this, a 1cm (1.25µg DNA) plug section was cut and washed for 30 minutes in two reagents – twice in TE (50 volumes) and once in 50 volumes of restriction enzyme buffer (50mM Tris pH 8, 10mM MgCl₂). The plug was then added to 2µl *Hinf*1 (20 units) in 150µl restriction enzyme buffer and incubated at 37°C for at least 16 hours.

Prior to their electrophoresis, the plugs were washed in 1ml 1xTAE (40mM Tris-acetate, 1mM EDTA), the electrophoresis buffer. They were then melted and analysed in a 0.5% (w/v) agarose gel along with the 1kb ladder and high molecular weight (HMW) DNA markers (Invitrogen). Electrophoresis was performed at 2.1V/cm.

After 16 hours, the gel was stained with ethidium bromide (0.5µg/ml) for 1 hour and washed with distilled water for 1-2 hours. Next, it was agitated with depurinating (0.125M HCl), denaturing (1.5M NaCl, 0.5M NaOH) and neutralising (1.5M NaOH, 0.5M Tris, pH 7.5) solutions for 20, 30 and 30 minutes respectively. Between each reagent wash, the gel was briefly bathed in distilled water. The gel was then blotted through capillary transfer with 20xSSC (0.3M Tris-sodium citrate, 3M NaCl, pH 7-8) to Hybond-*N* membrane (Amersham Pharmacia Biotech; Buckinghamshire) for at least 16 hours. The membrane was then UV cross-linked at 0.200joules/cm before the non-radioactive DIG system was employed. This used digoxigenin (DIG) to label DNA for hybridization and subsequent luminescent detection. Briefly, an oligonucleotide (TTAGGG)₄ labelled with DIG (Sigma-Genosys; Cambridge) was purified and hybridized to the membrane according to the manufacture's DIG High Prime DNA Labelling and Detection Starter Kit II (Roche; Lewes) instructions. Thereafter, the hybridized probes were immunodetected with anti-digoxigenin, Fab fragments conjugated to alkaline phosphatase and

visualised with the chemiluminescence substrate CSPD (DIG Luminescent Detection Kit; Roche). The enzymatic dephosphorylation of CSPD by alkaline phosphatase led to light emission at a maximum wavelength of 477nm which was recorded on X-ray films. After exposure, the telomeres were visualised on Kodak X-ray films (Sigma) and were analysed using the Alphamager™ 1220 analyser (Flowgen; Leicestershire) and EXCEL (Microsoft) software.

2.2.5 DNA REPAIR NUCLEOTIDE INCISION ASSAY

Primary endothelial cell cultures were established from human umbilical veins taken from umbilical cords at delivery. A colleague set up the initial cultures and froze the HUVECs for storage using standard techniques.^{443, 444, 445, 446} These were rejuvenated, seeded, maintained on 1% (v/v) gelatin coated 25cm² flasks with 4ml HUVEC media and incubated at 37°C (5% (v/v) CO₂–95% (v/v) air atmosphere) until usage. Separate HUVEC lines were used for every experiment. Next, the cells underwent their treatment (detailed in Chapter 6) before being harvested. For this, the flasks were aspirated, washed twice with 15ml warmed 1xMEM and incubated with 3ml warmed 0.1% (w/v) trypsin-0.02% (w/v) EDTA. After 2 minutes, 6ml warmed media was added, the HUVECs collected and centrifuged for 5 minutes at 172g. The resultant pellets were aspirated and then re-suspended in 1ml warmed media. Afterwards, the cells were centrifuged for 10 minutes at 620g at 4°C before being manually homogenised, re-suspended in 100µl freshly prepared DNA repair buffer (0.5M Tris pH 7.4, 0.5M KCl, 50mM magnesium acetate, 30mM EDTA, 1% (v/v) glycerol, 30mM β-mercaptoethanol, 5mM dithiothreitol (DTT), 0.1mg/ml PMSF, 10% (v/v) protease inhibitor cocktail (1.04M 4-(2-Aminoethyl)benzenesulfonyl fluoride (AEBSF), 800µM Aprotinin, 21mM Leupeptin, 36mM Bestatin, 15mM Pepstatin A, 14mM E-64), pH 7.4) and stored at -80°C overnight.

The following day, all the samples were dialysed against 1 litre HEPES-based buffer (20mM HEPES, 5mM EDTA, 5% (v/v) glycerol, 5mM DTT, 100mM KCl, pH 7.4) overnight at 4°C. After dialysis, the samples are drawn from the

dialysis membrane (12-14kDa molecular weight cut off; Medicell; London) and centrifuged for 1 minute at 3300g.

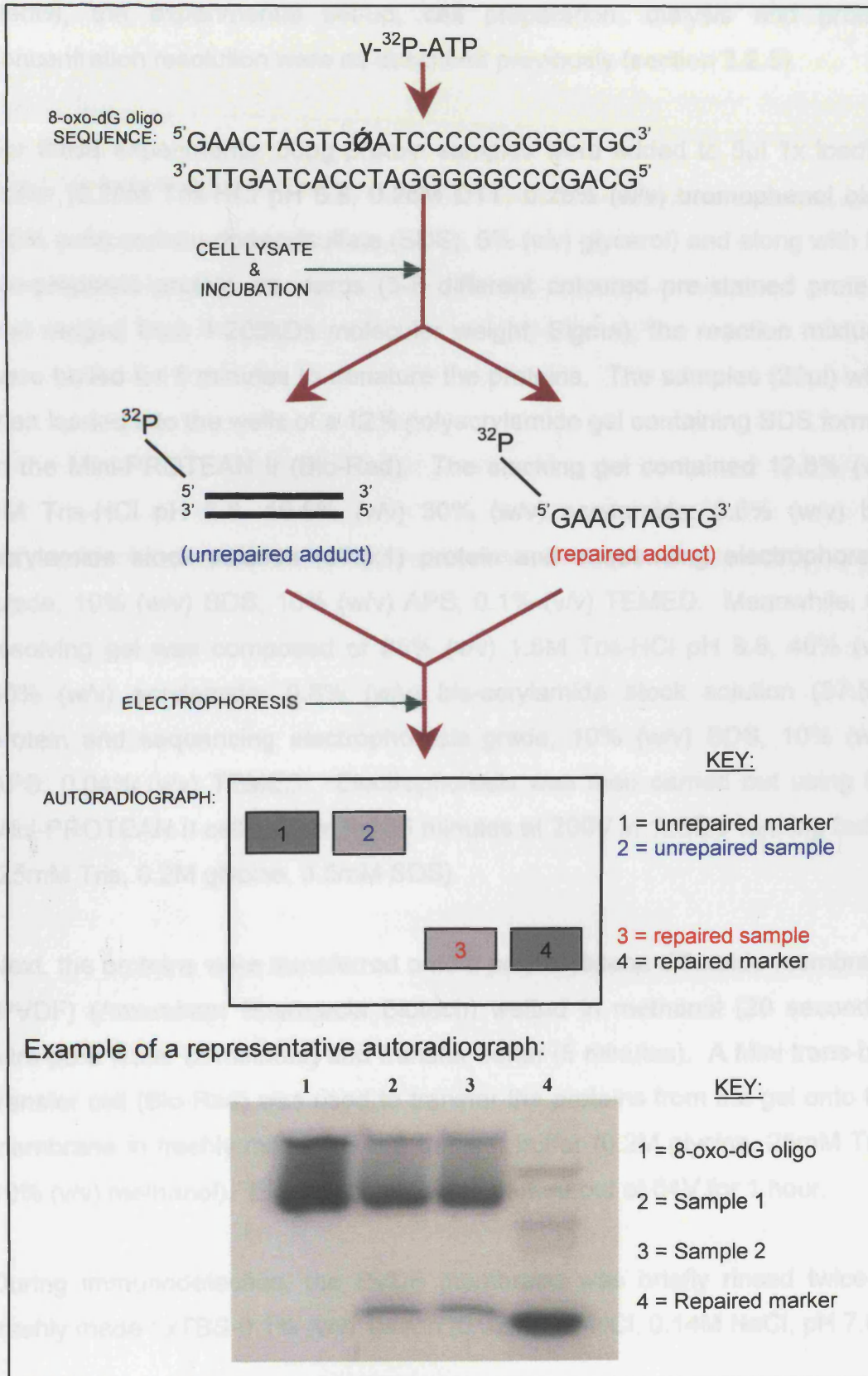
Next, the protein concentration was determined using the Bradford assay (Bio-Rad assay). The absorbance at 595nm (A_{595}) was measured for known concentrations of bovine serum albumin (BSA) samples ranging from 0-20 μ g/ml on addition of 200 μ l Bradford Assay Reagent Concentrate (Bio-Rad; Hemel Hempstead). A standard curve showing the relationship between A_{595} and the amount of BSA was constructed to determine the protein concentrations after measuring A_{595} of the samples containing 1-5 μ l of unknown proteins. To calculate the protein concentration, the concentration of BSA corresponding to the absorbance value of the specimen that intersected the standard curve was divided by the protein volume in that sample. An average protein concentration from the samples then gave the overall estimate.

After sample protein concentration determination, the oligonucleotide reagents required preparation. For this, both the 8-oxo-dG Oligonucleotide (Trevigen; Abingdon Oxon) and 9-mer repair product marker (a kind gift from Dr Karl Herbert) were labelled with 32 P (Amersham Pharmacia Biotech). The probe used had the following nucleotide sequence: $5'$ GAACTAGTG ϕ ATCCCCCGGGCTGC $3'$ (where ϕ was 8-oxoguanine).³¹¹ 8-oxo-dG (5pmol) was labelled with 5 μ l (1.85MBq) γ - 32 P-ATP in the presence of 5x forward reaction buffer (Invitrogen) and T4 polynucleotide kinase (Invitrogen). These reactions were incubated for 30 minutes at 37°C, heated at 75°C for 10 minutes and then placed on ice for 3 minutes. Subsequently, the reaction mixtures were spin pulsed and warmed to room temperature before Oligo Complement A (5pmol; Trevigen) was added to the labelled 8-oxo-dG Oligonucleotide and left at room temperature for 10 minutes to anneal. Thereafter, oligonucleotide purification ensued to ensure the removal of any enzymes, salts and unincorporated nucleotides. QIAquick Nucleotide Removal Kit (QIAGEN; Crawley) was used for this process according to the manufacture's instructions.

Next, 6 μ l (approximately 150fmols) purified labelled complemented 8-oxo-dG Oligonucleotide was added to the samples (50 μ g protein) and incubated at 37°C for 4 hours. For analysis, 10 μ l 3x denaturing buffer (300mM NaOH, 97% (v/v) de-ionizing formamide, 0.2% (w/v) bromophenol blue) was added to each specimen, heated to 95°C for 10 minutes and then rapidly cooled to 2°C for 5 minutes. Finally, the cleavage products were resolved by 20% denaturing polyacrylamide gel electrophoresis. The 20% acrylamide-TBE-UREA gel consisted of 50% (v/v) 30% (w/v) acrylamide: 0.8% (w/v) bis-acrylamide stock solution (37:5:1) protein and sequencing electrophoresis grade, 10% (v/v) 10xTBE (Bio-Rad), 42% (w/v) urea, 10% (w/v) ammonium peroxodisulphate (APS) and 0.15% (v/v) tetramethylethylenediamine (TEMED). It was pre-run using the Mini-PROTEAN II gel electrophoresis system (Bio-Rad) for 30 minutes at 15mA in 1xTBE (89mM Tris-borate, 2mM EDTA) before sample loading. Each sample and the 8-oxo-dG Oligonucleotide and 9-mer markers were loaded after which, the gel was run at 15mA for 90 minutes. Finally, the gel was gently rinsed in distilled water at room temperature for 2 minutes before being wrapped in cling film and subjected to autoradiography. After exposure, the bands were visualised on Kodak X-ray films and analysed using the Alphamager™ 1220 gel documentation system.

This procedure was employed to study the DNA repair activities of HG treated HUVECs to a radiolabelled synthetic oligonucleotide containing an 8-oxoguanine adduct. It worked on the principle that during cell manipulation, any increase in oxidative DNA damage would activate and/or up-regulate DNA repair. Furthermore, the enzymes and cofactors involved in subsequent DNA restoration would also be captured during sample collection and thus, they could be examined. Hence, upon the addition of the synthetic 24-mer oligonucleotide, hOGG1 would cleave the 8-oxoguanine, creating a 9-mer repair product that could then be separated by electrophoresis in a 20% polyacrylamide-TBE-UREA gel and visualised by autoradiography (figure 2-3, page 68).

Figure 2-3: Endonuclease assay used to assess HUVEC hOGG1 activity. Briefly, purified labelled double-stranded 8-oxo-dG oligonucleotide was incubated with the samples and the resultant cleavage products were resolved by gel electrophoresis. Finally, the gel was subjected to autoradiography. Ø, 8-oxoguanine; 8-oxo-dG oligo, double-stranded 8-oxo-dG oligonucleotide.



2.2.6 WESTERN BLOT ANALYSIS

The samples used in the nicking assay were additionally utilized for western blot analysis for the expression of repair endonuclease fraction 1 (Ref-1). Hence, the experimental set-up, cell preparation, dialysis and protein concentration resolution were as described previously (section 2.2.5).

For these experiments, 50 μ g protein samples were added to 5 μ l 1x loading buffer (0.25M Tris-HCl pH 6.8, 0.25M DTT, 0.25% (w/v) bromophenol blue, 2.5% (w/v) sodium dodecylsulfate (SDS), 5% (v/v) glycerol) and along with the pre-prepared protein standards (5-8 different coloured pre-stained proteins that ranged from 1-205kDa molecular weight; Sigma), the reaction mixtures were boiled for 5 minutes to denature the proteins. The samples (20 μ l) were then loaded into the wells of a 12% polyacrylamide gel containing SDS formed in the Mini-PROTEAN II (Bio-Rad). The stacking gel contained 12.6% (v/v) 1M Tris-HCl pH 6.8, 16.6% (v/v) 30% (w/v) acrylamide: 0.8% (w/v) bis-acrylamide stock solution (37:5:1) protein and sequencing electrophoresis grade, 10% (w/v) SDS, 10% (w/v) APS, 0.1% (v/v) TEMED. Meanwhile, the resolving gel was composed of 25% (v/v) 1.5M Tris-HCl pH 8.8, 40% (v/v) 30% (w/v) acrylamide: 0.8% (w/v) bis-acrylamide stock solution (37:5:1) protein and sequencing electrophoresis grade, 10% (w/v) SDS, 10% (w/v) APS, 0.04% (v/v) TEMED. Electrophoresis was then carried out using the Mini-PROTEAN II cell system for 55 minutes at 200V in 1xSDS running buffer (25mM Tris, 0.2M glycine, 3.5mM SDS).

Next, the proteins were transferred onto a polyvinylidene difluoride membrane (PVDF) (Amersham Pharmacia Biotech) wetted in methanol (20 seconds), ultra-pure water (2 minutes) and transfer buffer (5 minutes). A Mini trans-blot transfer cell (Bio-Rad) was used to transfer the proteins from the gel onto the membrane in freshly made 1.5 litre transfer buffer (0.2M glycine, 25mM Tris, 10% (v/v) methanol). Electrophoresis was carried out at 64V for 1 hour.

During immunodetection, the PVDF membrane was briefly rinsed twice in freshly made 1xTBS-0.1% (v/v) Tween (0.02M Tris-HCl, 0.14M NaCl, pH 7.6 –

0.1% (v/v) Tween-20), followed by a further two 5 minutes washes before being gently agitated in 100ml 10% (w/v) blocking solution (dried skimmed milk powder dissolved in TBS-0.1% (v/v) Tween) for 1 hour at room temperature. Afterwards, the membrane was again rinsed twice in TBS-0.1% (v/v) Tween before three 10 minute washes with gentle agitation. The excess TBS-0.1% (v/v) Tween was removed and the membrane incubated with the Ref-1 primary antibody (1:250 dilution in TBS-0.1% (v/v) Tween; BD Biosciences; Oxford) overnight at 4°C.

The next day, the membrane was briefly rinsed twice in freshly made TBS-0.1% (v/v) Tween, followed by another two 15 minute and two 5 minute TBS-0.1% (v/v) Tween washes. The membrane was then covered by the secondary antibody (anti-mouse Ig, horseradish peroxidase linked whole antibody (from sheep); Sigma) in 10% (w/v) blocking solution (1:5000 dilution) for 1 hour at room temperature, with gentle agitation. Thereafter, the excess secondary antibody was removed and the membrane rinsed twice with TBS-0.1% (v/v) Tween, followed by two 15 minute and four 5 minute TBS-0.1% (v/v) Tween washes with gentle agitation. Once the washes were completed, chemiluminescence detection was carried out with the Western blot reagent Enhanced Chemiluminescence Lighting System (ECL) (Amersham Pharmacia Biotech) and data were recorded on Hyperfilm ECL (Amersham Pharmacia Biotech). After exposure, bands were analysed using the Alphamager™ 1220 gel documentation system.

2.2.7 MITOCHONDRIAL STUDIES

2.2.7.1 CELL CULTURE

Primary endothelial cell cultures were established from human umbilical veins taken from three different umbilical cords at delivery. A colleague set up the initial cultures and froze these cells for storage using standard techniques.^{443, 444, 445, 446} At the start of the experiment, the HUVECs were rejuvenated, seeded on 75cm² flasks coated with 1% (v/v) gelatin and maintained in HUVEC media. Separate HUVEC lines were used for every experiment. All

the cultures were incubated in 12ml media at 37°C (5% (v/v) CO₂–95% (v/v) air atmosphere). When confluent, the HUVEC were passaged and 0.6 – 1x10⁶ cells were seeded per 75cm² flask (two per cell line). To study the effects of high glucose (HG), the growth media was supplemented with freshly prepared D-glucose to achieve a final concentration of 22mM. Exposure to HG began at passage three. The control glucose concentration (normal glucose; NG) was 5.5mM. Media was changed every two days to keep the glucose concentrations relatively constant. All the culture work was undertaken in dimmed light.

When sub-culturing, all the flasks were aspirated, washed twice with 15ml warmed PBS ((Dulbecco A; Oxoid, Hampshire) supplemented with penicillin (20iu/ml)-streptomycin (20µg/ml) mix and 0.5µg/ml fungizone) and incubated with 3ml warmed 0.1% (w/v) trypsin-0.02% (w/v) EDTA. After 2 minutes, 6ml warmed media was added, the HUVECs collected and centrifuged for 5 minutes at 172g. The resultant pellets were aspirated and then re-suspended in 3ml warmed media and left on ice. Next, the NG and HG cells were pooled into separate centrifuge tubes and stored on ice during counting. Cells were counted using 0.2% (w/v) Trypan blue in PBS, gently agitated for 2 minutes and counted in an Improved Neubauer haemocytometer. Next, 0.6 – 1x10⁶ cells were then added to 75cm² flasks coated with 1% (v/v) gelatin containing warmed HUVEC media and the HG flasks were supplemented with warmed D-glucose. The remaining cells were used for comet analysis, DNA isolation and protein separation (sections 2.2.7.2, 2.2.7.3 and 2.2.7.4, respectively).

2.2.7.2 COMET ASSAY

This stage proceeded as described earlier (section 2.2.1), except that instead of the 1xTE buffer washes, the slides (six per cell line) were rinsed in 1xFPG enzyme buffer (40mM HEPES, 0.1M KCl, 0.5mM EDTA, 0.2mg/ml BSA, pH 8.0) for 15 minutes. Thereafter, the excess buffer was drained and three of the slides were overlaid with 50µl FPG enzyme solution (1:10000 dilution with 1xFPG enzyme buffer; New England Biolabs; Hertfordshire) followed by a cover slip. Meanwhile, the other slides were treated with 50µl 1x FPG buffer

alone. Next, all the slides were incubated for 30 minutes at 37°C in a humidified atmosphere. The assay then proceeded as before and the subsequent comets were scored using the KOMET software.

2.2.7.3 DNA STUDIES

DNA ISOLATION

The total DNA collected from the cultured HUVECs were purified for Southern Blotting using the QIAamp DNA Mini Kit (QIAGEN) according to the manufacturer's instructions. Basically, the procedure comprised four steps utilizing QIAamp spin columns (QIAGEN) in a standard centrifuge to filter the DNA from proteins, nucleases and other contaminants or inhibitors. Initially, the cells were centrifuged for 3 minutes at 1700g, the supernatant aspirated and the HUVECs re-suspended in 200µl PBS. Subsequently, lysis followed. The lysate buffering conditions were adjusted to allow the optimal binding of the DNA to the QIAamp membrane before the sample was loaded onto the QIAamp spin column. The DNA was absorbed onto the QIAamp silica-gel membrane during a brief centrifugation, while the salt and pH conditions in the lysate ensured that proteins and other contaminants were not retained. The HUVEC DNA bound to the membrane was then washed in two further centrifugation steps to improve its purity. Thereafter, the refined DNA was removed from the spin column by an elution buffer that had been equilibrated to room temperature and incubated with the sample for 1 minute. Finally, all the specimens were stored at -20°C until quantification.

DNA QUANTIFICATION

DNA concentration was established by applying a Cytofluor plate reader (Applied Biosystems; California, USA) and the PicoGreen® double-stranded DNA (dsDNA) Quantitation Kit (Molecular Probes). The PicoGreen® dsDNA quantitation reagent used a sensitive fluorescent nucleic acid stain for

quantifying dsDNA in solution. The kit relies on the dye binding to dsDNA and subsequent fluorescence quantification with a standard spectrofluorometer. Briefly, a lambda DNA stock solution (2µg/ml) was prepared from the PicoGreen® dsDNA Quantitation Kit and this was used to create a series of DNA standards ranging from 0-1µg/ml. Additionally, the DNA samples isolated and purified using the QIAamp DNA Mini Kit were diluted by supplementing 1µl specimen to 1ml 1xTE (10mM Tris-HCl, 1mM EDTA, pH 7.5 (made in sterile, distilled, DNase-free water)). The standards were then placed in duplicate (100µl for each) into a 96-well flat-bottomed microplate (Nunc Brand Products) along with the diluted DNA specimens (100µl per sample). Thereafter, the PicoGreen reagent was readied by diluting PicoGreen reagent 200-fold in 1xTE in a blackened vessel. Next, 100µl PicoGreen reagent was quickly added to every well, gently mixed and kept in the dark. After 10 minutes, the fluorescence at excitation 485nm and emission 530nm wavelengths for each sample was read. Finally, EXCEL software was employed to calculate the sample concentrations.

MITOCHONDRIAL TO NUCLEAR DNA CONTENT RATIO ANALYSIS

Sample DNA (1µg) from selected long-term HUVEC sub-culturing, along with three HeLa DNA standards (0.5µg, 1µg and 2µg) were incorporated into a 40µl restriction enzyme digestion reaction mixture containing 1xNEBuffer 2 (New England Biolabs) and 40 units *Bam*HI (New England Biolabs). This digestion occurred at 37°C for at least 4 hours. Next, 5µl loading dye (10x bluejuice: 65% (w/v) sucrose, 10mM Tris-HCl, 10mM EDTA, 0.05% (w/v) bromophenol blue) was added to each specimen prior to their loading into a 0.5% (w/v) agarose gel in 1xTAE (40mM Tris-acetate, 1mM EDTA) containing 1µg/ml ethidium bromide. Additionally, the 1kb ladder (250ng) and HMW (400ng) DNA markers were appended prior to gel electrophoresis in 1xTAE containing 0.5µg/ml ethidium bromide for 38.5V/cm (performed for approximately 16 hours).

The following day, the gel was briefly rinsed in distilled water and visualized using the Alpha Innotech Gel Documentation System (Alpha Innotech Corporation; California, USA) to check for adequate sample migration and separation. Thereafter, the gel was cut to the appropriate size, agitated in depurinating solution (125mM HCl) for exactly 10 minutes and subsequently washed twice in Alkaline Blotting Buffer (ABB: 0.4M NaOH, 1M NaCl) for 15 and 20 minutes, respectively. The gel was then blotted through capillary transfer using standard Southern Blotting procedures with ABB to a Hybond-XL nylon membrane (Amersham Pharmacia Biotech) for at least 20 hours. Next, the membrane was baked at 80°C for 2 hours to fix the DNA. Meanwhile, the blotted gel was stained with 0.5µg/ml ethidium bromide for 30 minutes and reviewed using the Gel Documentation System to ensure a successful transfer.

After DNA fixation; the membrane was gently rinsed in distilled water, wrapped within a cleaned mesh (wetted with distilled water) and placed into a hybridization bottle containing 18ml hybridization buffer (0.5M PO₄, 1mM EDTA, 7% (w/v) SDS, 1% (w/v) BSA, pH 7.2). This pre-hybridization step was carried out in a rotary oven at 65°C for 3 hours having certified that the membrane had unwound completely. During this time, the radio-labelled probes (a kind gift from Dr Richard Hastings) were readied. The nuclear (20ng/µl), mitochondrial (20ng/µl), 1kb ladder (1ng/µl) and HMW (1ng/µl) probes were all heated at 100°C for 5 minutes and then rapidly cooled on ice for 5 minutes. Next, the denatured probes were transferred to Rediprime™ II (Random Prime Labelling System) tubes (Amersham Pharmacia Biotech) before 5µl (1.85MBq) α-³²P-dCTP (Amersham Pharmacia Biotech) was added to each probe, mixed thoroughly and incubated at 37°C for 10 minutes. Subsequently, 2µl 0.5M EDTA was included to stop each reaction and the probes were then purified using the QIAGEN's QIAquick Nucleotide Removal Kit according to their instructions. Afterwards, the nuclear (4ng), mitochondrial (1ng), HMW (20pg) and 1kb ladder (20pg) marker probes were boiled for 5 minutes and immediately placed on ice for 5 minutes prior to their supplementation into 8ml hybridization buffer. This latter solution was used to

replace the pre-hybridization reagent and hybridization was then continued at 65°C for a minimum of 19 hours.

Post-hybridization, the membrane was briefly rinsed in 1xSSC, 0.1% (w/v) SDS before being agitated in the following increasingly stringent buffers to remove the non-specific labelling: 1xSSC, 0.1% (w/v) SDS at room temperature for 10 minutes; 1xSSC, 0.1% (w/v) SDS at 65°C for 10 minutes; 0.5xSSC, 0.1% (w/v) SDS at 65°C for 10 minutes and finally; 0.25xSSC, 0.1% (w/v) SDS at 65°C for 15 minutes. Afterwards, the membrane was wrapped in cling film, its radioactivity monitored and then exposed to autoradiography on Kodak X-ray films. Thereafter, the Optical Densitometry ImageMaster ID Densitometry Software (Amersham Pharmacia Biotech) and Sharp JX-330 scanner were used to analyze the sample band intensities to establish their mitochondrial DNA to nuclear DNA content ratio relative to the HeLa DNA standards.

2.2.7.4 PROTEIN STUDIES

PROTEIN ISOLATION

HUVEC samples were also taken for protein analysis. Initially, the cells were centrifuged for 2 minutes at 1700g at 4°C, the supernatant discarded, the HUVECs re-suspended in 1ml cold PBS and then centrifuged again. Afterwards, the PBS was aspirated and the pellet re-suspended in PE buffer (87.5% (v/v) PBS, 1% (v/v) Triton X-100, 0.1% (w/v) SDS, 1mM EDTA, 0.2% (v/v) β -mercaptoethanol, 0.5mM DTT, 10% (v/v) protease inhibitor cocktail (1.04M AEBSF, 800 μ M Aprotinin, 21mM Leupeptin, 36mM Bestatin, 15mM Pepstatin A, 14mM E-64), pH 7.4) such that the final concentration was 1 μ l PE buffer for every 5×10^4 cells. All the specimens were kept on ice throughout these processes. Next, the resultant suspension was passed 5-6 times through a 21-gauge needle (BD Micolane 3; Fraga, Spain) using a 1ml syringe (Terumo; Leuven, Belgium) to shear the genomic DNA and make the solution less viscous. The lysate was then incubated on ice for 30-60

minutes, centrifuged at 10000g for 10 minutes at 4°C and the supernatant transferred to a fresh pre-chilled tube. Both the lysate and cell pellet were stored at -80°C until quantification.

PROTEIN QUANTIFICATION

The protein concentrations were determined through the Bradford assay (section 2.2.5).

WESTERN BLOTTING

The protein samples were utilized for western blot analysis for the expression of the mitochondrial respiratory chain complex IV (subunit I). Hence, the experimental set-up, cell preparation and protein concentration resolution were as described previously (section 2.2.5).

For these experiments, 40µg protein samples were supplemented with 1x loading buffer (50mM Tris-HCl pH 6.8, 100mM DTT, 0.01% (v/v) bromophenol blue, 4% (w/v) SDS, 12% (v/v) glycerol) and the reaction mixtures were left at room temperature for 25 minutes to denature the proteins. Concurrently, the pre-prepared protein standard (pre-stained protein marker, broad range from 6.5-175kDa; New England Biolabs) was heated at 95°C for 3 minutes. The samples (25µl) and marker (6µl) were then loaded into the wells of a 10% polyacrylamide gel containing SDS formed in the Mini-PROTEAN II casting unit (Bio-Rad). The stacking gel contained 25% (v/v) 0.5M Tris-HCl pH 6.2, 0.4% (w/v) SDS; 10% (v/v) 30% (w/v) acrylamide: 0.8% (w/v) bis-acrylamide stock solution (37:5:1) protein and sequencing electrophoresis grade; 1.2% (w/v) APS, 0.4% (v/v) TEMED. Meanwhile, the resolving gel was composed of 25% (v/v) 1.5M Tris-HCl pH 8.8, 0.4% (w/v) SDS; 33% (v/v) 30% (w/v) acrylamide: 0.8% (w/v) bis-acrylamide stock solution (37:5:1) protein and sequencing electrophoresis grade; 0.6% (w/v) APS, 0.14% (v/v) TEMED. Electrophoresis was then carried out using the Mini-PROTEAN II cell system

for 75-90 minutes at 120V in 1xSDS running buffer (25mM Tris, 192mM glycine, 0.1% (w/v) SDS).

Next, the proteins were transferred onto a PVDF membrane wetted in methanol (20 seconds), ultra-pure water (5 minutes) and the transfer buffer (10 minutes). A Mini trans-blot transfer cell (Bio-Rad) was used to transfer the proteins from the gel onto the membrane in freshly prepared 1x transfer buffer (192mM glycine, 25mM Tris, 10% (v/v) methanol). Electrophoresis was carried out at 150mA for 2 hours.

During immunodetection, the PVDF membrane was gently agitated in 40ml 5% (w/v) blocking solution (dried skimmed milk powder dissolved in 1xTBST (50mM Tris-HCl pH 7.5, 150mM NaCl, 0.05% (v/v) Tween-20) for 1 hour at room temperature. Afterwards, the excess solution was removed and the membrane incubated with the anti-OxPhos Complex IV subunit I, mouse IgG_{2a}, monoclonal primary antibody (1µg/ml in 5% (w/v) blocking buffer; Molecular Probes) overnight at 4°C.

The next day, the membrane was washed twice in freshly made 1xTBST for 10 minutes each time, followed by a single 10 minute bathing in 1xTBS (50mM Tris-HCl pH 7.5, 150mM NaCl). The membrane was then covered in the secondary antibody (anti-mouse Ig, horseradish peroxidase linked whole antibody (from sheep); Amersham Pharmacia Biotech) in 5% (w/v) blocking solution (1:5000 dilution) for 2 hours at room temperature, with gentle agitation. Thereafter, the excess secondary antibody was removed and the membrane washed three times with 1xTBST for 10 minutes at a time, followed a 10 minute 1xTBS wash with gentle agitation. Once the washes were completed, chemiluminescence detection was carried out with the Western blot reagent ECL and data were recorded on Hyperfilm ECL. After exposure, the bands were analysed using the Optical Densitometry ImageMaster ID Densitometry Software and Sharp JX-330 scanner.

Following ECL detection, the membrane was briefly rinsed in distilled water and incubated with stripping buffer (62.5mM Tris-HCl pH 6.7, 2% (w/v) SDS,

100mM β -mercaptoethanol) at 50°C for 30 minutes. The membrane was then soaked twice in 1xTBST for 10 minutes and covered in 5% (w/v) blocking buffer for 1 hour at room temperature, with gentle agitation. Next, the membrane was bathed with monoclonal anti- β -actin antibody (produced in mice; 1:5000 dilution in 5% (w/v) blocking buffer; Sigma) overnight at 4°C. Thereafter, the membrane was washed twice in 1xTBST for a total of 20 minutes and once in 1xTBS for 10 minutes before being covered in the secondary antibody (anti-mouse Ig, horseradish peroxidase linked whole antibody (from sheep); Amersham Pharmacia Biotech) in 5% (w/v) blocking solution (1:5000 dilution) for 2 hours at room temperature, with gentle agitation. Thereafter, the excess secondary antibody was removed and the membrane washed three times with 1xTBST for a total of 30 minutes, followed a 10 minute 1xTBS wash with gentle agitation. Once the washes were completed, chemiluminescence detection was carried out again with the Western blot reagent ECL and data were recorded on Hyperfilm ECL. After exposure, the bands were analysed using the Optical Densitometry ImageMaster ID Densitometry Software and Sharp JX-330 scanner.

2.2.8 STATISTICS

The results are expressed as the mean \pm the standard error of the mean (SEM). Comparisons were made using unpaired two-tailed *t*-tests or one-way Analysis of Variance (ANOVA) performed by the InStat Graphpad and EXCEL software. Significance levels were considered as $p < 0.05$.

CHAPTER 3 : GLUCOSE-INDUCED HUVEC

DNA DAMAGE

3.1 INTRODUCTION

DNA injury is one of the most critical threats to cellular homeostasis and life because it can cause disruption to DNA transcription and replication.^{46, 92, 100, 119, 308, 309} It has been estimated that around 2×10^4 DNA damaging events occur in every cell of the human body everyday and that a significant portion of this damage is caused by ROS.^{92, 310, 311}

ROS are thought to be ubiquitous and *in vitro* studies have demonstrated that about 2-4% of the oxygen consumed is converted into $O_2^{\bullet-}$.^{91, 92, 108-110} It has also been calculated that a typical human cell metabolises approximately 10^{12} oxygen molecules daily, and therefore, generates about 3×10^9 H_2O_2 molecules per hour.^{12, 111} Additionally, high ambient glucose has been shown to affect endothelial and other vascular cells at the cellular level through oxidative stress.^{21, 65, 66, 68, 69, 75, 81, 87-89} For example, Ho *et al.* (2000) discovered that high glucose treatment on HUVECs increased 2', 7'-dichlorofluorescein diacetate fluorescence in a time- and dose-dependent manner, while ascorbic acid addition was able to completely suppress this rise in fluorescence.^{67, 86, 90} Further, Graier *et al.* (1996) showed that high glucose could stimulate $O_2^{\bullet-}$ generation and enhance cell-mediated LDL peroxidation in endothelial cells.^{56,}
72

The targets of such radicals are proteins, lipids and DNA with the resultant oxidative damage to the latter producing large numbers of poorly characterised DNA adducts, abasic sites, and single- and double-stranded breaks.^{112, 113} Among the base modifications studied as a function of age and diabetes, the 8-oxo-dG lesion is the most extensively documented.¹¹⁹⁻¹²¹

Overall, genomic DNA injury is thought to play a central role in the progression of cell senescence and ageing.¹² Significantly, it has been suggested that alterations to cellular DNA may contribute to atherosclerotic plaque formation.⁴⁶ Oxidative DNA damage has been observed to accumulate in such plaques of humans and animals, while antioxidants like probucol, butylated hydroxytoluene, vitamin E and β -carotene are reported to inhibit this atherosclerotic development.³⁰⁵⁻³⁰⁷

3.2 AIM

The hypothesis that high ambient glucose causes heightened HUVEC DNA damage through an increase in oxidative stress was tested in this chapter. Thus, this section aimed to define and characterise the effects of elevated extracellular glucose concentrations on HUVEC DNA damage and to ascertain whether this glucose-induced HUVEC DNA damage was mediated via glucose-driven oxidative stress.

3.3 METHODS

DNA damage was quantified through “Single Cell Gel Electrophoresis” (SCGE; comet assay).^{447, 449} This well-validated technique was a relatively simple, rapid and sensitive method that measured global DNA strand breaks in individual cells.⁴⁴⁸ A HUVEC suspension was mixed with agarose, allowed to solidify into a thin layer on a microscope slide, treated and then lysed with a detergent and high salt to remove the cytoplasm, membranes and nuclear proteins. This left the “nucleoids” – supercoiled DNA arranged in loops that were attached to the nuclear matrix and morphologically similar to the original cell nucleus. Next, the gels were subjected to alkaline electrophoresis. The DNA was attracted towards the anode but, only the loops containing breakages (which relaxed the supercoiling) were free to migrate: they extended from the “nucleoid head” to form the “tail” of a comet-like image, as viewed by fluorescence microscopy. Critically, the comet tail size and its

fluorescence distribution were proven to be directly proportional to the number of single-stranded DNA breaks.^{308, 450}

The KOMET image analysis software, which was used later in these studies, provided a wealth of information for every comet including tail length, percentage DNA in the tail and the tail moment (the product of the fraction of DNA in the tail and the distance between the means of the head and tail distributions).^{427, 451, 452} The latter was thought to be a particularly sensitive DNA damage indicator and hence, was the parameter of choice.^{305, 427, 453, 454} Importantly, evidence had emphasized a close correspondence between the visual and computer scoring techniques.⁴⁵⁵ Indeed, a comparison of the comet valuations made on the same samples by manual and automated analysis systems revealed no significant differences.⁴⁵⁶

The comet grades were noted to vary between experiments. This observation may have been compounded by any inconsistencies with the cell passage number, cell cycle state and phenotype. Additionally, the clinical history of the umbilical chord donor was unknown. It was assumed that both the mother and child were healthy and that the pregnancy as well as the birth uncomplicated.

3.4 RESULTS

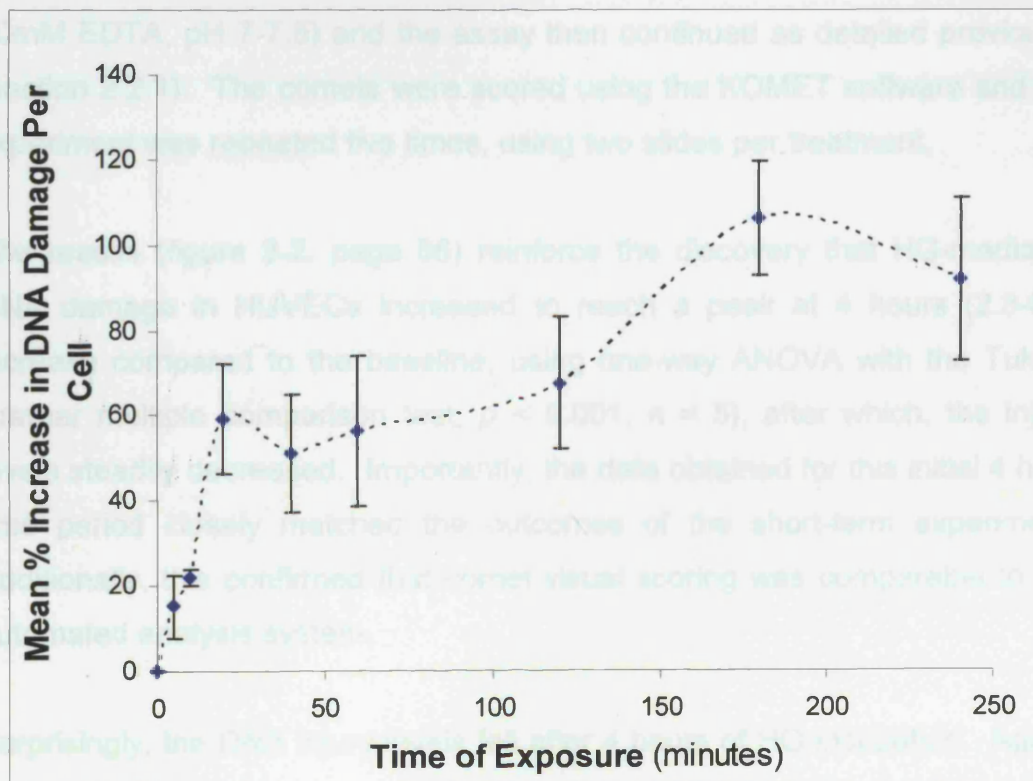
3.4.1 SHORT-TERM TIME COURSE OF GLUCOSE-INDUCED HUVEC DNA DAMAGE

Initially, it was important to discover the amount of glucose-induced DNA damage and to establish an optimal time point for the study of DNA injury. Hence, an experiment was designed to subject HUVECs to high glucose (HG) for varying times. Every effort was made to use young sub-confluent cells, as older HUVECs were more likely to be senescent, while confluent cells were known to produce fewer free radicals.¹⁷⁸ A maximal 4 hour exposure period was chosen. The glucose concentrations used were 5.5mM (normal glucose, as this was present in the HUVEC media) and 22mM (HG, because this represented the glycaemic levels reached in patients with poorly controlled diabetes).^{89, 335, 457} HG was attained by supplementing the HUVEC media with freshly prepared D-glucose.⁴⁵⁸ The experiment was repeated three times and used ten slides on each occasion – two were submerged in normal glucose (NG) for 4 hours, one was in HG for 4 hours, while the others all began in NG and were transferred into HG conditions to give additional exposure times of 5, 10, 20, 40, 60, 120 and 180 minutes. The slides were incubated in the Wilson jars throughout the treatment phase. This experiment then continued as detailed previously (section 2.2.1).

This comet assay (figure 3-1, page 83) showed that DNA damage occurred within 5 minutes of elevated D-glucose exposure. The level of injury continued to rise with the steepest increase appearing between 10-20 minutes of treatment. Surprisingly, in the next 20 minutes, the amount of DNA damage fell but was followed by a steady rise until 180 minutes, where the damage peaked. Interestingly, after 4 hours, the level of DNA injury decreased again. However, this may have been an artefact of the experiment – generally, the comet scores ranged from 0-2 in the shorter exposure times but the grades increased to 3-4 at the longer treatment periods. Hence, some

of the cells could have been so damaged that they were not recognisable as comets, and therefore, overlooked.

Figure 3-1: Short-term time course of high glucose (HG)-induced HUVEC DNA damage. Young HUVECs (passages 2-4) were isolated on to slides and then subjected to NG (normal glucose, 5.5mM) or HG (22mM) for varying times. HG was attained by supplementing the HUVEC media with freshly prepared D-glucose. Following their treatment, HUVECs were analysed through the comet assay technique and assessed using the visual scoring system. The experiment was conducted on three separate occasions (n = 3), using ten slides per experiment (two for the control, NG). The results are displayed as the mean percentage increases in DNA damage per cell compared to the control (\pm SEM) at each of the studied time points.



3.4.2 LONGER-TERM GLUCOSE-MEDIATED HUVEC DNA DAMAGE TIME COURSE

Following the short-term HG exposure data, it became equally important to discover the effects of longer-term HG incubations on DNA injury. Thus, a maximal 24 hour treatment period was chosen to subject young, sub-confluent cells to HG conditions. For this investigation, frozen HUVECs were taken from storage, seeded and maintained on two sets of six-well plates bathed in their media. At the start of the assay, in dimmed light, each well was aspirated and fed with fresh media. The experiment was designed so that all the samples could be collected simultaneously. The time points examined were 0 hour HG (24 hours NG), 1 hour HG (23 hours NG followed by 1 hour HG), 2 hours HG (22 hours NG then 2 hours HG), 3 hours HG (21 hours NG before 3 hours HG), 4 hours HG, 6 hours HG, 8 hours HG and finally 24 hours HG. After these exposure times, the cells were removed using the “mincing solution” (0.8X Hanks’ Balanced Salt Solution, 10% (v/v) dimethyl sulphoxide, 20mM EDTA, pH 7-7.5) and the assay then continued as detailed previously (section 2.2.1). The comets were scored using the KOMET software and the experiment was repeated five times, using two slides per treatment.

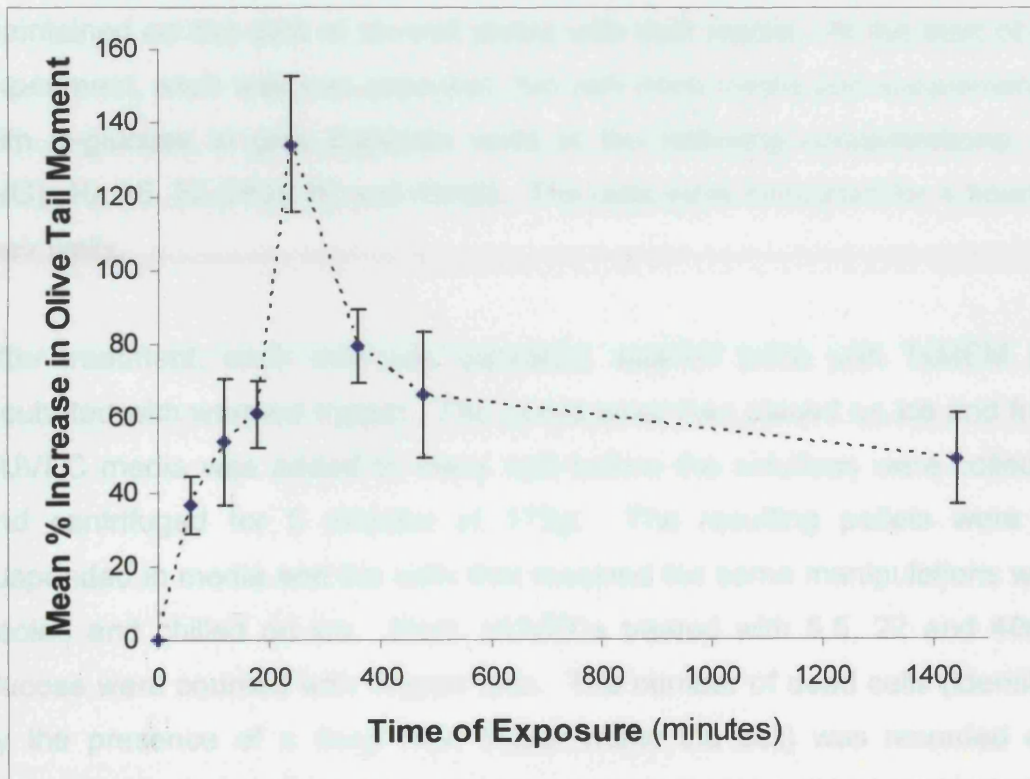
The results (figure 3-2, page 86) reinforce the discovery that HG-mediated DNA damage in HUVECs increased to reach a peak at 4 hours (2.3-fold increase compared to the baseline; using one-way ANOVA with the Tukey-Kramer multiple comparison test, $p < 0.001$, $n = 5$), after which, the injury levels steadily decreased. Importantly, the data obtained for this initial 4 hour time period closely matched the outcomes of the short-term experiment. Additionally, this confirmed that comet visual scoring was comparable to the automated analysis system.

Surprisingly, the DNA injury levels fell after 4 hours of HG incubation. Again, this was reflected in the visual appearance of the comets – those observed at 24 hours had much tighter nuclei than those noted at 4 hours of HG treatment. Previous research and preliminary experimental data (not shown) had lessened the possibility that these effects were potentiated by a significant

reduction in D-glucose concentration. Hence, it was possible that DNA repair may have been up regulated, particularly following 4 hours of conditioning as the greatest drop in DNA damage (1.3-fold decrease; using one-way ANOVA with the Tukey-Kramer multiple comparison test, $p < 0.05$, $n = 5$) occurred between 4 – 6 hours of HG exposure. Alternatively, the HUVECs could have adapted to their new environment by subtly altering their antioxidant defences.

Interestingly, the injury levels registered at 24 hours did not return to the “basal status”. Although the differences were not statistically significant, this was consistently the case and therefore, implied that D-glucose still elevated DNA damage levels after 24 hours of treatment. Moreover, very few apoptotic nuclei were observed (maximally, 1 per 150 comets) suggesting that HG-mediated HUVEC apoptosis may only become evident after more than 24 hours of continuous exposure, as confirmed by other studies.^{17, 89, 358, 459}

Figure 3-2: Longer-term time course of high glucose (HG)-induced HUVEC DNA injury. Low split HUVECs (passages 2-4) were maintained on six-well plates bathed in HUVEC media and subjected to NG (normal glucose, 5.5mM) and HG (22mM) for varying times. A maximal 24 hour exposure period was chosen. After treatment, the cells were removed and analysed with the comet assay. The comets were scored using the KOMET software and the experiment was conducted on five separate occasions (n = 5), using two slides for every time point. The results are presented as the mean percentage increases in olive tail moment (DNA damage) compared to the control (\pm SEM) at each of the examined time periods.



before (section 2.2.1). Each experiment was repeated three times and used three slides per treatment.

Data showed that HUVECs had a small elevation in γ -H2AX foci in HUVEC cells (on average 1.2% in NG and 3.2% in HG) HUVECs in 5.5 mM and 22 mM D-glucose, respectively, with increasing D-glucose concentrations. This was unlikely due to the differences seen in the gel scores were due to an increase in γ -H2AX.

3.4.3 EFFECT OF GLUCOSE CONCENTRATION ON HUVEC DNA DAMAGE

Previous experimental work had highlighted the possibility that during HG treatment, there could have been increased HUVEC cell death which would have, in turn, distorted the comet scoring. Hence, the SCGE technique was modified to allow for cell viability inspection through Trypan blue exclusion while simultaneously examining the DNA response to various D-glucose concentrations at the 4 hour time point.

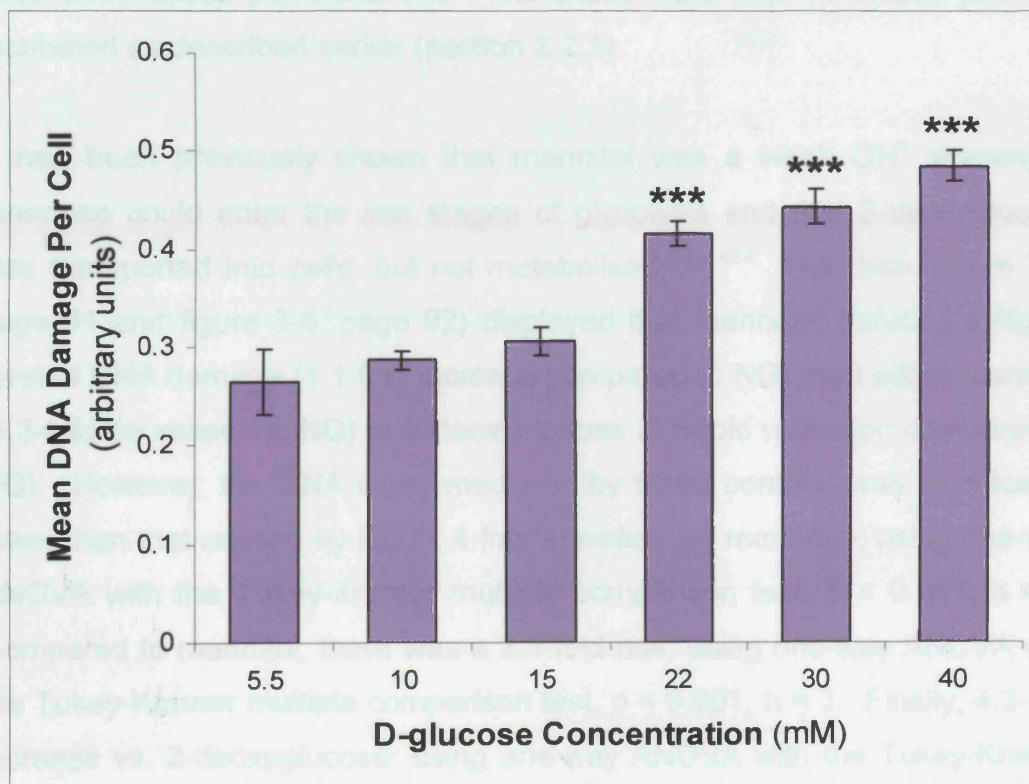
For this experiment, frozen HUVECs were taken from storage, seeded and maintained on two sets of six-well plates with their media. At the start of the experiment, each well was aspirated, fed with fresh media and supplemented with D-glucose to give duplicate wells at the following concentrations: 5.5 (NG), 10, 15, 22 (HG), 30 and 40mM. The cells were incubated for 4 hours in their wells.

After treatment, each well was aspirated, washed twice with 1xMEM and incubated with warmed trypsin. The plates were then placed on ice and fresh HUVEC media was added to every well before the solutions were collected and centrifuged for 5 minutes at 172g. The resulting pellets were re-suspended in media and the cells that received the same manipulations were pooled and chilled on ice. Next, HUVECs treated with 5.5, 22 and 40mM glucose were counted with Trypan blue. The number of dead cells (identified by the presence of a deep blue colour within the cell) was recorded and having ensured that the cell viabilities were similar, the assay continued as before (section 2.2.1). Each experiment was repeated three times and used three slides per treatment.

Data showed that there was only a small elevation in Trypan blue staining cells (on average; 2.5%, 2.9% and 3.2% dead HUVECs in 5.5, 22 and 40mM D-glucose, respectively) with increasing D-glucose concentrations. Thus, it was unlikely that the differences seen in the gel scores were due to the slight increases in cell death.

The results (figure 3-3, page 89) demonstrated that DNA damage was glucose concentration dependent. There was little difference between 5.5-15mM D-glucose and 20-40mM D-glucose, with comet scores of 0-2 dominating the former and 3-4 grades predominating in the latter. The greatest increase in DNA destruction materialised between 15-22mM D-glucose. This finding may be related to the discovery that PKC activity was maximised at 22mM D-glucose.^{460, 461} PKC activation could have caused an increase in intracellular free Ca^{2+} concentrations, which would have in turn, heightened the DNA damage. At higher D-glucose levels, PKC activity is dampened, thus, the continued increase in DNA injury may have resulted from the small rises in cell death, disruptions to the DNA repair enzymes and antioxidant defences mediated by the surges in ROS concentrations. Alternatively, the free radicals may have started to damage other cell organelles and this would have been undetected by the comet assay. Additionally, *in vivo*, such high glucose levels (40mM) may not consistently develop as glucose cell entry and glycolysis could become saturated. Furthermore, the late rise in DNA damage may have been an artefact of the technique. Very high glucose concentrations are known to induce endothelial apoptosis, a process that involves DNA fragmentation. Such cells would have been unnoticed by Trypan blue exclusion and could, therefore, have caused artificially high comet scores. However, this is unlikely as the amount of DNA injury reached a plateau at 22mM D-glucose.

Figure 3-3: HUVEC DNA damage induced by varying D-glucose concentrations. Young HUVECs (passages 2-4) were maintained on six-well plates, supplemented with fresh D-glucose to give the differing concentrations and incubated for 4 hours. After treatment, the cells were removed and assessed through the comet assay. The visual scoring system was used to grade the comets and the experiment was repeated three times, using three slides per treatment. The results are shown as the mean DNA damage per cell (\pm SEM) at the specific D-glucose concentrations. Using one-way ANOVA with the Tukey-Kramer multiple comparison test, 5.5mM vs. 22mM (** $p < 0.001$, $n = 3$); 5.5mM vs. 30mM (** $p < 0.001$, $n = 3$); 5.5mM vs. 40mM (** $p < 0.001$, $n = 3$) and 15mM vs. 22mM ($p < 0.01$, $n = 3$).



3.4.4 POSSIBLE MECHANISM FOR HIGH GLUCOSE-INFLICTED HUVEC DNA DAMAGE: OSMOSIS

It was necessary to exclude the possibility that the HG effects on DNA were osmotically mediated as the build up of osmotic pressure within cells would have caused them to eventually rupture and thus, distort their comet scores. Hence, in this investigation, HUVECs were exposed to osmotic controls (mannose, mannitol and 2-deoxyglucose), NG and HG for 4 hours. The HUVEC media was supplemented with the osmotic controls to give final concentrations of 22mM. Each experiment was repeated three times and used three slides per treatment. The slides were kept in Wilson jars and incubated as described earlier (section 2.2.1).

It had been previously shown that mannitol was a weak OH^\bullet scavenger, mannose could enter the late stages of glycolysis and that 2-deoxyglucose was transported into cells, but not metabolised.^{342, 462} The data (figure 3-4, page 91 and figure 3-5, page 92) displayed that mannose induced a higher level of DNA damage (1.1-fold increase compared to NG) than either mannitol (1.3-fold decrease vs. NG) or 2-deoxyglucose (1.8-fold reduction compared to NG). However, the DNA injury mediated by these controls was significantly lower than that caused by HG (1.4-fold elevation vs. mannose; using one-way ANOVA with the Tukey-Kramer multiple comparison test, $p < 0.001$, $n = 3$). Compared to mannitol, there was a 3.1-fold rise; using one-way ANOVA with the Tukey-Kramer multiple comparison test, $p < 0.001$, $n = 3$. Finally, 4.3-fold increase vs. 2-deoxyglucose; using one-way ANOVA with the Tukey-Kramer multiple comparison test, $p < 0.001$, $n = 3$). Thus, the HG observations were specific for D-glucose and dependent on D-glucose metabolism. Furthermore, the results were consistent with mannose being able to enter glycolysis, mannitol acting as a weak OH^\bullet scavenger and 2-deoxyglucose acting as a competitive inhibitor of D-glucose.

Figure 3-4: Mannose as an osmotic control for high glucose-induced HUVEC DNA damage. Low split HUVECs (passages 3-5) were isolated on to slides and then subjected to NG (normal glucose, 5.5mM), HG (high glucose, 22mM) or mannose (16.5mM mannose with 5.5mM D-glucose) for 4 hours. After their conditioning, the cells were removed and processed through the comet assay and visually scored. The experiment was repeated three times, using three slides per treatment. The results are displayed as the mean DNA damage per cell (\pm SEM) for each individual HUVEC treatment. Using one-way ANOVA with the Tukey-Kramer multiple comparison test, NG vs. HG (***) $p < 0.001$, $n = 3$) and HG vs. mannose (***) $p < 0.001$, $n = 3$).

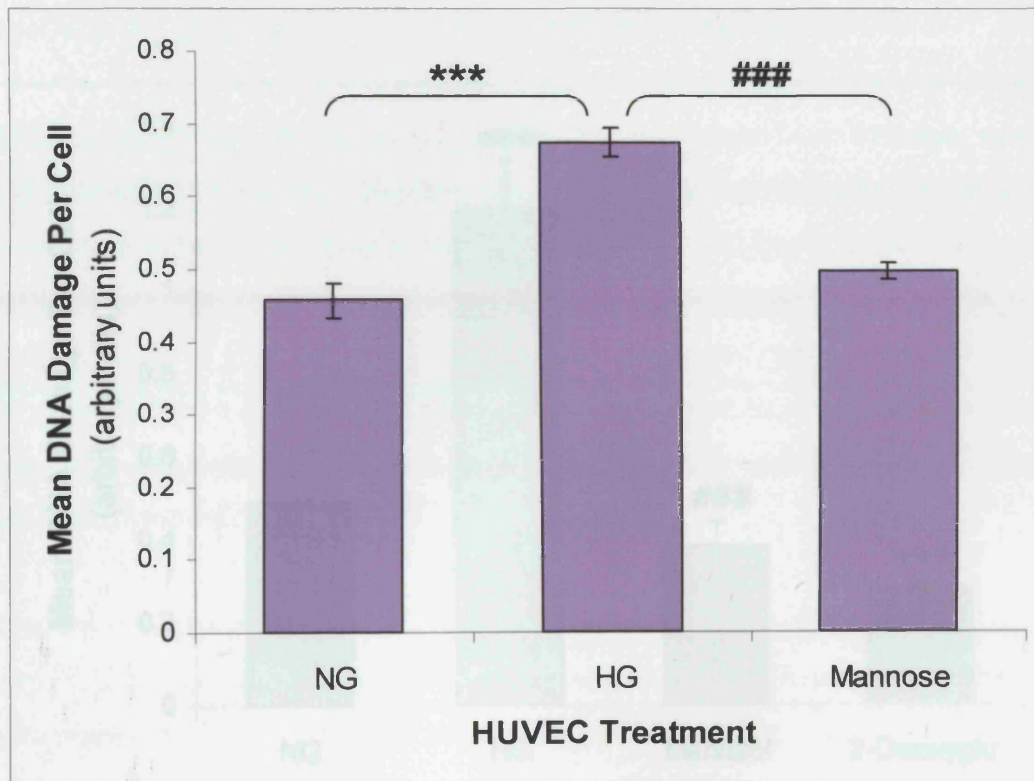
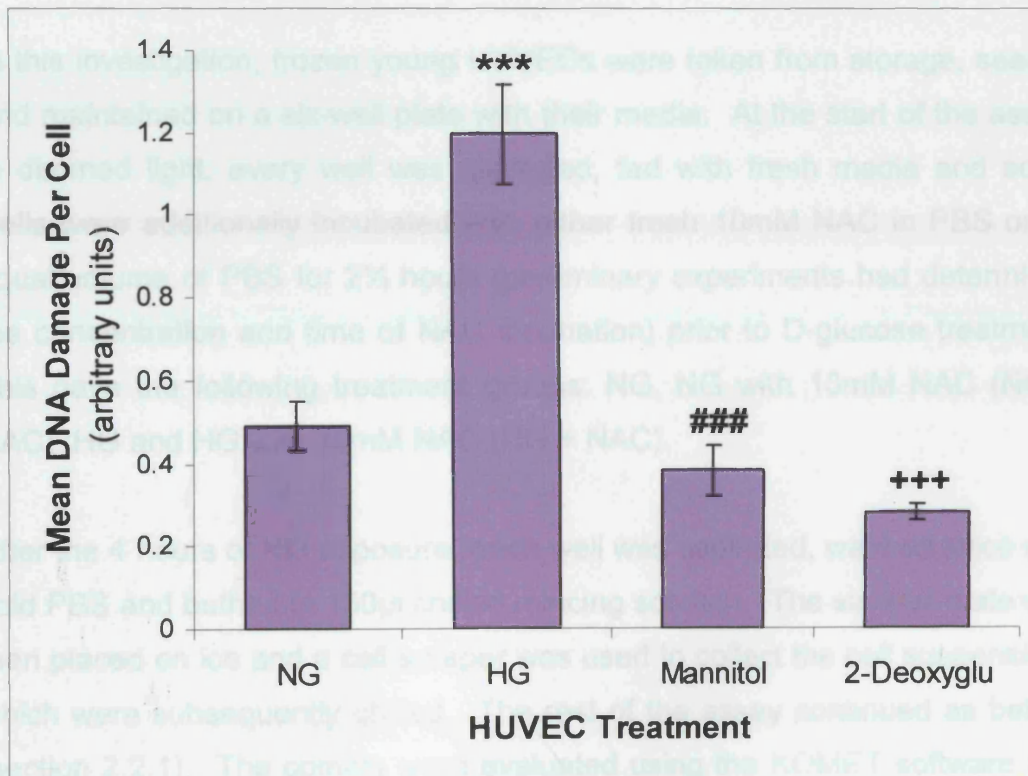


Figure 3-5: Mannitol and 2-deoxyglucose as further osmotic controls for high glucose-mediated HUVEC DNA injury. Young HUVECs (passages 3-5) were sequestered onto slides and then treated with NG (normal glucose, 5.5mM), HG (high glucose, 22mM), mannitol (16.5mM mannitol with 5.5mM D-glucose) and 2-deoxyglucose (16.5mM 2-deoxyglucose with 5.5mM D-glucose) for 4 hours. After their conditioning, cells were analysed through the comet assay and visual grading system. The experiment was repeated three times, using three slides for every treatment. The results are presented as the mean DNA damage per cell (\pm SEM) for each HUVEC treatment. Using one-way ANOVA with the Tukey-Kramer multiple comparison test, NG vs. HG (** $p < 0.001$, $n = 3$); HG vs. mannitol (### $p < 0.001$, $n = 3$) and HG vs. 2-Deoxyglu (+++ $p < 0.001$, $n = 3$). 2-Deoxyglu, 2-deoxyglucose.



3.4.5 EFFECT OF *N*-ACETYLCYSTEINE INCUBATION ON GLUCOSE-INDUCED HUVEC DNA INJURY

In order to confirm that the HG-induced DNA injury was mediated through heightened oxidative stress; an antioxidant, *N*-acetylcysteine (NAC), was used to neutralise the impact of increased ROS production. NAC was chosen because firstly, unlike SOD and catalase, it was known to enter HUVECs to act as a cysteine precursor for reduced glutathione (GSH) synthesis.^{32, 66, 379} Secondly, it was capable of directly scavenging some free radicals.¹² And finally, NAC supplementation had been demonstrated to improve human coronary and peripheral endothelium-dependent vasodilatation.⁴⁹

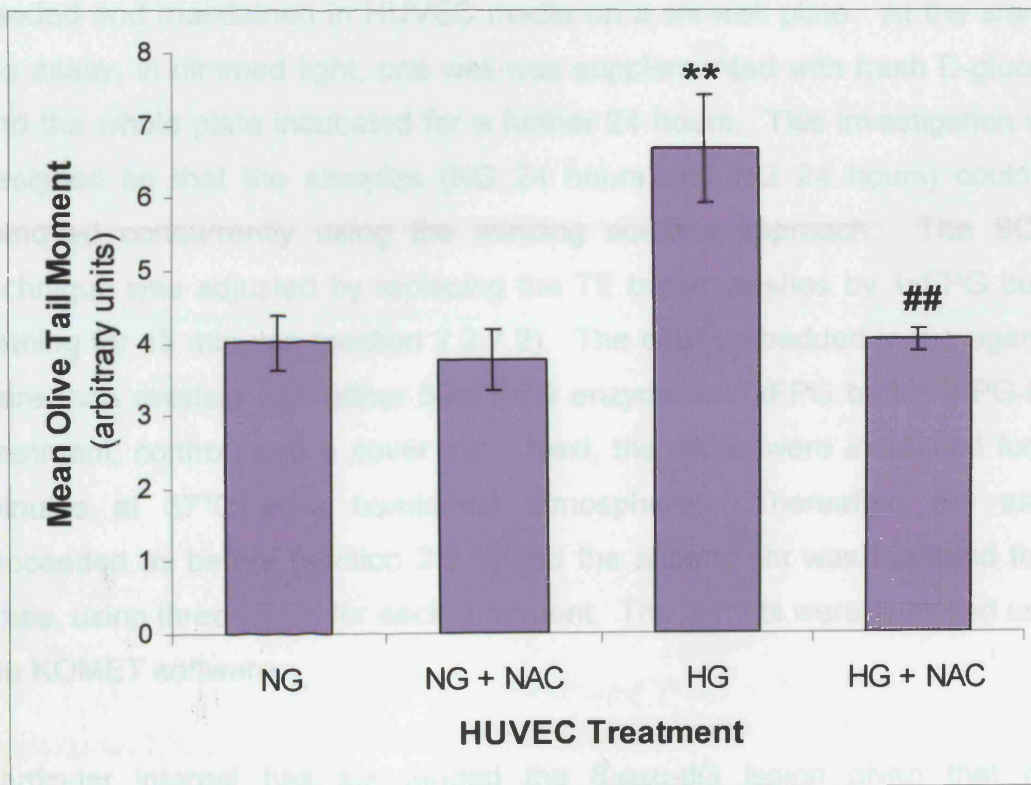
In this investigation, frozen young HUVECs were taken from storage, seeded and maintained on a six-well plate with their media. At the start of the assay, in dimmed light, every well was aspirated, fed with fresh media and some wells were additionally incubated with either fresh 10mM NAC in PBS or an equal volume of PBS for 2½ hours (preliminary experiments had determined the concentration and time of NAC incubation) prior to D-glucose treatment. This gave the following treatment groups: NG, NG with 10mM NAC (NG + NAC), HG and HG with 10mM NAC (HG + NAC).

After the 4 hours of HG exposure, each well was aspirated, washed twice with cold PBS and bathed in 150µl chilled mincing solution. The six-well plate was then placed on ice and a cell scraper was used to collect the cell suspensions which were subsequently chilled. The rest of the assay continued as before (section 2.2.1). The comets were evaluated using the KOMET software and the experiment was repeated four times, using three slides for each treatment.

Antioxidants are commonly used to assess for the presence of free radicals and these results clearly revealed that NAC pre-incubation prevented the HG-induced increase in DNA damage. After 4 hours of exposure, HG caused a 1.7-fold elevation in the mean olive tail moment recordings, while NAC supplementation prior to HG blocked any rise in DNA injury (figure 3-6, page

95). This was reflected visually too – the comets observed following HG conditioning were noticeably damaged with extended tails, however, both sets of NAC treated HUVECs produced tight, compact nucleoid structures with no obvious comet tails. Interestingly, the comet scores were very similar for the NG, NG + NAC and HG + NAC manipulated cells. Furthermore, the data for NG and NG + NAC closely resembled each other. Altogether, these findings suggest that NAC, and therefore, possibly the GSH system, is an effective antioxidant against HG-mediated DNA injury. This, in turn, could implicate ROS generation and H₂O₂ in the mechanism of HG-associated DNA damage.

Figure 3-6: Effects of *N*-acetylcysteine pre-incubation on high glucose-induced HUVEC DNA damage. Low split HUVECs (passages 2-4) were seeded on six-well plates and supplemented with either fresh 10mM *N*-acetylcysteine (NAC; an antioxidant) or an equal volume of ultra-pure distilled water for 2½ hours prior to D-glucose addition. After the 4 hour HG (high glucose, 22mM) exposure, cells were collected, subjected to the comet assay and evaluated using the KOMET software. The experiment was repeated four times, using three slides for every treatment. The results are shown as the mean olive tail moment (DNA damage; ± SEM) for each of the HUVEC treatments. Using one-way ANOVA with the Tukey-Kramer multiple comparison test, NG vs. HG (** $p < 0.01$, $n = 4$) and HG vs. HG + NAC (** $p < 0.01$, $n = 4$). NG, normal glucose (5.5mM).



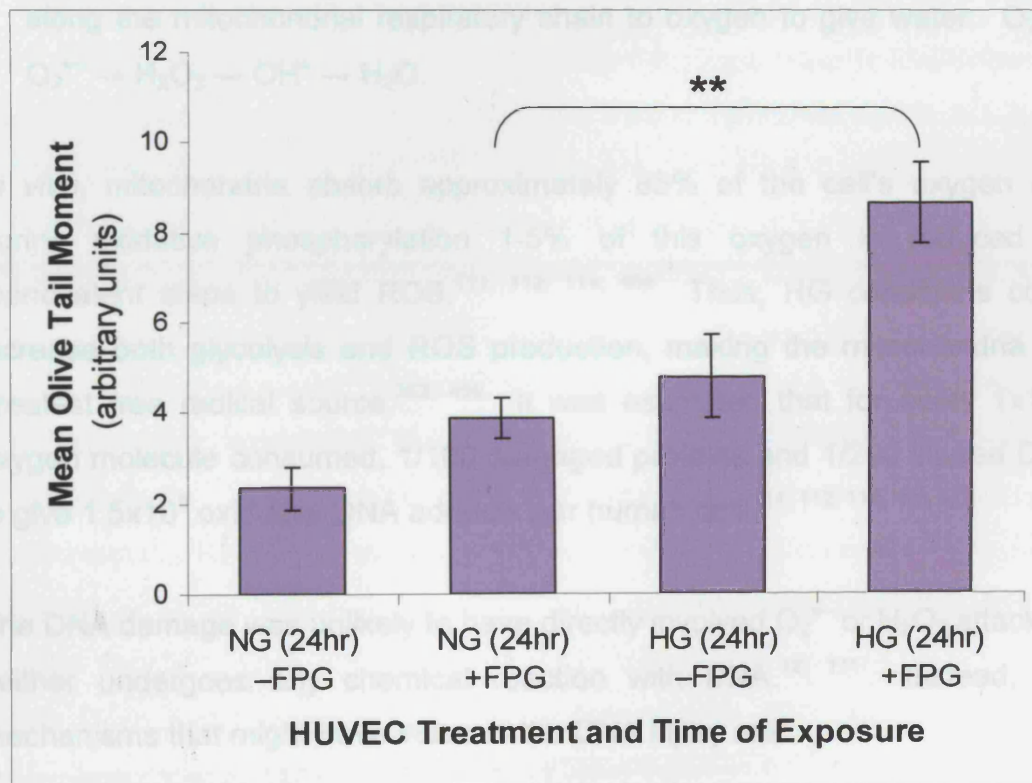
3.4.6 FPG COMET ANALYSIS OF HIGH GLUCOSE ASSOCIATED HUVEC DNA INJURY

In order to gain a further insight into the mechanisms of DNA injury caused by HG, the comet assay was adapted to incorporate the formamidopyrimidine DNA glycosylase (FPG) enzyme.⁴³⁷ This enzyme, when added to the DNA in the agarose gel layer after the lysis step, can convert altered purines, including 8-oxoguanine into DNA breaks. Thus, the comet tail and tail moment measurements would both increase and indicate a heightened level of DNA injury.

In these experiments, frozen young HUVECs were taken from storage, seeded and maintained in HUVEC media on a six-well plate. At the start of the assay, in dimmed light, one well was supplemented with fresh D-glucose and the whole plate incubated for a further 24 hours. This investigation was designed so that the samples (NG 24 hours and HG 24 hours) could be removed concurrently using the mincing solution approach. The SCGE technique was adjusted by replacing the TE buffer washes by 1xFPG buffer bathing for 15 minutes (section 2.2.7.2). The cells embedded in the agarose were then overlaid with either 50 μ l FPG enzyme or 1xFPG buffer (FPG-free treatment; control) and a cover slip. Next, the slides were incubated for 30 minutes at 37°C in a humidified atmosphere. Thereafter, the assay proceeded as before (section 2.2.1) and the experiment was repeated three times, using three slides for each treatment. The comets were analysed using the KOMET software.

Particular interest has surrounded the 8-oxo-dG lesion given that it is commonly used as a marker for oxidative DNA damage. The results (figure 3-7, page 97) demonstrated that over 24 hours, HG caused the accumulation of 8-oxo-dG lesions in HUVECs (FPG addition increased the olive tail moment by 2.2-fold compared to NG treated HUVECs). This, in turn, suggests that the HG-mediated DNA destruction seen previously in this chapter, probably occurred through an oxidative pathway.

Figure 3-7: Formamidopyrimidine DNA glycosylase (FPG) supplemented comet analysis of high glucose (HG)-mediated HUVEC DNA injury. Young HUVECs (passages 2-4) were maintained on a six-well plate and subjected to HG (22mM) for 24 hours. After the incubation phase, cells were removed, processed through the SCGE technique and the KOMET software graded the comets. This experiment was repeated three times, using three slides per treatment. The results are displayed as the mean olive tail moment (DNA damage; \pm SEM) for each of the HUVEC treatments. Using one-way ANOVA with the Tukey-Kramer multiple comparison test, NG (24hr) + FPG vs. HG (24hr) + FPG (** $p < 0.01$, $n = 3$) and HG (24hr) – FPG vs. HG (24hr) + FPG ($p < 0.05$, $n = 3$). NG, normal glucose (5.5mM).



3.5 DISCUSSION

Cellular respiration enables the complete oxidation of organic fuels to carbon dioxide and water over three stages.^{332, 463-467} These include:

- Glycolysis → glucose oxidation to acetyl-coenzyme A (acetyl-CoA);
- Citric Acid Cycle → enzymatically oxidises acetyl groups from acetyl-CoA to produce carbon dioxide with the freed energy being conserved in NADH and FADH₂; and
- Oxidative Phosphorylation → NADH and FADH₂ are oxidised to release energy (in the form of ATP) and electrons, which are then transferred along the mitochondrial respiratory chain to oxygen to give water: $O_2 \rightarrow O_2^{\bullet-} \rightarrow H_2O_2 \rightarrow OH^{\bullet} \rightarrow H_2O$.

In vivo, mitochondria absorb approximately 85% of the cell's oxygen and during oxidative phosphorylation 1-5% of this oxygen is reduced by monovalent steps to yield ROS.^{111, 112, 114, 468} Thus, HG conditions could increase both glycolysis and ROS production, making the mitochondria the greatest free radical source.^{363, 469} It was estimated that for every 1×10^{12} oxygen molecule consumed, 1/100 damaged proteins and 1/200 injured DNA to give 1.5×10^5 oxidative DNA adducts per human cell.^{111, 112, 114, 468, 470}

The DNA damage was unlikely to have directly involved $O_2^{\bullet-}$ or H_2O_2 attack as neither undergoes any chemical reaction with DNA.^{12, 111} Instead, the mechanisms that might have induced the DNA injury are:

- Damage by $OH^{\bullet} \rightarrow H_2O_2$ crosses biological membranes to penetrate the nucleus and then reacts with iron or copper ions to give OH^{\bullet} ,^{111, 291} or
- Nuclease activation → oxidative stress triggers a series of metabolic events that leads to nuclease enzyme stimulation, which then cleaves the DNA backbone.^{111, 291}

Conceivably, both processes could have occurred. However, the first suggestion is only feasible if the metal ions are either bound or very close to the DNA. The former is more probable as DNA would effectively act as a large anion with its numerous negatively charged phosphate groups. Moreover, copper ions are reported to bind preferentially to GC residues and promote H₂O₂-dependent damage (through OH[•] formation) to isolated and chromatin covered DNA *in vitro*.¹² The second possibility is that oxidative stress causes metal ion release, which then binds to the DNA. *In vitro* studies have shown that increasing the extracellular iron ion concentration heightened the level of oxidative DNA damage.¹²

The time course assays had suggested that DNA damage reached a peak after 240 minutes of HG exposure. This may have been due to DNA damage clustering, given that injury to a DNA base may enhance its susceptibility for further damage at that site.^{310, 415} Alternatively, the DNA damage may have become maximised due to an elevation in the sorbitol, glycolysis and pentose phosphate pathways depleting the cofactors (NAD⁺, NADH, NADPH, ATP) necessary for cellular respiration.⁴⁶³ Additionally, certain steps in each stage of cellular respiration are regulated by negative feedback mechanisms and H₂O₂ has been suggested to directly inhibit the phosphofructokinase and glyceraldehyde 3-phosphate dehydrogenase glycolysis enzymes.⁴⁷¹ Furthermore, HG has also been demonstrated to induce the poly(ADP-ribose)polymerase enzyme in HUVECs.⁴⁷² Single-stranded DNA breaks caused by O₂^{•-}, OH[•], ONOO⁻ and H₂O₂ trigger the enzyme, which then initiates an energy consuming cycle by transferring ADP ribose units from NAD⁺ to nuclear proteins.⁴⁷² This would have resulted in additional NAD⁺ and ATP losses that, in turn, would have slowed glycolysis and mitochondrial respiration further and added to the cell's dysfunction.

The NADPH depletions are particularly important because enzymes such as, glutathione reductase and NOS are NADPH-dependent.^{473, 474} Consequently, it could be that their losses in HG treated endothelial cells are directly

responsible for the NOS inhibition and endothelium-dependent vasodilatation suppressions observed in diabetic blood vessels.

These experiments also provided evidence that HG caused heightened ROS production. There is additional proof from other studies.⁹ For example, endothelial cell incubation with sequentially increasing glucose concentrations showed ROS production with a significant elevation being observed at 10mM D-glucose.^{9, 475} Additionally, hyperglycaemia induced heightened $O_2^{\bullet-}$ production in a concentration dependent manner in porcine and bovine aortic endothelial cells (BAECs).^{56, 399} In particular, 23mM D-glucose treated BAECs raised $O_2^{\bullet-}$ production after just three hours and the intracellular ROS levels increased 2.5-fold after 24 hours in 30mM D-glucose.^{62, 65} Further, Rosen *et al.* (1997) demonstrated that prolonged HG exposure raised endothelial NO synthase (eNOS) expression, nitrite release and $O_2^{\bullet-}$ production in human aortic endothelial cells.^{17, 476} A marked increase in eNOS expression was also noted in HUVECs within 2-24 hours of HG treatment followed by a gradual decline after 24 hours.^{17, 362} In addition, ONOO⁻ generation in HG subjected endothelial cells was shown.⁹

AGE formation has also been shown to stimulate ROS production.³⁷⁷ Giardino *et al.* (1998) even showed that intracellular AGE generation and lipid peroxidation were closely dependent processes, such that the blockage of lipid peroxidation prevented AGE formation.^{477, 478} Additionally, Wolff *et al.* (1991, 1993) demonstrated that the autoxidation of glucose led to ROS production.^{14, 478, 479} Alternatively, HG may induce ROS formation through increased glycolysis as evidenced by elevated citric acid cycle flux and decreased ROS generation by 2-deoxyglucose treated cells.⁹⁰ HG also activates the polyol pathway.⁹ This leads to a depletion of NADPH which is essential in the regeneration of antioxidant molecules such as reduced glutathione, ascorbate and tocopherol from their oxidised forms. Further, the NADH/NAD⁺ ratio becomes raised and this leads to pseudohypoxia as well as $O_2^{\bullet-}$ production, possibly via the NADH-driven stimulation of hydroperoxidase activity converting prostaglandin G₂ to prostaglandin H₂. Thus, overall, the

mechanisms underpinning these HG-mediated ROS increases are still unclear.

Together, these effects probably culminated in the heightened HUVEC DNA damage detected by the comet assay. Interestingly, Cerami and coworkers (1991) had suggested that glucose could modify nucleotide bases itself.^{121, 312} The resultant glucose-derived DNA addition products were then proposed to cause strand breaks and impair DNA repair in cultured human endothelial cells.^{259, 284} Importantly, HUVECs cultured in HG media were shown to have significantly higher FPG-sensitive sites after five days of incubation.⁴⁷⁹

3.6 CONCLUSIONS

This chapter, via the use of the sensitive comet assay, has established that HG conditions increased HUVEC DNA damage after four hours of treatment. This effect appeared to be dependent upon glucose concentration with near maximal DNA damage at 22mM. It was also specific for D-glucose, as it could not be reproduced by the osmotic controls (22mM mannose, 22mM mannitol and 22mM 2-deoxyglucose). The DNA damage was visible after just five minutes in HG and reached a peak after four hours of exposure. Furthermore, NAC pre-incubation prevented the HG-induced increase in DNA damage and over 24 hours, HG caused an elevation in HUVEC 8-oxo-dG accumulation. Therefore, this study has shown that exposure to raised extracellular glucose concentrations promoted human endothelial cell DNA injury, possibly through an oxidative pathway.

3.7 FUTURE WORK

To further clarify the underlying mechanisms of glucose-driven DNA injury, the effects of various antioxidants (other than NAC) on the level of HG-induced DNA damage should be examined. In particular, SOD supplementation should be investigated as previous research has highlighted the possibility that HG increases $O_2^{\bullet-}$ production.

CHAPTER 4 : GLUCOSE-INDUCED HUVEC

SENESCENCE

4.1 INTRODUCTION

Most mammalian cells will senesce, including endothelial cells.^{201, 202} Accompanying the inability to respond to stimulation by physiologic mitogens, senescent cells demonstrate a decrease in cell cycle regulated enzymatic activity, protein synthesis and degradative efficiency.^{197, 204} Moreover, nuclear and chromosomal aberrations occur at a higher frequency.²⁰⁴ Furthermore, some cells acquire resistance to the induction of apoptosis.^{121, 205-208}

Research has indicated that ROS are important in the development of the senescent phenotype.^{98, 100, 229} For example, fibroblasts treated with H₂O₂ activated a rapid, senescence-like growth arrest and this was reversed by ambient oxygen reduction and antioxidant supplementation.^{146, 228} Further, DNA oxidation measurements revealed that senescent cells suffered greater oxidative DNA damage than young cells. In fact, they contained 30% more 8-oxo-dG.^{12, 94} Additionally, elevated oxidative stress levels have been observed in the SAMP (accelerated senescence-prone, short-lived) mice strains.²³¹

The senescence response can induce changes to differentiated cellular functions. For instance, some senescent cells can over express and secrete molecules that act to disrupt both the local environment and distant tissues. A variety of known senescence-specific changes also have the potential to contribute to atherosclerosis.^{39, 201} For example, stimuli that would in a young endothelial cell be met with a proliferative response might, in an old vessel, lead to death and endothelial denudation.^{70, 209} Similarly, in an old artery, proliferating cells could rapidly senesce and lead to a friable intima.⁴⁸

4.2 AIM

A central theme to the hypothesis was that the high glucose-induced DNA injury would have led to disturbances in endothelial cell growth. Therefore, it was necessary to determine the effects of elevated extracellular glucose concentrations on the growth characteristics of HUVECS and in the development of cell senescence.

4.3 METHODS

The long-term effects of glucose on HUVEC proliferation were examined through cell culturing as this system was often used as a model for the physiological events that occur *in vivo*.^{109, 480} Three long-term cultures were allotted using HUVECs from different sources. This was done to confirm that HG would consistently disrupt endothelial cell growth and that the effects were not due to variations in the replicative potential of individual cells. HUVECs were plated at low densities and passaged when sub-confluent. The greatest HG effects were expected at these densities as the cells would have been free to proliferate rapidly (without contact inhibition). Samples were taken to enable analyses into HUVEC growth characteristics (section 2.2.2), level of DNA damage accumulation (section 2.2.7.2) and extent of senescence (section 2.2.3) in both NG and HG environments.

Senescent cells were identified through the senescence biomarker, SA- β -Gal. This enzymatic marker had been identified in aged cells from both *in vitro* and *in vivo* conditions and was originally discovered in the skin biopsy specimens from elderly individuals. Interestingly, strong SA- β -Gal staining was also noted in coronary artery atherosclerotic lesions.⁴¹

4.4 RESULTS

4.4.1 HUVEC PROLIFERATION

The initial HUVEC culture showed that the rate of population doublings (PDs) decreased over time in both NG and HG conditions (figure 4-1, page 106 and figure 4-2, page 107). Intriguingly, the rates of this decline were very similar even though, generally, HG cell numbers were lower (on average, HG counts were 15% less than NG numbers). This indicated that HG might have induced cell death or delayed endothelial S-phase cell cycle entry, rather than preventing it. The data also suggested that HUVECs underwent cyclical PDs. For example, after the opening sub-cultures, sudden bursts of proliferation were often preceded by slower growth rates (data not shown). Surprisingly, after 80 days of sub-culture, the cells had neither exhausted nor signalled an absolute reduction in their replicative potential (figure 4-1, page 106).

Figure 4-1: Growth curve for the long-term cell culture of HUVECs bathed in NG (normal glucose) and HG (high glucose) conditions. Primary endothelial cell cultures were established from human umbilical veins taken from umbilical cords at delivery. All cultures were incubated at 37°C (5% CO₂ – 95% air atmosphere) and passaged, using standard protocols, when sub-confluent. To study the effects of HG, the growth media was supplemented with fresh D-glucose to achieve a final concentration of 22mM. Exposure to HG began at passage 3. The control glucose concentration (NG) was 5.5mM. The media was refreshed every two days. The data are depicted as HUVEC growth (as measured by the sum of the population doublings) over time for three independent experiments.

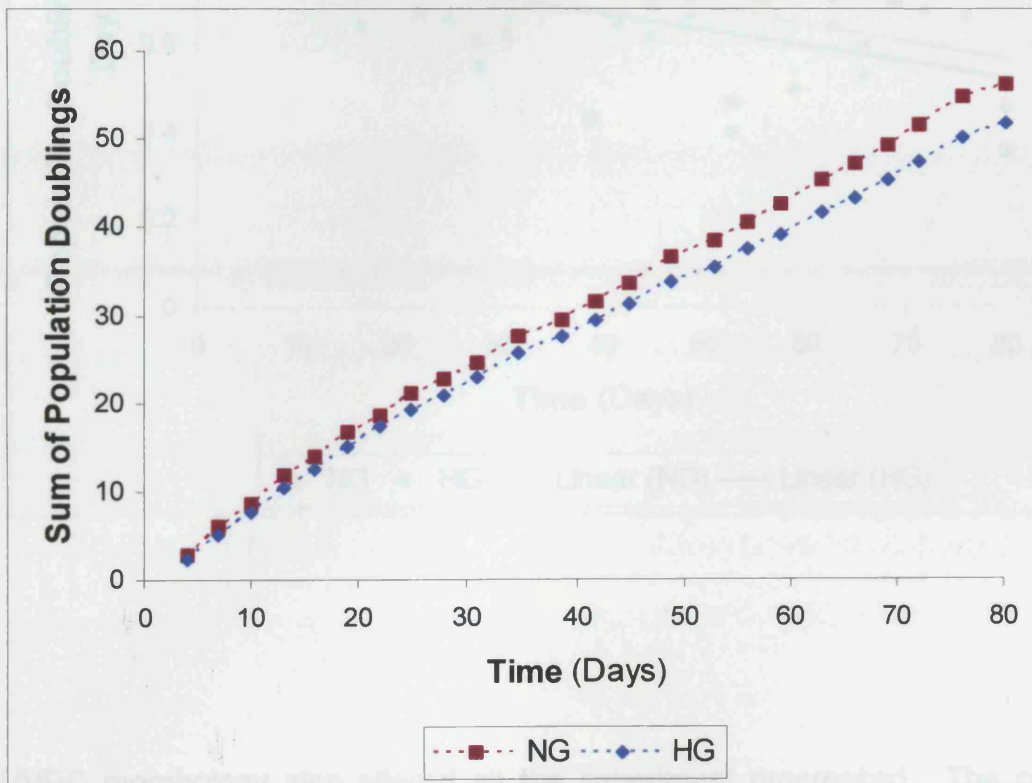
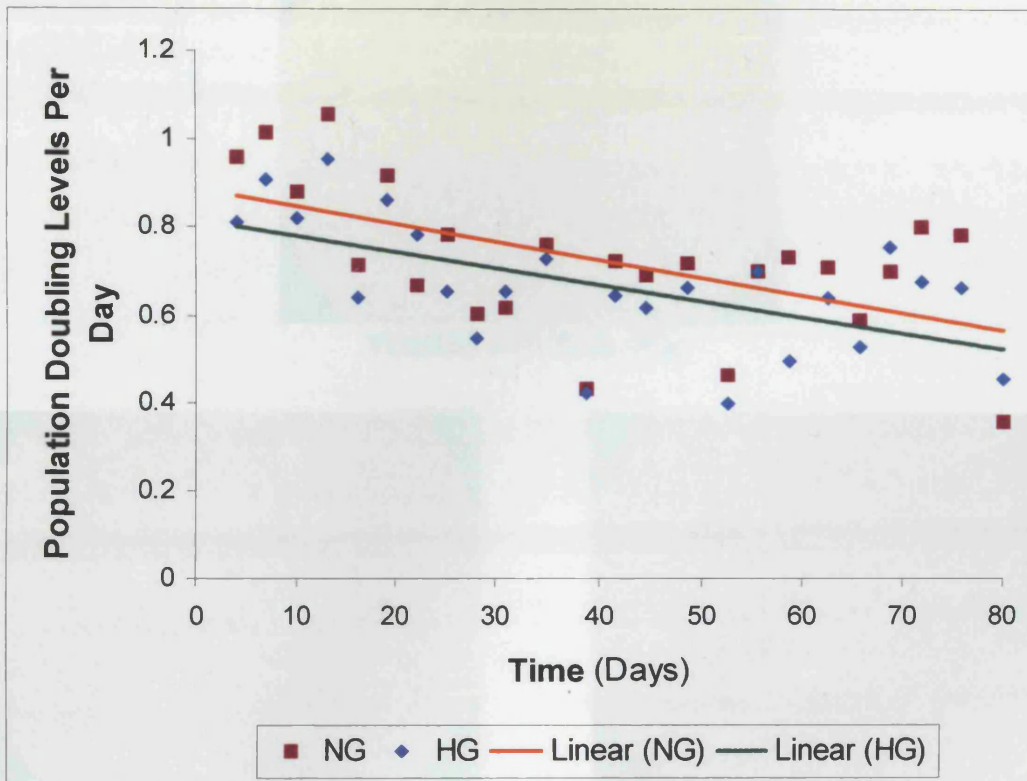
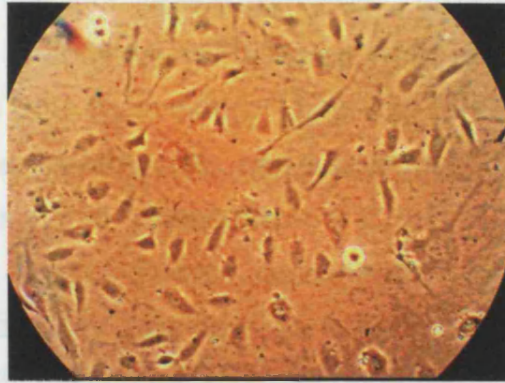


Figure 4-2: HUVEC growth rate during the preliminary long-term cell culture. The linear lines for NG (orange) and HG (green) treated HUVECs simply generalise the pattern of declining growth rate with time. The growth rate was gauged by the population doubling level per day. NG, normal glucose (5.5mM); HG, high glucose (22mM).

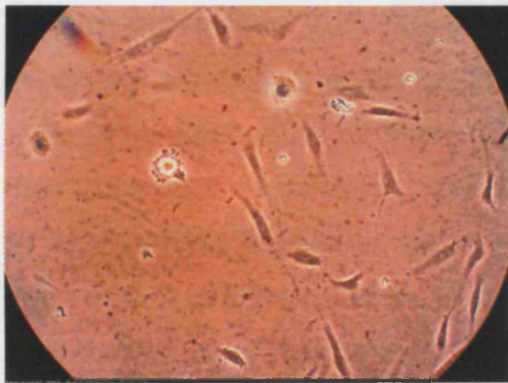


HUVEC morphology also altered as the experiment progressed. The cells became noticeably larger (by increasing their cytoplasmic content), irregular, multinucleated, stretched and lost their typical cobblestone appearance at confluency. These “senescent” cells were neither dead nor dying as they re-established themselves on new culture vessel surfaces. Additionally, they did not mix evenly with their normal counterparts instead, they tended to form their own islands. The characteristic appearance of senescent HUVECs in culture is shown in figure 4-3, page 108.

Figure 4-3: Micrographs of HUVECs at the beginning and end of the long-term culture. Morphologically, HG (22mM) bathed cells lost their cobblestone appearance sooner, had greater numbers of enlarged cells that tended to cluster together and grew to a lower saturation density. P, passage number; NG, normal glucose (5.5mM); HG, high glucose. (x40 magnification)



YOUNG HUVECs (P3)



OLDER NG HUVECs (P25)



OLDER HG HUVECs (P25)

Comparisons between the proliferation experiments are difficult but they all followed a similar growth pattern. Any differences between the three cultures could have been due to variations in the cell origin, time of passage, cell storage conditions and duration or the deviations in the conditions employed, which are never identical. The glucose effects possibly altered with the cell density, duration and concentration of exposure, culture medium and whether the cells were quiescent or proliferating.

4.4.2 HUVEC DNA DAMAGE DURING PROLONGED HIGH GLUCOSE EXPOSURE

The data collected from the comet assay and HUVEC cell cultures had suggested that the HG-induced DNA damage may be responsible for the reduced proliferation of HG treated HUVECs. In order to investigate this hypothesis, primary endothelial cell cultures were established from human umbilical veins taken from three different umbilical cords at delivery. To study the effects of HG, the growth media was supplemented with freshly prepared D-glucose to achieve a final concentration of 22mM. Exposure to HG began at passage 3. The control glucose concentration was 5.5mM (NG). The media was changed every two days to keep the glucose concentrations relatively constant. All the culture work was undertaken under subdued light.

At each sub-culture, HUVECs were taken for DNA damage analysis through the comet assay and details of their growth were also recorded. This enabled a direct comparison to be made between the level of HUVEC DNA injury and their subsequent replication. Additionally, the SCGE technique was adapted to include FPG supplementation (section 2.2.7.2). This was undertaken to demonstrate whether 8-oxo-dG lesions continued to accumulate in HUVECs during continuous sub-culture. The comets were evaluated using the KOMET software and the cell cultures terminated at passage 6.

The comet results (figure 4-4, page 111) showed that generally, HUVEC DNA damage increased as the cells aged. Moreover, the HG treated samples tended to have higher levels of DNA damage at each passage, although this was not statistically significant (on average, 2.8 (± 0.49) NG olive tail moment vs. 3.7 (± 1.0) HG olive tail moment; $p > 0.05$, $n = 4$). The comet variations between each cell line were very similar, until passage 6 (HG), where the greatest variation occurred, as reflected in figure 4-4 (page 111). The data for the same cells, when subjected to FPG, showed a uniform trend (figure 4-5, page 112). The FPG supplemented comets looked more damaged for both treatments and displayed elevating DNA injury levels with advancing HUVEC

age. However, the increases were much greater in HG (on average, 5.5 (± 0.90) NG olive tail moment vs. 8.3 (± 1.4) HG olive tail moment; $p > 0.05$, $n = 4$). Furthermore, the data showed statistical significant differences in the DNA damage levels registered between NG and HG treated HUVECs at passages 4 and 5 (figure 4-5, page 112). Overall, as expected, FPG heightened the olive tail moment scores, especially for HG-treated HUVECs (figure 4-6, page 113). Although this increase was not quite statistically significant, the data displayed a trend that 8-oxo-dG lesions accumulated to a higher extent in HG treated HUVECs than in NG conditions (figure 4-5, page 112).

Figure 4-4: HUVEC DNA damage sustained during their sub-culture. Primary endothelial cell cultures were established from human umbilical veins taken from three different umbilical cords at delivery. All cultures were incubated at 37°C (5% CO₂ – 95% air atmosphere) and passaged in dimmed light using standard protocols, when sub-confluent. To study the effects of HG, the growth media was supplemented with fresh D-glucose to achieve a final concentration of 22mM. Exposure to HG began at passage 3. The control glucose concentration (NG) was 5.5mM. The media was refreshed every two days. After the initial passages (2 – 6), cells were taken and processed using the FPG adapted comet assay technique to study the levels of DNA damage (as measured by the olive tail moment) during HUVEC culture. The results are presented as the mean olive tail moment scores (\pm SEM) without FPG treatment at each passage examined. P, passage number; NG, normal glucose; HG, high glucose.

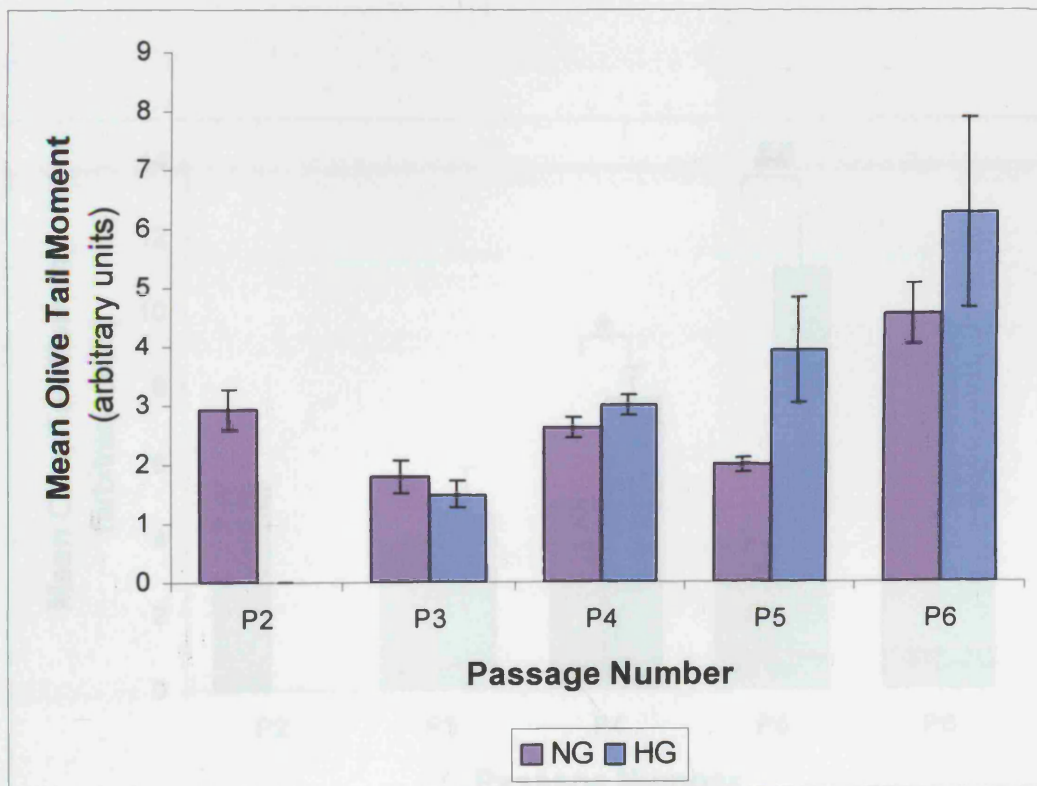


Figure 4-5: HUVEC oxidative DNA damage sustained during their sub-culture. Primary endothelial cell cultures were established from human umbilical veins taken from three different umbilical cords at delivery. All cultures were incubated at 37°C (5% CO₂ – 95% air atmosphere) and passaged in dimmed light using standard protocols, when sub-confluent. To study the effects of HG, the growth media was supplemented with fresh D-glucose to achieve a final concentration of 22mM. Exposure to HG began at passage 3. The control glucose concentration (NG) was 5.5mM. The media was refreshed every two days. After the initial passages (2 – 6), cells were taken and processed using the FPG adapted comet assay technique to study the levels of DNA damage (as measured by the olive tail moment) during HUVEC culture. The results are depicted as the FPG supplemented (1:10000 dilution) olive tail moment scores (\pm SEM) at every passage examined. Using unpaired two-tailed t-tests, NG (+ FPG) P4 vs. HG (+ FPG) P4 (* $p = 0.03$, $n = 3$) and NG (+ FPG) P5 vs. HG (+ FPG) P5 (## $p = 0.008$, $n = 3$). P, passage number; NG, normal glucose; HG, high glucose; FPG, formamidopyrimidine DNA glycosylase.

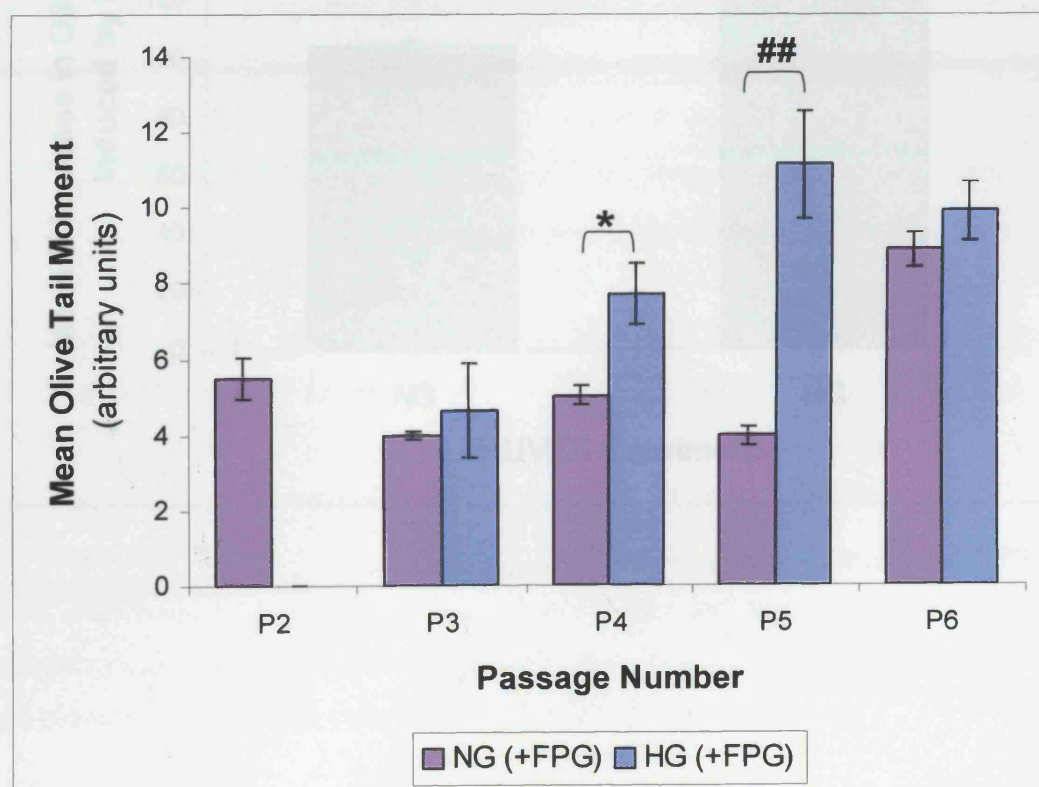
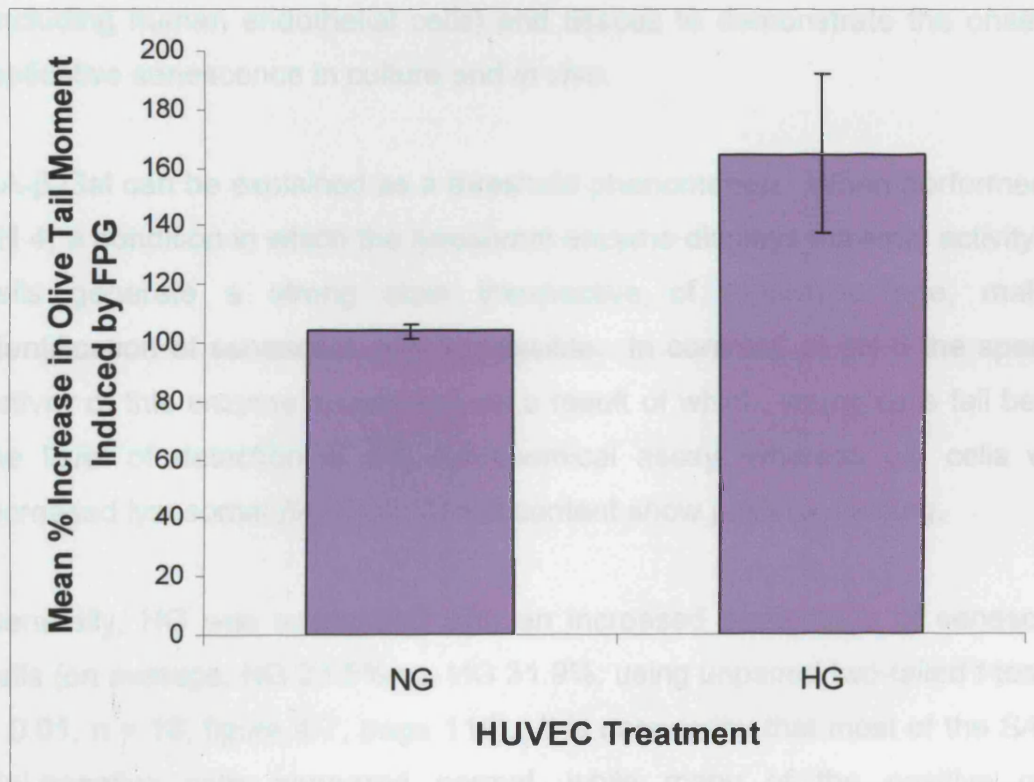


Figure 4-6: Summary of HUVEC DNA damage with FPG treatment. The results are displayed as the mean percentage increases in the olive tail moment (\pm SEM) induced by FPG for NG (5.5mM) and HG (22mM) HUVEC conditions. The percentage increases were calculated by comparing the comet scores for FPG-treated NG and HG HUVECs against FPG-untreated NG and HG cells. The data reflects the comet scores obtained from the initial passages (2 – 6) from the three separate cell lines. Using unpaired two-tailed t-test, NG vs. HG ($p = 0.05$, $n = 5$). NG, normal glucose; HG, high glucose; FPG, formamidopyrimidine DNA glycosylase.



4.4.3 β -GALACTOSIDASE ACTIVITY

Most cells express lysosomal β -galactosidase activity, which is optimally detectable at pH 4, using the X-Gal substrate.^{481, 482} However, Dimri *et al* described a pH 6 β -galactosidase activity, which was found specifically in senescent human fibroblast cultures, but not in quiescent or terminally differentiated cells.^{216, 483} Furthermore, this pH 6 activity enabled the identification of senescent fibroblasts and keratinocytes in biopsies of aged human skin, and subsequently became known as SA- β -Gal. Various laboratories have since used the SA- β -Gal assay on a variety of cells (including human endothelial cells) and tissues to demonstrate the onset of replicative senescence in culture and *in vivo*.

SA- β -Gal can be explained as a threshold phenomenon. When performed at pH 4, a condition in which the lysosomal enzyme displays maximal activity, all cells generate a strong stain irrespective of replicative age, making identification of senescent cells impossible. In contrast, at pH 6 the specific activity of this enzyme is very low, as a result of which, young cells fall below the level of detection of the cytochemical assay, whereas old cells with increased lysosomal β -galactosidase content show positive staining.

Generally, HG was associated with an increased percentage of senescent cells (on average, NG 23.5% vs. HG 31.9%; using unpaired two-tailed *t*-test, *p* = 0.01, *n* = 18; figure 4-7, page 115). It is noteworthy that most of the SA- β -Gal-negative cells appeared normal, while many of the positive cells demonstrated senescent morphology (figure 4-8, page 116). Occasionally, false positives and negatives may have been generated and there were staining inconsistencies with some cells staining more strongly than others. Additionally, some cells were stained for different time periods.

Figure 4-7: High glucose (22mM) effects on HUVEC senescence as indicated by β -galactosidase staining. Cells were seeded on flasks and stained 48 hours later. HUVECs were washed in warmed phosphate buffered saline (PBS), fixed with formalin in PBS, washed again with PBS and then incubated for 24 hours at 37°C with warmed senescence-associated β -galactosidase (SA- β -Gal; pH 6.0). β -galactosidase staining was microscopically revealed by the presence of a blue, insoluble precipitate within the cell. Data was recorded for NG (5.5mM) and HG treated HUVECs between passages 3-8, 10-15 and 20-25. The combined results are displayed as the mean percentages of SA- β -Gal-positive cells (\pm SEM) for both NG and HG cells. Using unpaired two-tailed t-test, NG vs. HG (* $p < 0.05$, $n = 18$). NG, normal glucose; HG, high glucose.

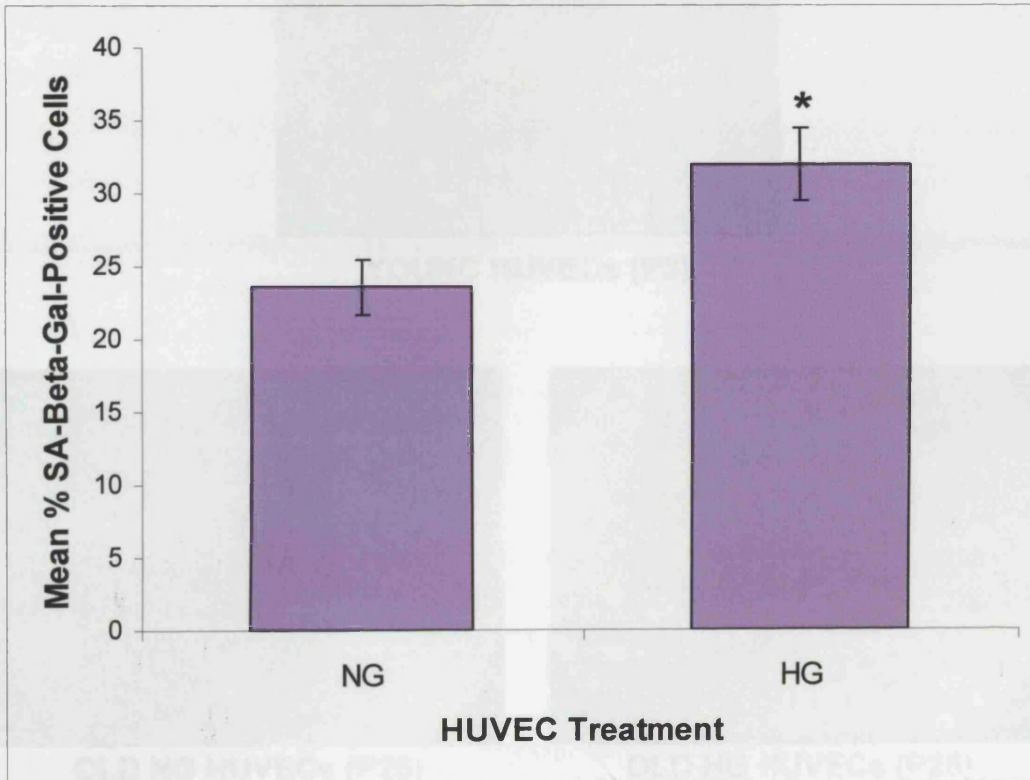
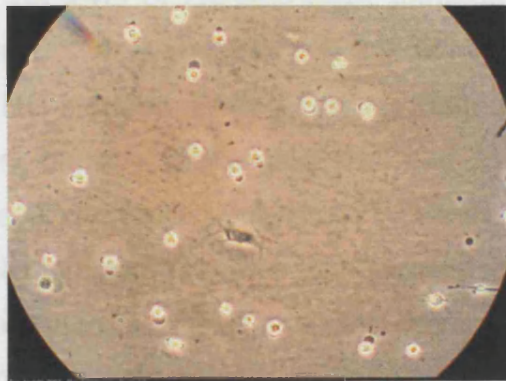
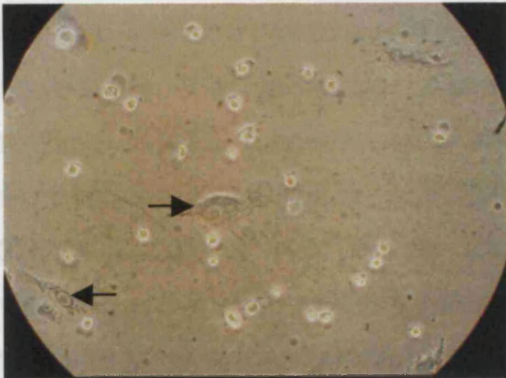


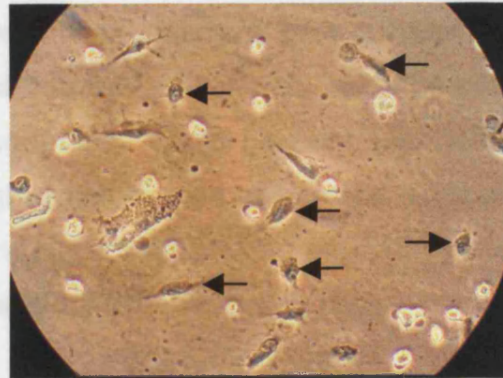
Figure 4-8: Examples of senescent HUVECs as indicated by β -galactosidase staining. Cells were seeded on flasks and stained 48 hours later. HUVECs were washed in warmed phosphate buffered saline (PBS), fixed with formalin in PBS, washed again with PBS and then incubated for 24 hours at 37°C with warmed senescence-associated β -galactosidase (SA- β -Gal; pH 6.0). β -galactosidase staining was microscopically revealed by the presence of a blue, insoluble precipitate within the cell. The arrows indicate some of the senescent cells. Young HUVECs (P3) demonstrated very little staining, older HUVECs (P25) treated with NG (5.5mM) showed a little staining; whereas, old cells (P25) bathed in HG (22mM) exhibited much more staining. P, passage number; NG, normal glucose; HG, high glucose. (x40 magnification)



YOUNG HUVECs (P3)



OLD NG HUVECs (P25)



OLD HG HUVECs (P25)

4.5 DISCUSSION

HUVEC subculturing had shown an attenuation in endothelial cell proliferation during HG treatment and highlighted the possibility of a prolonged endothelial cell cycle. This has been previously demonstrated in bovine aortic endothelial cells and fibroblasts cultured with high glucose concentrations.^{331, 364} Interestingly, these observations were thought to involve increased ROS production as antioxidant supplementation was able to reverse the HG-mediated reduction in endothelial cell numbers.^{21, 331} Further, previous work had suggested that the level of HUVEC DNA damage correlated with their lowered replicative rate.³²² It is possible that the cell cycle checkpoints would have detected the HG-induced DNA damage, halted cell replication and initiated DNA repair, thereby prolonging the cell cycle.⁴⁸⁴ Later, other checkpoints would have identified the restored DNA and allowed cell cycle re-entry. The mechanisms governing this HG-associated cell cycle delay are unknown but probably involve p53, as studies have shown that DNA injury elicits a p53-induced cell cycle arrest.^{116, 485} The results suggest that this process is very efficient as the cells survived in HG for more than 80 days.

However, it is also possible that the transient suspension of growth could have allowed the cells to adapt to prevent further HG insults, and therefore, increase HUVEC longevity. Cellular adaptation could be very important *in vivo* because it provides a route through which human cells could cope with ROS generated by their own respiration, auto-oxidation, the respiratory burst of neighbouring cells and the metabolism of ROS producing drugs or toxins (cigarette smoke, for example).

Cell cycle delay could also have other implications. For instance, normally, the endothelium operates as an anti-thrombotic surface *in vivo* and thus, any injury to it would heighten the risk of thrombosis.¹ Usually, denuded areas would be covered by the migration of surrounding cells and eventually, newly grown cells.¹ However, the HG-mediated inhibition of proliferation and increase in cell death would force these regions to remain exposed for longer.

Subsequently, the probability of thrombosis and neutrophil attraction would increase with the latter amplifying the oxidative injuries.⁴⁸⁶

Replicative senescence may have important physiological associations. Firstly, it could reflect the processes that occur during normal ageing and could even constitute an underlying cause of ageing.¹² Secondly, it is a known tumour suppressive mechanism as it could prevent cells from acquiring the multiple mutations necessary for malignant transformation.¹² Additionally, senescent cells may influence endothelial function. For example, persistent vessel wall coverage with surviving but dysfunctional cells may have more profound effects than cell loss followed by normal rapid regrowth given that endothelial senescence has been linked to atherosclerosis.⁴⁸⁷ Moreover, in a growth factor-rich environment, senescent cells are no more likely to be deleted than their growing counterparts.⁷⁷ This, therefore, strongly implies that they will persist long enough *in vivo* to be of physiological significance in the pathogenesis of vascular disease.

Examinations of the endothelium at atherosclerotic lesions and in vessels from elderly subjects have detected multinucleated enlarged cells – alterations characteristic of replicative senescence.⁷⁷ In addition, similar changes in gene expression have been demonstrated in endothelial cells ageing *in vivo* and in HUVEC models of senescence. For instance, senescent HUVECs in culture over express the intercellular adhesion molecule-1 (ICAM-1) and endothelin, while atherosclerotic lesions have elevated ICAM-1 and patients with advanced atherosclerosis have increased plasma endothelin levels.⁷⁷ Therefore, HUVEC ageing *in vitro* has comparable characteristics to endothelial cell ageing *in vivo*. Furthermore, senescent endothelial cells *in vitro* show an approximate 50-fold rise in PAI-1 and urokinase-type plasminogen activator.²¹⁸ Both these molecules play a central role in the regulation of haemostasis and the altered PAI-1 regulation has been strongly implicated in the pathogenesis of age-related cardiovascular disease.^{193, 218, 233} Similarly, senescent HUVECs in culture appear unable to induce NO production, which has potential *in vivo* consequences for the regulation of vascular tone.⁷⁷

It is well established that endothelial cells exhaust their division potential after a finite number of population doublings.²⁰² Although this was not conclusively displayed in the growth curves, it is expected that with further serial passaging, HUVEC replication would have curtailed. In fact, previous research has suggested that endothelial senescence is reached after 65 cumulative PDs.^{77, 416} However, the β -galactosidase HUVEC staining was consistent with previous findings. Most young cells (with less than 20 sum of PDs) stained negative for SA- β -Gal; whereas, in senescent cultures (48 cumulative PDs) most cells were positive.^{77, 216, 233} Even after cessation of proliferation, most senescent cells including endothelial cells remain metabolically active in cell culture and probably *in vivo* as well.²⁰²

Senescent cells secrete molecules that can have far-reaching and deleterious effects in tissues. These molecules include matrix-degrading enzymes (like metalloproteinases), pro-inflammatory cytokines, anti-angiogenic factors and pro-thrombotic factors.¹²¹ Over expression of any of these secreted molecules would be expected to compromise the integrity and function of tissues. As these molecules can act at a distance within tissues, only a few senescent cells may be needed for them to have adverse effects.

Generally, senescent cells show functional changes.¹²¹ However, the nature of these changes tend to be cell type-specific. For instance, senescent fibroblasts show elevated H₂O₂ generation and a three-fold increase in catalase activity.²³⁰ Additionally, it is claimed that various senescent biomarkers like enlarged cell size, SA- β -Gal activity, lowered induction of *c-fos* and raised metalloproteinase activity also appear after exposure to subcytotoxic oxidative stress and DNA damaging agents.¹⁷⁶ This has suggested the possibility that oxidative stress, DNA damage and senescence are all connected.

The comet assays undertaken with NAC supplemented HUVECs showed that the HG-induced DNA damage was potentially mediated through increased ROS generation (Chapter 3). Additionally, the experiments conducted with the FPG enzyme showed that HG caused an accumulation of oxidative

HUVEC DNA damage through elevated 8-oxo-dG formation over both 24 hours and in the long-term (Chapters 3 and 4). This cause-effect relationship between oxidative stress, DNA damage and ageing was also investigated in human diploid fibroblasts. Wolf *et al.* (2002) demonstrated that DNA injury in old (58 PDs) cells reflected both a heightened susceptibility to oxidative stress, induced by an acute exposure to sub-lethal concentration of H₂O₂ and a reduced efficiency of repair mechanisms.^{14, 488} Furthermore, chronic oxidative stress, mediated by prolonged exposure to 5µM H₂O₂ accelerated fibroblast ageing. This treatment raised 8-oxo-dG levels, SA-β-Gal activity and induced G0/G1 cell cycle arrest in middle aged (41 PDs) cells – making them similar to H₂O₂-untreated old (58 PDs) cells.

4.6 CONCLUSIONS

This chapter showed that DNA damage increased as the HUVECs aged with the HG treated cells tending to have the greater levels of DNA injury. Further, cell culture demonstrated that HG exposure prolonged the HUVEC population doubling times. In addition, the HUVECs were observed to change in morphology with large, irregular and stretched cell islands becoming more prominent with time. Moreover, the application of SA-β-Gal staining confirmed that HG was linked to a higher percentage of senescent cells. Thus, this study provided an association between glucose-induced DNA injury, prolonged cell population doubling times and premature HUVEC senescence.

4.7 FUTURE WORK

The cell culture work could be furthered by the addition of an antioxidant to the HUVEC media. This would allow an examination into the role of ROS in the development of senescence. The antioxidant supplementation could potentially reverse the decrease in the HUVEC proliferation rate and prevent the acceleration of senescence noted in HG treated HUVECs. Additionally, these *in vitro* experiments could be used to study the HUVEC cell cycle. This,

in turn, would enhance the current knowledge regarding cell cycle transition times and checkpoint protein expression during senescence.

CHAPTER 5 : HUVEC TELOMERE

ATTRITION

5.1 INTRODUCTION

Human telomeres consist of $5'$ TTAGGG $3'$ repeats that cap the ends of chromosomes.^{134, 135} The discovery that they shortened with each cell division in human somatic cells, but not in immortal tumour cells, led to the suggestion that they might act as “mitotic clocks”, counting the number of cell divisions and activating senescence as an ultimate DNA damage checkpoint.^{133, 136, 137}

Oxidative DNA damage is thought to preferentially target the telomere as the G-triplet within its structure has been demonstrated to be especially sensitive to oxidative injury.^{3, 114-116} Additionally, deficiencies in the telomeric repair of oxidatively generated single-stranded breaks have been described.^{3, 37, 115-118, 178} Furthermore, it has been illustrated that H₂O₂-induced oxidative DNA damage is sufficient to promote the instability of repetitive sequences.^{114, 115, 149, 183} In fact, fibroblast telomeres have been shown to diminish five times faster when subjected to chronic hyperoxia or subtoxic concentrations of either H₂O₂ or *tert*-butyl-hydroperoxide.^{176, 177} Conversely, the rate of telomere loss was decreased when the fibroblasts were treated with various antioxidants, like EC-SOD.¹⁷⁹ Measurements of telomere shortening rates in these contexts showed that they lessened by about 100 bp/PD under basal culture conditions and by more than 600 bp/PD under mild hyperoxia.^{180, 181} Meanwhile, the telomere attrition rates in fibroblast strains with highly efficient antioxidant defences were as low as 15-20 bp/PD under both conditions.⁹⁴ Altogether, this data strongly indicated that oxidative DNA damage was a major mechanism in triggering rapid telomere attrition.^{116, 118, 144}

5.2 AIM

Diabetes mellitus is associated with premature atherosclerosis and accelerated endothelial cell ageing.¹⁷⁻¹⁹ Additionally, raised glucose concentrations were linked to heightened oxidative stress levels, with the latter known to induce genomic DNA injury. Furthermore, there was evidence that telomeric DNA, an index of cell age, was especially susceptible to oxidation. Thus, this chapter aimed to define the effects of extracellular glucose concentrations on the rate of HUVEC telomere shortening and whether any enhanced attrition was dependent on glucose-driven oxidative stress.

5.3 METHODS

The effects of glucose on HUVEC telomere shortening were examined through cell culturing (section 2.2.2) as this system is often used as a model for the physiological events that occur *in vivo*.^{109, 480} Preliminary Southern analyses (section 2.2.4) revealed early prominent changes in telomere length with replication of HUVECs. Hence, three long-term cultures were established to investigate the effects of high glucose on telomere attrition (section 2.2.2). Furthermore, to implicate an underlying oxidative mechanism for any telomere reductions noted with HG treatment, experiments were designed to examine the effects of antioxidant supplementation on the telomere lengths of HUVECs subjected to NG and HG environments.

The determination of telomere length is traditionally performed by Southern blotting and densitometry, to give a mean telomere restriction fragment (TRF) value for the total cell population studied.^{150, 489, 490} Here, Southern analysis utilized the DIG System, which used digoxigenin (DIG) to label DNA probes for hybridisation and subsequent chemiluminescent detection by enzyme immunoassay (section 2.2.4). The telomeres were visualised on radiographic films that were exposed for 1-5 minutes. The average length per lane was

then calculated as the weighted mean of the optical density using the following formula:⁴⁹¹

$$\frac{\Sigma (\text{optical densities})}{\Sigma (\text{optical densities/molecular weight})}$$

5.4 RESULTS

5.4.1 GLUCOSE-INDUCED TELOMERE ATTRITION

An analysis into a spread of samples taken from the preliminary cell culture experiments (figure 5-1, page 125) revealed small changes in the TRF length (figure 5-2, page 126 and figure 5-3, page 127). In this assay, after 80 days, the telomere lengths had fallen by 13.5% and 16% in NG and HG respectively. Although the total TRF lengths fell, the actual differences between NG and HG (on average, 1.07% NG vs. 1.27% HG per population doubling) were not statistically significant.

Interestingly, the preliminary cell culture also demonstrated that the cell populations at passages 16 (NG, HG) and 21 (NG, HG) had unusually long telomeres. This finding may have resulted from deteriorations in DNA quality or from inherent problems in the experimental methodology. For example, heterogeneous cell suspensions, unequal sample loadings, poor DNA smear intensities, inadequate probes and samples running out of alignment during electrophoresis all affect the outcome.

Figure 5-1: Example of Southern analysis autoradiograph used in the measurement of telomere restriction fragment (TRF) lengths from the long-term HUVEC cultures. The horizontal lines represent the positions of certain markers and the numbers on the left-hand side indicate some of their sizes in kilo bases. P, passage number; NG, normal glucose; HG, high glucose.

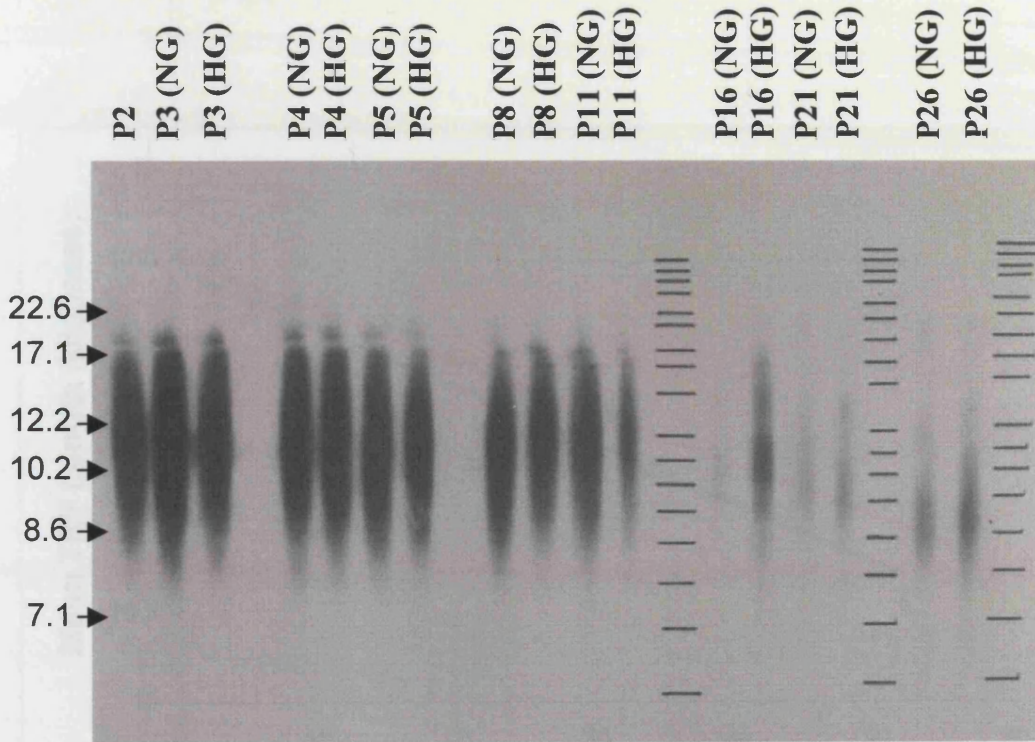


Figure 5-2: Long-term telomere shortening from HUVEC culture. The results are presented as the mean telomere restriction fragment (TRF) length at specific sums of HUVEC population doublings. Each sample was measured three times and the subsequent mean TRF (\pm SEM) was plotted. The linear lines for NG (orange) and HG (green) treatments simply emphasize the general trend of declining telomere length with advancing HUVEC age. NG, normal glucose (5.5mM); HG, high glucose (22mM).

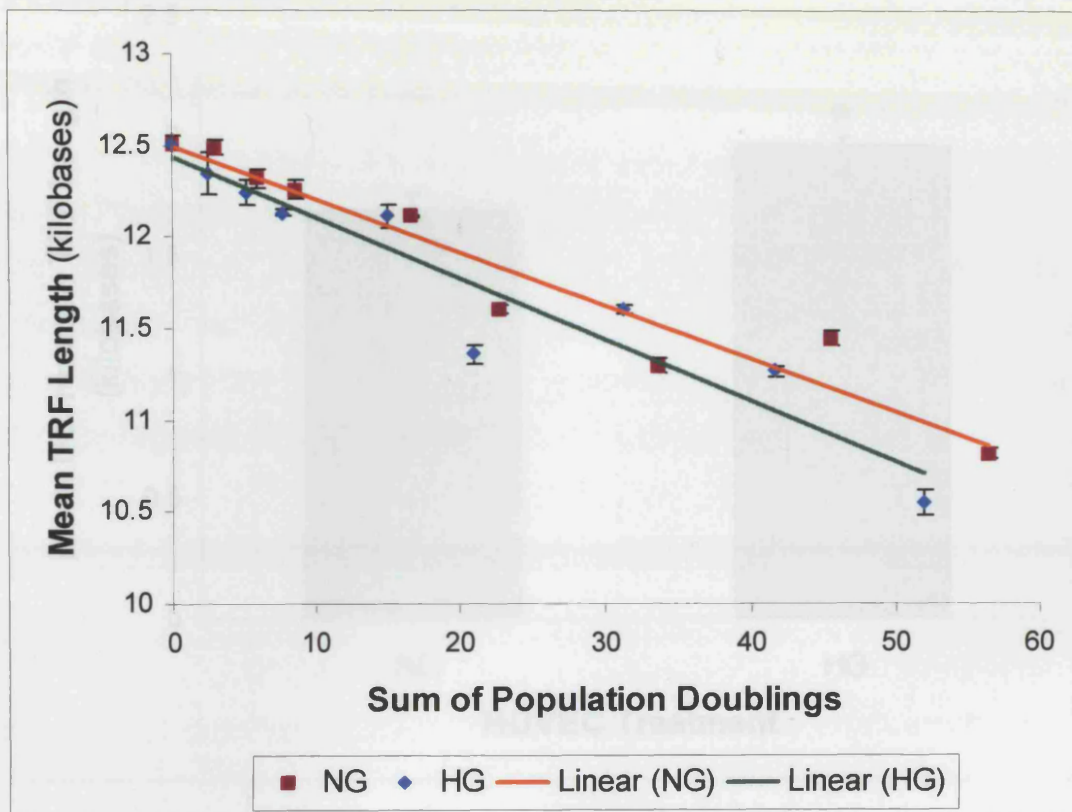
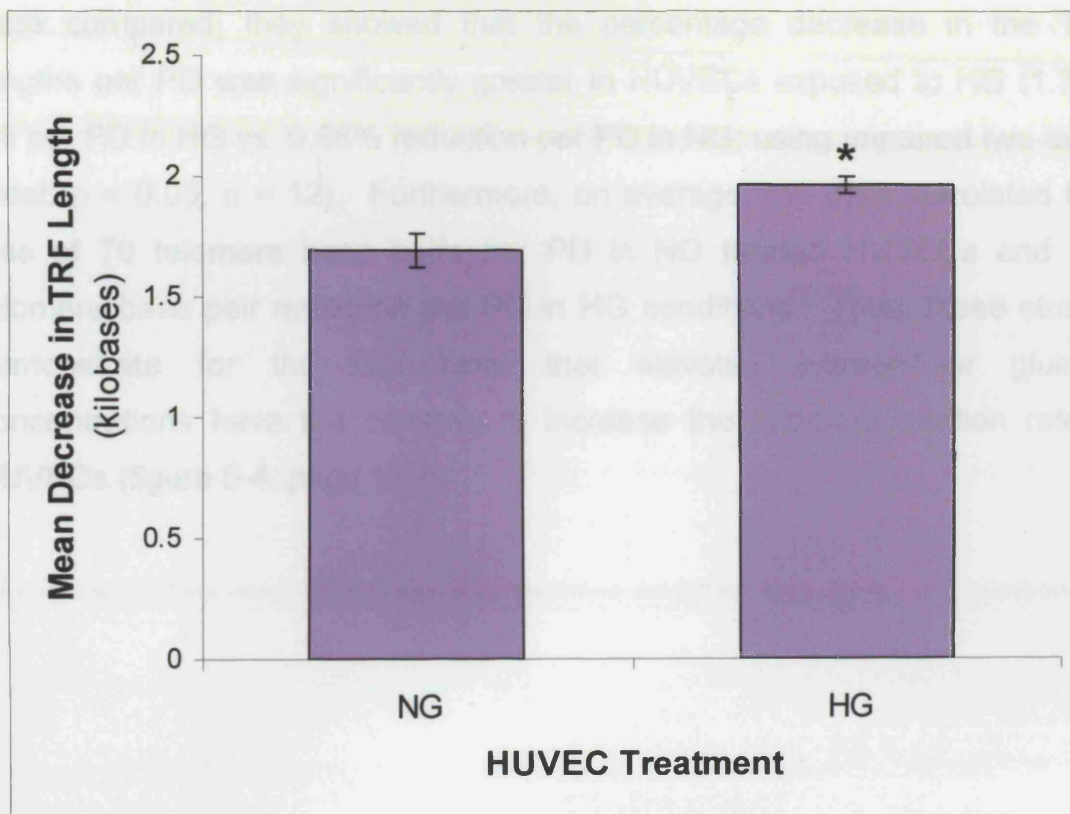
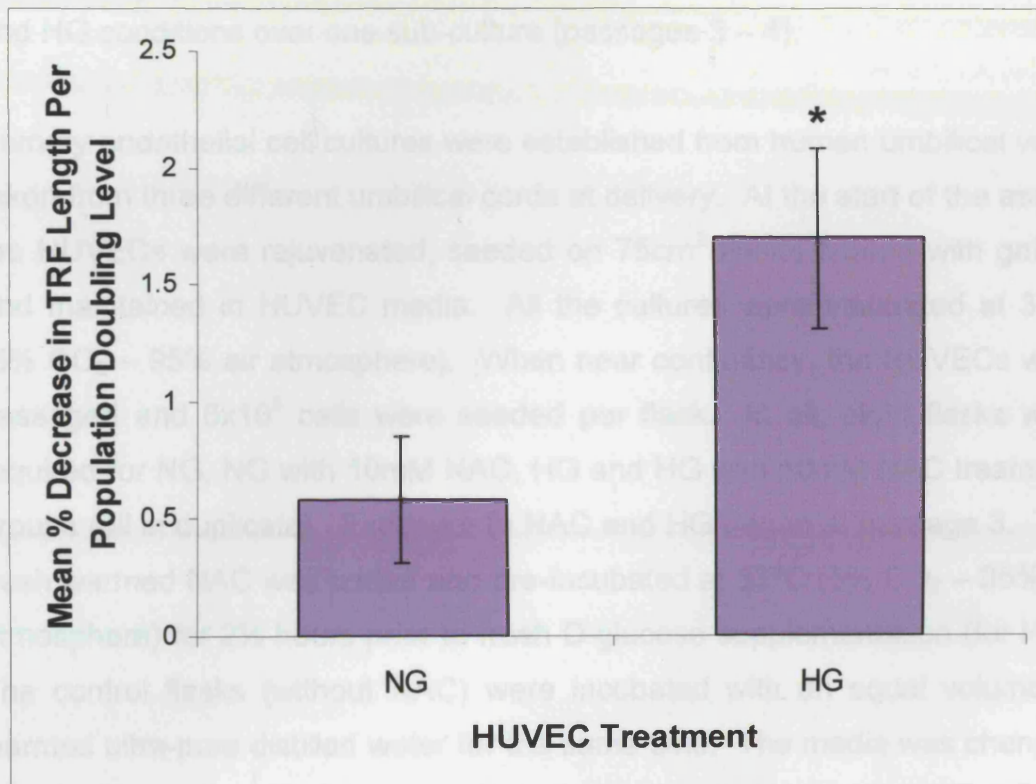


Figure 5-3: Summary of long-term HUVEC telomere attrition from the cell cultures. The results are shown as the total fall in telomere restriction fragment (TRF) length (\pm SEM) over the whole HUVEC culture and demonstrate that HG (22mM) accelerated the telomere shortening rate in this cell line. Using unpaired two-tailed t-test, NG vs. HG (* $p = 0.02$, $n = 3$ measurements). NG, normal glucose (5.5mM); HG, high glucose.



This telomere shortening effect was considered to be an underestimation because glucose could influence cell proliferation (Chapter 4) and increase cell death.⁴⁷ This, in turn, could have led to the selection of clones of cells (“clonal selection”) with less damaged telomeres. The only way around this problem was to examine the telomere shortening over a small number of population doublings. Therefore, a second set of cell cultures (on three new cell lines) was conducted encompassing cell passages 2, 3 (NG, HG) and 4 (NG, HG). When all the data from passages 3 (NG, HG) and 4 (NG, HG) were compared, they showed that the percentage decrease in the TRF lengths per PD was significantly greater in HUVECs exposed to HG (1.70% fall per PD in HG vs. 0.58% reduction per PD in NG; using unpaired two-tailed *t*-test, $p = 0.03$, $n = 12$). Furthermore, on average, the data correlated to a loss of 70 telomere base pairs per PD in NG treated HUVECs and 220 telomere base pair reduction per PD in HG conditions. Thus, these studies demonstrate for the first time, that elevated extracellular glucose concentrations have the capacity to increase the telomere attrition rate in HUVECs (figure 5-4, page 129).

Figure 5-4: Telomere reduction over initial passages (3 – 4) of all HUVEC cultures. The fall in the telomere restriction fragment (TRF) length was studied in four different HUVEC cell lines. The results are indicated as the mean percentage decreases in TRF length per population doubling level (\pm SEM) for both NG (5.5mM) and HG (22mM) treatments. Using unpaired two-tailed t-test, NG vs. HG (* $p = 0.03$, $n = 12$). NG, normal glucose; HG, high glucose.



5.4.2 TELOMERE REDUCTION WITH N-ACETYLCYSTEINE

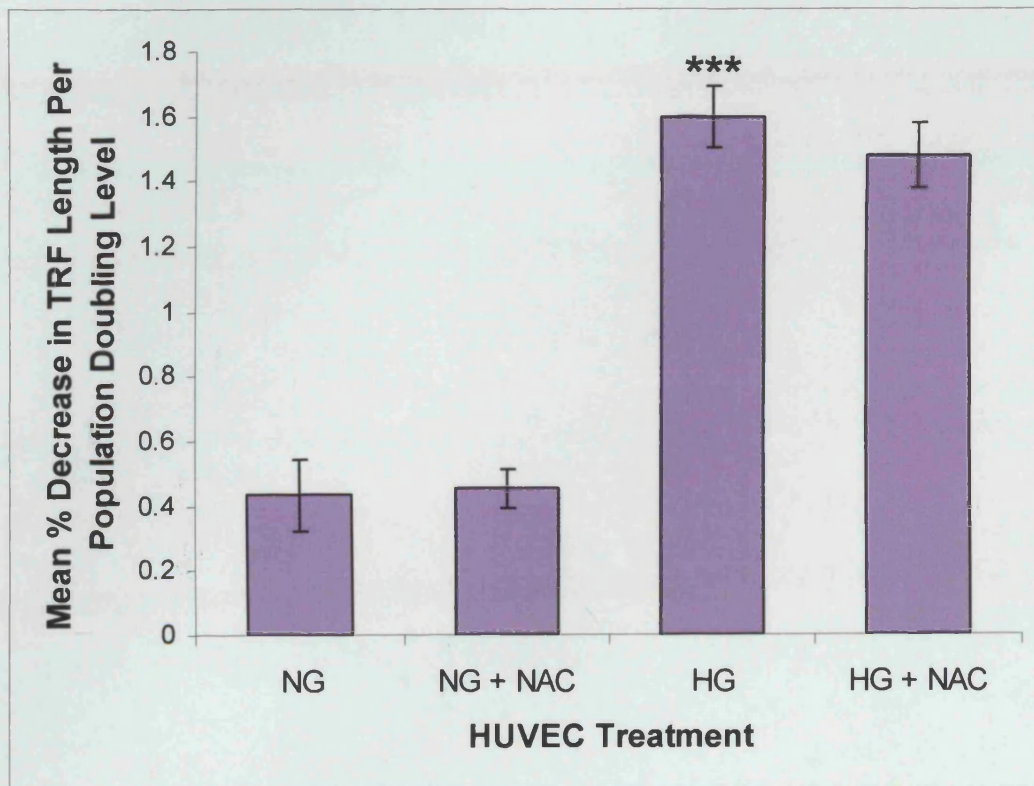
As a result of the HG-induced accelerated telomere shortening data, it became important to ascertain whether the observed quickened pace of telomere attrition could be prevented by antioxidant supplementation. This, in turn, would implicate a free radical mechanism for the telomere reductions noted with HG treatment. Therefore, experiments were designed to examine the effects of NAC addition on the TRF values of HUVECs subjected to NG and HG conditions over one sub-culture (passages 3 – 4).

Primary endothelial cell cultures were established from human umbilical veins taken from three different umbilical cords at delivery. At the start of the assay, the HUVECs were rejuvenated, seeded on 75cm² flasks coated with gelatin and maintained in HUVEC media. All the cultures were incubated at 37°C (5% CO₂ – 95% air atmosphere). When near confluency, the HUVECs were passaged and 6x10⁵ cells were seeded per flask. In all, eight flasks were required for NG, NG with 10mM NAC, HG and HG with 10mM NAC treatment groups (all in duplicate). Exposure to NAC and HG began at passage 3. The fresh warmed NAC was added and pre-incubated at 37°C (5% CO₂ – 95% air atmosphere) for 2½ hours prior to fresh D-glucose supplementation (for HG). The control flasks (without NAC) were incubated with an equal volume of warmed ultra-pure distilled water for the same time. The media was changed every two days until the sub-culture to passage 4, where all the three experiments were terminated. The passaging technique and Southern analysis were completed as described before (section 2.2.4).

The data (figure 5-5, page 131) again demonstrated that HG was able to hasten the pace of telomere shortening. Additionally, this experiment had highlighted that HG caused a 3.7-fold reduction in mean TRF length per PD which compared favourably to the 2.9-fold decrease found previously. Overall, 10mM NAC supplementation was unable to prevent the telomere trimming that occurred in both NG and HG conditions. However, there was a slight trend that NAC may have started to block the HG accelerated telomere

shortening rate as the telomere base pair loss per PD for NG, NG + NAC, HG and HG + NAC treatments were 70, 70, 260 and 240, respectively.

Figure 5-5: HUVEC telomere attrition with N-acetylcysteine (NAC) supplementation. Exposure to NAC (10mM) and HG (22mM) began at passage 3. Fresh warmed NAC was added and pre-incubated at 37°C (5% CO₂ – 95% air atmosphere) for 2½ hours prior to fresh D-glucose supplementation. The media was changed every two days until the sub-culture to passage 4, where all three separate experiments were terminated. The results are displayed as the mean percentage decreases in telomere restriction fragment (TRF) length per population doubling level (\pm SEM) for each HUVEC treatment. Using one-way ANOVA with the Tukey-Kramer multiple comparison test, NG vs. HG (***) $p < 0.001$, $n = 9$) and HG vs. HG + NAC (not significant; $p > 0.05$, $n = 9$). NG, normal glucose (5.5mM); HG, high glucose.



5.5 DISCUSSION

It is now widely accepted that the endothelium is a major target organ for cardiovascular risk factors such as hypercholesterolaemia, hypertension, ageing, smoking and diabetes.¹ This qualifies the ensuing endothelial dysfunction as both a marker and potential mediator of injury. In particular, it is well established that the endothelium plays a central role in atherosclerosis.⁴⁹ Thus, in this thesis, it was essential to use endothelial cell culture as an experimental model system.

HUVEC culture nullified the contributions made by individual cells and allowed investigations into the long-term effects of HG on cell function as well as the telomere-senescence-ageing interrelationship. However, this approach was not without its problems. For example, the changes made to the cellular environment would have perturbed the HUVECs from their typically quiescent *in vivo* state into an activated phenotype with the probable loss of some of their specialised functions during this process.^{493, 494} Furthermore, the hormonal and nutritional milieus were altered. This would have created a climate that favoured HUVEC spreading, migration and proliferation. Another inherent problem was that with each successive subculture, the rapidly proliferating cells would have gradually dominated while the senescent and slower replicating cells were “diluted out”. This “clonal selection” may have been why the telomere lengths increased in passages 16 (NG, HG) and 21 (NG, HG) (figure 5-1, page 125 and figure 5-2, page 126). The observed differences in HUVEC replicative capacity may have also been compounded by the varying abilities of these cells to withstand the traumas of trypsinization, transfer, changes to the media : cell ratio and plating on plastic.⁴⁹⁵

Ideally, a method that could have generated the resting human arterial endothelium *in vitro* should have been used, as this would have represented the *in vivo* situation more closely. However, we have not yet established such a model within the laboratory. Thus, the results obtained should be considered in the context of the cell source and *ex vivo* culture conditions.

Southern blotting was used to measure the telomere lengths of the HUVEC samples because it was the most commonly utilised and robust tool.⁴⁹⁶⁻⁴⁹⁸ Briefly, the fragments obtained by digestion of genomic DNA with *Hinf1* were resolved by electrophoresis and hybridised to labelled probes specific for the telomeric repeats. The resulting TRF smear represented the mean telomeric length of all chromosomes and the TRF values were quantified by densitometric analysis. Thus, the TRF values were subject to variation based on the site of restriction in the sub-telomeric region. Another drawback was that the TRF value attained represented an assessment for the cell population rather than the individual chromosomes, thereby affecting the interpretation of results. However, even with these disadvantages, research had shown that the values obtained through Southern analysis related well to the measurements gained from other procedures.^{496, 498, 499}

Recently, telomere length was inversely correlated to atherosclerotic grade and replicative ageing was suggested as a trigger mechanism for plaque formation.^{41, 196} In this study, the data confirmed that the vascular endothelium undergoes age-dependent telomere attrition (loss of 70 telomere base pairs per PD in NG). It also implied that the rate was hastened by HG treatment (220 telomere base pair reduction per PD). However, Chang and Harley (1995) estimated that HUVECs lost approximately 190 base pairs per PD in telomere length *in vitro*.³⁹ This discrepancy may have been due to culturing variations – for instance, in the cell plating efficiencies and in the concentrations of growth factors and/ or foetal calf serum used in our studies. Moreover, cell culture is often performed with cell culture media that contains a higher concentration of glucose (i.e. >10mmol/l) and this may explain the higher rates of TRF loss noted in other studies in which the cells have been grown in “normal” media.

Importantly, in this thesis, Southern analyses indicated that the acceleration of HG-mediated telomere shortening could be related to the HG-induced increase in HUVEC senescence (Chapter 4). Unexpectedly, Hsiao *et al.* (1997) discovered strong telomerase activity in proliferating HUVECs.⁵⁰⁰ They showed that telomerase was active for up to three weeks following the initial

subculture, inactivated after 20 PDs (even though the cells continued to replicate) and that the enzyme's activity was growth related. These findings are crucial, as the telomerase could have lengthened the HG affected telomeres, and therefore, may have resulted in an underestimation of telomere loss.^{140, 207} Nevertheless, this would be very difficult to confirm because clonal selection would occur in all long-term experiments.

Generally, antioxidants have been shown to reverse the accelerated telomere attrition induced by heightened oxidative stresses. HUVEC and fibroblast treatment with either ascorbic acid 2-O-phosphate or with α -phenyl-*t*-butyl-nitron (free radical scavenger) prolonged their replicative lifespans and slowed down their telomere shortening compared to their controls.^{178, 501} In this study, HUVEC incubation with 10mM NAC was unable to reproduce these findings even though this concentration of NAC was sufficient to inhibit DNA damage as measured by the comet assay (Chapter 3). Perhaps conditioning with NAC at a higher concentration would have prevented the observed quickened HG-mediated HUVEC telomere attrition rate. Additionally, the previous studies had investigated telomere shortening rates over long time periods, as opposed to the attrition rate over the one subculture examined here.^{178, 501} Overall, it is unlikely that the rate of telomere attrition is an innate constant.¹⁷⁸ Instead, evidence suggests that it probably varies from cell to cell as a function of the oxidative milieu, antioxidant defences and level of DNA repair. The latter is especially important because the presence of unrepaired telomeric oxidative lesions during cellular replication could cause large amounts of telomere loss.¹⁶⁰

The HUVEC exposure time to HG would have governed the level of cellular adaptation – the longer the incubation, the more likely that the endothelial cells would have become more resistant to the HG-induced damage. Such acclimatisation could have been mediated through the up-regulation of DNA repair and antioxidant defences.^{77, 486}

The common antioxidant enzymes are SOD, catalase and glutathione peroxidase. In fact, the exposure of human endothelial cells to 20mM D-

glucose for seven and fourteen days was associated with an increase in the mRNA expression of CuZnSOD, MnSOD, catalase and glutathione peroxidase along with a corresponding elevation in their activities.^{21, 28, 299} In the protection against DNA injury, both SOD and catalase have limited roles because $O_2^{\bullet-}$ crosses cell membranes poorly and unless it combines with NO or forms H_2O_2 , it will not cause DNA injury.⁵⁰² Catalases, on the other hand, are exclusively found in peroxisomes and unless they can rapidly diffuse into other cell compartments, they too, are restricted. Thus, in the experimental conditions used, glutathione peroxidase was the likely major defence against HG-mediated ROS generation.⁴⁷³ Additionally, studies have demonstrated that plasma glutathione peroxidase activity is elevated in both types of diabetes.⁵⁰³ Furthermore, other small molecules, such as ascorbate, contribute to antioxidant defences but these become oxidised and impotent after reacting. Moreover, ROS elimination would have also depended upon the cell number and the amount of glucose available to each cell.

After these safeguards, the free radicals could attack proteins, DNA and lipids to produce oxidative damage. Through enzymic damage, ROS could have impaired the DNA repair and antioxidant defences.^{9, 383, 470, 504} Oxidation at an enzyme's active site would have serious implications, for example, it was revealed that glutathione peroxidase glycation caused a decrease in its affinity and contributed to the hyperaggregability of diabetic platelets.⁵⁰³ Different forms of protein oxidation occur ranging from protein carbonyl formation, amino acid attack, sulphhydryl group oxidation, disulphide reduction, aldehyde reaction, protein-protein cross-linking to peptide fragmentation.¹² Normally, oxidised proteins are recognised and degraded by proteases.³³² However, these are insufficient to prevent the age associated increase in oxidised proteins. The accumulation of such proteins is detrimental to the cell, and therefore, they have been implicated in diseases. For instance, premature ageing syndromes have reportedly shown an increased accumulation of oxidised proteins at abnormally high rates.¹²

5.6 CONCLUSIONS

This chapter showed that the percentage decrease in TRF length per PD was significantly greater in HUVECs exposed to HG. On average, the data correlated to a loss of 70 telomere base pairs per PD in NG treated HUVECs and 220 telomere base pair reduction per PD in HG conditions. In addition, NAC supplementation was unable to prevent this accelerated telomere shortening. Therefore, this study suggested, for the first time, that elevated extracellular glucose concentrations had the capacity to increase the HUVEC telomere attrition rate. Further studies are necessary to more fully evaluate whether this effect of HG can be attenuated by a wider range of antioxidants than used in the present study.

5.7 FUTURE WORK

The experiments that examined whether antioxidant supplementation could prevent the glucose-driven increase in HUVEC telomere shortening should be repeated. In future assays, the NAC concentration should be increased and alternative antioxidants should be evaluated. Moreover, it will be important to study the impact of HG on telomerase activity to get a fuller appreciation of the impact of HG on telomere dynamics. Telomerase is thought to have the capacity to anneal to the G-rich strand of the telomere repeat array, and thus, to synthesize telomeric DNA *de novo*. However, very little is known about the amount and duration of telomerase expression as well as the activating and inhibitory signals.

Chapter 6 : HUVEC DNA REPAIR

6.1 INTRODUCTION

Oxidatively damaged DNA bases, including 8-oxo-dG, are mostly restored by BER. This lesion is widely investigated because its presence can induce GC → TA transversions unless it is repaired prior to DNA replication.⁴⁶ Secondly, it is probably the most abundant DNA base oxidation product. In fact, aside from abasic sites, 8-oxo-dG is the most frequent adduct found after DNA exposure to OH[•].^{121, 310} Furthermore, it has been calculated that approximately 7500 8-oxo-dG lesions form daily in mammalian cells, which represents about 5% of all oxidised insults and 10% of the total base adducts.^{82, 266, 309, 505} Thirdly, 8-oxo-dG has been linked to diabetes, atherosclerosis and ageing.^{46, 49, 121, 140, 309, 393} Age-related rises in 8-oxo-dG were observed in female C57BL/6 mice, while Hamilton *et al.* (2001) reported elevating 8-oxo-dG as a function of an age-related sensitivity to oxidative stress in rats.^{49, 309} In addition, primary antioxidant enzymes have been reported to remain unchanged between young and old animals. Hence, these findings were taken to suggest that older animals are unable to adapt to escalating oxidative stress as a function of their increasing age.⁴⁹ Additionally, there is a correlative rise in oxidative mitochondrial DNA damage with age as reported by measured raised 8-oxo-dG levels.^{121, 266}

The major mammalian DNA glycosylase responsible for removing 8-oxo-dG is the 8-oxoG-DNA glycosylase 1 (OGG1).^{375, 439} Without it, mice display 8-oxo-dG accumulation along with an increased DNA mutation frequency.⁵⁰⁶⁻⁵⁰⁸ However, OGG1 does not act alone and there are other enzymes that play roles in 8-oxo-dG elimination (table 6-1, page 138). Additionally, there are different isoforms of the OGG1 protein.³⁷⁵ It appears that there is an alternative last exon of the *ogg1* gene that upon differential splicing directs the

bifunctional OGG1 to either the nucleus (exon 7) or mitochondria (exon 8).³⁷⁵
439, 440, 509, 510

Table 6-1: The enzymes involved in the repair of human cellular 8-oxo-dG. A, adenosine; G, guanine; C, cytosine; 8-oxoG, 8-oxoguanine; hOGG, human 8-oxoG-DNA glycosylase; *E. Coli*, Esherichia Coli. (Adapted from references 46, 191, 247, 266, 309, 321, 375, 418, 422, 423, 430, 439, 505-524)

ENZYME	FUNCTION	LOCALISATION
hOGG1	Removes 8-oxoG from 8-oxoG: C pairs	Type 1a – nucleus (mostly) and mitochondria Types 1b, 1c and 2 – mitochondria
hOGG2	Removes 8-oxoG from 8-oxoG: A and 8-oxoG: G pairs	Nucleus (Mitochondria – possibly)
hMYH human homolog of mut Y (<i>E. Coli</i>)	Removes A from A: 8-oxoG pairs	Type 1 – mitochondrial matrix and cytosol Type 2 – nucleus
hMTH1 human homolog of mut L (<i>E. Coli</i>)	Prevents incorporation of 8-oxodGTP from nucleotide precursor pools	Cytosol and mitochondria
hNTH1 human homolog of nth endonuclease III-like 1 (<i>E. Coli</i>)	Mainly responsible for oxidised pyrimidine removal, but evidence suggests that it could remove 8-oxoG from 8-oxoG: G pairs	Nucleus and mitochondria

6.2 AIM

It has been hypothesised that raised oxidative stress levels may interfere with DNA repair. Therefore, this chapter aimed to examine the efficiency of 8-oxoguanine DNA restoration in HUVECs and to appraise the impact of elevated extracellular glucose concentrations on such DNA repair.

6.3 METHODS

The DNA repair nucleotide incision assay (section 2.2.5) was employed to study the DNA repair activities of HG treated HUVECs to a radiolabelled synthetic oligonucleotide containing an 8-oxoguanine adduct. It worked on the principle that, any increase in oxidative DNA damage would activate and/or up-regulate DNA repair. Furthermore, the enzymes and cofactors involved in subsequent DNA restoration would also be captured during sample collection and thus, they could be examined. Hence, upon the addition of the synthetic 24-mer oligonucleotide, hOGG1 would cleave the 8-oxoguanine, creating a 9-mer repair product that could then be separated by electrophoresis in a 20% polyacrylamide-TBE-UREA gel and visualised by autoradiography.

The samples that were collected for use in the above assay were further utilised to explore for the expression of the repair endonuclease fraction 1 (Ref-1) protein through western blot analysis (section 2.2.6). It was necessary to assess the role of Ref-1 (also known as APE) as recent studies had shown that mouse Ogg-1 activity could be increased by its expression.³¹¹ Additionally, other studies demonstrated that, in the presence of excess Ref-1, the glycosylase activity of hOGG1 was thought to be augmented by up to five-fold.^{507, 514} Furthermore, several DNA repair proteins were demonstrated to be up regulated in the plaques of carotid endarterectomy specimens when compared with non-atherosclerotic vessels. In fact, a strong nuclear immunoreactivity for Ref-1 and DNA-dependent protein kinase was present in the entire plaque (> 90% of the total area) in both macrophages and SMCs.³⁰⁷

6.4 RESULTS

6.4.1 COMPARISON OF 8-oxo-dG INCISION IN HeLa, HUVECs AND HUASMCs

This experiment was undertaken to define the optimal conditions and sensitivity of the endonuclease assay. This investigation was of particular interest as it could establish, for the first time, any differences in 8-oxo-dG repair between three cell types. Low passage cells were used throughout the endonuclease assays as research by Homme *et al* (1994) and Hirano *et al* (1995) had disclosed that repair of oxidative DNA damage was more efficient in cells with fewer population doublings.^{12, 121}

HeLa, HUVECs and HUASMCs were grown from frozen storage, seeded, maintained on two 75cm² flasks each with their respective media and incubated at 37°C (5% CO₂ – 95% air atmosphere) until usage (section 2.2.5). The cells were washed twice with warmed 1xMEM, aspirated and incubated with warmed trypsin. After 4 minutes, warmed media (dependent on the cell type) was added, the cells collected, pooled and centrifuged for 5 minutes at 172g. The resultant pellets were aspirated, then re-suspended in 1ml warmed media and placed on ice. Next, the cells were centrifuged for 10 minutes at 620g at 4°C, homogenised and re-suspended in 100µl fresh DNA repair buffer. Finally, the samples were stored at -80°C until dialysis. The rest of the procedure was continued as related before (section 2.2.5) and was repeated with four separate experimental samples. The optical densities of the 9-mer repair products were measured from autoradiographs exposed for 1 hour as this provided the optimal optical density evaluations (figure 6-1, page 142).

These results demonstrated, for the first time, that HeLa cells are able to incise the most 8-oxoguanine lesions during the 4 hour incubation period, followed by HUVECs, with HUASMCs generating the least 9-mer repair product (figure 6-2, page 143). Ideally, a ratio of unrestored (24-mer) to

repaired oligonucleotide should have been calculated. However, this was impossible as the unrepaired sequences produced smears on the autoradiograph films rather than distinct bands (figure 6-1, page 142). Though unexpected, this was common and reported by other investigators.^{264, 525, 526}

Overall, it appears that untreated HUVECs have a good capacity to sense and initiate 8-oxoguanine repair (figure 6-2, page 143). This may reflect either the abundance of DNA renovation proteins in HUVECs or their heightened sensitivity to oxidative damage. Intriguingly, HUASMCs showed a 3.3- (using one-way ANOVA with the Tukey-Kramer multiple comparison test, $p < 0.001$, $n = 4$) and 1.9-fold (not significant) reduction in 9-mer intensity when compared to HeLa and HUVECs respectively.

Figure 6-1: Example of an autoradiograph comparing the 8-oxo-dG incision capacities of young HeLa, HUVECs and HUASMCs. Low passage HeLa, HUVECs and HUASMCs (passages 2-10) were trypsinised, collected, homogenised and re-suspended in fresh DNA repair buffer. Next, the samples were dialysed against a HEPES-based buffer and their concentrations determined through the Bradford assay. Thereafter, purified labelled complemented 8-oxo-dG oligonucleotide was added to the samples (50µg protein) and incubated at 37°C for 4 hours. Afterwards, 3x denaturing buffer was added to each specimen, heated to 95°C for 10 minutes and then rapidly cooled to 2°C for 5 minutes. Finally, the cleavage products were resolved by 20% denaturing polyacrylamide gel electrophoresis. Next, the gel was subjected to autoradiography and the optical densities of the 9-mer bands were measured from autoradiographs exposed for 1 hour. The methodology is described in more detail in section 2.2.5. 8-oxo-dG, synthetic 24-mer 8-oxo-dG oligonucleotide.

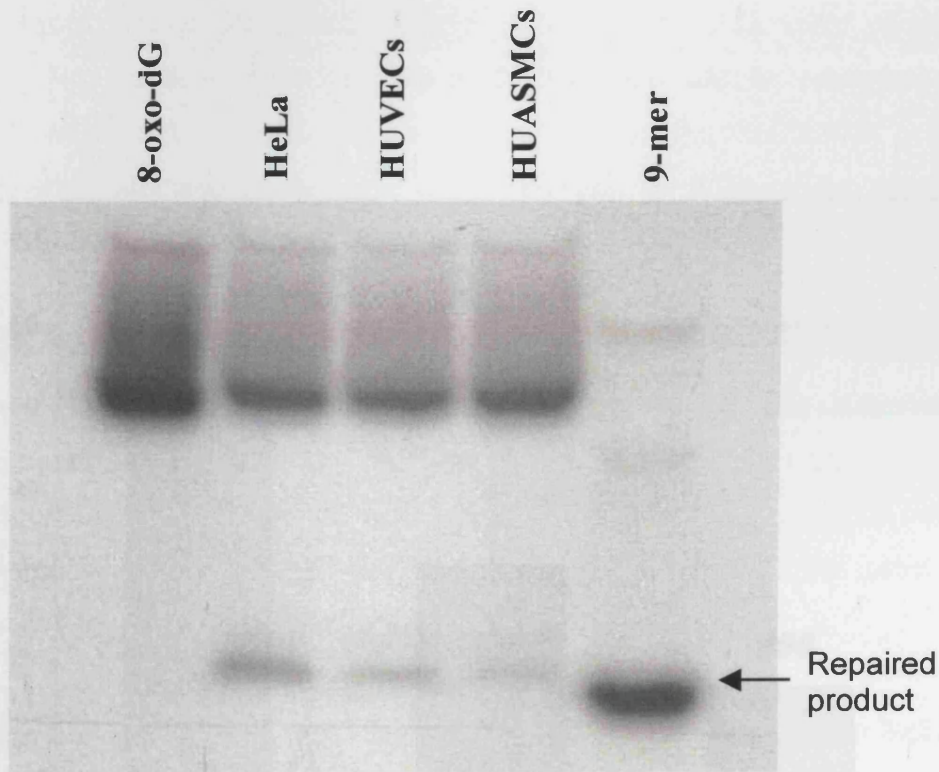
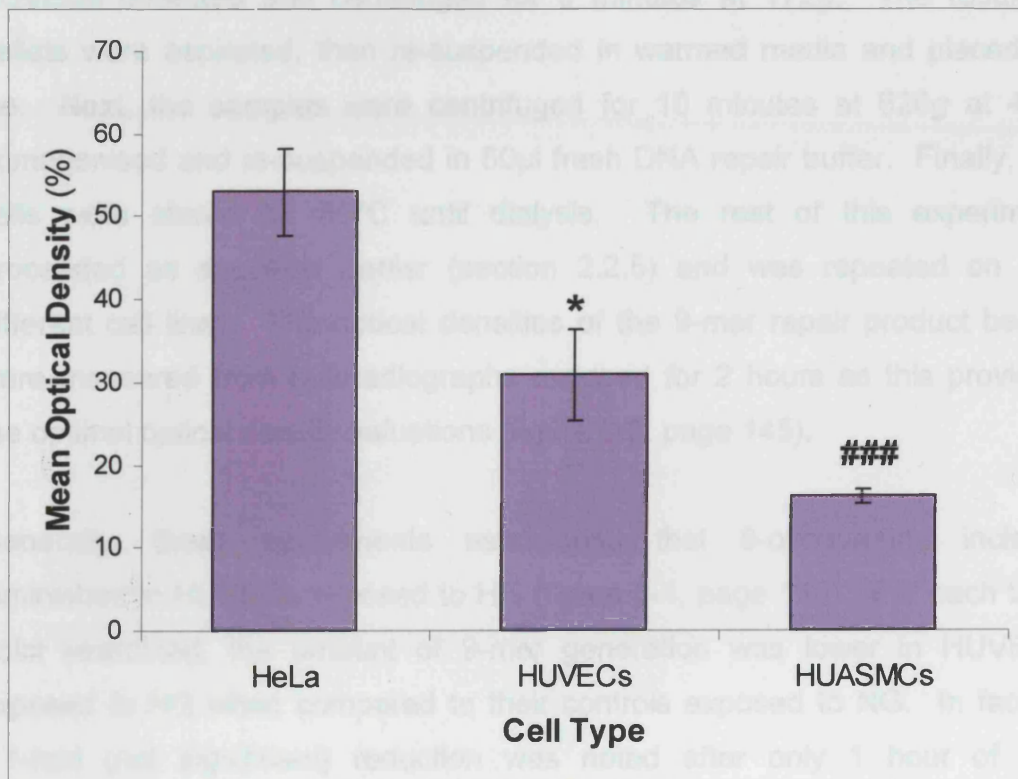


Figure 6-2: 8-oxo-dG incision in HeLa, HUVECs and HUASMCs. Low passage HeLa, HUVECs and HUASMCs (passages 2-10) were trypsinised, collected, homogenised and re-suspended in fresh DNA repair buffer. Next, the samples were dialysed against a HEPES-based buffer and their concentrations determined through the Bradford assay. Thereafter, purified labelled complemented 8-oxo-dG oligonucleotide was added to the samples (50µg protein) and incubated at 37°C for 4 hours. Afterwards, 3x denaturing buffer was added to each specimen, heated to 95°C for 10 minutes and then rapidly cooled to 2°C for 5 minutes. Finally, the cleavage products were resolved by 20% denaturing polyacrylamide gel electrophoresis. Next, the gel was subjected to autoradiography and the optical densities of the 9-mer bands were measured from autoradiographs exposed for 1 hour. The experiment was repeated on four different cell lines and the results are expressed as the mean percentage optical densities (\pm SEM) of the 9-mer repair products for each of the cell types. Using one-way ANOVA with the Tukey-Kramer multiple comparison test, HeLa vs. HUVECs (* $p < 0.05$, $n = 4$) and HeLa vs. HUASMCs (### $p < 0.001$, $n = 4$).



6.4.2 EFFECT OF HIGH GLUCOSE ON 8-oxo-dG EXCISION IN HUVECs

This assay was designed to study whether HG influenced the extent of 8-oxo-dG repair and to examine whether HG increased hOGG1 expression in HUVECs. Low passage HUVECs were rejuvenated from frozen storage, seeded and maintained on gelatin coated 75cm² flasks with HUVEC media and incubated at 37°C (5% CO₂ – 95% air atmosphere) until usage. Flasks were established to enable the following time points to be examined: NG (0 hours; baseline control), NG (1 hour), HG (1 hour), NG (6 hours), HG (6 hours), NG (24 hours) and HG (24 hours). All the flasks were fed with fresh warmed HUVEC media 7 hours before the start of the experiment to allow the cells to settle before D-glucose addition. All the HUVECs were removed together. The flasks were washed twice with warmed 1xMEM, aspirated and incubated with warmed trypsin. After 2 minutes, warmed media was added, HUVECs collected and centrifuged for 5 minutes at 172g. The resultant pellets were aspirated, then re-suspended in warmed media and placed on ice. Next, the samples were centrifuged for 10 minutes at 620g at 4°C, homogenised and re-suspended in 50µl fresh DNA repair buffer. Finally, the cells were stored at -80°C until dialysis. The rest of this experiment proceeded as specified earlier (section 2.2.5) and was repeated on five different cell lines. The optical densities of the 9-mer repair product bands were measured from autoradiographs exposed for 2 hours as this provided the optimal optical density valuations (figure 6-3, page 145).

Generally, these experiments established that 8-oxoguanine incision diminished in HUVECs exposed to HG (figure 6-4, page 146). For each time point examined, the amount of 9-mer generation was lower in HUVECs exposed to HG when compared to their controls exposed to NG. In fact, a 1.1-fold (not significant) reduction was noted after only 1 hour of HG incubation and by 24 hours, a 16% fall had been detected (using one-way ANOVA with the Tukey-Kramer multiple comparison test, $p < 0.05$, $n = 5$). These decreases may have been due to either damage to the repair enzymes

and/or their cofactors or impairment of DNA repair due to energy depletion within the cell, as DNA repair consumes substantial amounts of cellular ATP.

Figure 6-3: Example of an autoradiograph obtained from a time course study into the effects of high glucose (22mM) on HUVEC 8-oxo-dG incision. Young HUVECs (passages 2-5) were trypsinised, collected, homogenised and re-suspended in fresh DNA repair buffer. Next, the samples were dialysed against a HEPES-based buffer and their concentrations determined through the Bradford assay. Thereafter, purified labelled double-stranded 8-oxo-dG oligonucleotide was added to the samples (50µg protein) and incubated at 37°C for 4 hours. Afterwards, 3x denaturing buffer was added to each specimen, heated to 95°C for 10 minutes and then rapidly cooled to 2°C for 5 minutes. Finally, the cleavage products were resolved by 20% denaturing polyacrylamide gel electrophoresis. Next, the gel was subjected to autoradiography and the optical densities of the 9-mer bands were measured from autoradiographs exposed for 2 hours. The methodology is described in more detail in section 2.2.5. The numbers in brackets represent the HUVEC treatment times (in hours). Oligo, 8-oxo-dG oligonucleotide; NG, normal glucose (5.5mM); HG, high glucose.

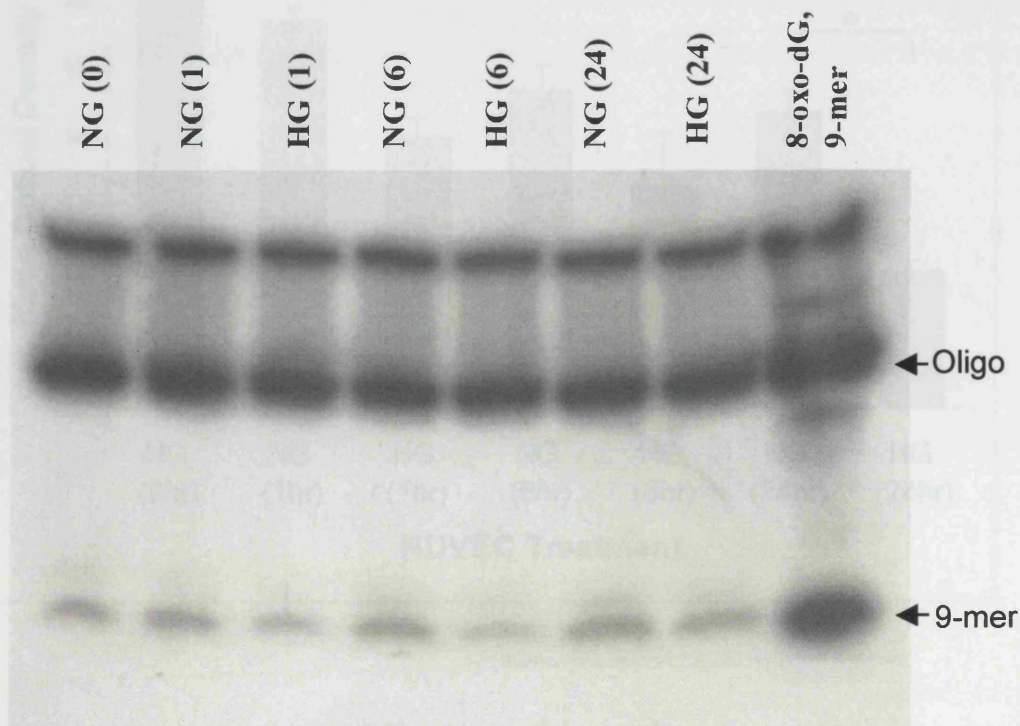
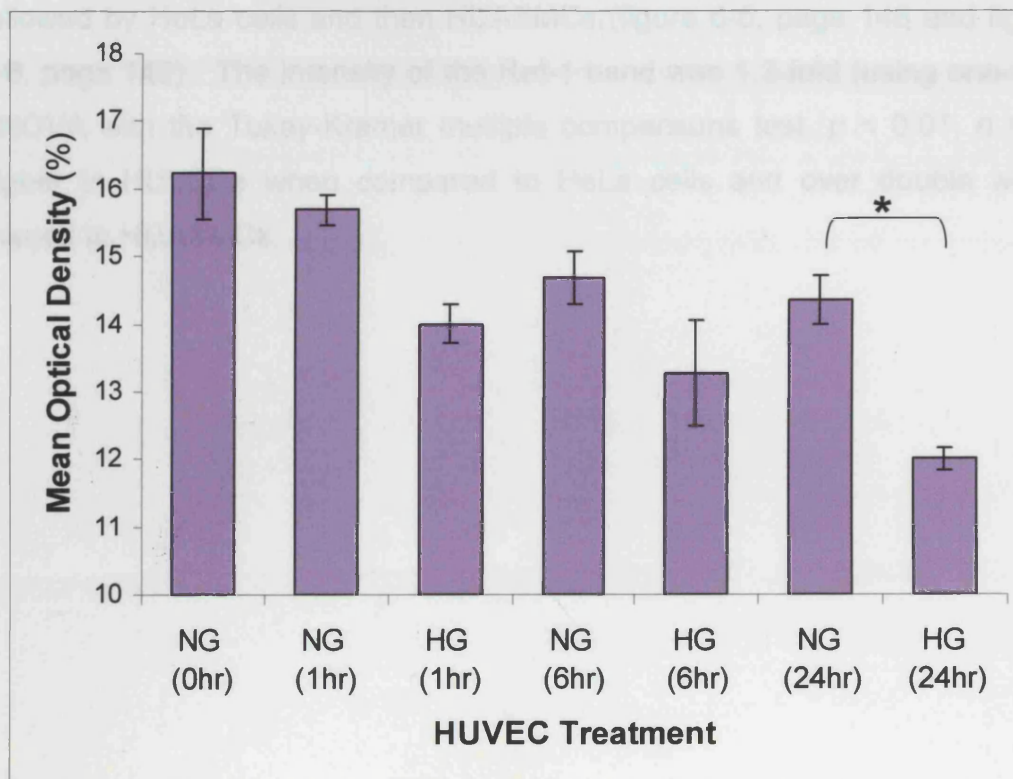


Figure 6-4: High glucose (22mM) induced 8-oxo-dG excision time course in HUVECs. Young HUVECs (passages 2-5) were trypsinised, collected, homogenised and re-suspended in fresh DNA repair buffer. Next, the samples were dialysed against a HEPES-based buffer and their concentrations determined through the Bradford assay. Thereafter, purified labelled double-stranded 8-oxo-dG oligonucleotide was added to the samples (50µg protein) and incubated at 37°C for 4 hours. Afterwards, 3x denaturing buffer was added to each specimen, heated to 95°C for 10 minutes and then rapidly cooled to 2°C for 5 minutes. Finally, the cleavage products were resolved by 20% denaturing polyacrylamide gel electrophoresis. Next, the gel was subjected to autoradiography and the optical densities of the 9-mer bands were measured from autoradiographs exposed for 2 hours. The experiment was repeated on five different HUVEC lines and the results are expressed as the mean percentage optical densities (\pm SEM) of the 9-mer repair products for every time period examined. Using one-way ANOVA with the Tukey-Kramer multiple comparison test, NG (24 hours) vs. HG (24 hours) (* $p < 0.05$, $n = 5$) and the reductions in the NG samples were not significant ($p > 0.05$, $n = 5$). NG, normal glucose (5.5mM); HG, high glucose.



6.4.3 Ref-1 EXPRESSION IN HeLa, HUVECs AND HUASMCs

The next series of studies examined the feasibility of measuring Ref-1 expression in different cell types and optimised the conditions, sensitivity and specificity for Ref-1 detection. Moreover, these studies would indicate how the 8-oxo-dG endonuclease assay correlated with the Western analysis of Ref-1 expression, given the reported interaction of hOGG and Ref-1 in 8-oxo-dG repair. The experiment was performed as outlined earlier (section 2.2.6). The optical density of the 36kDa Ref-1 band was measured from autoradiographs exposed for 15 seconds (figure 6-5, page 148). Such autoradiographs provided the peak optical density values, minimised background signals and lessened any inter-blot differences. The assay was repeated on four separate experimental samples for each cell type.

Western analysis showed that untreated HUVECs expressed the most Ref-1, followed by HeLa cells and then HUASMCs (figure 6-5, page 148 and figure 6-6, page 149). The intensity of the Ref-1 band was 1.3-fold (using one-way ANOVA with the Tukey-Kramer multiple comparisons test, $p < 0.01$, $n = 4$) higher in HUVECs when compared to HeLa cells and over double when likened to HUASMCs.

Figure 6-5: Example of an autoradiograph obtained from Western analysis of Ref-1 expression in HeLa, HUVECs and HUASMCs. The protein samples (50 μ g) were added to 1x loading buffer, boiled, loaded into the wells of a 12% polyacrylamide gel containing SDS and separated by electrophoresis for 55 minutes at 200V in 1xSDS running buffer. Thereafter, the proteins were transferred onto a PVDF membrane through electrophoresis at 64V for 1 hour. Next, immunodetection was carried out with Ref-1 primary antibody and a secondary antibody (anti-mouse Ig, horseradish peroxidase linked whole antibody (from sheep)). This was followed by a number of TBS-0.1% (v/v) Tween washes and chemiluminescent detection with Western blot analysis reagent ECL with the data being recorded on Hyperfilm ECL. The methodology is described in more detail in section 2.2.6. kDa, kilo Daltons.

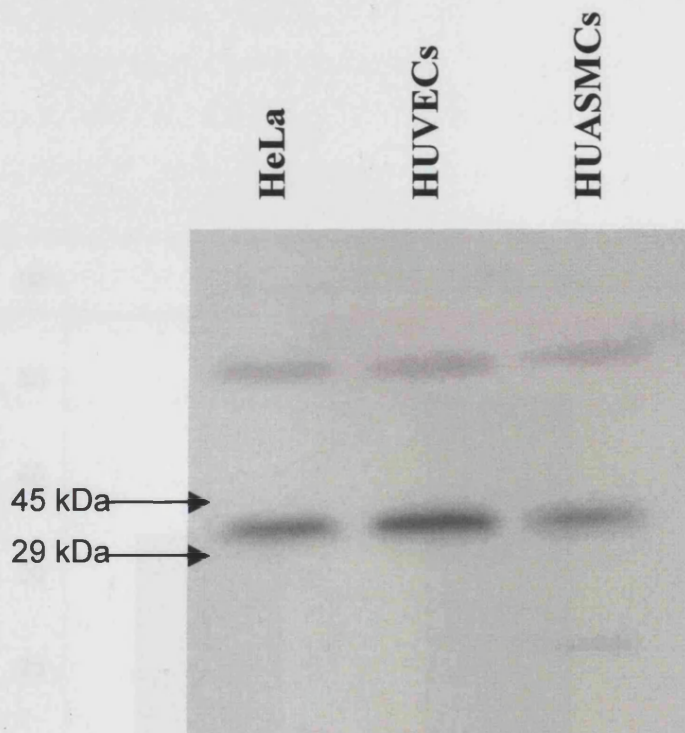
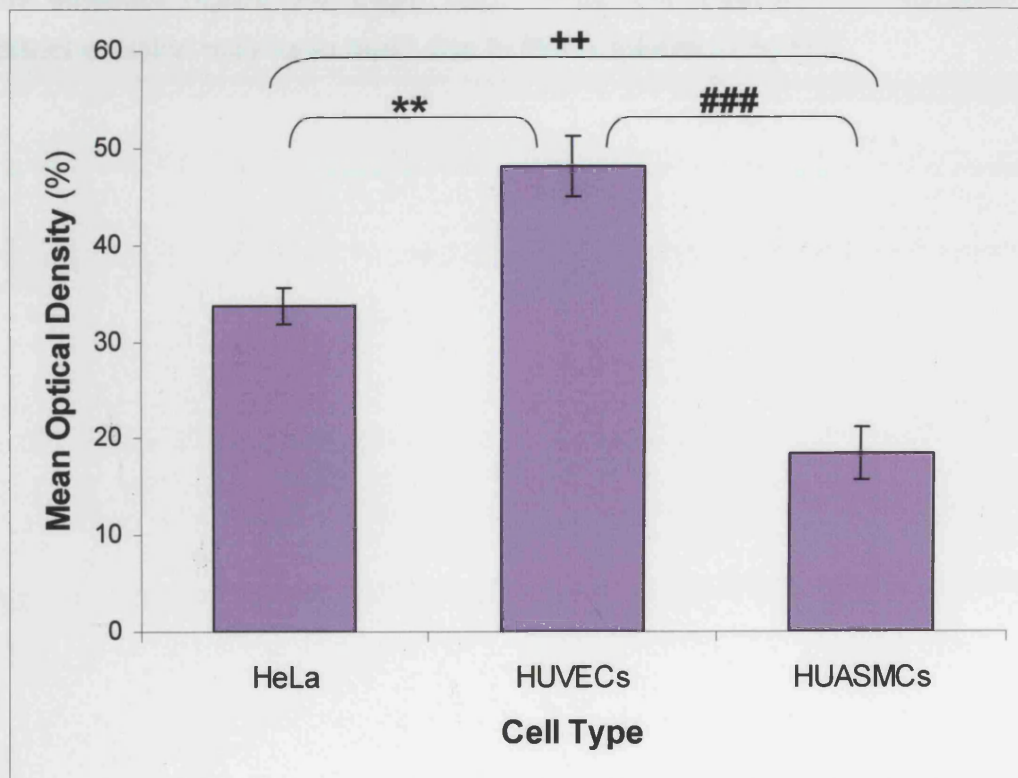


Figure 6-6: Ref-1 expression in HeLa, HUVECs and HUASMCs. The protein samples (50 μ g) were added to 1x loading buffer, boiled, loaded into the wells of a 12% polyacrylamide gel containing SDS and separated by electrophoresis for 55 minutes at 200V in 1xSDS running buffer. Thereafter, the proteins were transferred onto a PVDF membrane through electrophoresis at 64V for 1 hour. Next, immunodetection was carried out with Ref-1 primary antibody and a secondary antibody (anti-mouse Ig, horseradish peroxidase linked whole antibody (from sheep)). This was followed by a number of TBS-0.1% (v/v) Tween washes and chemiluminescent detection with Western blot analysis reagent ECL with the data being recorded on Hyperfilm ECL. The experiment was repeated with four different cell lines for every cell type. After exposure, the bands were analysed and the results are presented as the mean percentage optical densities (\pm SEM) of the 36kDa Ref-1 protein for each of the cell types. Using one-way ANOVA with the Tukey-Kramer multiple comparison test, HeLa vs. HUVECs (** $p < 0.01$, $n = 4$); HUVECs vs. HUASMCs (### $p < 0.001$, $n = 4$) and HeLa vs. HUASMCs (++ $p < 0.001$, $n = 4$).



6.4.4 Ref-1 EXPRESSION IN HIGH GLUCOSE-TREATED HUVECs

This assay was undertaken to discover whether the expression of Ref-1 in HUVECs mirrored the repair activities of these cells to the 8-oxo-dG lesion. It was performed as explained previously (section 2.2.6). Again, the optical densities of the 36kDa Ref-1 bands were measured from autoradiographs exposed for 15 seconds (figure 6-7, page 151). The experiment was repeated on three different cell lines.

These Western blots showed that Ref-1 expression (figure 6-8, page 152) mirrored the incision activity of HUVECs to the 8-oxo-dG lesion (section 6.4.2). The levels of Ref-1 decreased with increasing HUVEC HG exposure times, such that after 24 hours, a 1.8-fold fall (using one-way ANOVA with the Tukey-Kramer multiple comparison test, $p < 0.01$, $n = 3$) in Ref-1 expression was detected (figure 6-8, page 152). Thus, the reduction in 8-oxoguanine adduct excision may have been due to Ref-1 alteration by HG.

Figure 6-7: Example of an autoradiograph obtained from Western analysis of Ref-1 expression in HUVECs treated with HG (22mM). The protein samples (50µg) were added to 1x loading buffer, boiled, loaded into the wells of a 12% polyacrylamide gel containing SDS and separated by electrophoresis for 55 minutes at 200V in 1xSDS running buffer. Thereafter, the proteins were transferred onto a PVDF membrane through electrophoresis at 64V for 1 hour. Next, immunodetection was carried out with Ref-1 primary antibody and a secondary antibody (anti-mouse Ig, horseradish peroxidase linked whole antibody (from sheep)). This was followed by a number of TBS-0.1% (v/v) Tween washes and chemiluminescent detection with Western blot analysis reagent ECL with the data being recorded on Hyperfilm ECL. The methodology is described in more detail in section 2.2.6. The numbers in brackets represent the HUVEC treatment times (in hours). kDa, kilo Daltons; NG, normal glucose (5.5mM); HG, high glucose.

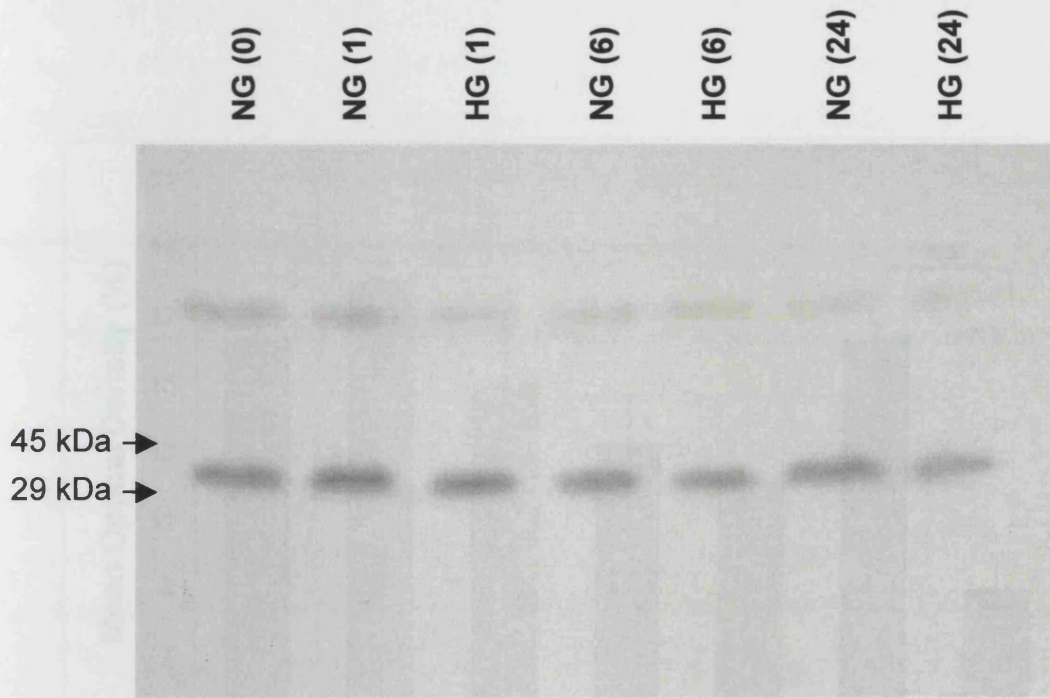
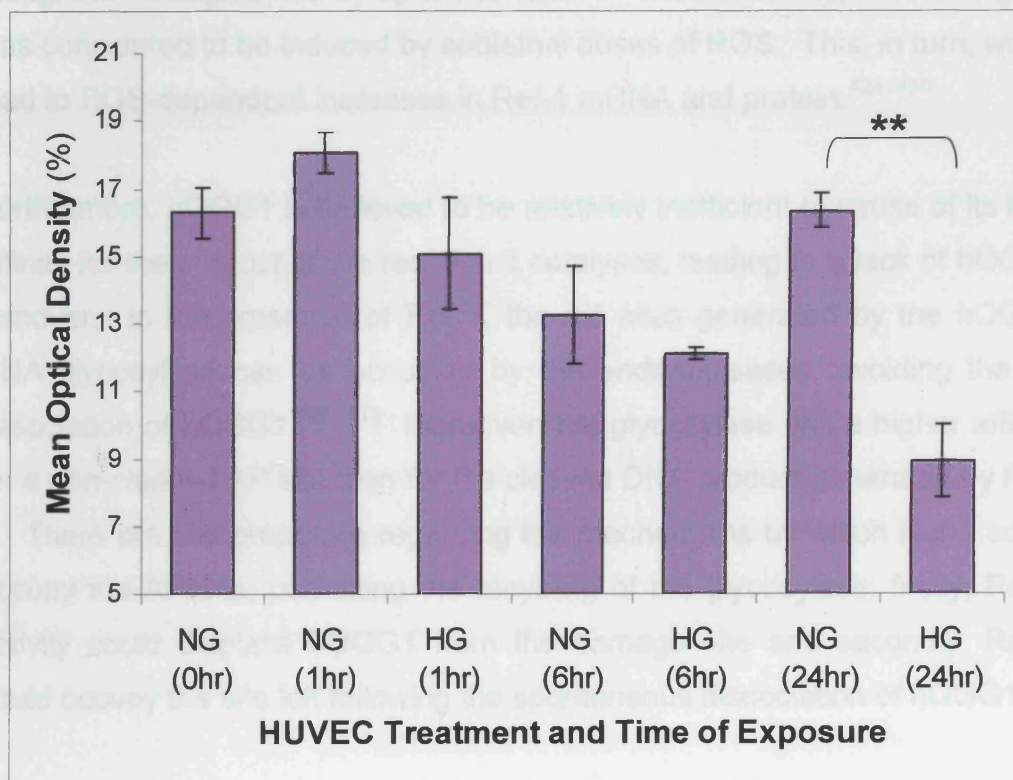


Figure 6-8: Time course of Ref-1 expression in high glucose (22mM) treated HUVECs. The protein samples (50µg) were added to 1x loading buffer, boiled, loaded into the wells of a 12% polyacrylamide gel containing SDS and separated by electrophoresis for 55 minutes at 200V in 1xSDS running buffer. Thereafter, the proteins were transferred onto a PVDF membrane through electrophoresis at 64V for 1 hour. Next, immunodetection was carried out with Ref-1 primary antibody and a secondary antibody (anti-mouse Ig, horseradish peroxidase linked whole antibody (from sheep)). This was followed by a number of TBS-0.1% (v/v) Tween washes and chemiluminescent detection with Western blot analysis reagent ECL with the data being recorded on Hyperfilm ECL. The experiment was repeated with three different HUVEC lines. After exposure, the bands were analysed and the results are presented as the mean percentage optical densities (\pm SEM) of the 36kDa Ref-1 protein at every time point studied. Using one-way ANOVA with the Tukey-Kramer multiple comparison test, NG (24 hour) vs. HG (24 hour) (** $p < 0.01$, $n = 3$). NG, normal glucose (5.5mM); HG, high glucose.



6.5 DISCUSSION

DNA not only appears as a unique copy within a cell, but is also larger than any other macromolecule and the template for all cellular proteins. In addition, DNA is also the primary target of evolutionary change, thus, alteration in this molecule is of particular importance.^{92, 121} In particular, interest surrounds 8-oxo-dG lesions because it has been linked to diabetes, atherosclerosis and ageing.^{46, 49, 121, 140, 309, 393}

In this study, the endonuclease assay was used to estimate hOGG1 activity. Previous results had suggested that the *OGG1* gene was not significantly induced in cells under severe oxidative stress, however, the activity of hOGG1 could be partly enhanced by an increase in the amount of Ref-1 protein.⁵⁰⁷ In fact, in the presence of excess Ref-1, the glycosylase activity of hOGG1 was thought to be augmented by up to five-fold.^{507, 514} Additionally, the *Ref-1* gene was considered to be induced by sublethal doses of ROS. This, in turn, would lead to ROS-dependent increases in Ref-1 mRNA and protein.^{424, 438}

Furthermore, hOGG1 is believed to be relatively inefficient because of its high affinity for the product of the reaction it catalyses, leading to a lack of hOGG1 turnover. In the presence of Ref-1, the AP sites generated by the hOGG1 DNA glycosylase can be occupied by the endonucleases, avoiding the re-association of hOGG1.^{507, 513} Moreover, the glycosylase has a higher affinity for a non-cleaved AP site than for the cleaved DNA product generated by Ref-1. There are two proposals regarding the mechanisms by which Ref-1 could occupy the AP site, permitting the recycling of the glycosylase: firstly, Ref-1 activity could displace hOGG1 from the damage site and secondly, Ref-1 could occupy the site left following the spontaneous dissociation of hOGG1.⁵¹³

The endonuclease assay demonstrated that HeLa cells were able to excise the most 8-oxoguanine lesions, followed by HUVECs and then HUASMCs. This was supplemented by Western blot analysis into Ref-1 expression, which showed that untreated HUVECs had the most Ref-1, followed by HeLa and

HUASMCs, respectively. These results may not have matched directly for a number of reasons. For instance, the heterogeneity of response could be caused by differing growth media, oxygen and nutritional status, metabolic properties and growth characteristics of the cells. Further, differing 8-oxoguanine repair mechanisms may exist in the different cell types. For example, HeLa cells could be more reliant on hOGG1 activity, while HUVECs may require excess Ref-1 expression to aid hOGG1 efficiency.

The HG treated HUVEC time course experiments displayed a gradual decline in 8-oxoguanine repair with increasing HG exposure. This was correlated with a fall in Ref-1 expression in the same cells. Importantly, the decrease in 8-oxoguanine repair was not as a result of lessening 8-oxoguanine formation as the FPG supplemented comet assay displayed HUVEC 8-oxoguanine lesion accumulation during 24 hours of HG incubation. Given that earlier experiments had suggested that HUVECs may have been reliant on Ref-1 expression to help hOGG1 activity, the decline in Ref-1 expression may have caused the tail-off in hOGG1 activity. The fall in Ref-1 expression could have resulted from HG-induced protein damage, possibly via a free radical mechanism. Overall, the fall in 8-oxoguanine excision may be counter-acted *in vivo* by repair through alternative pathways. For example, NER may heighten its contribution to oxidative DNA damage repair.⁴³⁷

Although HUVEC Ref-1 expression was studied, nothing is known about Ref-1 activity. It is possible that cells respond to DNA damage by altering the activity rather than the expression of their DNA repair enzymes. For instance, DNA damage to mammalian cells initiates transient phosphorylation cascades in which different proteins and sites on individual proteins undergo phosphorylation and dephosphorylation.⁵²⁷ However, not all the phosphorylations may be functional. Hence, the significance of these phosphorylations is still under consideration. They may represent a brief but widespread “alarm” response, from which only a few alterations are actually employed for a particular damage.

Western blot analysis and immunohistochemical stains have indicated that there are several DNA repair enzymes (like Ref-1) that are up-regulated in the atherosclerotic plaque.³⁰⁷ The significance of this Ref-1 up-regulation in atherosclerosis is still unclear. For example, Herring *et al.* (1999) could not demonstrate increased resistance to DNA damage in cells overexpressing Ref-1, indicating that elevated Ref-1 could not improve repair efficiency.^{121, 307} It is important to note that Ref-1 is also a redox factor and thus, a widespread regulator of transcription factors that control multiple events in the life cycle of various cell types.

6.6 CONCLUSIONS

This chapter demonstrated, for the first time, that HeLa cells incised the most 8-oxoguanine lesions during a four hour incubation period, followed by HUVECs and then HUASMCs. Interestingly, HUVECs expressed the most Ref-1, followed by HeLa cells and finally, HUASMCs. Moreover, the DNA repair nucleotide incision assay displayed a gradual decline in 8-oxoguanine repair with increasing HUVEC HG exposure. Further, Western analysis showed a similar fall in Ref-1 expression in the same cells. Therefore, this study suggests that HG has the potential to decrease the efficiency of HUVEC 8-oxoguanine repair.

6.7 FUTURE WORK

Examinations into the other DNA repair molecules and oxidative DNA lesions could be conducted. Furthermore, it would be interesting and important to study the repair activities of pancreatic cells in NG and HG conditions.

Chapter 7 : HUVEC MITOCHONDRIAL DNA

CONTENT

7.1 INTRODUCTION

Mitochondrial DNA injury is now considered to be an important factor in ageing caused, in part, by ROS released from the “electron transport chain”.^{94, 96, 124, 126} Mitochondria are the targets of their own deleterious oxidant yields and consequently, their steady-state oxidative damage levels are relatively higher than in other organelles.^{100, 125, 127-129} Further, the percentage of oxygen converted into $O_2^{\bullet-}$ increases with age.^{130, 131} This, in turn, leads to a spiralling cycle of elevated cellular injury to the nuclear, cytosolic and mitochondrial compartments, which would then adversely affect cell function and ultimately result in a loss of ATP-generating capacity. This could become especially important in times of great energy demand (DNA repair, for instance) as vital ATP-dependent reactions would be compromised.¹³²

Alterations to mt-DNA structure, mediated by mt-DNA damage, are proposed to play a role in mt-DNA deletion generation.²⁶⁷ Age-related changes in mt-DNA oxidative adduct aggregation and deletions are also consistent with this idea.^{12, 121, 127, 234} Furthermore, there is evidence of an increase in the incidence of point mutations in mt-DNA with age.^{262, 267, 269, 270}

Mitochondrial integrity and function is influenced by the presence of diabetes too.^{234, 269} Approximately 0.5-1.5% of all diabetic patients exhibit pathogenic mt-DNA mutations such as duplications, point mutations and large-scale deletions (especially the “common 4977 base pair deletion”).^{94, 127, 281} High glucose concentrations have been shown to contribute to common deletion accumulation as well as to the development of other mutations in VSMCs *in vitro*.^{43, 282} Such glucose-related mt-DNA deletions have additionally been seen in HUVECs.²⁸² Diabetes also shows quantitative changes in mt-DNA.

For example, Antonetti *et al.* (1995) reported that mt-DNA copy number was approximately 50% lower in the skeletal muscles of both type 1 and 2 diabetic patients.^{121, 283-286} In addition, Lee *et al.* (1998) claimed that lymphocyte mt-DNA copy number decreased prior to type 2 diabetic development and suggested that the fall might be a causal factor in diabetic pathogenesis.²⁸³⁻²⁸⁶

7.2 AIM

Oxidative injuries to cellular DNA, both nuclear and mitochondrial, are ubiquitous insults that occur under normal physiological conditions that may be enhanced by environmental agents and ageing.^{121, 234, 256} Additionally, mt-DNA is proposed to be more vulnerable to oxidant damage than nuclear DNA.^{83, 264} Furthermore, mitochondrial integrity and function are influenced by ageing and diabetes.^{234, 269} Therefore, this chapter aimed to determine whether elevated extracellular glucose concentrations led to an accelerated loss of mitochondrial DNA in HUVECs.

7.3 METHODS

Initially, primary endothelial cell cultures were formed from human umbilical veins taken from three different umbilical cords at delivery (section 2.2.7.1). These three cell lines were grown for 85 days and to study the effects of HG, the growth media was supplemented with freshly prepared D-glucose to achieve a final concentration of 22mM. Exposure to HG began at passage 3. The media was changed every two days to keep the glucose concentrations relatively constant. At each passage, HUVEC samples were taken for DNA analysis as detailed earlier (sections 2.2.7.3 and 2.2.7.4).

The mitochondrial genome copy number was established using a probe specific to a sequence of mitochondrial DNA (between 12663 – 13662 base pairs, which encodes the NADH-dehydrogenase subunit 5 protein). Meanwhile, the nuclear DNA copy number was ascertained using a probe

limited to 18S ribosomal DNA (a multi-copy gene). Densitometry was used to quantify the intensities of the nuclear and mitochondrial DNA bands (section 2.2.7.3). The relative mitochondrial DNA copy number was then calculated by normalizing the mitochondrial DNA to the nuclear DNA in every examined sample and then comparing it to the HeLa standards to account for any inter-gel variability.

7.4 RESULTS

In these experiments, it was assumed that the nuclear DNA copy number (content) would be constant and the levels of mitochondrial DNA would vary with HG treatment. Indeed, the autoradiographs for each HUVEC culture reflected this (figure 7-1, page 159). That is, there were visible differences in the mitochondrial content between NG and HG exposed HUVECs (figure 7-1, page 159). However, the nuclear DNA content unexpectedly varied between the NG and HG conditioned cells at most passages (figure 7-1, page 159). This, as yet, is unexplained and entails that the data must be interpreted with caution.

Overall, the combined data (figure 7-2, page 160) from the three long-term cultures suggested that there was little difference in the relative mitochondrial DNA contents of NG and HG treated HUVECS (on average, 3.8 NG vs. 4.1 HG relative HUVEC mitochondrial DNA content, not statistically significant). It is possible that during the prolonged HUVEC culture clonal selection for cells with high mitochondrial DNA content may have masked the results for these experiments. For instance, on closer inspection, over the first few passages, there was a tendency for HG incubated HUVECs to demonstrate lower relative mitochondrial DNA content (on average, 4.2 NG vs. 3.1 HG relative HUVEC mitochondrial DNA content, not statistically significant). But, in the later passages, this pattern was reversed.

Figure 7-1: Example of an autoradiograph displaying the mitochondrial DNA (mt-DNA) and nuclear DNA (n-DNA) in a HUVEC line. Initially, the total DNA collected from the long-term culture of HUVECs were purified and quantified. Sample DNA (1 μ g) along with three HeLa DNA standards (0.5 μ g, 1 μ g and 2 μ g) were incorporated into a restriction enzyme digestion mixture containing 1xNEBuffer 2 and BamH1. Digestion occurred at 37°C for 4 hours before each specimen was separated by electrophoresis in a 0.5% agarose gel in 1xTAE for approximately 16 hours. Next, alkaline Southern blotting, DNA fixation and radio-labelling with specific probes was undertaken. The mitochondrial genome copy number was established from a probe specific to a sequence of mt-DNA (between 12663 – 13662 base pairs, which encodes the NADH-dehydrogenase subunit 5 protein). Meanwhile, the nuclear DNA copy number was ascertained by a probe limited to 18S ribosomal DNA (a multi-copy gene). Finally, autoradiography was performed to visualize the DNA bands. (A more detailed description of the methodology is contained in section 2.2.7.3). P, passage number; HMW, high molecular weight; kb, kilo base; NG, normal glucose (5.5mM); HG, high glucose (22mM).

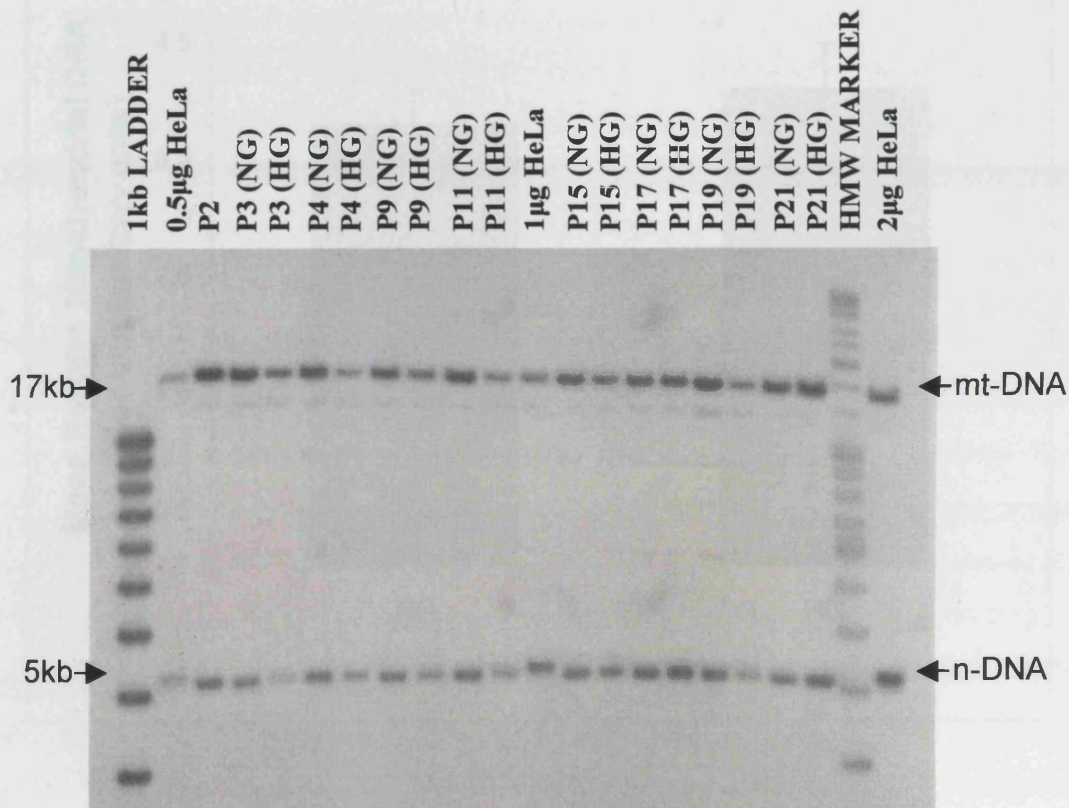
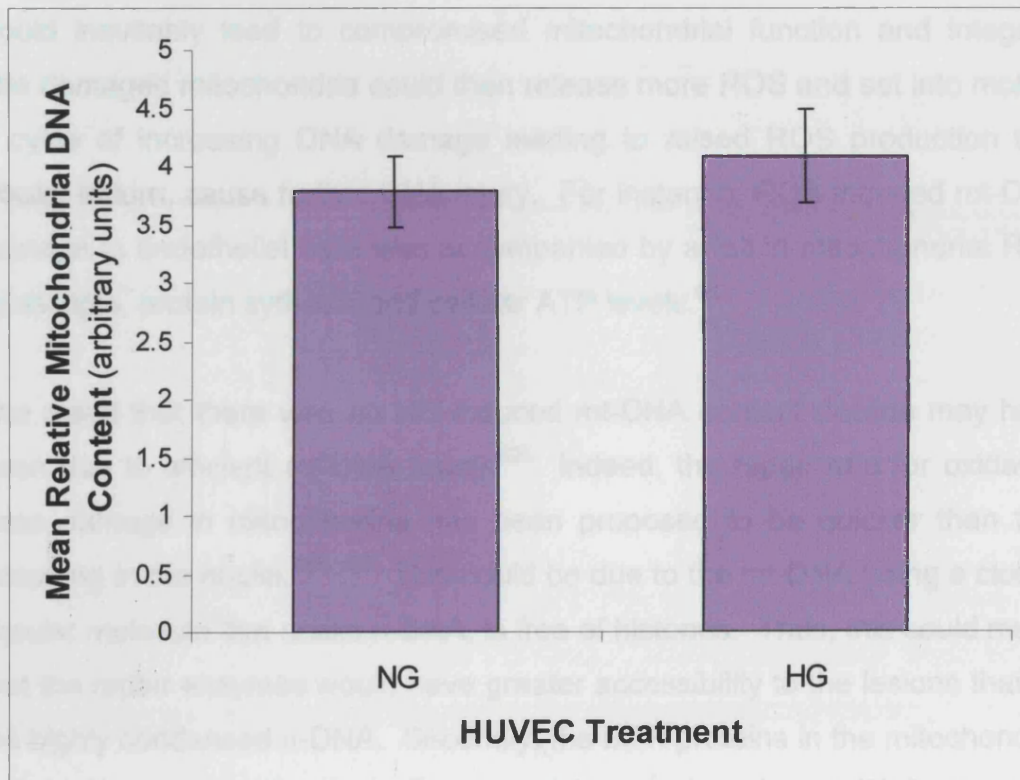


Figure 7-2: Long-term effect of high glucose (22mM) on HUVEC mitochondrial DNA content. Primary endothelial cell cultures were established from umbilical veins taken from three different umbilical cords at delivery. A sample of cells was taken from selected passages (2, 3, 4, 9, 11, 15, 17, 19 and 21) for mitochondrial to nuclear DNA analysis. The specimens underwent DNA isolation and quantification before alkaline Southern blotting, DNA fixation, radio-labelling with specific probes and autoradiography. Thereafter, densitometry was undertaken to establish the mitochondrial DNA to nuclear DNA content ratios relative to the HeLa DNA standards. The results are expressed as the mean relative mitochondrial DNA contents (\pm SEM) for all studied HUVEC passages treated with either NG (normal glucose; 5.5mM) or HG (high glucose) conditions from three independent experiments.



7.5 DISCUSSION

The finding that HG had no effect on the HUVEC mt-DNA content was unexpected. It is known from experiments with cultured BAECs that hyperglycaemia increases the mitochondrial production of ROS via the transport of cytoplasmic pyruvate into the mitochondria.^{9, 377} Additionally, the spatial proximity to the process of oxidative phosphorylation renders mt-DNA highly vulnerable to ROS.⁴³⁹ In fact, HG media has been shown to induce oxidative damage to mt-DNA and reduce mitochondrial gene expression through increased mitochondrial electron transport chain $O_2^{\bullet-}$ production.⁴³ In parallel, mitochondrial generation of $O_2^{\bullet-}$ was augmented in HUVECs incubated with HG.⁹⁰ It was thought that the increasing damage to mt-DNA would inevitably lead to compromised mitochondrial function and integrity. The damaged mitochondria could then release more ROS and set into motion a cycle of increasing DNA damage leading to raised ROS production that would, in turn, cause further DNA injury. For instance, ROS-induced mt-DNA damage in endothelial cells was accompanied by a fall in mitochondrial RNA transcripts, protein synthesis and cellular ATP levels.⁶⁸

The result that there was no HG-induced mt-DNA content decline may have been due to efficient mt-DNA repair.⁵²⁴ Indeed, the repair rate for oxidative base damage in mitochondria has been proposed to be quicker than that occurring in the nuclei.^{439, 520} This could be due to the mt-DNA being a closed circular molecule that unlike n-DNA, is free of histones. Thus, this could mean that the repair enzymes would have greater accessibility to the lesions than in the highly condensed n-DNA. Secondly, the BER proteins in the mitochondria and nucleus are not identical. The alternative splicing of pre-mRNA gives rise to at least two isoforms of OGG1, which are transported to the different cellular compartments. Both the OGG1 isoforms have glycosylase and AP-lyase activity, but they differ in their C-terminus, and therefore, it is possible that the activity varies between them. Thirdly, the concentration of the active enzyme in the different cellular compartments may differ.

Although the role of mitochondria in ageing is currently attracting much attention, several factors contribute to the uncertainties that surround the importance of mitochondrial dysfunction. For example, the dual genetic control of biogenesis and function of mitochondria results in the difficulty of differentiating the nuclear and mitochondrial DNA involvement, due to the complicated cross-talk between the nucleus and mitochondria. In fact, certain strains of yeast are able to cope with mt-DNA damage by activating a suitable nuclear response and increasing lifespan.⁵²⁸ This compensatory mechanism is known as the “retrograde response (RR)”. It acts to adjust the activity of nuclear genes according to the strength of a signal generated by the mitochondrion. It has been suggested that RR may also be present in mammals such that damaged mitochondria are removed and replaced through interplay with the nucleus. However, as yet, no evidence exists for this in humans.⁵²⁹ Another significant factor is that mt-DNA are present in mammalian cells in thousands of copies, but virtually nothing is known about their physical organisation within the cell.²⁴⁰ The traditional view of mitochondria as discrete and semi-permanent entities has now given way to a more dynamic model, in which individual organelles are seen as exchanging materials with each other, via a continuous process of fusion and budding.⁵²⁹

7.6 CONCLUSIONS

This chapter suggests that there was very little difference in the relative mt-DNA contents between the NG and HG treated HUVECs. In fact, there was a slight increase in the level of mt-DNA in the HG exposed HUVECs.

7.7 FUTURE WORK

Very little is known about the potential roles for mt-DNA in diabetes and its complications. Thus, further research is essential. The quantitative polymerase chain reaction technique could be used to re-examine the mt-DNA content of HG treated HUVECs. Additionally, this method could be

employed to analyse the levels of glucose-driven HUVEC mt-DNA injury. Also, investigations into pancreatic β -cell mt-DNA damage are important as this cell's mitochondria play a pivotal role in glucose stimulated insulin secretion.

Chapter 8 : HUVEC MITOCHONDRIAL

COMPLEX IV EXPRESSION

8.1 INTRODUCTION

Approximately 85-90% of the oxygen taken up by a cell is utilized by the mitochondria to manufacture most of the ATP needed.¹² The essence of metabolic energy production involves the oxidization of food materials: they lose electrons, which are accepted by electron carriers, such as NAD⁺ and flavins (FMN, FAD).^{249, 250} The resulting reduced NADH and flavins (FMNH₂, FADH₂) are then re-oxidised by oxygen in mitochondria, forming ATP.^{251, 252} This oxidation is catalysed in a stepwise manner by a chain of five enzyme complexes in the electron transport chain, so that the energy is released gradually.^{12, 253}

Mitochondrial O₂^{•-} production occurs primarily at two discrete points in the electron transport chain, namely at complex I (NADH dehydrogenase) and at complex III (ubiquinone-cytochrome c reductase).^{49, 125, 247, 256-260} Under normal metabolic conditions, complex III is the main site for ROS production.⁹⁵ The rate of electron leakage and hence, O₂^{•-} production, by mitochondria is increased at elevated oxygen concentrations.^{12, 102} For example, in rat lung slices exposed to air, about 9% of the total oxygen taken up led to O₂^{•-} formation. However, in an atmosphere that contained 85% oxygen, O₂^{•-} accumulation accounted for 18% of the total oxygen uptake.¹² The generation of ROS, therefore, becomes predominantly a function of the metabolic rate and, as such, the rate of living can be indirectly translated to a corresponding scale of oxidative stress.^{262, 263}

On the whole, ageing is thought to increase ROS mitochondrial production. Ageing defects in this organelle's electron transport chain are believed to be the probable sources for the raised oxidative injury.^{49, 127, 277} Investigations

have highlighted decreases in the activity of complexes I, III and IV with age advancement but complex II appears unaltered.^{70, 127, 270, 277-279} Significantly, many of the subunits comprising complexes I, III and IV are partly encoded by mt-DNA while complex II is entirely encoded by nuclear DNA. Additionally, it is reported that complex II could be involved in the ROS elevation seen in diabetics – a role for it has been suggested in AGE formation and sorbitol accumulation.^{256, 280}

8.2 AIM

Mitochondria are the targets of their own deleterious oxidant yields and consequently, their steady-state oxidative damage levels are relatively higher than in other organelles.^{100, 125, 127-129} Mitochondrial DNA injury is now considered to be an important factor in ageing and diabetes caused, in part, by ROS released from the “electron transport chain”.^{94, 96, 124, 126} Thus, this chapter aimed to determine the effects of elevated extracellular glucose concentrations on the expression of mitochondrial electron transport chain proteins in HUVECs.

8.3 METHODS

Initially, primary endothelial cell cultures were formed from human umbilical veins taken from three different umbilical cords at delivery (section 2.2.7.1). These three cell lines were grown for 85 days and to study the effects of HG, the growth media was supplemented with freshly prepared D-glucose to achieve a final concentration of 22mM. Exposure to HG began at passage 3. The media was changed every two days to keep the glucose concentrations relatively constant. At each passage, HUVEC samples were taken for protein analysis as detailed earlier (sections 2.2.7.3 and 2.2.7.4).

During the serial passaging, HUVECs were processed for mitochondrial electron transport chain (ETC) complex IV, subunit I expression (section

2.2.7.4). This part of the ETC was chosen as it is encoded for by mitochondrial DNA. Densitometry was conducted to quantify the bands for the 37kDa sized protein subunit. These bands (figure 8-1, page 167) were normalized against β -actin expression (figure 8-2, page 168) and then standardized using the P18 (NG) sample (to allow for inter-western comparisons).

8.4 RESULTS

Overall, the results (figure 8-3, page 169) showed that HG decreased the HUVEC expression of complex IV, subunit I (2.8-fold fall in HG vs. NG). Moreover, the lower expression of the subunit was consistent for nearly all the passages studied. The most dramatic differences were seen at passage 5 (0.2 arbitrary units NG vs. 0.05 arbitrary units HG, using unpaired two-tailed *t*-test; $p = 0.01$, $n = 3$), passage 8 (0.4 arbitrary units NG vs. 0.07 arbitrary units HG, using unpaired two-tailed *t*-test; $p = 0.005$, $n = 3$) and passage 14 (0.3 arbitrary units NG vs. 0.03 arbitrary units HG, not significant).

Figure 8-1: Example of an autoradiograph obtained through Western analysis of HUVEC complex IV, subunit I expression (37kDa). Primary endothelial cell cultures were established from human umbilical veins taken from three different umbilical cords at delivery. Samples of cells were taken from selected passages for complex IV, subunit I expression. The specimens underwent protein isolation and quantification before Western blotting was performed. Immunodetection was carried out using the anti-OxPhos complex IV (subunit I), mouse IgG_{2a}, monoclonal primary antibody and a secondary antibody (anti-mouse Ig, horseradish peroxidase linked whole antibody (from sheep)). Thereafter, chemiluminescent detection was undertaken with Western blot reagent ECL. (A more detailed explanation of the methodology is contained in section 2.2.7.4). P, passage number; kDa, kilo Daltons; NG, normal glucose (5.5mM); HG, high glucose (22mM).

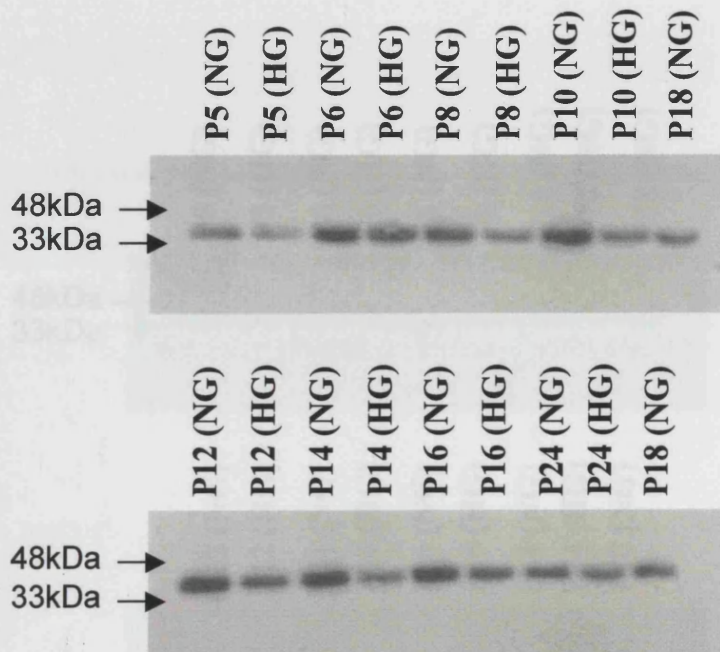


Figure 8-2: Example of an autoradiograph acquired during Western analysis for β -actin (42kDa) in HUVECs at selected passages. Primary endothelial cell cultures were established from human umbilical veins taken from three different umbilical cords at delivery. Samples of cells were taken from selected passages for complex IV, subunit I expression. The specimens underwent protein isolation and quantification before Western blotting was performed. Immunodetection was carried out using the anti-OxPhos complex IV (subunit I), mouse IgG_{2a}, monoclonal primary antibody and a secondary antibody (anti-mouse Ig, horseradish peroxidase linked whole antibody (from sheep)). Thereafter, chemiluminescent detection was undertaken with Western blot reagent ECL. Next, the blot was stripped and immunodetection for β -actin was conducted using the monoclonal anti- β -actin antibody and a secondary antibody (anti-mouse Ig, horseradish peroxidase linked whole antibody (from sheep)). Thereafter, chemiluminescent detection was undertaken with Western blot reagent ECL. (A more detailed description of the methodology is contained in section 2.2.7.4). P, passage number; kDa, kilo Daltons; NG, normal glucose (5.5mM); HG, high glucose (22mM).

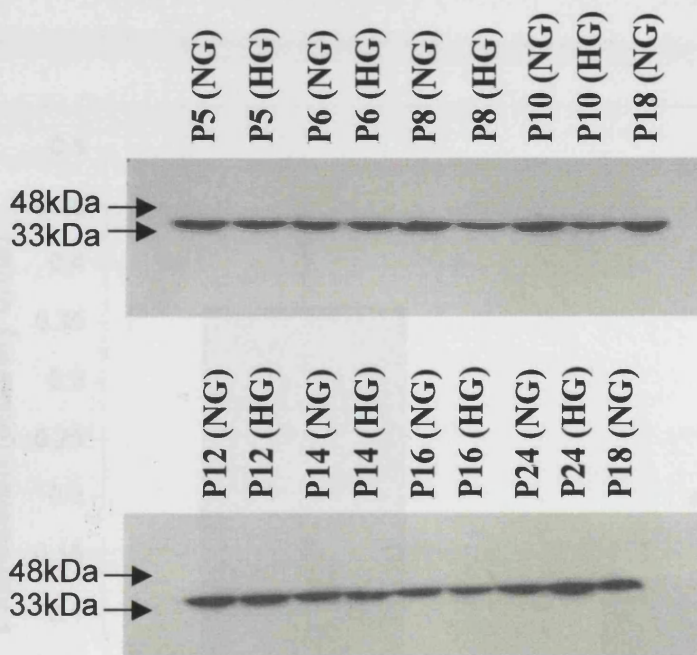
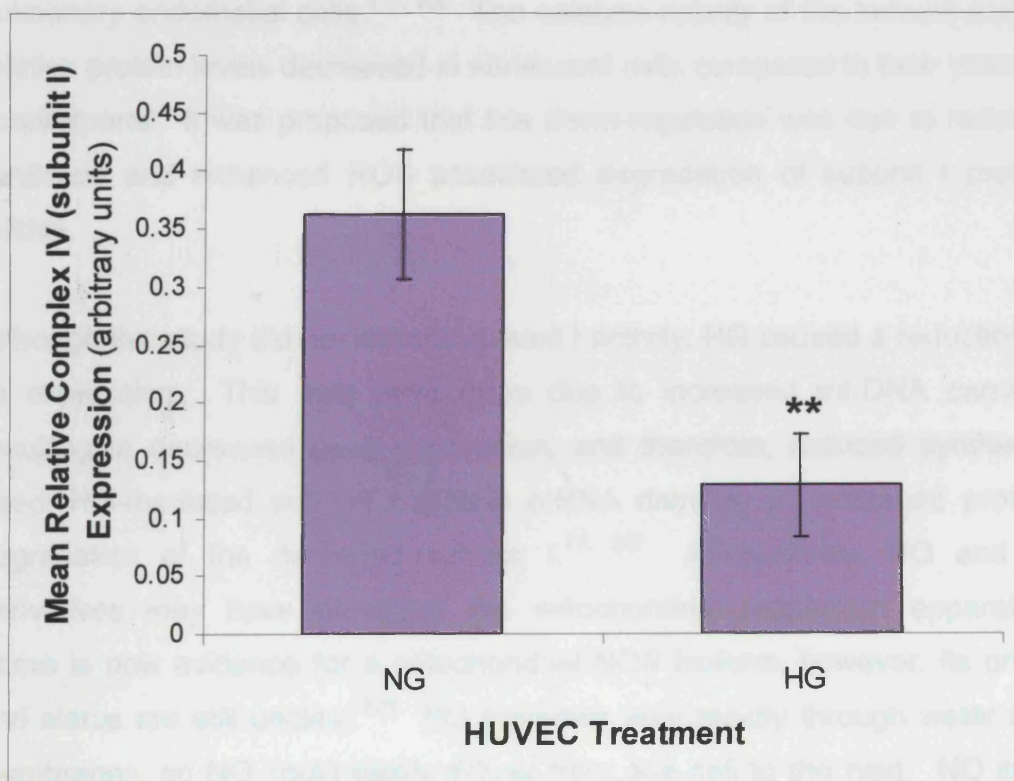


Figure 8-3: Long-term effect of high glucose (22mM) on HUVEC electron transport chain complex IV, subunit I expression. Primary endothelial cell cultures were established from human umbilical veins taken from three different umbilical cords at delivery. Samples of cells were taken from selected passages for complex IV, subunit I expression. The specimens underwent protein isolation and quantification before Western blotting was performed. Immunodetection was carried out using the anti-OxPhos complex IV (subunit I), mouse IgG_{2a}, monoclonal primary antibody and a secondary antibody (anti-mouse Ig, horseradish peroxidase linked whole antibody (from sheep)). Thereafter, chemiluminescent detection was undertaken with Western blot reagent ECL. Next, the blot was stripped and immunodetection for β -actin was conducted. The densitometry evaluated complex IV, subunit I expressions were normalized to β -actin expressions for both NG (normal glucose, 5.5mM) and HG (high glucose) exposures. The results are presented as the mean relative complex IV, subunit I expressions (\pm SEM) for each of the HUVEC treatments. Using unpaired two-tailed t-test, NG vs. HG (** $p = 0.006$, $n = 8$).



8.5 DISCUSSION

Complex IV (cytochrome *c* oxidase) is the terminal enzyme complex of the respiratory chain and determines the rate of electron exit from the respiratory chain. In eukaryotes, it is located in the inner mitochondrial membrane where it catalyses the transfer of electrons from reduced cytochrome *c* to molecular oxygen.⁵³⁰ This reaction is coupled to the translocation of protons across the inner membrane and the resulting electrochemical gradient is used to drive ATP synthesis and ion transport.⁵³¹ Human complex IV is composed of three subunits (I, II and III) encoded by mt-DNA and ten subunits (IV, Va, Vb, VIa, VIb, VIc, VIIa, VIIb, VIIc and VIII) encoded by nuclear DNA.⁵³² Subunit I is one of the three subunits that forms the active core of complex IV. Thus, a lack of subunit I could affect complex IV assembly and lead to its deficiency.⁵³³ Zhang *et al.* (2002) examined the relationship between complex IV subunit I gene expression and its activity in young and senescent porcine pulmonary endothelial cells.^{277, 506} The catalytic activity of the subunit and its relative protein levels decreased in senescent cells compared to their younger counterparts. It was proposed that this down-regulation was due to reduced synthesis and enhanced ROS associated degradation of subunit I protein mRNA.

Although this study did not assess subunit I activity, HG caused a reduction in its expression. This may have been due to increased mt-DNA damage resulting in decreased gene expression, and therefore, reduced synthesis; direct HG-mediated subunit I protein mRNA damage or increased protein degradation of the damaged subunit I.^{70, 267} Alternatively, NO and its derivatives may have damaged the mitochondrial respiration apparatus. There is now evidence for a mitochondrial NOS isoform, however, its origin and status are still unclear.²⁷⁹ NO traverses very rapidly through water and membranes, so NO could easily diffuse from one cell to the next. NO itself causes a rapid, selective, potent but reversible inhibition of cytochrome *c* oxidase.^{122, 125, 279} Meanwhile, reactive nitrogen species (RNS) cause a slow,

nonselective, weak but irreversible blockage of many mitochondrial compartments (for example, ONOO⁻ can impede complex IV).^{68, 122, 125, 279}

This hindrance to the respiratory chain may, in fact, enhance ROS formation. At moderate levels, NO could acutely increase O₂^{•-} and H₂O₂ production by inhibiting mitochondrial respiration, while at higher levels, it could prevent H₂O₂ production by scavenging the precursor O₂^{•-}, resulting in ONOO⁻ generation.¹² In addition to stimulating ROS formation, NO or RNS could also inhibit catalase, deplete cellular glutathione and inhibit glutathione peroxidase, thus increasing intracellular H₂O₂ levels. Moreover, Ballinger and colleagues (2000) demonstrated that HUVEC mt-DNA was damaged by H₂O₂ and ONOO⁻.⁸³

8.6 CONCLUSIONS

This chapter, through Western analysis, showed that HG decreased the expression of HUVEC ETC complex IV, subunit I.

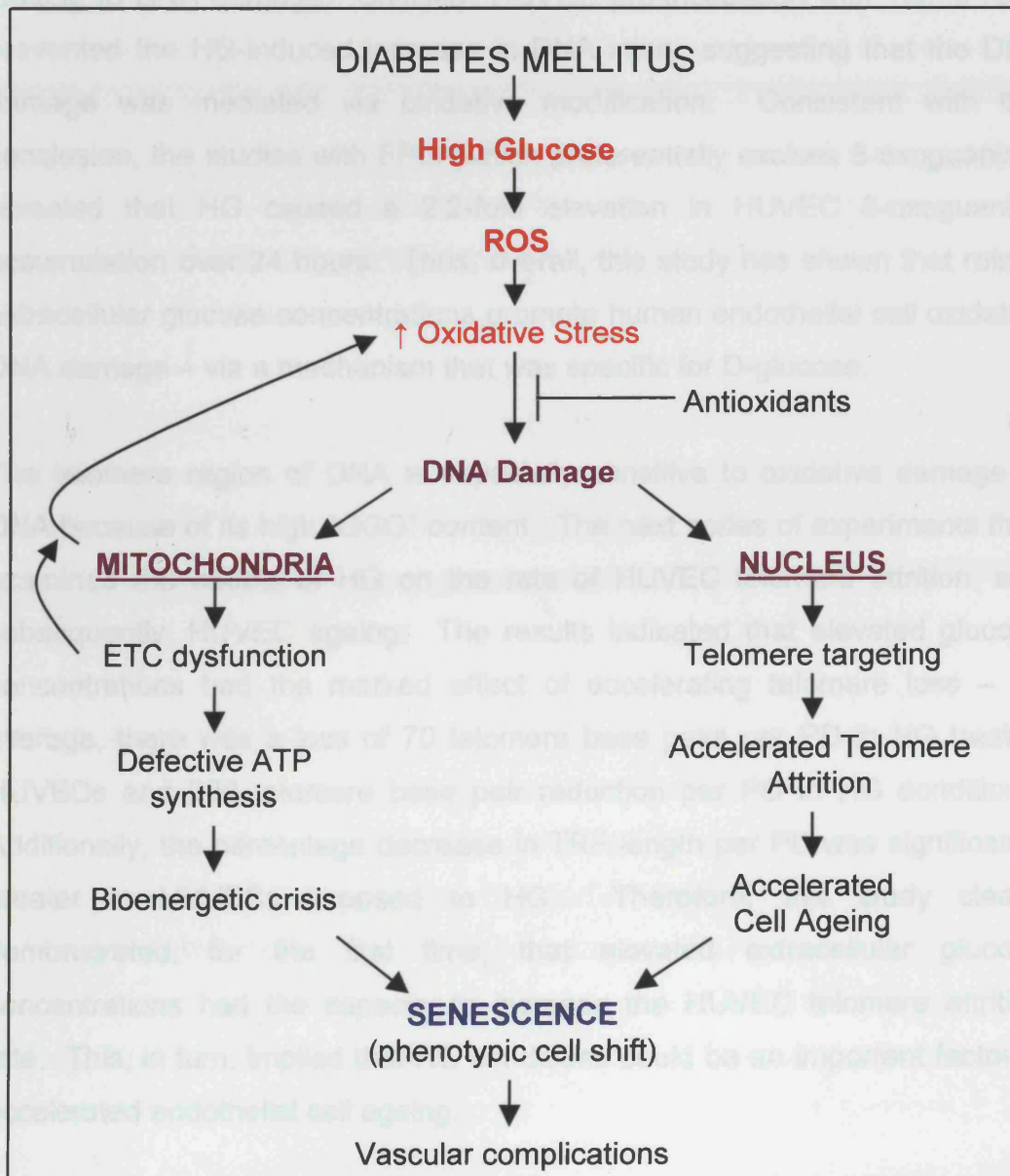
8.7 FUTURE WORK

Further research should examine the remaining ETC complexes, especially those thought to participate in ROS generation. Additionally, the complexes encoded for by nuclear DNA could be compared to those encoded by the mt-DNA. Moreover, the addition of ETC complex inhibitors should help to highlight the potential role for mitochondrial ROS production in the HG-induced DNA damage observed in Chapter 3. For example, thenoyltrifluoroacetone (TTFA) could be used to block complex II activity.

Chapter 9 : SUMMARY AND FINAL CONCLUSIONS

Diabetes is believed to be a state of accelerated vascular ageing. Thus, this thesis set out to examine whether this ageing was due to glucose-driven oxidative damage to telomeric DNA, culminating in premature endothelial cell senescence (figure 9-1).

Figure 9-1: Summary of the rationale behind the hypothesis that diabetes is a state of accelerated vascular ageing. ROS, reactive oxygen species.



Initially, it was important to define the effects of elevated extracellular glucose concentrations on HUVEC DNA and to ascertain whether any glucose-induced DNA damage was mediated through an oxidative pathway. The results in Chapter 3 established that HUVEC DNA injury was detectable after just five minutes of HG treatment and reached a peak after four hours of exposure. Additionally, these effects appeared to be dependent upon the glucose concentration with near maximal DNA injury occurring at 22mM D-glucose. Further, the data was specific for D-glucose, as it was not reproduced by the osmotic controls (22mM mannose, 22mM mannitol and 22mM 2-deoxyglucose). The latter was particularly significant because it suggested that glucose metabolism was an important part in the pathway leading to DNA damage. Critically, HUVEC pre-incubation with 10mM NAC prevented the HG-induced increase in DNA injury, suggesting that the DNA damage was mediated via oxidative modification. Consistent with this conclusion, the studies with FPG (which preferentially excises 8-oxoguanine) revealed that HG caused a 2.2-fold elevation in HUVEC 8-oxoguanine accumulation over 24 hours. Thus, overall, this study has shown that raised extracellular glucose concentrations promote human endothelial cell oxidative DNA damage – via a mechanism that was specific for D-glucose.

The telomere region of DNA is especially sensitive to oxidative damage to DNA because of its high “GGG” content. The next series of experiments thus examined the effects of HG on the rate of HUVEC telomere attrition, and subsequently, HUVEC ageing. The results indicated that elevated glucose concentrations had the marked effect of accelerating telomere loss – on average, there was a loss of 70 telomere base pairs per PD in NG treated HUVECs and 220 telomere base pair reduction per PD in HG conditions. Additionally, the percentage decrease in TRF length per PD was significantly greater in HUVECs exposed to HG. Therefore, this study clearly demonstrated, for the first time, that elevated extracellular glucose concentrations had the capacity to increase the HUVEC telomere attrition rate. This, in turn, implied that HG conditions could be an important factor in accelerated endothelial cell ageing.

This study was then extended to determine whether the enhanced telomere shortening rate could be prevented by the addition of an antioxidant (NAC). Interestingly, HUVEC NAC supplementation decreased the telomere base pair loss per PD induced by HG, however, the reduction was not statistically significant. In light of the fact that NAC clearly attenuated HG-induced DNA damage, it seems likely that glucose-induced ROS production is the likely mechanism to account for glucose-induced telomere attrition. However, more detailed studies of the impact of a range of antioxidants on the glucose-induced telomere attrition will be necessary to further evaluate this possibility.

The HG-induced DNA damage noted in Chapter 3 is likely to result in disturbances in endothelial cell growth. Further, genomic DNA injury has been shown to play a central role in the progression of cell senescence and ageing. Hence, the next series of studies investigated the effects of HG on the growth characteristics of HUVECs and in their development of cellular senescence. With repeated cell passage, the HUVEC morphology altered. For instance, the cells became noticeably larger, irregular, stretched and lost their typical cobblestone appearance when confluent. These cells were neither dead, nor dying as they re-established themselves when passaged onto fresh culture plates. Additionally, the cells with altered morphology tended to cluster in groups, forming their own cell islands. Furthermore, the studies revealed that there was a trend leading to the increased accumulation of 8-oxoguanine lesions with advancing HUVEC age and this occurred to a greater extent in the HG treated cells.

Overall, Chapter 4 showed that DNA damage increased as the HUVECs aged with the HG treated cells tending to have the greater levels of DNA injury. Further, the cell cultures demonstrated that HG exposure prolonged the HUVEC population doubling times. In addition, the HUVECs were observed to change in their morphology and the application of SA- β -Gal staining clearly confirmed that HG conditioned HUVECs contained a higher percentage of senescent cells. Thus, all in all, this study demonstrated a clear association between elevated extracellular glucose concentrations and endothelial cell

DNA injury, prolonged population doubling times, accumulation of oxidative DNA damage and premature senescence.

Cellular senescence is accompanied by changes in cell function, morphology and gene expression. These changes in cell phenotype may contribute to age-associated diseases, including atherosclerosis. For example, the evidence that endothelial cells with senescence-associated phenotypes exist in human atherosclerotic lesions suggests that the functional changes in senescent endothelial cells *in vivo* may play a key role in the pathophysiology of atherosclerosis.^{41, 47} This is important because it represents a paradigm shift in our thinking about vascular cell injury – it is no longer solely about cell death, but rather it is the subtle shifts in cellular function and growth that markedly disturb the function of the vasculature.⁴⁷

This thesis was further broadened to include an investigation of the impact of elevated glucose concentrations on DNA repair. In Chapter 6 the studies focussed on the efficiency of repair of an 8-oxoguanine lesion in HUVECs and the impact of HG on this repair process. The results showed that different cell types exhibit differences in their repair capacity with HUVECs being more efficient at excising 8-oxoguanine lesions than HUASMCs. Interestingly, HUVECs also expressed more Ref-1, than HUASMCs. Elevated glucose concentrations did significantly impair DNA repair, which was most noticeable after 24 hours exposure to HG. Furthermore, Western analysis demonstrated a similar trend in the fall in Ref-1 protein expression in the same cells. Therefore, this study suggests that as well as increasing oxidative DNA injury, elevated extracellular glucose concentrations have the potential to decrease the efficiency of endothelial cell 8-oxoguanine repair.

Mitochondrial DNA injury has been documented in patients with diabetes and is considered an important factor in ageing. This injury is in part caused by ROS released from the ETC.^{94, 96, 124, 126} Thus, it was important to determine whether HG conditions could lead to an accelerated loss of HUVEC mt-DNA and effect the expression of the ETC proteins. Chapter 7 suggested that there was very little difference in the relative mt-DNA contents between the

NG and HG treated HUVECs. However, the studies reported in Chapter 8 did demonstrate that HG decreased the expression of HUVEC ETC complex IV, subunit I. Thus, although the total amount of mt-DNA does not appear to be reduced, it is conceivable that there may be selective deletion or damage to mt-DNA regions encoding key mitochondrial ETC proteins. If true, our finding that there is a reduction in the level of key ETC complexes, could provide a basis for ETC dysfunction and a cellular energy deficit. Moreover, inefficient ETC function would in turn, lead to a spiralling cycle of elevated ROS production and thus, further mitochondrial damage. A deficit in ATP-generating capacity could become especially important in times of great energy demand (DNA repair, for example) as vital ATP-dependent reactions would be compromised.¹³²

9.1 LIMITATIONS OF THE STUDY AND FUTURE DIRECTIONS

The comet assay technique was used to measure DNA damage through the detection of DNA strand breaks. However, temporary strand breaks are also generated during DNA repair. Thus, the assay actually measures a combination of DNA damage and repair. Nevertheless, the data would still mainly reflect upon the level of DNA injury because repair would only be initiated once DNA damage had occurred. Although the aforementioned limitation would be encountered by any procedure that analysed DNA strand breaks, it may prove beneficial to support the comet assay data with another method that monitors DNA damage. For example, the alkaline unwinding technique could be used.

There are several protocols that are used in the quantification of cellular oxidative DNA damage. In this thesis, the FPG enzyme was utilised as it has been demonstrated to give reliable and reproducible results by other researchers. Once again, the use of a complementary technique, such as high performance liquid chromatography (HPLC), may help to strengthen the

data presented. However, HPLC has come under recent heavy criticism for the artefactual induction of oxidative DNA damage during the DNA isolation phase of the procedure. Thus, it should be employed with caution.

ROS production by endothelial cells grown in HG is well characterised, however, it may have been useful to directly measure the levels of ROS in our system. This project, like many others in the literature, implied the possibility of increased HUVEC ROS generation by demonstrating elevated DNA damage and heightened oxidative DNA lesion accumulation in HG conditions. In the future, ROS generation by HG could be confirmed through the application of florescent indicators such as the 2', 7'-dichlorofluorescein diacetate reagent.

Further, this thesis did not specifically measure the levels of telomeric DNA injury. Techniques to investigate this exist, like the S1 nuclease assay; however, they have also been subject to criticism. As an alternative, it may be possible to adapt the Southern analysis methodology to include the use of the FPG enzyme. The latter should identify and highlight the DNA damage to the G-triplet of the telomere.

It would also be of interest to extend our observations to the study of people with diabetes, using accessible cells, such as those from blood. Such a study is ongoing in the Clinical Research Unit. It has focussed on measuring DNA damage in whole blood, studying people with and without diabetes and will employ many of the same techniques described in this thesis, providing a good example of how this laboratory-based work will be translated into clinical research.

REFERENCES

1. Kumar P, Clark M. *Clinical Medicine*. 3rd ed. London: W B Saunders, 1994.
2. Stehouwer CDA, Lambert J, Donker AJM, van Hinsbergh VWM. Endothelial dysfunction and the pathogenesis of diabetic angiopathy. *Cardiovascular Research* 1997; **34**: 55-68.
3. Petersen S, Saretzki G, von Zglinicki T. Preferential accumulation of single-stranded regions in telomeres of human fibroblasts. *Experimental Cell Research* 1998; **239**: 152-160.
4. Baynes JW, Thorpe SR. Role of oxidative stress in diabetic complications: a new perspective on an old paradigm. *Diabetes* 1999; **48**: 1-9.
5. Giugliano D, Ceriello A, Paolisso G. Oxidative stress and diabetic vascular complications. *Diabetes Care* 1996; **19**: 257-267.
6. Griending KK, Harrison DG. Dual role of reactive oxygen species in vascular growth. *Circulation Research* 1999; **85**: 562-563.
7. Plutzley J, Viberti G, Haffner S. Atherosclerosis in type 2 diabetes mellitus and insulin resistance: mechanistic links and therapeutic targets. *Journal of Diabetes and its Complications* 2002; **16**: 401-415.
8. Deedwania P. Diabetes and vascular disease: common links in the emerging epidemic of coronary artery disease. *American Journal of Cardiology* 2003; **91**: 68-71.
9. Rosen P, Nawroth PP, King G, Moller W, Tritschler H-J, Packer L. The role of oxidative stress in the onset and progression of diabetes and its complications. *Diabetes Metabolism Research Reviews* 2001; **17**: 189-212.
10. Zimmet P, Alberti KGMM, Shaw J. Global and societal implications of the diabetic epidemic. *Nature* 2001; **414**: 782-787.
11. Barnett AH. *Management of diabetic vascular disease*. 1st ed. London: Medical Education Partnership, 2003.

12. Halliwell B, Gutteridge JMC. *Free radicals in biology and medicine*. 3rd ed. Oxford: Oxford University Press, 1998.
13. Tuomilehto J. Glucose peaks – the hidden danger in type 2 diabetes. *Practical Diabetes International* 2001; **18**: 57-59.
14. Wolff SP. Diabetes mellitus and free radicals. *British Medical Bulletin* 1993; **49**: 642-652.
15. Yki-Jarvinen H. Toxicity of hyperglycaemia in type 2 diabetes. *Diabetes Metabolism Reviews* 1998; **14**: S45-S50.
16. Donnelly R. Vascular complications in type 2 diabetes: current perspectives. *Practical Diabetes International* 2001; **18**: S19-S24.
17. Ho FM, Liu SH, Liao CS, Huang PJ, Shiah SG, Lin-Shiau SY. Nitric oxide prevents apoptosis of human endothelial cells from high glucose exposure during early stage. *Journal of Cell Biochemistry* 1999; **75**: 258-263.
18. Trngakos IP, Poulakou M, Stathatos M, Chalikia A, Melidonis A, Gonos ES. Serum levels of the senescence biomarker clusterin/ apolipoprotein J increase significantly in diabetes type II and during development of coronary heart disease or at myocardial infarction. *Experimental Gerontology* 2002; **37**: 1175-1187.
19. Hunt BJ, Poston L, Schachter M, Halliday A. *An introduction to vascular biology*. 2nd ed. Cambridge: Cambridge University Press, 2002.
20. Laakso M. Hyperglycaemia and cardiovascular disease in type 2 diabetes. *Diabetes* 1999; **48**: 937-942.
21. Sharpe PC, Liu W-H, Yue KKM, *et al*. Glucose-induced oxidative stress in vascular contractile cells. *Diabetes* 1998; **47**: 801-809.
22. Gutterman DD. Vascular dysfunction in hyperglycaemia. Is protein kinase C the culprit? *Circulation Research* 2002; **90**: 5-7.
23. Sumpio BE, Riley JT, Dardik A. Cells in focus: endothelial cell. *International Journal of Biochemistry and Cell Biology* 2002; **34**: 1508-1512.
24. Wu KK, Thiagarajan P. Role of endothelium in thrombosis and haemostasis. *Annual Review of Medicine* 1996; **47**: 315-331.

25. Matsuoka H. Endothelial dysfunction associated with oxidative stress in humans. *Diabetes Research and Clinical Practice* 2001; **54**: S65-S72.
26. De Vriese AS, Verbeuren TJ, van de Voorde J, Lameire NH, Vanhoutte PM. Endothelial dysfunction in diabetes. *British Journal of Pharmacology* 2000; **130**: 963-974.
27. Taylor PD, Poston L. Endothelium-mediated vascular function in insulin-dependent diabetes mellitus. *Clinical Sciences* 1995; **88**: 245-255.
28. Laight DW, Carrier MJ, Anggard EE. Endothelial cell dysfunction and the pathogenesis of diabetic macroangiopathy. *Diabetes Metabolism Research Reviews* 1999; **15**: 274-282.
29. Williams B. *Diabetes and hypertension*. 1st ed. Kent: Publishing Initiatives Books, 1996.
30. Stevens T, Garcia JGN, Shasby DM, Bhattacharya J, Malik AB. Mechanisms regulating endothelial cell barrier function. *American Journal of Physiology Lung Cellular and Molecular Physiology* 2000; **279**: L419-L422.
31. Mombouli J-V, Vanhoutte PM. Endothelial dysfunction: from physiology to therapy. *Journal of Molecular and Cellular Cardiology* 1999; **31**: 61-74.
32. Voskoboinik I, Soderholm K, Cotgreave IA. Ascorbate and glutathione homeostasis in vascular smooth muscle cells: cooperation with endothelial cells. *American Journal of Physiology Cell Physiology* 1998; **275**: C1031-C1039.
33. De Meyer GRY, Herman AG. Vascular endothelial dysfunction. *Progress in Cardiovascular Diseases* 1997; **41**: 325-342.
34. Cohen RA. Dysfunction of vascular endothelium in diabetes mellitus. *Circulation* 1993; **87**: V67-V76.
35. Verma S, Anderson TJ. Fundamentals of endothelial function for the clinical cardiologist. *Circulation* 2002; **105**: 546-549.
36. Newby A. Atherosclerosis. *Medicine* 1997; **24**: 31-34.
37. Napoli C, de Nigris F, Palinski W. Multiple roles of reactive oxygen species in the arterial wall. *Journal of Cellular Biochemistry* 2001; **82**: 674-682.

38. Droge W. Free radicals in the physiological control of cell function. *Physiological Reviews* 2002; **82**: 47-95.
39. Chang E, Harley CB. Telomere length and replicative ageing in human vascular tissues. *Proceedings of the National Academy of Sciences of the United States of America* 1995; **92**: 11190-11194.
40. Shizukuda Y, Buttrick PM. Oxygen free radicals and heart failure: new insight into an old question. *American Journal of Physiology Lung Cellular and Molecular Physiology* 2002; **283**: L237-L238.
41. Minamino T, Miyauchi H, Yoshida T, Ishida Y, Yoshida H, Komuro I. Endothelial cell senescence in human atherosclerosis. Role of telomere in endothelial dysfunction. *Circulation* 2002; **105**: 1541-1544.
42. Lusis AJ. Atherosclerosis. *Nature* 2000; **407**: 233-241.
43. Fukagama NK, Li M, Timblin CR, Mossman BT. Modulation of cell injury and survival by high glucose and advancing age. *Free Radical Biology and Medicine* 2001; **31**: 1560-1569.
44. Weissberg PL, Clesham GJ, Bennett MR. Is vascular smooth muscle cell proliferation beneficial? *Lancet* 1996; **347**: 305-307.
45. Li M, Absher PM, Liang P, Russell JC, Sobel BE, Fukagawa NK. High glucose concentrations induce oxidative damage to mitochondrial DNA in explanted vascular smooth muscle cells. *Experimental Biology and Medicine* 2001; **226**: 450-457.
46. Olinski R, Gackowski D, Foksinski M, Rozalski R, Rozalski K, Jaruga P. Oxidative DNA damage: assessment of the role in carcinogenesis, atherosclerosis and acquired immunodeficiency syndrome. *Free Radical Biology and Medicine* 2002; **33**: 192-200.
47. Guo ZM, Mitchell-Raymundo F, Yang H, *et al.* Dietary restriction reduces atherosclerosis and oxidative stress in the aorta of apolipoprotein E-deficient mice. *Mechanisms of Ageing and Development* 2002; **123**: 1121-1131.
48. Bennett MR, MacDonald K, Shiu-Wan C, Boyle JJ, Weissberg PL. Cooperative interactions between RB and p53 regulate cell proliferation, cell senescence, and apoptosis in human vascular smooth muscle cells from atherosclerotic plaques. *Circulation Research* 1998; **82**: 704-712.

49. Hagen T. *Advances in cell ageing and gerontology (volume II). Mechanisms of cardiovascular ageing*. 1st ed. Amsterdam: Elsevier, 2002.
50. Weinbrenner T, Cladellas M, Covas MI, *et al*. High oxidative stress in patients with stable coronary heart disease. *Atherosclerosis* 2003; **168**: 99-106.
51. Ceriello A, Quatraro A, Giugliano D. Diabetes mellitus and hypertension: the possible role of hyperglycaemia through oxidative stress. *Diabetologia* 1993; **36**: 265-266.
52. Hua C, Harrison DG. Endothelial dysfunction in cardiovascular diseases: the role of oxidative stress. *Circulation Research* 2000; **87**: 840-844.
53. Laight DW, Anggard EE, Carrier MJ. Antioxidants, diabetes and endothelial dysfunction. *Cardiovascular Research* 2000; **47**: 457-464.
54. Susic D. Hypertension, ageing and atherosclerosis: the endothelial interface. *Medical Clinics of North America* 1997; **81**: 1231-1240.
55. Schaffler A, Arnt H, Scholmerich J, Palitzsch KD. Acute hyperglycaemia causes severe disturbances of mesenteric microcirculation in an *in vivo* rat model. *European Journal of Clinical Investigation* 1998; **28**: 886-893.
56. Graier WF, Posch K, Fleischhacker E, Washer TC, Kostner GM. Increased superoxide anion formation in endothelial cells during hyperglycaemia: an adaptive response or initial step of vascular dysfunction? *Diabetes Research and Clinical Practice* 1999; **45**: 153-160.
57. Lorenzi M, Montisano DF, Toledo S, Barrieux A. High glucose induces DNA damage in cultured human endothelial cells. *Journal of Clinical Investigation* 1986; **77**: 322-325.
58. Poston L. Endothelial control of vascular tone in diabetes mellitus. *Diabetologia* 1997; **40**: S113-S114.
59. Hink U, Li H, Mollnau H, *et al*. Mechanisms underlying endothelial dysfunction in diabetes mellitus. *Circulation Research* 2001; **88**: e14-e22.
60. Freener EP, King GL. Vascular dysfunction in diabetes mellitus. *Lancet* 1997; **350**: 9-13.

61. Tomlinson DR. Mitogen-activated protein kinases as glucose transducers for diabetic complications. *Diabetologia* 1999; **42**: 1271-1281.
62. Giardino I, Edelstein D, Brownlee M. Bcl-2 expression or antioxidants prevent hyperglycaemia-induced formation of intracellular advanced glycation endproducts in bovine endothelial cells. *Journal of Clinical Investigation* 1996; **97**: 1422-1428.
63. Betteridge JD. What is oxidative stress? *Metabolism* 2000; **49**: 3-8.
64. Tooke JE, Goh KL. Vascular function in type 2 diabetes mellitus and pre-diabetes: the case for intrinsic endotheliopathy. *Diabetic Medicine* 1999; **16**: 710-715.
65. Kimura C, Oika M, Koyama T, Ito Y. Impairment of endothelial nitric oxide production by acute glucose overload. *American Journal of Physiology Endocrinology and Metabolism* 2001; **280**: E171-E178.
66. Liu W, Schoenkerman A, Lowe WL. Activation of members of the mitogen-activated protein kinase family by glucose in endothelial cells. *American Journal of Physiology Endocrinology and Metabolism* 2000; **279**: E782-E790.
67. Nightingale AK, James PP, Morris-Thurgood J, *et al.* Evidence against oxidative stress as mechanism of endothelial dysfunction in methionine loading model. *American Journal of Physiology Heart and Circulatory Physiology* 2001; **280**: H1334- H1339.
68. Ramachandran A, Levonen A-L, Brookes PS, *et al.* Mitochondria, nitric oxide and cardiovascular dysfunction. *Free Radical Biology and Medicine* 2002; **33**: 1465-1474.
69. Cepinskas G, Rui T, Kvietys PR. Interaction between reactive oxygen metabolites and nitric oxide in oxidant tolerance. *Free Radical Biology and Medicine* 2002; **33**: 433-440.
70. Kumazaki T, Sakano T, Yoshida T, *et al.* Enhanced expression of mitochondrial genes in senescent endothelial cells and fibroblasts. *Mechanisms of Ageing and Development* 1998; **101**: 91-99.
71. Ballinger SW, Patterson C, Yan C-N, *et al.* Hydrogen peroxide- and peroxy-nitrite-induced mitochondrial DNA damage and dysfunction in vascular endothelial and smooth muscle cells. *Circulation Research* 2000; **86**: 960-966.

72. Kunsch C, Medford RM. Oxidative stress as a regulator of gene expression in the vascular. *Circulation Research* 1999; **85**: 753-766.
73. Hu G. Copper stimulates proliferation of human endothelial cells under culture. *Journal of Cell Biochemistry* 1998; **69**: 326-335.
74. Hastie LE, Patton WF, Hechtman HB, Shepro D. Metabolites of the phospholipase D pathway regulate H₂O₂-induced filamin redistribution in endothelial cells. *Journal of Cell Biochemistry* 1998; **68**: 511-524.
75. Sohal RS. Effects of simulated hyperglycaemia, insulin and glucagons on endothelial nitric oxide synthase expression. *American Journal of Physiology Endocrinology and Metabolism* 2000; **279**: E11-E17.
76. Okayama N, Kevil CRG, Correia L, *et al.* Nitric oxide enhances hydrogen peroxide-mediated endothelial permeability *in vitro*. *American Journal of Physiology Cell Physiology* 1997; **273**: C1581-1587.
77. Carlisle R, Rhoads CA, Aw TY, Harrison L. Endothelial cells maintain a reduced redox environment even as mitochondrial function declines. *American Journal of Physiology Cell Physiology* 2002; **283**: C1675-C1686.
78. van der Loo B, Labugger R, Skepper JN, *et al.* Enhanced peroxynitrite formation is associated with vascular ageing. *Journal of Experimental Physiology* 2000; **192**: 1731-1743.
79. Lum H, Roebuck KA. Oxidative stress and endothelial cell dysfunction. *American Journal of Physiology Cell Physiology* 2001; **280**: C719-C741.
80. Yu BP, Chung HY. Oxidative stress and vascular ageing. *Diabetes Research and Clinical Practice* 2001; **54**: S73-S80.
81. Inoguchi T, Li P, Umeda F, *et al.* High glucose level and free fatty acid stimulate reactive oxygen species production through protein kinase C-dependent activation of NAD(P)H Oxidase in cultured vascular cells. *Diabetes* 2001; **49**: 1939-1945.
82. Wolin MS, Mohazzab-H KM. *Mediation of signal transduction by oxidants*. In: Scandalios JG, ed. *Oxidative stress and the molecular biology of antioxidant defences*. 1st ed. USA: Cold Harbour Laboratory Press, 1997.
83. Grishko V, Solomon M, Wilson GL, Lebourg SP, Gillespie MN. Oxygen radical-induced mitochondrial DNA damage and repair in pulmonary vascular endothelial cell phenotypes. *American Journal of Physiology Lung Cellular and Molecular Physiology* 2001; **280**: L1300-L1308.

84. Gow AJ, Branco F, Christofidou-Solomidou M, Black-Schultz L, Albelda SM, Muzykantov VR. Immunotargeting of glucose oxidase: intracellular production of H₂O₂ and endothelial oxidative stress. *American Journal of Physiology* 1999; **277**: L271-L281.
85. King GL, Shiba T, Oliver J, Inoguchi T, Bursell S-E. Cellular and molecular abnormalities in the vascular endothelium of diabetes mellitus. *Annual Review of Medicine* 1994; **45**: 179-188.
86. Ho FM, Liu SH, Liao CS, Huang PJ, Lin-Shiau SY. High glucose-induced apoptosis in human endothelial cells is mediated by sequential activations of c-Jun NH₂-terminal kinase and capase-3. *Circulation* 2000; **101**: 2618-2624.
87. Risso A, Mercuri F, Quagliari L, Damante G, Ceriello A. Intermittent high glucose enhances apoptosis in human umbilical vein endothelial cells in culture. *American Journal of Physiology Endocrinology and Metabolism* 2001; **281**: E924-E930.
88. Gupta S, Chough E, Daley J, *et al.* Hyperglycaemia increases endothelial superoxide that impairs smooth muscle cell Na⁺-K⁺-ATPase activity. *American Journal of Physiology Cell Physiology* 2002; **282**: C560-C566.
89. Itoh M, Omi H, Okouchi M, *et al.* The mechanisms of inhibitory actions of gliclazide on neutrophils – endothelial cells adhesion and surface expression of endothelial adhesion molecules mediated by a high glucose concentration. *Journal of Diabetes and its Complications* 2003; **17**: 22-26.
90. Brodsky SV, Go S, Li H, Goligorsky MS. Hyperglycaemic switch from mitochondrial nitric oxide to superoxide production in endothelial cells. *American Journal of Physiology Heart and Circulatory Physiology* 2002; **283**: H2130-H2139.
91. Wei Y-H. Oxidative stress and mitochondrial DNA mutations in human ageing. *PSEBM* 1998; **217**: 53-63.
92. Barzilai A, Rotman G, Shiloh Y. ATM deficiency and oxidative stress: a new dimension of defective response to DNA damage. *DNA Repair* 2002; **1**: 3-25.
93. Finch CE, Ruukun G. The genetics of ageing. *Annual Review of Genomics and Human Genetics* 2001; **2**: 435-462.

94. von Zglinicki T, Burkle A, Kirkwood TBL. Stress, DNA damage and ageing – an integrative approach. *Experimental Gerontology* 2001; **36**: 1049-1062.
95. Finkel T, Holbrook NJ. Oxidants, oxidative stress and the biology of ageing. *Nature* 2000; **408**: 239-247.
96. Sohal SR. Role of oxidative stress and protein oxidation in the ageing process. *Free Radical Biology and Medicine* 2002; **33**: 37-44.
97. Melov S. Animal models of oxidative stress, ageing and therapeutic antioxidant interventions. *International Journal of Biochemistry and Cell Biology* 2002; **34**: 1395-1400.
98. Sohal RS, Mockett RJ, Orr WC. Mechanisms of ageing: an appraisal of the oxidative stress hypothesis. *Free Radical Biology and Medicine* 2002; **33**: 575-586.
99. Van Voorhies WA. Metabolism and ageing in the nematode *Caenorhabditis Elegans*. *Free Radical Biology and Medicine* 2002; **33**: 587-596.
100. Fukagawa NK. Ageing: is oxidative stress a marker or is it causal? *PSEBM* 1999; **222**, 293-298.
101. Zhang Y, Herman B. Ageing and apoptosis. *Mechanisms of Ageing and Development* 2002; **123**: 245-260.
102. Beckman KB, Ames BN. *Oxidants, antioxidants and ageing*. In: Scandalios, ed. *Oxidative stress and the molecular biology of antioxidants defences*. USA: Cold Spring Harbour Laboratory Press, 1997; 201-235.
103. Warner HR, Sierra F. Models of accelerated ageing can be informative about the molecular mechanisms of ageing and/ or age-related pathology. *Mechanisms of Ageing and Development* 2003; **124**: 581-587.
104. Erden-Inal M, Sunal E, Kanbak G. Age-related changes in the glutathione redox system. *Cell Biochemistry and Function* 2002; **20**: 61-66.
105. Barja G. Rate of generation of oxidative stress-related damage and animal longevity. *Free Radical Biology and Medicine* 2002; **33**: 1167-1172.

106. Jones DP, Mody VC, Carlson JL, Lynn MJ, Sternberg P. Redox analysis of human plasma allows separation of pro-oxidant events of ageing from decline in antioxidant defences. *Free Radical Biology and Medicine* 2002; **33**: 1290-1300.
107. Cristofalo VJ, Allen RG, Pignolo RJ, Martin BG, Beck JC. Relationship between donor age and the replicative lifespan of human cells in culture; a re-evaluation. *Proceedings of the National Academy of Sciences of the United States of America* 1998; **95**: 10614-10619.
108. Morre DM, Lenaz G, Morre DJ. Surface oxidase and oxidative stress propagation in ageing. *Journal of Experimental Biology* 2000; **203**: 1513-1521.
109. Thannickal VJ, Fanburg BL. Reactive oxygen species in cell signalling. *American Journal of Physiology Lung Cellular and Molecular Physiology* 2000; **279**: L1005-L1028.
110. Yoon S-O, Yun C-H, Chung A-S. Dose effect of oxidative stress on signal transduction in ageing. *Mechanisms of Ageing and Development* 2002; **123**: 1597-1604.
111. Aust AE, Eveleigh JF. Mechanisms of DNA oxidation. *PSEBM* 1999; **222**: 246-252.
112. Martin GM, Anstad SN, Johnson TE. Genetic analysis of ageing: role of oxidative damage and environmental stresses. *Nature Genetics* 1996; **13**: 25-34.
113. Gilchrest BA, Bohr VA. Ageing processes, DNA damage and repair. *FASEB Journal* 1997; **11**: 322-330.
114. Fukagawa NK. Ageing: is oxidative stress a marker or is it causal? *PSEBM* 1999; **22**: 293-298.
115. Oikawa S, Kawanishi S. Site-specific DNA damage at GGG sequence by oxidative stress may accelerate telomere shortening. *FEBS Letters* 1999; **453**: 365-368.
116. Saretzki G, Sitte N, Merkel U, Wurm RE, von Zglinicki T. Telomere shortening triggers a p53-dependent cell cycle arrest via the accumulation of G-rich single stranded DNA fragments. *Oncogene* 1999; **18**: 5148-5158.

117. Blackburn EH, Greider CW, eds. *Telomeres*. 1st ed. USA: Cold Spring Harbor Laboratory Press, 1995.
118. von Zglinicki T, Rilger R, Sitté N. Accumulation of single-strand breaks is the major cause of telomere shortening in human fibroblasts. *Free Radical Biology and Medicine* 2000; **28**: 64-74.
119. von Zglinicki T, Saretzki G, Docke W, Lotze C. Mild hypoxia shortens telomeres and inhibits proliferation of fibroblasts: a model for senescence? *Experimental Cell Research* 1995; **220**: 186-193.
120. Collins AR, Raslova K, Somorovska M, *et al.* DNA damage in diabetes: correlation with a clinical marker. *Free Radical Biology and Medicine* 1998; **25**: 373-377.
121. Gilchrest BA, Bohr VA, eds. *Advances in cell ageing and gerontology (volume IV). The role of DNA damage and repair in cell ageing*. 1st ed. Amsterdam: Elsevier, 2001.
122. Hausladen A, Fridovich I. Superoxide and peroxynitrite inactivate aconitases, but nitric oxide does not. *Journal of Biological Chemistry* 1994; **269**: 29405-29408.
123. Bernardi P, Scorrano L, Colonna R, Petronilli V, DiLisa F. Mitochondria and cell death. Mechanistic aspects and methodological issues. *European Journal of Biochemistry* 1999; **264**: 687-701.
124. Lopez-Torres M, Gredilla R, Sanz A, Barja G. Influence of ageing and long-term caloric restriction on oxygen radical generation and oxidative DNA damage in rat liver mitochondria. *Free Radical Biology and Medicine* 2002; **32**: 882-889.
125. Merry BJ. Molecular mechanisms linking calorie restriction and longevity. *International Journal of Biochemistry and Cell Biology* 2002; **34**: 1340-1354.
126. Hagen TM, Liu J, Lykkesfeld J, *et al.* Feeding acetyl-L-carnitine and lipoic acid to old rats significantly improves metabolic function while decreasing oxidative stress. *Proceedings of the National Academy of Sciences of the United States of America* 2002; **99**: 1870-1875.
127. Van Remmen H, Richardson A. Oxidative damage to mitochondria and ageing. *Experimental Gerontology* 2001; **31**: 957-968.

128. Diaz F, Byona-Bafaluy MP, Rana M, Mora M, Hao H, Moraes CT. Human mitochondrial DNA with large deletions repopulates organelles faster than full-length genomes under relaxed copy number control. *Nucleic Acids Research* 2002; **30**: 4626-4623.
129. Rustin P, von Kleist-Retzow J-C, Vajo Z, Rotig A, Munnich A. For debate: defective mitochondria, free radicals, cell death, ageing – reality or myth-ochondria? *Mechanisms of Ageing and Development* 2000; **114**: 201-206.
130. Pamplona R, Portero-Otin M, Requena J, Gredilla R, Barja G. Oxidative, glycoxidative and lipoxidative damage to rat heart mitochondrial proteins is lower after 4 months of caloric restriction than in age-matched controls. *Mechanisms of Ageing and Development* 2002; **123**: 1437-1446.
131. Raha S, Robinson BH. Mitochondria, oxygen free radicals, disease and ageing. *Trends in Biochemical Sciences* 2000; **25**: 502-508.
132. Tavazzi B, DiPierro D, Amorini AM, *et al.* Energy metabolism and lipid peroxidation of human erythrocytes as a function of increased oxidative stress. *European Journal of Biochemistry* 2000; **267**: 684-689.
133. Aviv A, Aviv H. Reflections on telomeres, growth, ageing and essential hypertension. *Hypertension* 1997; **29**: 1067-1072.
134. De Bono DP. Olovnikov's clock: telomeres and vascular biology. *Heart* 1998; **80**: 110-111.
135. Wellinger RJ, Ethier K, Labrecque P, Zakian VA. Evidence for a new step in telomere maintenance. *Cell* 1996; **85**: 423-433.
136. Chiu CP, Harley CB. Replicative senescence and cell immortality: the role of telomeres and telomerase. *Society for Experiment Biology and Medicine* 1997; **214**: 99-106.
137. Lundblad V, Wright WE. Telomeres and telomerase: a simple picture becomes complicated. *Cell* 1996; **87**: 869-375.
138. Slagboom PE, Droog S, Boomsma DI. Genetic determination of telomere size in humans: a twin study of three age groups. *American Journal of Human Genetics* 1994; **55**: 876-882.
139. Proctor CJ, Kirkwood TBL. Modelling telomere shortening and the role of oxidative stress. *Mechanisms of Ageing and Development* 2002; **123**: 351-363.

140. Mattson MP, ed. *Advances in cell ageing and gerontology (volume VIII). Telomerase, ageing and disease*. 1st ed. Amsterdam: Elsevier, 2001.
141. Broccoli D, Cooke H. Ageing, healing and the metabolism of telomeres. *American Journal of Human Genetics* 1993; **52**: 657-660.
142. Allsopp RC, Harley CB. Evidence for a critical telomere length in senescent human fibroblasts. *Experimental Cell Research* 1995; **219**: 130-136.
143. Mera SL. The role of telomeres in ageing and cancer. *British Journal of Biomedical Science* 1998; **55**: 221-225.
144. Greider CW. Telomeres and senescence: the history, the experiment, the future. *Current Biology* 1998; **8**: R178-R181.
145. Mikhelson VM. Replicative mosaicism might explain the seeming contradictions in the telomere theory of ageing. *Mechanisms of Ageing and Development* 2001; **122**: 1361-1365.
146. Beckman KB, Ames BN. The free radical theory of ageing. *Physiological Reviews* 1998; **78**: 547-581.
147. Cherif H, Tarry JL, Ozanne SE, Hales CN. Ageing and telomeres: a study into organ- and gender- specific telomere shortening. *Nucleic Acids Research* 2003; **31**: 1576-1583.
148. Sitte N, Saretzki G, von Zglinicki T. Accelerated telomere shortening in fibroblasts after extended periods of confluency. *Free Radical Biology and Medicine* 1998; **24**: 885-893.
149. Fossel M. Telomerase and the ageing cell. *Journal of the American Medical Association* 1998; **279**: 1732-1735.
150. Kakuo S, Asaoka K, Ide T. Human is a unique species among primates in terms of telomere length. *Biochemical and Biophysical Research Communications* 1999; **263**: 308-314.
151. Ahmed S, Henderson E. Formation of novel hairpin structures by telomeric C-strand oligonucleotides. *Nucleic Acids Research* 1992; **20**: 507-511.

152. Zakin VA. Telomeres: beginning to understand the end. *Science* 1995; **270**: 1601-1607.
153. Cerni C. Telomeres, telomerase and myc. *Mutation Research* 2000; **462**: 31-47.
154. Hernann MT, Greider CW. G-strand overhangs on telomeres in telomerase-deficient mouse cells. *Nucleic Acids Research* 1999; **27**: 3964-3969.
155. Urquidi V, Tarin D, Goodison S. Role of telomerase in cell senescence and oncogenesis. *Annual Review of Medicine* 2000; **51**: 65-79.
156. Graakjaer J, Bischoff C, Korsholm L, *et al.* The pattern of chromosome-specific variations in telomere length in humans is determined by inherited, telomere-near factors and is maintained throughout life. *Mechanisms of Ageing and Development* 2003; **124**: 629-640.
157. Dionne I, Wellinger RJ. Cell cycle-regulated generation of single-stranded G-rich DNA in the absence of telomerase. *Proceedings of the National Academy of Sciences of the United States of America* 1996; **93**: 13902-13907.
158. Makarov VL, Hirose Y, Langmore JP. Long G tails at both ends of human chromosomes suggest a C-strand degradation mechanism for telomere shortening. *Cell* 1997; **88**: 657-666.
159. Huffman KE, Levene SD, Tesmer VM, Shay JW, Wright WE. Telomere shortening is proportional to the size of the G-rich telomeric 3'-overhang. *Journal of Biological Chemistry* 2000; **275**: 19719-19722.
160. Cimino-Reale G, Pascale E, Battiloro E, Starace G, Verna R, D'Ambrosio E. The length of telomeric G-rich strand 3'-overhang measured by oligonucleotide ligation assay. *Nucleic Acids Research* 2001; **29**: e35-e41.
161. Wellinger RJ, Sen D. The DNA structure at the ends of eukaryotic chromosomes. *European Journal of Cancer* 1997; **33**: 735-749.
162. Greider CW. Telomeres do D-loop-T-loop. *Cell* 1999; **97**: 503-514.
163. Griffith JD, Comeau L, Rosenfield S, *et al.* Mammalian telomeres end in a large duplex loop. *Cell* 1999; **97**: 503-514.

164. Shore D. Telomeres – unsticky ends. *Science* 1998; **281**: 1818-1819.
165. van Steensel B, de Lange T. Control of telomere length by the human telomeric protein TRF 1. *Nature* 1997; **385**: 740-743.
166. Ancelin K, Brun C, Gilson E. Role of the telomeric DNA-binding protein TRF2 in the stability of human chromosome ends. *BioEssays* 1998; **20**: 879-883.
167. Rippmann JF, Damm K, Schnapp A. Functional characterisation of the Poly(ADP-ribose)polymerase activity of tankyrase 1, a potential regulator of telomere length. *Journal of Molecular Biology* 2002; **323**: 217-224.
168. Martens UM, Charez EA, Poon SS, Schmoor C, Lansdorp PM. Accumulation of short telomeres in human fibroblasts prior to replicative senescence. *Experimental Cell Research* 2000; **256**: 291-299.
169. Campisi JH, Kim S, Lim C-S, Rubio M. Cellular senescence, cancer and ageing: the telomere connection. *Experimental Gerontology* 2001; **36**: 1619-1637.
170. Bertuch AA. Telomeres: the molecular events during end-to-end fusions. *Current Biology* 2002; **12**: R738-R740.
171. Martin GM. Genetic modulation of telomeric terminal restriction-fragment length: relevance for clonal ageing and late-life disease. *American Journal of Human Genetics* 1994; **55**: 866-869.
172. Linger J, Cooper JP, Cech TR. Telomerase and DNA end replication: no longer a lagging strand problem? *Science* 1995; **269**: 1533-1534.
173. Levy ZM, Allsopp RC, Futcher AB, Greider CW, Harley CB. Telomere end-replication problem and cell ageing. *Journal of Molecular Biology* 1992; **225**: 951-960.
174. Allsopp RC, Vaziri H, Patterson C, *et al.* Telomere length predicts replicative capacity of human fibroblasts. *Proceedings of the National Academy of Sciences of the United States of America* 1992; **89**: 10114-10118.
175. Finkel E. Telomeres: keys to senescence and cancer. *Lancet* 1998; **351**: 1186.

176. Toussaint O, Remacle J, Dierick J-F, *et al.* From the Hayflick mosaic to the mosaics of ageing. Role of stress-induced premature senescence in human ageing. *International Journal of Biochemistry and Cell Biology* 2002; **34**: 1415-1429.
177. Renault V, Thornell L-E, Butter-Browne G, Mouly V. Human skeletal muscle satellite cells: ageing, oxidative stress and the mitotic clock. *Experimental Gerontology* 2002; **37**: 1229-1236.
178. von Zglinicki T. Oxidative stress shortens telomeres. *Trends in Biochemical Sciences* 2002; **27**: 339-344.
179. Serra V, von Zglinicki T, Lorenz M, Saretzki G. Extracellular superoxide dismutase is a major antioxidant in human fibroblasts and slows telomere shortening. *Journal of Biological Chemistry* 2003; **278**: 6824-6930.
180. Hodes RJ. Telomere length, ageing and somatic cell turnover. *Journal of Experimental Medicine* 1999; **190**: 153-156.
181. Saretzki G, Sitte N, Merkal U, Wurm RE, von Zglinicki T. Telomere shortening triggers a p53-dependent cell cycle arrest via accumulation of G-rich single stranded DNA fragments. *Oncogene* 1999; **18**: 5148-5158.
182. Bohr VA. DNA repair fine structure and its relations to genomic instability. *Carcinogenesis* 1995; **16**: 2885-2892.
183. Vaziri H, Schachter F. Loss of telomeric DNA during ageing of normal and trisomy 21 human lymphocytes. *American Journal of Human Genetics* 1993; **52**: 661-667.
184. Lansdorp PM. Repair of telomeric DNA prior to replicative senescence. *Mechanisms of Ageing and Development* 2000; **114**: 69-77.
185. Kruk PA, Rampino NJ, Bohr VA. DNA damage and repair in telomeres: relation to ageing. *Proceedings of the National Academy of Sciences of the United States of America* 1995; **92**: 258-262.
186. von Zglinicki T. Telomeres: influencing the rate of ageing. *Annals of the New York Academy of Sciences* 1998; **854**: 318-327.
187. Wesierska-Gadek J, Schmid G. Overexpressed poly(ADP-ribose)polymerase delays the release of rat cells from p53-mediated G₁ checkpoint. *Journal of Cell Biochemistry* 2000; **80**: 85-103.

188. Milyavsky M, Mimran A, Senderovich S, *et al.* Activation of p53 protein by telomeric (TTAGGG)_n repeats. *Nucleic Acids Research* 2001; **29**: 5207-5215.
189. Wright WE, Shay JW. Time, telomeres and tumours: is cellular senescence more than an anticancer mechanism? *Trends in Cell Biology* 1995; **5**: 293-297.
190. Campisi J. The biology of replicative senescence. *European Journal of Cancer* 1997; **33**: 703-709.
191. Harley CB, Sherwood SW. Telomerase, checkpoints and cancer. *Cancer Surveys* 1998; **29**: 263-284.
192. Woodring WE, Shay JW. Telomere positional effects and the regulation of cellular senescence. *Trends in Genetics* 1992; **8**: 193-197.
193. Hensler PJ, Pereira-Smith OM. Human replicative senescence. *American Journal of Pathology* 1995; **147**: 1-8.
194. Reddel RR. A reassessment of the telomere hypothesis of senescence. *BioEssays* 1998; **20**: 985-999.
195. Rotman G, Shilon Y. The ATM gene and protein: possible roles in genome surveillance, checkpoint controls and cellular defence against oxidative stress. *Cancer Surveys* 1998; **29**: 285-304.
196. Klapper W, Parwaresch R, Krupp G. Telomere biology in human ageing and ageing syndromes. *Mechanisms of Ageing and Development* 2001; **122**: 695-712.
197. Holt SE, Wright WE, Shay JW. Multiple pathways for the regulation of telomerase activity. *European Journal of Cancer* 1997; **33**: 761-766.
198. Kipling D. Telomerase: immortality enzyme or oncogenes? *Nature Genetics* 1995; **9**: 104-106.
199. Holt SE, Shay JM. Role of telomerase in cellular proliferation and cancer. *Journal of Cellular Physiology* 1999; **180**: 10-18.
200. von Zglinicki T. Telomeres and replicative senescence: is it only length that counts? *Cancer Letters* 2001; **168**: 111-116.

201. Bennett MR, MacDonald K, Chan S-W, Boyle JJ, Weissberg PL. Cooperative interactions between RB and p53 regulate cell proliferation, cell senescence and apoptosis in human vascular smooth muscle cells from atherosclerotic plaques. *Circulation Research* 1998; **82**: 704-712.
202. Zhang J, Patel JM, Block ER. Enhanced apoptosis in prolonged cultures of senescent porcine pulmonary artery endothelial cells. *Mechanisms of Ageing and Development* 2002; **123**: 613-625.
203. Campisi J. Replicative senescence: an old lives' tale? *Cell* 1996; **84**: 497-500.
204. Chen Q, Ames BN. Senescence-like growth arrest induced by hydrogen peroxide in human diploid fibroblast F65 cells. *Proceedings of the National Academy of Sciences of the United States of America* 1994; **91**: 4130-4134.
205. Neumeister P, Albanese C, Balent B, Grealley J, Pestell RG. Senescence and epigenetic dysregulation in cancer. *International Journal of Biochemistry and Cell Biology* 2002; **34**: 1475-1490.
206. Itahana K, Dimri G, Campisi J. Regulation of cellular senescence by p53. *European Journal of Biochemistry* 2001; **268**: 2784-2791.
207. Tominaga K, Olgun A, Smith JR, Pereira-Smith OM. Genetics of cellular senescence. *Mechanisms of Ageing and Development* 2002; **123**:927-936.
208. Zhang Y, Herman B. Apoptosis and successful ageing. *Mechanisms of Ageing and Development* 2002; **123**: 563-565.
209. Campisi J. Cellular senescence and apoptosis: how cellular responses might influence ageing phenotypes. *Experimental Gerontology* 2003; **38**: 5-11.
210. Bodnar AG, Ouellette M, Frolkis M, *et al.* Extension of life-span by introduction of telomerase into normal human cells. *Science* 1998; **279**: 349-352.
211. Jeanclos E, Schork NJ, Kyvik KO, Kimura M, Skurnick JH, Aviv A. Telomere length inversely correlates with pulse pressure and is highly familial. *Hypertension* 2000; **36**: 195-200.

212. Meyyappan M, Wheaton K, Riabowol KT. Decreased expression and activity of the immediate-early growth response (*Egr-1*) gene product during cellular senescence. *Journal of Cellular Physiology* 1999; **179**: 29-39.
213. Cawthon RM, Smith KR, O'Brein E, Sivatchenko A, Kerber RA. Association between telomere length in blood and mortality in people aged 60 years or older. *Lancet* 2003; **361**: 393-395.
214. Cristofalo VJ, Gerhard GS, Pignolo RJ. Molecular biology of ageing. *Surgical Clinics of North America* 1994; **74**: 1-21.
215. West MD. The cellular and molecular biology of skin ageing. *Archives of Dermatology* 1994; **130**: 87-95.
216. Kurz DJ, Decary S, Hong Y, Erusalimsky JD. Senescence-associated β -galactosidase reflects an increase in lysosomal mass during replicative ageing of human endothelial cells. *Journal of Cell Science* 2000; **113**: 3613-3622.
217. Vojta PJ, Barrett JC. Genetic analysis of cellular senescence. *Biochimica et Biophysica Acta* 1995; **1242**: 29-41.
218. Faragher RGA, Kipling D. How might replicative senescence contribute to human ageing? *BioEssays* 1998; **20**: 985-999.
219. Shelton DN, Chang E, Whitter PS, Choi D, Funk WD. Microarray analysis of replicative senescence. *Current Biology* 1999; **9**: 939-945.
220. de Lange T. Telomeres and senescence: ending the debate. *Science* 1998; **279**: 334-335.
221. Wynford-Thomas D. p53: guardian of cellular senescence. *Journal of Pathology* 1996; **180**: 118-121.
222. Hwang ES. Replicative senescence and senescence-like state induced in cancer-derived cells. *Mechanisms of Ageing and Development* 2002; **123**: 1681-1694.
223. Wagner M, Hampel B, Bernhard D, Hala M, Zwerschke W, Jansen-Durr P. Replicative senescence of human endothelial cells *in vitro* involves G1 arrest, polyploidization and senescence-associated apoptosis. *Experimental Gerontology* 2001; **36**: 1327-1347.

224. Sasaki M, Kumazaki T, Takano H, Nishiyama M, Mitsui Y. Senescent cells are resistant to death despite low Bcl-2 level. *Mechanisms of Ageing and Development* 2001; **122**: 1695-1706.
225. Sayama K, Shirakata K, Midorikawa K, Hanakawa Y, Hashimoto K. Possible involvement of p21 but not of p16 or p53 in keratinocyte senescence. *Journal of Cellular Physiology* 1999; **179**: 40-44.
226. O'Reilly MA. DNA damage and cell cycle checkpoints in hyperoxic lung injury: braking to facilitate repair. *American Journal of Physiology Lung Cellular and Molecular Physiology* 2001; **281**: L291-L305.
227. Frippiat C, Remacle J, Toussaint O. Down-regulation and decreased activity of cyclin-dependent kinase 2 in H₂O₂-induced premature senescence. *International Journal of Biochemistry and Cell Biology* 2003; **35**: 246-254.
228. Hutter E, Unterluggauer H, Uberall F, Schramek H, Jansen-Durr P. Replicative senescence of human fibroblasts: the role of Ras-dependent signalling and oxidative stress. *Experimental Gerontology* 2002; **37**: 1165-1174.
229. Nohl H. Involvement of free radicals in ageing: a consequence or cause of senescence. *British Medical Bulletin* 1993; **49**: 653-667.
230. Allen RG, Tresini M, Keogh BP, Doggett DL, Cristofalo VJ. Differences in electron transport potential, antioxidant defences and oxidant generation in young and senescent foetal lung fibroblasts (WI-38). *Journal of Cellular Physiology* 1999; **180**: 114-122.
231. Hosokawa M. A higher oxidative status accelerates senescence and aggravates age-dependent disorders in SAMP strains of mice. *Mechanisms of Ageing and Development* 2002; **123**: 1553-1561.
232. Hosokawa M, Fujisawa H, Ax S, Zahn-Daimler G, Zahn RK. Age-associated DNA damage is accelerated in the senescence-accelerated mice. *Mechanisms of Ageing and Development* 2000; **118**: 61-70.
233. Kalashnik L, Bridgeman CJ, King AR, *et al.* A cell kinetic analysis of human umbilical vein endothelial cells. *Mechanisms of Ageing and Development* 2000; **120**: 23-32.
234. Zeng Z, Zhang Z, Yu H, Corbley MJ, Tang Z, Tong T. Mitochondrial DNA deletions are associated with ischemia and ageing in Balb/c mouse brain. *Journal of Cell Biochemistry* 1999; **73**: 545-553.

235. Gerbitz KD. Does the mitochondrial DNA play a role in the pathogenesis of diabetes? *Diabetologia* 1992; **35**: 1181-1186.
236. Mathews CE, Berdancier CD. Non-insulin-dependent diabetes mellitus as a mitochondrial genomic disease. *PSEBM* 1998; **219**: 97-108.
237. Wei Y-H, Lee H-C. Oxidative stress, mitochondria DNA mutation and impairment of antioxidant enzymes in ageing. *Experimental Biology and Medicine* 2002; **227**: 671-682.
238. Fernandez-Silva P, Enriquez JA, Montoya J. Replication and transcription of mammalian mitochondrial DNA. *Experimental Physiology* 2003; **88**: 41-56.
239. Chinnery PF, Samuels DC. Relaxed replication of mtDNA: A model with implications for the expression of disease. *American Journal of Human Genetics* 1999; **64**: 1158-1165.
240. Jacobs HT, Lehtinen SK, Spelbrink JN. No sex please, we're mitochondria: a hypothesis on the somatic unit of inheritance of mammalian mtDNA. *BioEssays* 2000; **22**: 564-572.
241. Rose G, Passarino G, Franceschi C, DeBenedictis G. The variability of the mitochondrial genome in human ageing: a key for life and death? *International Journal of Biochemistry and Cell Biology* 2002; **34**: 1449-1460.
242. Ide T, Tsutsui H, Hayashidani S, *et al.* Mitochondrial DNA damage and dysfunction associated with oxidative stress in failing hearts after myocardial infarction. *Circulation Research* 2001; **88**: 529-535.
243. Imai H, Nakagawa Y. Biological significance of phospholipids hydroperoxide glutathione peroxidase (PHGPx, GPx 4) in mammalian cells. *Free Radical Biology and Medicine* 2003; **34**: 145-169.
244. Passarella S, Atlante A, Valenti D, de Bari L. The role mitochondrial transport in energy metabolism. *Mitochondrion* 2003; **2**: 319-343.
245. Shadel GS, Clayton DA. Mitochondrial DNA maintenance in vertebrates. *Annual Review of Biochemistry* 1997; **66**: 409-435.
246. Kagawa Y, Cha SH, Hasegawa K, Hamamoto T, Endo H. Regulation of energy metabolism in human cells in ageing and diabetes: F₀F₁, mtDNA, UCP and ROS. *Biochemical and Biophysical Research Communications* 1999; **266**: 662-676.

247. Sawyer DE, Houten BV. Repair of DNA damage in mitochondria. *Mutation Research* 1999; **434**: 161-176.
248. Stryer L. *Biochemistry*. 4th ed. New York: W H Freeman, 1995.
249. Boss O, Hagen T, Lowell BB. Uncoupling proteins 2 and 3. Potential regulators of mitochondrial energy metabolism. *Diabetes* 2000; **49**: 143-156.
250. Richter C, Schweizer M. *Oxidative stress in mitochondria*. In: Scandalios JG, ed. *Oxidative stress and the molecular biology of antioxidant defences*. 1st ed. USA: Cold Harbour Laboratory Press, 1997.
251. Steward VC, Heales SJR. Nitric oxide-induced mitochondrial dysfunction: implications for neuro-degeneration. *Free Radical Biology and Medicine* 2003; **34**: 287-303.
252. Brand MD. Uncoupling to survive? The role of mitochondrial inefficiency in ageing. *Experimental Gerontology* 2000; **35**: 811-820.
253. Schultz AC, Chan GS. Structures and proton-pumping strategies of mitochondrial respiratory enzymes. *Annual Review of Biophysics and Biomolecular Structure* 2001; **30**: 23-65.
254. van der Heuvel L, Smeitink J. The oxidative phosphorylation (OXPHOS) system: nuclear genes and human genetic disorders. *BioEssays* 2001; **23**: 518-525.
255. Wojtczak L, Teplova VV, Bogucka K, *et al*. Effects of glucose and deoxyglucose on the redistribution of calcium in Ehrlich ascites tumour and Zajdela hepatoma cells and its consequences for mitochondrial energetics. *European Journal of Biochemistry* 1999, **263**: 495-501.
256. Gniadecki R, Thorn T, Vicanova J, Petersen A, Wulf HC. Role of mitochondria in ultraviolet-induced oxidative stress. *Journal of Cellular Biochemistry* 2000; **80**: 216-222.
257. Nicholls DG. Mitochondrial function and dysfunction in the cell: its relevance to ageing and ageing-related disease. *International Journal of Biochemistry and Cell Biology* 2002; **34**: 1372-1381.

258. Kulisz A, Chen N, Chandel NS, Shao Z, Schumacker PT. Mitochondrial ROS initiate phosphorylation of p38 MAP kinase during hypoxia in cardiomyocytes. *American Journal of Physiology Lung Cellular and Molecular Physiology* 2002; **282**: L1324-L1329.
259. Takeshi N, Diane E, Liang DX, *et al.* Normalising mitochondrial superoxide production blocks three pathways of hyperglycaemic damage. *Nature* 2000; **404**: 787-790.
260. Fleury C, Mignotte B, Vayssiere J-L. Mitochondrial reactive oxygen species in cell death signalling. *Biochimie* 2002; **84**: 131-141.
261. Esposito LA, Melov S, Panov A, Cottrell BA, Wallace DC. Mitochondrial disease in mouse results in increased oxidative stress. *Proceedings of the National Academy of Sciences of the United States of America* 1999; **96**: 4820-4825.
262. Golden TR, Melov S. Mitochondrial DNA mutations, oxidative stress and ageing. *Mechanisms of Ageing and Development* 2001; **122**: 1577-1589.
263. Cadenas E, Davies KJA. Mitochondrial free radical generation, oxidative stress and ageing. *Free Radical Biology and Medicine* 2000; **29**: 222-230.
264. Dobson AW, Grishko V, LeDoux SP, Kelley MR, Wilson GL, Gillespie MN. Enhanced mtDNA repair capacity protects pulmonary artery endothelial cells from oxidant-mediated death. *American Journal of Physiology Lung Cellular and Molecular Physiology* 2002; **283**: L205-L210.
265. Richter C, Suter M. Fragmented mitochondrial DNA is the predominant carrier of oxidised DNA bases. *Biochemistry* 1999; **38**: 459-464.
266. Yakes FM, Van Houten B. Mitochondrial DNA damage is more extensive and persists longer than nuclear DNA damage in human cells following oxidative stress. *Proceedings of the National Academy of Sciences of the United States of America* 1997; **94**: 514-519.
267. Goyns MH. Genes, telomeres and mammalian ageing. *Mechanisms of Ageing and Development* 2002; **123**: 791-799.
268. Kang D, Hamasuki N. Maintenance of mitochondrial DNA integrity: repair and degradation. *Current Genetics* 2002; **41**: 311-322.

269. Li M, Absher PM, Liang P, Russell JC, Sobal BE, Fukagawa NK. High glucose concentrations induce oxidative damage to mitochondrial DNA in explanted vascular smooth muscle cells. *Experimental Biology and Medicine* 2001; **226**: 450-457.
270. Chinnery PF, Samuels DC, Elson J, Turnbull DM. Accumulation of mitochondrial DNA mutations in ageing, cancer and mitochondrial disease: is there a common mechanism? *Lancet* 2002; **360**: 1323-1325.
271. Iossa S, Lionetti L, Mollica MP, Barletta A, Liverini G. Oxidative activity in mitochondria isolated from rat liver at different stages of development. *Cell Biochemistry and Function* 1998; **16**: 261-268.
272. Liu VWS, Zhang C, Nagley P. Mutations in mitochondrial DNA accumulate differentially in three different human tissues during ageing. *Nucleic Acids Research* 1998; **26**: 1268-1275.
273. Smith RAJ, Porteous CM, Coulter CV, Murphy MP. Selective targeting of an antioxidant to mitochondria. *European Journal of Biochemistry* 1999; **263**: 709-716.
274. Babsky A, Doliba N, Savchrnko A, Wehrli S, Osbakken M. Na⁺ effects on mitochondrial respiration and oxidative phosphorylation in diabetic hearts. *Experimental Biology and Medicine* 2001; **226**: 543-551.
275. Kajander OA, Karhunen PJ, Jacobs HT. The relationship between somatic mtDNA rearrangements, human heart disease and ageing. *Human Molecular Genetics* 2002; **11**: 317-324.
276. Anson MR, Hudson E, Bohr VA. Mitochondrial endogenous oxidative damage has been overestimated. *FASEB Journal* 2000; **14**: 355-360.
277. Zhang J, Block ER, Patel JM. Down-regulation of mitochondrial cytochrome c oxidase in senescent porcine pulmonary artery endothelial cells. *Mechanisms of Ageing and Development* 2002; **123**: 1363-1374.
278. Gow AJ, Ischiropoulos H. Nitric oxide chemistry and cellular signalling. *Journal of Cellular Physiology* 2001; **187**: 277-282.
279. Brown GC, Borutaite V. Nitric oxide inhibition of mitochondrial respiration and its role in cell death. *Free Radical Biology and Medicine* 2002; **33**: 1440-1464.

280. Elgawish A, Glomb M, Friedlander M, Monnier UM. Involvement of hydrogen peroxide in collagen cross-linking by high glucose *in vitro* and *in vivo*. *Journal of Biological Chemistry* 1996; **271**: 12964-12971.
281. Attardi G. Role of mitochondrial DNA in human ageing. *Mitochondrion* 2002; **2**: 27-37.
282. Fukagawa NK, Li M, Liang P, Russell JC, Sobel BE, Absher PM. Aging and high concentrations of glucose potentiate injury to mitochondrial DNA. *Free Radical Biology and Medicine* 1999; **27**: 1437-1443.
283. Park K-S, Nam J-K, Kim J-W, *et al.* Depletion of mitochondrial DNA alters glucose metabolism in SK-Hep 1 cells. *American Journal of Physiology Endocrinology and Metabolism* 2001; **280**: E1007-E1014.
284. Suzuki S, Hinokio Y, Komatu K, *et al.* Oxidative damage to mitochondrial DNA and its relationship to diabetic complications. *Diabetes Research and Clinical Practice* 1999; **45**: 161-168.
285. Choi YS, Kim S, Pak YK. Mitochondrial transcription factor A (mt TFA) and diabetes. *Diabetes Research and Clinical Practice* 2001; **54**: S65-S72.
286. Lee HK, Song JH, Shin CS, *et al.* Decreased mitochondrial DNA content in peripheral blood precedes the development of non-insulin-dependent diabetes mellitus. *Diabetes Research and Clinical Practice* 1998; **42**: 161-167.
287. Rhian MT. Oxidative stress and vascular damage in hypertension. *Current Hypertension Reports* 2000; **2**: 98-105.
288. Jones SA, O'Donnell VB, Wood JD, Broughton JP, Hughes EJ, Jones OTG. Expression of phagocyte NADPH oxidase components in human endothelial cells. *American Journal of Physiology* 1996; **271**: H1626-H1634.
289. Chan S, Schopfer P. Hydroxyl-radical production in physiological reactions — a novel function of peroxidase. *European Journal of Biochemistry* 1999; **260**: 726-735.
290. Dreher D, Junod AF. Role of oxygen free radicals in cancer development. *European Journal of Cancer* 1996; **32A**: 30-38.

291. Halliwell B, Aruoma OI. DNA damage by oxygen-derived species – its mechanisms and measurement in mammalian systems. *FEBS Letters* 1991; **281**: 9-19.
292. Kietzmann T, Fandrey J, Acker H. Oxygen radicals as messengers in oxygen-dependent gene expression. *News in Physiological Science* 2000; **15**: 202-208.
293. Kasai N, Sugimoto K, Horiba N, Suda T. Effect of D-glucose on nitric oxide release from glomerular endothelial cells. *Diabetes Metabolism Research Reviews* 2001; **17**: 217-222.
294. Castro L, Rodriguez M, Radi R. Aconitase is readily inactivated by peroxynitrite, but not by its precursor, nitric oxide. *Journal of Biological Chemistry* 1994; **269**: 29409-29415.
295. Radi R, Cassina A, Hodara R, Quijano C, Castro L. Peroxynitrite reactions and formation in mitochondria. *Free Radical Biology and Medicine* 2002; **33**: 1451-1474.
296. Okuda M, Inoue N, Azumi H, *et al.* Expression of glutaredoxin in human coronary arteries. Its potential role in antioxidant protection against atherosclerosis. *Arteriosclerosis, Thrombosis and Vascular Biology* 2001; **21**: 1483-1487.
297. Kritharides L, Stocker R. The use of antioxidant supplements in coronary heart disease. *Atherosclerosis* 2002; **164**: 211-219.
298. de Hann JB, Cristiano F, Iannello R, Bladier C, Kelner MJ, Kola I. Elevation in the ratio of Cu/ Zn-superoxide dismutase to glutathione peroxidase activity induces features of cellular senescence and this effect is mediated by hydrogen peroxide. *Human Molecular Genetics* 1996; **5**: 283-292.
299. Oliveira HR, Curi R, Carpinelli AR. Glucose induces an acute increase of superoxide dismutase activity in incubated rat pancreatic islets. *American Journal of Physiology Cell Physiology* 1999; **245**: C507-C510.
300. Indik JH, Goldman S, Gaballa MA. Oxidative stress contributes to vascular endothelial dysfunction in heart failure. *American Journal of Physiology Heart and Circulatory Physiology* 2001; **281**: H1767-H1770.
301. Oberley TD. Oxidative damage and cancer. *American Journal of Pathology* 2002; **164**: 403-408.

302. Antunes F, Han D, Cadenas E. Relative contributions of heart mitochondria glutathione peroxidase and catalase to H₂O₂ detoxification in *in vivo* conditions. *Free Radical Biology and Medicine* 2002; **33**: 1260-1267.
303. Schaffer FQ, Buettner GR. Redox environment of the cell as viewed through the redox state of the glutathione disulphide/ glutathione couple. *Free Radical Biology and Medicine* 2001; **30**: 1191-1212.
304. Hu H-L, Forsey RJ, Blades TJ, Barratt MEJ, Parmar P, Powell JR. Antioxidants may contribute in the fight against ageing: an *in vitro* model. *Mechanisms of Ageing and Development* 2000; **121**: 217-230.
305. Guo ZM, Yang H, Hamilton ML, Van Remmen H, Richardson A. Effects of age and food restriction on oxidative DNA damage and antioxidant enzyme activities in the mouse aorta. *Mechanisms of Ageing and Development* 2001; **122**: 1771-1736.
306. Zahn RK, Zahn-Daimler G, Ax S, *et al.* DNA damage susceptibility and repair in correlation to calendric age and longevity. *Mechanisms of Ageing and Development* 2000; **119**: 101-112.
307. Martinet W, Knaapen M, Meyer GD, Herman A, Kockx M. Elevated levels of oxidative DNA damage and DNA repair enzymes in human atherosclerotic plaques. *Circulation* 2002; **106**: 927-932.
308. Sampson MJ, Astley S, Richardson T, *et al.* Increased DNA oxidative susceptibility without increased plasma LDL oxidisability in type II diabetes: effects of α -tocopherol supplementation. *Clinical Science* 2001; **101**: 235-241.
309. Hamilton ML, Van Remmen H, Drake JA, *et al.* Does oxidative damage to DNA increase with age? *Proceedings of the National Academy of Sciences of the United States of America* 2001; **98**: 10469-10474.
310. Collins AR. Oxidative DNA damage, antioxidants and cancer. *BioEssays* 1999; **21**: 238-246.
311. Cardozo-Pelaez F, Stedeford TJ, Brooks PJ, Song S, Sanchez-Ramos JR. Effects of diethylmaleate on DNA damage and repair in the mouse brain. *Free Radical Biology and Medicine* 2002; **33**: 292-298.
312. Bucala R, Model P, Cerami A. Modification of DNA by reducing sugars: a possible mechanism for nucleic acid ageing and age-related dysfunction in gene expression. *Proceedings of the National Academy of Sciences of the United States of America* 1984; **81**: 105-109.

313. Barbouti A, Doulias P-T, Nouis L, Tenopouloou M, Galaris D. DNA damage and apoptosis in hydrogen peroxide-exposed Jurkat cells: Bolus addition versus continuous generation of H₂O₂. *Free Radical Biology and Medicine* 2002; **33**: 691-702.
314. Ikeda M, Ariyoshi H, Kambayashi J, *et al.* Separate analysis of nuclear and cytosolic Ca²⁺ concentrations in human umbilical vein endothelial cells. *Journal of Cellular Biochemistry* 1996; **63**: 23-36.
315. Djuric Z, Potter DW, Taffe BG, Strasburg GM. Comparison of iron-catalysed DNA and lipid oxidation. *Journal of Biochemical and Molecular Toxicology* 2001; **15**: 114-119.
316. Villani P, Altavista PL, Castaldi L, Leter G, Cordelli E. Analysis of DNA oxidative damage related to cell proliferation. *Mutation Research* 2000; **464**: 229-237.
317. Arosio P, Levi S. Ferritin, iron homeostasis and oxidative damage. *Free Radical Biology and Medicine* 2002; **33**: 457-463.
318. Aust AE, Eveleigh JF. Mechanisms of DNA oxidation. *PSEBM* 1999; **222**: 246-252.
319. Boone E, Schuster GB. Long-range oxidative damage in duplex DNA: the effect of bulged G in a G-C tract and tandem G/A mispairs. *Nucleic Acids Research* 2002; **30**: 830-837.
320. Gjese B. Long-distance electron transfer through DNA. *Annual Review of Biochemistry* 2002; **71**: 51-70.
321. Wallace SS. Biological consequences of free radical-damaged DNA bases. *Free Radical Biology and Medicine* 2002; **33**: 1-14.
322. Kaneko T, Tahara S, Taguchi T, Kondo H. Accumulation of oxidative DNA damage, 8-oxo-2'-deoxyguanosine and change of repair systems during *in vitro* cellular ageing of cultured human skin fibroblasts. *Mutation Research* 2001; **487**: 19-30.
323. Graziewicz MA, Day BJ, Copeland WC. The mitochondrial DNA polymerase as a target of oxidative damage. *Nucleic Acids Research* 2002; **30**: 2817-2824.
324. Pieper GM, Jordan M, Dondlinger LA, Adams MB, Roza AM. Peroxidative stress in diabetic blood vessels. *Diabetes* 1995; **44**: 884-889.

325. Dandona P, Thusu K, Cook S, *et al.* Oxidative damage to DNA in diabetes mellitus. *Lancet* 1996; **347**: 444-445.
326. Ghosh R, Mitchell DL. Effect of oxidative DNA damage in promoter elements on transcription factor binding. *Nucleic Acids Research* 1999; **27**: 3213-3218.
327. Nuttall SL, Dunne F, Kendall MJ, Martin U. Age-dependent oxidative stress in elderly patients with non-insulin dependent diabetes mellitus. *Quarterly Journal of Medicine* 1999; **92**: 33-38.
328. Giugliano D, Ceriello A, Paolisso G. Diabetes mellitus, hypertension and cardiovascular disease: which role for oxidative stress? *Metabolism* 1995; **44**: 363-368.
329. West IC. Radicals and oxidative stress in diabetes. *Diabetic Medicine* 2000; **43**: 562-571.
330. Chappey OC, Dosquet M-P, Wautier J-L. Advanced glycation end-products, oxidative stress and vascular lesions. *European Journal of Clinical Investigation* 1997; **27**: 97-108.
331. Kamal K, Du W, Mills I, Sumpio BE. Antiproliferative effect of elevated glucose in human microvascular endothelial cells. *Journal of Cell Biochemistry* 1998; **71**: 491-501.
332. Lehninger AL, Nelson DL, Cox MM. *Principles of Biochemistry*. 2nd ed. New York: Worth Publishers, 1993: 359-542.
333. Van Wynsberghe D, Noback CR, Carola R. *Human Anatomy and Physiology*. 3rd ed. New York: McGraw-Hill, 1995: 852-862.
334. Guyton AC, Hall JE. *Human Physiology and Mechanisms of Disease*. 6th ed. London: WB Saunders Company, 1997: 625-633.
335. Zayzafoon M, Stell C, Irwin R, McCabe LR. Extracellular glucose influences osteoblast differentiation and c-Jun expression. *Journal of Cell Biochemistry* 2000; **79**: 301-310.
336. Lange K. Role of microvillar cell surfaces in the regulation of glucose uptake and organisation of energy metabolism. *American Journal of Physiology Cell Physiology* 2002; **282**: C1-C26.

337. Berne RM, Levy MN. *Principles of Physiology*. 1st ed. London: Mosby, 1990: 16-17.
338. Quinn LA, McCumbee WD. Regulation of glucose transport by angiotensin II and glucose in cultured vascular smooth muscle cells. *Journal of Cellular Physiology* 1998; **177**: 94-102.
339. Sasson S, Gorowitz N, Joost HG, King GL, Cerasi E, Kaiser N. Regulation by metformin of the hexose transport system in vascular endothelial and smooth muscle cells. *British Journal of Pharmacology* 1996; **117**: 1318-1324.
340. Kaiser N, Sasson S, Feener EP, *et al*. Differential regulation of glucose transport and transporters by glucose in vascular endothelial and smooth muscle cells. *Diabetes* 1993; **42**: 80-89.
341. Behrooz A, Ismail-Beigi F. Stimulation of glucose transport by hypoxia: signals and mechanisms. *News in Physiological Science* 1999; **14**: 105-110.
342. Kishi Y, Schmelzer JD, Yae JK, *et al*. α -lipoic acid: effect on glucose uptake, sorbitol pathway and energy metabolism in experimental diabetic neuropathy. *Diabetes* 1999; **48**: 2045-2051.
343. Mann GE, Yudilevich DL, Sobreria L. Regulation of amino acid and glucose transporters in endothelial and smooth muscle cells. *Physiological Reviews* 2003; **83**: 183-252.
344. Boileau P, Mrejen C, Girard J, Monzon SH-d. Overexpression of GLUT 3 Placental glucose transporter in diabetic rats. *Journal of Clinical Investigation* 1995; **96**: 309-317.
345. Mouzon SH-d, Challier JC, Kacemi A, Cauzac M, Malek A, Girard J. The GLUT 3 glucose transporter isoform is differentially expressed within human placental cell types. *Journal of Clinical Endocrinology and Metabolism* 1997; **82**: 2689-2694.
346. Peiro C, Lafuente N, Matesanz N, *et al*. High glucose induces cell death of cultured human aortic smooth muscle cells through the formation of hydrogen peroxide. *British Journal of Pharmacology* 2001; **133**: 967-974.

347. Pennathur S, Wagner JD, Leeuwenburgh C, Litwak KN, Heinecke JW. A hydroxyl radical-like species oxidises cynomolgus monkey artery wall proteins in early diabetic vascular disease. *Journal of Clinical Investigation* 2001; **107**: 853-860.
348. Zhao X, Alexander JS, Zhang S, *et al.* Redox regulation of endothelial barrier integrity. *American Journal of Physiology Lung Cellular and Molecular Physiology* 2001; **281**: L879-L886.
349. Van den Eenden MK, Nyengaard JR, Ostrow E, Burgan JH, Williamson JR. Elevated glucose levels increase retinal glycolysis and sorbitol pathway metabolism. Implications for diabetic retinopathy. *Investigative Ophthalmology and Visual Science* 1995; **36**: 1675-1685.
350. Tangiuchi N, Kaneto H, Asahi M, *et al.* Involvement of glycation and oxidative stress in diabetic macroangiopathy. *Diabetes* 1996; **45**: S81-S83.
351. Spychar SE, Tabataba-Vakili S, O'Donnell VB, Palomloa L, Azzi A. Aldose reductase induction: a novel response to oxidative stress of smooth muscle cells. *FASEB Journal* 1997; **11**: 181-188.
352. Yabe-Nishimura C. Aldose reductase in glucose toxicity: a potential target for the prevention of diabetic complications. *Pharmacological Reviews* 1998; **50**: 21-33.
353. Baynes JW. Role of oxidative stress in development of complications in diabetes. *Diabetes* 1991; **40**: 405-412.
354. Dominguez C, Ruiz E, Gussinye M, Carrascosa A. Oxidative stress at onset and in early stages of type 1 diabetes in children and adolescents. *Diabetes Care* 1998; **21**: 1736-1742.
355. Ceriello A, Bortolotti N, Motz E, *et al.* Meal-generated oxidative stress in type 2 diabetics patients. *Diabetes Care* 1998; **21**: 1529-1533.
356. Cameron NE, Cotter MA. Metabolism and vascular factors in the pathogenesis of diabetic neuropathy. *Diabetes* 1997; **46**: 31-37.
357. Ido Y, Kilo C, Williamson JR. Cytosolic NADH/ NAD⁺, free radicals and vascular dysfunction in early diabetes mellitus. *Diabetologia* 1997; **40**: S115-S117.

358. Wu QD, Wang JH, Fennessy F, Redmond HP, Bouchier HD. Taurine prevents high-glucose-induced human vascular endothelial cell apoptosis. *American Journal of Physiology Cell Physiology* 1999; **277**: C1229-C1238.
359. Yang ES, Richter C, Chun J-S, Huh T-L, Kang S-S, Park J-W. Inactivation of NADP⁺-dependent isocitrate dehydrogenase by nitric oxide. *Free Radical Biology and Medicine* 2002; **33**: 927-937.
360. Ammar RF, Gutterman DD, Brookes LA, Dellsperger KC. Impaired dilation of coronary arterioles during increases in myocardial O₂ consumption with hyperglycaemia. *American Journal of Physiology Endocrinology and Metabolism* 2000; **279**: E868-E874.
361. Honing MLH, Morrison PJ, Banga JD, Stores ESG, Rabelink TJ. Nitric oxide availability in diabetes mellitus. *Diabetes Metabolism Reviews* 1998; **14**: 241-249.
362. Carlos F, Susana R, Claudio A, *et al.* Rapid stimulation of 1-Arginine transport by D-glucose involves p42/44^{mapk} and nitric oxide in human umbilical vein endothelium. *Circulation Research* 2003; **92**: 64-72.
363. Wahlberg G, Adamson U, Svensson J. Pyridine nucleotides in glucose metabolism and diabetes: a review. *Diabetes Metabolism Research Reviews* 2000; **16**: 33-42.
364. Hehenberger K, Hansson A. High glucose-induced growth factor resistance in human fibroblasts can be reversed by antioxidants and protein kinase C-inhibitors. *Cell Biochemistry and Function* 1997; **15**: 197-201.
365. Koya D, King GL. Protein kinase C activation and the development of diabetic complications. *Diabetes* 1998; **47**: 859-866.
366. Ha H, Lee HB. Reactive oxygen species as glucose signalling molecules in mesangial cells cultured under high glucose. *Kidney International* 2000; **58**: S19-S25.
367. Lyons TJ. Glycation and oxidation: a role in the pathogenesis of atherosclerosis. *American Journal of Cardiology* 1993; **71**: 26B-31B.
368. Brownlee M. Negative consequences of glycation. *Metabolism* 2000; **49**: 9-13.
369. Lee AT, Cerami A. Role of glycation in ageing. *Annals of the New York Academy of Sciences* 2000; **908**: 63-71.

370. Yan SD, Schmidt AM, Anaderson GM, *et al.* Enhanced cellular oxidant stress by the interaction of advanced glycation end-products with their receptors/ binding proteins. *Journal of Biological Chemistry* 1994; **269**: 9889-9897.
371. Ho H-Y, Cheng M-L, Lu F-J, *et al.* Enhanced oxidative stress and accelerated cellular senescence in glucose-6-phosphate dehydrogenase (G6PD)-deficient human fibroblasts. *Free Radical Biology and Medicine* 2000; **29**: 156-159.
372. Vlassara H, Bucala R. Recent progress in advanced glycation and diabetic vascular disease: role of advanced glycation end-product receptors. *Diabetes* 1996; **45**: S65-S66.
373. Brownlee M. Advanced protein glycosylation in diabetes and ageing. *Annual Review of Medicine* 1995; **46**: 223-234.
374. Featherstone C, Jackson SP. DNA double-strand break repair. *Current Biology* 1999; **20**: R759-R761.
375. Horton JK, Baker A, Vande Berg BJ, Sobol RW, Wilson SH. Involvement of DNA polymerase β in protection against the cytotoxicity of oxidative DNA damage. *DNA Repair* 2002; **1**: 317-333.
376. Stanaway SERS, Gill GV. Protein glycosylation in diabetes mellitus: biochemical and clinical considerations. *Practical Diabetes International* 2000; **17**: 21-25.
377. Talasz H, Wasserer S, Puschendorf B. Non-enzymatic glycation of histones *in vitro* and *in vivo*. *Journal of Cellular Biochemistry* 2002; **85**: 24-34.
378. Chi MM-Y, Hoehn A, Moley KH. Metabolic changes in the glucose-induced apoptotic blastocyst suggest alterations in mitochondrial physiology. *American Journal of Physiology Endocrinology and Metabolism* 2002; **283**: E226-E232.
379. Wautier M-P, Chappey O, Corda S, Stern DM, Schmidt M, Wautier J-L. Activation of NADPH oxidase by AGE links oxidant stress to altered gene expression via RAGE. *American Journal of Physiology Endocrinology and Metabolism* 2001; **280**: E685-E694.
380. Wautier J-L, Zoukourian C, Chappey O, *et al.* Receptor-mediated endothelial cell dysfunction in diabetic vasculopathy. *Journal of Clinical Investigation* 1996; **97**: 238-243.

381. Ceriello A. Acute hyperglycaemia and oxidative stress generation. *Diabetic Medicine* 1997; **14**: S45-S49.
382. Dincer Y, Alademir Z, Ilkova H, Akcay T. Susceptibility of glutathione and glutathione-related antioxidant activity to hydrogen peroxide in patients with type 2 diabetes: effect of glycaemic control. *Clinical Biochemistry* 2002; **35**: 297-301.
383. Aydin A, Orhan H, Sayal A, Ozata M, Sahrin G, Isimer A. Oxidative stress and nitric oxide related parameters in type II diabetes mellitus: effects of glycaemic control. *Clinical Biochemistry* 2001; **34**: 65-70.
384. Barbieri M, Rizzo MR, Manzella D, *et al.* Glucose regulation and oxidative stress in healthy centenarians. *Experimental Gerontology* 2003; **38**: 137-143.
385. Gopaul NK, Anggard EE, Mallet AI, Betteridge DJ, Wolff SP, Nourooz-Zahah J. Plasma 8-epi PGF_{2α} levels are elevated in individuals with non-insulin dependent diabetes mellitus. *FEBS Letters* 1995; **368**: 225-229.
386. Nourooz-Zadeh J, Tajaddini-Sarmadi J, McCarthy S, Betteridge DJ, Wolff SP. Elevated levels of authentic plasma hydroperoxidase in NIDDM. *Diabetes* 1995; **44**: 1054-1058.
387. Nourooz-Zadeh J, Rahimi A, Tajaddini-Sarmadi J. Relationships between plasma measures of oxidative stress and metabolic control in NIDDM. *Diabetologia* 1997; **40**: 647-653.
388. Davi G, Ciaboattoni G, Consoli A. *In vivo* formation of 8-iso-prostaglandin F_{2α} and platelet activation in diabetes mellitus: effects of improved metabolic control and vitamin E supplementation. *Circulation* 1999; **99**: 224-229.
389. Ceriello A. Oxidative stress and glycaemic regulation. *Metabolism* 2000; **49**: 27-29.
390. Paolisso G, Giugliano D. Oxidative stress and insulin action: is there a relationship? *Diabetologia* 1996; **39**: 357-363.
391. Shin CS, Moon BS, Park KS, *et al.* Serum 8-hydroxy-guanine levels are increased in diabetic patients. *Diabetes Care* 2001; **24**: 733-737.
392. Matteucci E, Giampietro O. Oxidative stress in families of type I diabetic patients. *Diabetes Care* 2000; **23**: 1182-1186.

393. Hinokio Y, Suzuki S, Hirai M, Chiba M, Hirai A, Toyota T. Oxidative DNA damage in diabetes mellitus: its association with diabetic complications. *Diabetologia* 1999; **42**: 995-998.
394. Zobali F, Avai A, Canbolta O, Karasu C. Effects of vitamin A and insulin on the antioxidative state of diabetic rat heart: a comparison study with combination treatment. *Cell Biochemistry and Function* 2002; **20**: 75-80.
395. Jeanclos E, Krolewski A, Skurnick J, *et al.* Shortened telomere length in white blood cells of patients with IDDM. *Diabetes* 1998; **47**: 482-486.
396. Krapfenbauer K, Birnbacher R, Vierhapper H, Herkner K, Kampel D, Lubec G. Glycooxidation and protein and DNA oxidation in patients with diabetes mellitus. *Clinical Science* 1998; **95**: 331-337.
397. Vlassara H. Recent progress in advanced glycation end-products and diabetic complications. *Diabetes* 1997; **46**: S19-S24.
398. Varvarovska J, Racek J, Stozicky F, Soucek J, Trefil L, Pomahacova R. Parameters of oxidative stress in children with type I diabetes mellitus and their relatives. *Journal of Diabetes and its Complications* 2003; **17**: 7-10.
399. Graier WF, Simecek S, Kukovetz WR, Kostner GM. High D-glucose-induced changes in endothelial Ca^{2+} /EDRF signalling are due to generation of superoxide anions. *Diabetes* 1996; **45**: 1386-1395.
400. Gesquiere L, Loreau N, Minnich A, Davignon J, Blache D. Oxidative stress leads to cholesterol accumulation in vascular smooth muscle cells. *Free Radical Biology and Medicine* 1999; **27**: 134-145.
401. Oakley TJ, Hickson ID. Defending genome integrity during S-phase: putative roles for RecQ helicases and topoisomerase III. *DNA Repair* 2002; **1**: 175-207.
402. Wallace SS. *Oxidative damage to DNA and its repair*. In: Scandalios JG, ed. *Oxidative stress and the molecular biology of antioxidant defences*. 1st ed. USA: Cold Harbour Laboratory Press, 1997.
403. DePinho RA. The age of cancer. *Nature* 2000; **408**: 248-254.

404. Lee H-S, Lee Y-S, Kim H-S, Choi J-Y, Hasen HM, Chung M-H. Mechanism of regulation of 8-hydroxyguanine endonuclease by oxidative stress: roles of FNR, ArcA and Fur. *Free Radical Biology and Medicine* 1998; **24**: 1193-1201.
405. Aquilina G, Bignami M. Mismatch repair in correction of replication errors and processing of DA damage. *Journal of Cellular Physiology* 2001; **187**: 145-154.
406. Chen Y, Lee W-H, Chew HK. Emerging roles of BRCA1 in transcriptional regulation and DNA repair. *Journal of Cellular Physiology* 1999; **181**: 385-392.
407. Paul R, Dalibart R, Lemoine S, Lestienne P. Expression of *E. Coli* RecA targeted to mitochondria of human cells. *Mutation Research* 2001; **485**: 169-176.
408. Chang CL, Marra G, Chauhan DP, *et al.* Oxidative stress inactivates the human DNA mismatch repair system. *American Journal of Physiology Cell Physiology* 1999; **276**: C1061-C1068.
409. Ono T, Uehara Y, Saito Y, Ikehata H. Mutation theory of ageing, assessed in transgenic mice and knockout mice. *Mechanisms of Ageing and Development* 2002; **123**: 1543-1552.
410. Mason PA, Matheson EC, Hall AG, Lightowlers RN. Mismatch repair activity in mammalian mitochondria. *Nucleic Acids Research* 2003; **31**: 1052-1058.
411. Frosina G. Overexpression of enzymes that repair endogenous damage to DNA. *European Journal of Biochemistry* 2000; **267**: 2135-2149.
412. Marti TM, Kunz C, Fleck O. DNA mismatch repair and mutation avoidance pathways. *Journal of Cellular Physiology* 2002; **191**: 28-41.
413. Shall S. Poly(ADP-ribosylation) – a common control process? *BioEssays* 2002; **24**: 197-201.
414. Burkle A. Physiology and pathophysiology of poly(ADP-ribosylation). *BioEssays* 2001; **23**: 795-806.
415. Dianov GL, O'Neill P, Goodhead DT. Securing genome stability by orchestrating DNA repair: removal of radiation-induced clustered lesions in DNA. *BioEssays* 2001; **23**: 745-749.

416. Ziegler M, Oei SL. A cellular survival switch: poly(ADP-ribosylation) stimulates DNA repair and silences transcription. *BioEssays* 2001; **23**: 543-548.
417. Caley KW. Mammalian DNA single-strand break repair: an X-rayed affair. *BioEssays* 2001; **23**: 447-455.
418. Scharer OD, Jiricny J. Recent progress in the biology, chemistry and structural biology of DNA glycosylases. *BioEssays* 2001; **23**: 270-281.
419. Radaelli A, Magrassi R, Bonassi S, Abboridandolo A, Frosina G. AP Endonuclease activity in humans: development of a simple assay and analysis of ten normal individuals. *Teratogenesis, Carcinogenesis and Mutagenesis* 1998; **18**: 17-26.
420. Bohr VA. Repair of oxidative DNA damage in nuclear and mitochondrial DNA and some changes with ageing in mammalian cells. *Free Radical Biology and Medicine* 2002; **32**: 804-812.
421. Burkle A. PARP-1: a regulator of genomic stability linked with mammalian longevity. *ChemBiochem* 2001; **2**: 725-728.
422. Lehmann AR. Dual functions of DNA repair genes: molecular, cellular and clinical implications. *BioEssays* 1998; **20**: 146-155.
423. Dodson ML, Lloyd RS. Backbone dynamics of DNA containing 8-oxoguanine: importance for substrate recognition by base excision repair glycosylases. *Mutation Research* 2001; **487**: 93-108.
424. Mitra S, Izumi T, Boldogh I, Bhakat KK, Hill JW, Hazra TK. Choreography of oxidative damage repair in mammalian genomes. *Free Radical Biology and Medicine* 2002; **33**: 15-28.
425. Wilson III DM, Barsky D. The major human abasic endonuclease: formation, consequences and repair of abasic lesions in DNA. *Mutation Research* 2001; **485**: 283-307.
426. Fortini P, Pascucci B, Belisario F, Doglitti E. DNA polymerase β is required for efficient DNA strand break repair induced by methyl methanesulfonate but not by hydrogen peroxide. *Nucleic Acids Research* 2000; **28**: 3040-3046.
427. Vodenichaeov MD, Sallmann FR, Satoh MS, Poirier GG. Base excision repair is efficient in cells lacking poly(ADP-ribose)polymerase 1. *Nucleic Acids Research* 2000; **28**: 3887-3896.

428. Trucco C, Oliver FJ, de Murica G, Menissier-de Murcia J. DNA repair defect in poly(ADP-ribose)polymerase-deficient cell lines. *Nucleic Acids Research* 1998; **26**: 2644-2649.
429. Chen K-H, Yakes FM, Srivastava DK, *et al.* Up-regulation of base excision repair correlates with enhanced protection against a DNA damaging agent in mouse cell lines. *Nucleic Acids Research* 1998; **26**: 2001-2007.
430. Ziegler M. New functions of a long-known molecule. Emerging roles of NAD in cellular signalling. *European Journal of Biochemistry* 2000; **267**: 1550-1564.
431. Lunec J, Holloway KA, Cooke MS, Faux S, Griffiths HR, Evans MD. Urinary 8-oxo-2'-deoxyguanosine: redox regulation of DNA repair *in vivo*? *Free Radical Biology and Medicine* 2002; **33**: 875-885.
432. Titan K, McTigue M, de los Santos C. Sorting the consequences of ionizing radiation: processing of 8-oxoguanine/ abasic site lesions. *DNA repair* 2002; **1**: 1039-1049.
433. Hubscher U, Maga G, Spaderi S. Eukaryotic DNA polymerases. *Annual Review of Biochemistry* 2002; **71**: 133-163.
434. McCullough AK, Dodson ML, Lloyd RS. Initiation of base excision repair: glycosylase mechanisms and structures. *Annual Review of Biochemistry* 1999; **68**: 255-285.
435. Vidal AE, Boiteux S, Hickson ID, Radicella JP. XRCC1 coordinates the initial and late stages of DNA abasic site repair through protein-protein interactions. *EMBO Journal* 2001; **20**: 6530-6539.
436. Xu Y-j, DeMott MS, Hwang JT, Greenberg MM, Demple B. Action of human apurinic endonuclease (Ape-1) on C1'-oxidised deoxyribose damage in DNA. *DNA Repair* 2003; **2**: 175-185.
437. Oliver FJ, de Murica JM, de Murica G. Poly(ADP-ribose)polymerase in the cellular response to DNA damage, apoptosis and disease. *American Journal of Human Genetics* 1999; **64**: 1282-1288.
438. Fortini P, Parlanti E, Sidorkina OM, Laval J, Dogliotti E. The type of DNA glycosylase determines the base excision repair pathway in mammalian cells. *Journal of Biological Chemistry* 1999; **274**: 15230-15236.

439. Ramana CV, Bolgogh I, Izumi T, Mitra S. Activation of apurinic/apyrimidinic endonuclease in human cells by reactive oxygen species and its correlation with their adaptive response to genotoxicity of free radicals. *Proceedings of the National Academy of Sciences of the United States of America* 1998; **95**: 5061-5066.
440. Thorslund T, Sunesen M, Bohr VA, Stevnsner T. Repair of 8-oxoG is slower in endogenous nuclear genes than in mitochondrial DNA and is without strand bias. *DNA Repair* 2002; **1**: 261-273.
441. Bohr VA, Stevnsner T, de Souza-Pinto NC. Mitochondrial DNA repair of oxidative damage in mammalian cells. *Gene* 2002; **286**: 127-134.
442. Digweed M, Reis A, Sperling K. Nijmegen Breakage Syndrome: consequences of defective DNA double strand break repair. *BioEssays* 1999; **21**: 649-656.
443. Freshney IR. *Culture of animal cells*. 4th edition. New York: Wiley-Liss, 1985.
444. Hastings R, Qureshi M, Verma R, Lacy PS, Williams B. Telomere attrition and acculuation of senescent cells in cultured human endothelial cells. *Cell Proliferation* 2004; **37**: 317-324.
445. Hewett PW, Murray JC. Human microvessel endothelial cells: isolation, culture and characterisation. *In Vitro Cellular and Developmental Biology* 1993; **29**: 823-830.
446. Sudonikova EY, Martynov AV, Danilor SM. Long-term serial cultivation of human vascular endothelial cells. *Biomedical Science* 1990; **1**: 199-205.
447. Wei C, Skopp R, Takata M, Takeda S, Price CM. Effects of double-strand break repair proteins on vertebrate telomere structure. *Nucleic Acids Research* 2002; **30**: 2862-2870.
448. Anderson D, Yu T-W, Wright J, Ioannides C. An examination of DNA strand breakage in the comet assay and antioxidant capacity in diabetic patients. *Mutation Research* 1998; **398**: 151-161.
449. Tice RR, Vasquez M. Protocol for the application of the pH>13 alkaline single cell gel (SCG) assay to the detection of DNA damage in mammalian cells. Komet@ils-inc.com; 1999.
450. Comet assay interest group website URL:
<http://www.geocites.com/cometassay//fixed/collins.htm>

451. Cadet J, Douki T, Frelon S, Sauvaigo S, Pouget J-P, Ravanat J-L. Assessment of oxidative base damage to isolated and cellular DNA by HPLC-MS/MS measurement. *Free Radical Biology and Medicine* 2002; **33**: 441-449.
452. Lovell DP, Thomas G, Dubow R. Issues related to the experimental design and subsequent statistical analysis of *in vivo* and *in vitro* comet studies. *Teratogenesis, Carcinogenesis and Mutagenesis* 1999; **19**: 109-119.
453. Sierens J, Hartley JA, Campell MJ, Leathem AJC, Woodside JV. Effect of phytoestrogen and antioxidant supplementation on oxidative DNA damage assessed using the comet assay. *Mutation Research* 2001; **485**: 169-176.
454. Anderson D, Yu T-W, Dobrzynska MM, Ribas G, Marcos R. Effects in the comet assay of storage conditions on human blood. *Teratogenesis, Carcinogenesis and Mutagenesis* 1997; **17**: 115-125.
455. Horvathova E, Slamenova D, Hlincikova L, Mandal TK, Gabelova A, Collins AR. The nature and origin of DNA single-strand breaks determined with the comet assay. *Mutation Research* 1998; **409**: 163-171.
456. Collins A, Dusinska M, Franklin M, *et al.* Comet assay in human biomonitoring studies: reliability, validation and applications. *Environmental and Molecular Mutagenesis* 1997; **30**: 139-146.
457. Bocker W, Rolf W, Bauch T, Muller W-U, Streffer C. Automated comet assay analysis. *Cytometry* 1999; **35**: 134-144.
458. Rutter GA, Tavare JM, Palmer DG. Regulation of mammalian gene expression by glucose. *News in Physiological Science* 2000; **15**: 149-154.
459. Singh G, Lakkis CL, Laucinica R, Epner DE. Regulation of prostate cancer cell division by glucose. *Journal of Cellular Physiology* 1999; **180**: 431-438.
460. Yang J, Chang E, Cherry AM, *et al.* Human endothelial cell life extension by telomerase expression. *Journal of Biological Chemistry* 1999; **274**: 26141-26148.
461. Williams B, Schrier RW. Characterisation of glucose-induced *in situ* protein kinase C activity in cultured vascular smooth muscle cells. *Diabetes* 1992; **41**: 1464-1472.

462. Williams B. Glucose-induced vascular smooth muscle dysfunction: the role of protein kinase C. *Journal of Hypertension* 1995; **13**: 477-486.
463. Toussaint O, Remacle J, Clark BFC, Gonos ES, Franceschi C, Kirkwood TBL. Biology of ageing. *BioEssays* 2000; **22**: 954-956.
464. Williamson JR, Chang K, Frangos M, *et al.* Hyperglycaemic pseudohypoxia and diabetic complications. *Diabetes* 1993; **42**: 801-813.
465. Wolfe RR. Metabolic interactions between glucose and fatty acids in humans. *American Journal of Clinical Nutrition* 1998; **67**: 519S-526S.
466. Greene DA, Stevens MJ, Obrosova I, Feldman EL. Glucose-induced oxidative stress and programmed cell death in diabetic neuropathy. *European Journal of Pharmacology* 1999; **375**: 217-223.
467. Mueckler M. Facilitative glucose transporters. *European Journal of Biochemistry* 1994; **219**: 713-725.
468. Wright EM, Hirsch JR, Loo DD, Zampighi GA. Regulation of Na⁺/glucose co-transporters. *Journal of Experimental Biology* 1997; **200**: 287-293.
469. Shigenaga MK, Hagen TM, Ames BN. Oxidative damage and mitochondrial decay in ageing. *Proceedings of the National Academy of Sciences of the United States of America* 1994; **91**: 10771-10778.
470. Morre DM, Lenaz G, Morre JD. Surface oxidase and oxidative stress propagation in ageing. *Journal of Experimental Biology* 2000; **203**: 1513-1521.
471. Beckman KB, Ames BN. Oxidative decay of DNA. *Journal of Biological Chemistry* 1997; **272**: 19633-19636.
472. Kashiwagi A, Asahina T, Nishio Y, *et al.* Glycation, oxidative stress and scavenger activity. *Diabetes* 1996; **45**: S84-S86.
473. Soriano FG, Virag L, Jagtap P, *et al.* Diabetic endothelial dysfunction: the role of poly(ADP-ribose)polymerase activation. *Nature Medicine* 2001; **7**: 108-113.
474. Asahina T, Kashiwagi A, Nishio Y, *et al.* Impaired activation of glucose oxidation and NADPH supply in human endothelial cells exposed to H₂O₂ in high glucose medium. *Diabetes* 1995; **44**: 520-526.

475. Hattori Y, Hattori S, Sato N, Kasai K. High-glucose-induced nuclear factor κ B activation in vascular smooth muscle cells. *Cardiovascular Research* 2000; **46**: 188-197.
476. Du XL, Stockklauser-Faber K, Rosen P. Generation of reactive oxygen intermediates, activation of NF- κ B and induction of apoptosis in human endothelial cells by glucose: role of nitric oxide synthase? *Free Radical Biology and Medicine* 1999; **27**: 752-763.
477. Franceso C, Keiichi H, Zvonimir K, Luscher T. High glucose increases nitric oxide synthase expression and superoxide anion generation in human aortic endothelial cells. *Circulation* 1997; **96**: 25-28.
478. Giardino I, Fard AK, Hatchell DL, Brownlee M. Aminoguanidine inhibits reactive oxygen species formation, lipid peroxidation and oxidant-induced apoptosis. *Diabetes* 1998; **47**: 1114-1120.
479. Wolff SP, Jiang ZY, Hundt JV. Protein glycation and oxidative stress in diabetes mellitus and ageing. *Free Radical Biology and Medicine* 1991; **10**: 339-352.
480. Shimoi K, Okitsu A, Green MHL, *et al.* Oxidative DNA damage induced by high glucose and its suppression in human umbilical vein endothelial cells. *Mutation Research* 2001; **480-481**: 371-378.
481. Allen CB, White CW. Glucose modulates cell death due to normobaric hyperoxia by maintaining cellular ATP. *American Journal of Physiology* 1998; **274**: L159-L164.
482. van der Loo B, Fenton M, Erusalimsky JD. Cytochemical detection of a senescence associated- β -Galactosidase in endothelial and smooth muscle cells from human and rabbit blood vessels. *Experimental Cell Research* 1998; **241**: 309-315.
483. Dimri GP, Lee X, Basile G, Acosta M, Scott G, Roskelley C. A biomarker that identifies senescent human cells in culture and in ageing skin *in vivo*. *Proceedings of the National Academy of Sciences of the United States of America* 1995; **92**: 9363-9367.
484. Goyns MH, Lavery WL. Telomerase and mammalian ageing: a critical appraisal. *Mechanisms of Ageing and Development* 2000; **114**: 69-77.

485. Hiroishi G, Kobayasi S, Nishimura J, Inomata H, Kamaide H. High D-glucose stimulates the cell cycle from the G₁ to the S and M phases, but has no competent effect on the G₀ phase, in vascular smooth muscle cells. *Biochemical and Biophysical Research Communications* 1995; **211**: 619-626.
486. Dulic V, Kaufmann WK, Wilson SJ, *et al.* p53-dependent inhibition of cyclin-dependent kinase activities in human fibroblasts during radiation-induced G1 arrest. *Cell* 1994; **76**: 1013-1023.
487. Ceriello A, Russo P, Amstad P, Cerutti P. High glucose induces antioxidant enzymes in human endothelial cells in culture. *Diabetes* 1996; **45**: 471-477.
488. Ceriello A, Pirisi M. Is oxidative stress the missing link between insulin resistance and atherosclerosis? *New England Journal of Medicine* 1998; **344**: 1484.
489. Wolf FI, Torsello L, Covacci V, *et al.* Oxidative DNA damage as a marker of ageing in WI-38 human fibroblasts. *Experimental Gerontology* 2002; **37**: 647-656.
490. Poon SSS, Martens UM, Wrad RK, Lansdorp PM. Telomere length measurements using digital fluorescence microscopy. *Cytometry* 1999; **36**: 267-278.
491. Oexle K. Telomere length distribution and southern blot analysis. *Journal of Theoretical Biology* 1998; **190**: 369-377.
492. Friedrich U, Griese E-U, Schwab M, Fritz P, Thon K-P, Klotz U. Telomere length in different tissues of elderly patients. *Mechanisms of Ageing and Development* 2000; **119**: 89-99.
493. Freshney RI. *Culture of Animal Cells*. 1st ed. New York: Alan R Liss, 1984:7-14.
494. Kvietys PR, Granger DN. Endothelial cell monolayers as a tool for studying microvascular pathophysiology. *American Journal of Physiology* 1997; **273**: G1189-G1199.
495. Sherr CJ, DePinho RA. Cellular senescence: mitotic clock or culture shock? *Cell* 2000; **102**: 407-410.

496. Hultin M, Gronlund E, Norback KF, Eriksson-Lindstrom E, Just T, Roos G. Telomere analysis by fluorescence *in situ* hybridization and flow cytometry. *Nucleic Acids Research* 1998; **26**: 3651-3656.
497. Saldanha SN, Andrews LG, Tollefsbol TO. Assessment of telomere length and factors that contribute to its stability. *European Journal of Biochemistry* 2003; **270**: 389-403.
498. Lansdrop PM, Verwoerd NP, van de Rijke FM, *et al.* Heterogeneity in telomere length of human chromosomes. *Human Molecular Genetics* 1996; **5**: 685-691.
499. Cawthon RM. Telomere measurement by quantitative PCR. *Nucleic Acids Research* 2002; **30**: e47-e50.
500. Hsiao R, Sharma HW, Ramakrishnan S, Keith E, Narayanan R. Telomerase activity in normal human endothelial cells. *Anticancer Research* 1997; **17**: 827-832.
501. Furumoto K, Inoue E, Nagao N, Hiyama E, Miwa N. Age-dependent telomere shortening is slowed down by enrichment of intracellular vitamin C via suppression of oxidative stress. *Life Sciences* 1998; **63**: 935-948.
502. Spycher SE, Tabataba-Vakili S, O'Donnell VB, Palomloa L, Azzi A. Aldose reductase induction: a novel response to oxidative stress of smooth muscle cells. *FASEB Journal* 1997; **11**: 181-188.
503. Bonnefont-Rousselot D, Bastard JD, Jandon MC, Delattre J. Consequences of the diabetic status on the oxidant/ antioxidant balance. *Diabetes and Metabolism* 2000; **26**: 163-176.
504. Keenoy BM, Vertommen J, Leeuw ID. Divergent effects of different oxidants on glutathione homeostasis and protein damage in erythrocytes from diabetic patients: effects of high glucose. *Molecular and Cellular Biochemistry* 2001; **225**: 59-73.
505. Hamilton ML, Guo Z, Fuller CD, *et al.* A reliable assessment of 8-oxo-2-deoxyguanosine levels in nuclear and mitochondrial DNA using the sodium iodide method to isolate DNA. *Nucleic Acids Research* 2001; **29**: 2117-2126.
506. Janssen K, Schlink K, Gotte W, Hippler B, Kaina B, Oesch F. DNA repair activity of 8-oxoguanine DNA glycosylase 1 (OGG1) in human lymphocytes is not dependent on genetic polymorphism Ser³²⁶/ Cys³²⁶. *Mutation Research* 2001; **486**: 207-216.

507. Saitoh T, Shinmura K, Yamaguchi S, *et al.* Enhancement of OGG1 protein AP lyase activity by increase of APEX protein. *Mutation Research* 2001; **486**: 31-40.
508. Dantzer F, Luna L, Bjoras M, Seeberg E. Human OGG1 undergoes serine phosphorylation and associates with the nuclear matrix and mitotic chromatin *in vivo*. *Nucleic Acids Research* 2002; **30**: 2349-2357.
509. Souza-Pinto NC, Croteau DL, Hudson EK, Hansford RG, Bohr VA. Age-associated increase in 8-oxo-deoxyguanosine glycosylase/ AP lyase activity in rat mitochondria. *Nucleic Acids Research* 1999; **27**: 1935-1942.
510. Cooke MS, Lunec J, Evans MD. Progress in the analysis of urinary oxidative DNA damage. *Free Radical Biology and Medicine* 2002; **33**: 1601-1614.
511. Chung JH, Suh M-J, Park YI, Tainer JA, Han YS. Repair activities of 8-oxoguanine DNA glycosylase from *Archaeoglobus fulgidus*, a hyperthermophilic archaeon. *Mutation Research* 2001; **486**: 99-111.
512. Matsumoto Y, Zhang Q-M, Takao M, Yasui A, Yonei S. Escherichia Coli Nth and human hNTH1 DNA glycosylases are involved in removal of 8-oxoguanine from 8-oxoguanine/ guanine mispairs in DNA. *Nucleic Acids Research* 2001; **29**: 1975-1981.
513. Vidal AE, Hickson ID, Boiteux S, Radicella JP. Mechanism of stimulation of the DNA glycosylase activity of hOGG1 by the major human AP endonuclease: bypass of the AP lyase activity step. *Nucleic Acids Research* 2001; **29**: 1285-1292.
514. Hill JW, Hazra TK, Izumi T, Mitra S. Stimulation of human 8-oxoguanine-DNA glycosylase by AP-endonuclease: potential coordination of the initial steps in base excision repair. *Nucleic Acids Research* 2001; **29**: 430-438.
515. David-Cordonnier M-H, Boiteux S, O'Neill P. Excision of 8-oxoguanine within clustered damage by the yeast OGG1 protein. *Nucleic Acids Research* 2001; **29**: 1107-1113.
516. Dherin C, Radicella JP, Dizdaroglu M, Boiteux S. Excision of oxidatively damaged DNA bases by the human α -hOGG1 protein and the polymorphic α -hOGG1 (Ser 326 Cys) protein which is frequently found in human populations. *Nucleic Acids Research* 1999; **27**: 4001-4007.

517. Takao M, Zhang Q-M, Yonei S, Yasui A. Differential subcellular localization of human Mut Y homolog (hMYH) and the functional activity of adenine: 8-oxoguanine DNA glycosylase. *Nucleic Acids Research* 1999; **27**: 3638-3644.
518. Takao M, Aburatani H, Kobayashi K, Yasui A. Mitochondrial targeting of human DNA glycosylases for repair of oxidative DNA damage. *Nucleic Acids Research* 1998; **26**: 2917-2922.
519. Morland I, Rolseth V, Luna L, Rognes T, Bjoras M, Seeberg E. Human DNA glycosylases of the bacterial Fpg/ MutM superfamily: an alternative pathway for the repair of 8-oxoguanine and other oxidation products in DNA. *Nucleic Acids Research* 2002; **30**: 4926-4936.
520. Stevnsner T, Thorsland T, de Souza-Pinto NC, Bohr VA. Mitochondrial repair of 8-oxoguanine and changes with ageing. *Experimental Gerontology* 2002; **37**: 1189-1196.
521. Tsuruya K, Furuichi M, Tominaga Y, *et al.* Accumulation of 8-oxoguanine in the cellular DNA and the alteration of the OGG1 expression during ischaemia-reperfusion injury in the rat kidney. *DNA Repair* 2003; **2**: 211-229.
522. Bogenhagen D. Repair of mtDNA in vertebrates. *American Journal of Human Genetics* 1999; **64**: 1276-1281.
523. Croteau DL, Stienum RH, Bohr VA. Mitochondrial DNA repair pathways. *Mutation Research* 1999; **434**: 137-148.
524. LeDoux SP, Driggers WJ, Hollensworth BS, Wilson GL. Repair of alkylation and oxidative damage in mitochondrial DNA. *Mutation Research* 1999; **434**: 149-159.
525. Sobal RW, Prasad R, Evenski, *et al.* The lyase activity of the DNA repair protein β -polymerase protects from DNA-damage-induced cytotoxicity. *Nature* 2000; **405**: 807-810.
526. Allinson SL, Dianova II, Dianov GL. DNA polymerase β is the major dRPase involved in repair of oxidative base lesions in DNA by mammalian cell extracts. *EMBO Journal* 2001; **20**: 6919-6926.
527. Cleaver JE, Karplus K, Kashami-Sabet M, Limoli CL. Nucleotide excision repair "a legacy of creativity". *Mutation Research* 2001; **485**: 23-36.

528. Kojda G, Harrison D. Interactions between NIO and reactive oxygen species: pathophysiological importance in atherosclerosis, hypertension, diabetes and heart failure. *Cardiovascular Research* 1999; **43**: 562-571.
529. Benedictis GD, Carrieri G, Garasto S, *et al.* Does a retrograde response in human ageing and longevity exist? *Experimental Gerontology* 2000; **35**: 795-801.
530. Capaldi RA. Structure and function of cytochrome *c* oxidase. *Annual Review of Biochemistry* 1990; **59**: 569-596.
531. Hatefi HH. The mitochondrial electron transport and oxidative phosphorylation system. *Annual Review of Biochemistry* 1985; **54**: 1015-1069.
532. Tsukihara T, Aoyama H, Yamashita E, *et al.* The whole structure of the 13-subunit oxidised cytochrome *c* oxidase at 2.8 Å. *Science* 1996; **272**: 1136-1144.
533. Hanson BJ, Carozzo R, Piemonte F, Tessa A, Robinson BH, Capaldi RA. Cytochrome *c* oxidase-deficient patients have distinct subunit assembly profiles. *Journal of Biological Chemistry* 2001; **276**: 16296-16301.